INDEX

FOREWORD

In this thesis, the modeling of biotechnological and food-industry processes was studied. Even if characterized by an apparent dissimilarity, the analyzed processes share the necessity of process intensification. From one side, biotechnological processes exploit the catalytic activity of enzymes or whole cells to produce valuable products; however, except for well-consolidated biotechnological productions, the industrial applications are often limited by economic reasons. On the other side, food-industry processes need a continuous innovation and optimization in order to fulfil the qualitative standards required by the markets and the safety standards required by the regulations.

For the processes at hand, different modeling approaches were tested and discussed and, finally, an optimal modeling strategy was identified for each of the analyzed case-studies. On the basis of the obtained results , the hybrid neural modeling was proposed as an effective support to design and control the considered processes.

According to the so-called "*papers model dissertation*" (Dunleavy, 2003), the thesis was structured as a collection of already published and ready-to-be-submitted papers, summarizing the research activity performed during the PhD course. After a brief introduction to the overall work the thesis was then divided, without sacrificing the unity of the proposed approach, into two main chapters: in Chapter 1, the modeling of biotechnological processes was discussed; whereas, the application of hybrid neural modeling to food-industry processes was treated in Chapter 2.

Each chapter is, actually, a series of interrelated and consequential papers introduced by a short description aimed at emphasizing the strong relationships existing among the presented papers, whose novelty was pointed out in a short opening note containing a list of highlights.

The work is closed by a biographical paragraph containing all the references cited in the text.

INTRODUCTION

The aim of this chapter is to present an overview of hybrid neural modeling and to explain the motivation of this PhD thesis.

The so-called "model identification step" is, generally, aimed at identifying a mathematical model, which determines the relationship(s) existing between the input and the output variables of a physical process (Fig.1) (Stephanopoulos, 1984).

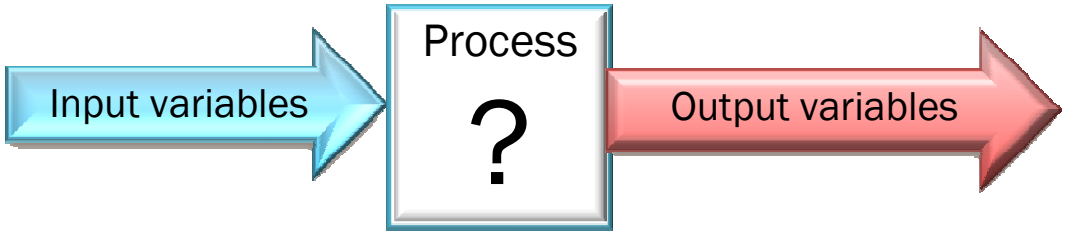

Fig.1. The "model identification" step.

This step is preliminary to any kind of rational process development being necessary to process optimization and control.

The classical approach used to model a chemical process is the fundamental or theoretical approach. Based on the so-called "first principles", it consists in writing the mass, energy and momentum balance equations referred to the considered system; being physically-based, the model predictions are usually very reliable even in extrapolation. However, this approach is no longer applicable if the process under study is characterized by an inherent complexity; in this case, the resulting rigorous model, could become a cumbersome system of non-linear partial differential equations very often unsuitable for practical purposes, such as the implementation of on-line optimal control strategies.

On the contrary, the "empirical, or black-box, approach" depicts the process input-output dynamics using a "best-fitting" mathematical model. The main advantage of this approach relies in the simplified representation of the process that usually corresponds to a simple-to-manage model. Unfortunately, due to the lack of any kind of physical interpretation, the exploitation of empirical models is limited to a validity domain corresponding to that in which the experimental data used during their set-up were actually collected; empirical models, therefore, provide unreliable predictions when

they are called to interpret the system behavior outside the range of the available data.

If a very complex process, such as the prediction of a bioreactor behavior, has to be described in a consistent way, it could be necessary to formulate advanced and alternative modeling approaches that combine the advantages of theoretical modeling to the simplicity of black-box models.

In the present PhD thesis, it will be shown that hybrid neural modeling, given as the combination of a rigorous fundamental model, used to represent the available process knowledge by well-assessed theoretical relationships, with an empirical model, used to describe very difficult-to-interpret physical phenomena, allows reliably represent the behavior of biotechnological and food-industry processes.

With respect to "pure" empirical models, the key advantage of hybrid models (HMs) is represented by the possibility of performing extrapolation. This capability, however, has always to be proved by the so-called "model validation phase" since HMs cannot be considered as general as a first principles models. With reference to the theoretical approach, HMs represents an effective alternative in the case of not fully understood phenomena such as for processes involving a series of very complex (bio-)chemical reactions and for systems in which the simultaneous transfer of momentum, heat and mass transfer actually occurs (Kahrs and Marquardt, 2007).

Hybrid neural models (HNMs), in particular, are hybrid models whose empirical part is constituted by an artificial neural network. A brief digression about ANNs is hereafter reported.

Among the available empirical models, Artificial Neural Networks (ANNs) make themselves conspicuous owing to their ability to "learn" complex dynamics from examples, thus performing a mapping from an input space to an output space (Psichogios and Hungar, 1992).

Originally, the aim of ANNs developers was to set-up a tool inspired to human brain functioning, capable, therefore, to compute, learn and optimize like humans do. Still distant from this target, ANNs did actually exhibit powerful pattern classification and pattern recognition capabilities (Zhang et al., 1998). An ANN is a data-driven model constituted by an interconnection of simple processing elements called "neurons" or "nodes"; each neuron receives, as input, a series of signals from the other neurons and processes it through an activation function that, typically, is non linear.

Neurons are usually inserted in a multiple-layer structure which can be classified according to the way of positioning the neurons in the network and to the actual mechanism of transfer information. For our purposes, the most interesting network structure is represented by the multi-layer perceptron (MLP) whose schematic is given in Fig. 2. In MLP the input information is fed to the first and lower layer of the structure, i.e. the " input layer", whereas the output variables of the system are provided by the last

layer of the structure, i.e. the “output layer”. Between the first and the last layer , many intermediate (or hidden) layers could exist. Through these layers the information passes from a lower to a higher layer so as to follow a feed-forward scheme.

In order to use a neural model for any kind of forecasting task, the network architecture should be defined and the so-called “training procedure” accomplished. The choice of the neural network architecture, i.e. the definition of the number of layer(s) composing the net and the number of neurons composing each layer, is usually the results of a trial and error procedure. However, even if the network architecture has been preliminary defined, the actual completion of neural network development can be achieved by the so-called network training. During the training phase the ANN learns how to correlate the input to the output variables properly changing a set of other variables, namely the neurons weights, interconnecting each node; more specifically, the network is submitted to a definite set of available data and, according to an error minimization algorithm, the network weights are progressively adjusted. Not all the available data are actually provided to the ANN during the training phase; a considerable number of experimental points is to be used during the post-training analysis, i.e. the test and validation phases. The necessity of post training analysis is due to the black-box nature of the neural models since it is always necessary to verify the model reliability beyond the training dataset.

During the test phase, the neural network is called to predict the output values corresponding to an input combination not belonging to the training set: if satisfactory results are obtained, the chosen network structure could be considered suitable to map the considered input-output dynamics. Finally, the validation phase represents a real validation for the considered process since it is an analysis aimed at proving the reliability of the already determined model (Zhang et al., 1998).

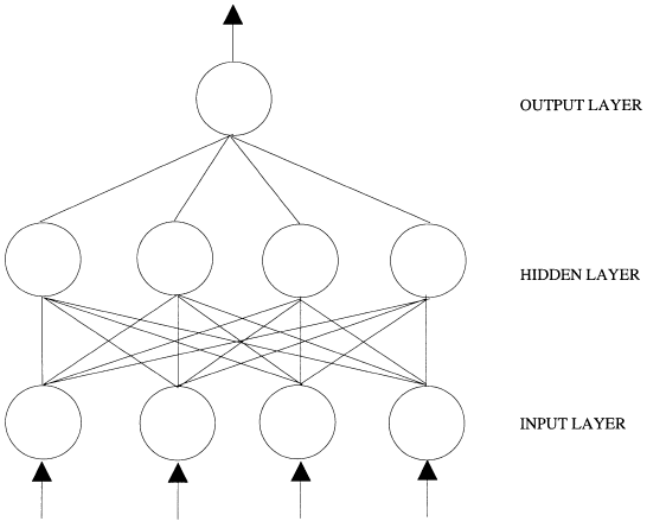

Fig.2.ANNs structure

When an ANNs is used in a hybrid model two general structures can be defined on the basis of the interaction existing between the theoretical and the black-box part of the model: in a parallel architecture, the error existing between the theoretical part of the model and the experimental data is filtered by the neural network that play the role of a "residuals estimator"; in a serial model structure, the neural network is used to estimate a difficult-to-measure process variable that subsequently is fed to the theoretical part of the model.

As anticipated before, the hybrid neural approach was exploited to model both biotechnological and food-industry processes.

Biotechnological processes are performed on biological materials or making use of biological agents such as cells, enzymes or antibodies (Bailey and Ollis, 1986). For these processes, the modeling step represents a key issue to achieve, for instance the implementation of proper control systems aimed at process optimization; the success of this step depends on the capability to integrate the knowledge about the true biological pathways and the actual kinetics and transport phenomena involved in the transformations (Lubbert & Jorgensen, 2001; Bailey & Ollis, 1986). In this PhD thesis the kinetic modeling of two types of bioprocess: a) processes using whole cells as catalytic agents, i.e. fermentations; b) processes using enzymes as catalytic agents, was performed.

Both in fermentations and enzymatic processes many parallel-serial reaction steps are involved as well as several transport phenomena that may limit the observed reaction rates; this aspect is more relevant in fermentations since product formation is actually the result of cell metabolism and of the control and regulatory mechanisms occurring in living cells. For the above-mentioned reasons, the rigorous kinetic modeling of bio-processes results in a series of complex reactions whose resolution either necessitates a set of simplifying hypotheses, which may not be applicable in several cases, or is too onerous and time consuming for practical purposes (Feyo de Azevedo et al., 1997).

As far as food-industry processes are concerned, the convective drying of vegetables was investigated. Food drying is a preservation technique aimed at decreasing the water activity thus limiting the microbial spoilage and prolonging food shelf-life. Without a proper control of drying conditions, i.e. the operating variables chosen to operate the convective ovens, either very poor quality or unsafe foods could be obtained . The starting point for an efficient automatic control of drying process is represented by the availability of a suitable predictive model. It is worthwhile remarking that an exhaustive analysis of the transport phenomena involved in drying process is burdensome. In fact, heat is transferred from air to the material and simultaneously water, both as liquid and as vapor, is transported, both by a pressure gradient and a concentration gradient, from the food core to its surface, where finally is transported to the drying air, which flows, in turbulent conditions, around the food sample, whose shape and dimensions continuously change as drying proceeds. The above phenomena can be described solving a set of unsteady-state, non-linear, partial differential equations. Similarly to biotechnological processes, the problem solution either necessitates a set of simplifying hypotheses, which may not be applicable in several cases, or is too onerous and time consuming for practical purposes.

On the basis of the considerations reported in this introductory paragraph the main motivation that drove the author to model bioprocesses and drying kinetics by means of different modeling approaches, especially by the hybrid approach, should be clear. In the following, a more detailed analysis of each of the considered processes will be presented.

CHAPTER 1

KINETIC MODELING OF BIOPROCESSES

Introduction

In this chapter the papers dealing with modeling of biotechnological process are sequentially reported as:

Paper 1: *A hybrid neural approach to model batch fermentation of "ricotta cheese whey" to ethanol*. It has been published on *Computers & Chemical Engineering, 2010,* 34 (10), 1590-1596.

Paper 2: *A comparison between different modeling techniques for the production of bioethanol from dairy industry wastes.* It will be published on *Chemical and Biochemical Engineering Quarterly,* 2011, 25 (4).

Paper 3: *Biodiesel production from waste oils by enzymatic trans-esterification: process modeling with hybrid neural model.* An abstract of this work has been published on *Journal of Biotechnology,* 2010, 150, 371. At present, this paper is ready to be submitted for publication on ISI ranked scientific journals.

Paper 4: *How hybrid neural model might help on the optimization of biofuels product.* The work was presented at the 19th Biomass Conference and Exhibition held in Berlin, 6-9 June, 2011. It was submitted to Biomass & Bioenergy and at present, it is under review.

Paper 5: *A mass transport/kinetic model for the description of inulin hydrolysis by immobilized enzyme.* At present, this paper is ready to be submitted for publication on ISI ranked scientific journals

In particular, papers 1-4 concern the development of hybrid neural models aimed at describing biofuels production processes.

The urgency to identify a sustainable fuel source has become clear during the XX century and in this context, biofuels have been proposed as the most attractive alternative due to energy independence, mitigation of climate change and rural development. In spite of an initial success, biofuels produced by food crops, the so called “first generation biofuels”, showed few advantages if compared with fossil fuels and were widely criticized being foodstuff competitive. To overcome these limits, another kind of biofuels was actually considered, the “second generation biofuels”; in this case, biofuels are produced starting from either dedicated energy crops or waste biomass, obtained from agriculture and food-industry (Luque et al., 2011).

Among suitable conversion processes aimed at “second generation biofuels” production, biochemical conversion using enzymes as well as fermentative paths play a key role; these processes, however, are far from being optimized and their kinetic modeling represents only the first step for a more comprehensive knowledge about the influence on biofuel yields of both operating variables and substrate characteristics, often a mixture of several complex biomasses. Papers 1 and 2, in particular, deal with the modeling of “ricotta cheese whey” fermentation aimed at bioethanol production. Ricotta cheese whey (RCW) is a dairy industry waste characterized by a high lactose content (about 50 g/l) that can be directly fermented into ethanol by the yeast *Kluyveromices Marxianus.* The aim of the work summarized in these two papers was the development of a model capable of predicting the time evolution of lactose, biomass and ethanol concentrations, i.e. the key reacting species monitored during the lab-scale fermentation runs. In Paper 1 a multiple hybrid neural model was proposed to accomplish this task, whereas in Paper 2, the obtained model was compared with a pure neural model and with a very simple analytical model; a better forecasting capability was finally observed when the proposed hybrid approach was exploited.

In Paper 3, a kinetic study was performed on the enzymatic trans-esterification of triglycerides aimed at biodiesel production. The enzymatic conversion of triglycerides using lipase represents an innovative procedure for biodiesel production, since it is less energy intensive and more environmental friendly than traditional processes, which make use of alkaline or acid catalysts.

The starting point to develop the study was represented by a simplified theoretical model, already

available to describe the reaction kinetics on the basis of a series of simplifying hypotheses necessary to solve the mathematical model. The original contribution of paper 3 consisted, therefore, in the formulation of a hybrid neural model whose neural part was aimed at determining the actual relationships existing between the substrate(s) and the reaction product(s). This allowed removing some of the hypotheses previously formulated. Even if developed making use of a set of experimental data collected feeding the bioreactor with simulating oil, the model reliability was also tested on a low quality olive husk oil, showing a good agreement between HNM predictions and the experimental data.

In Paper 4, three case-studies were analyzed with the aim to show how ANNs, in some cases combined with well-assessed theoretical equations, can be used to model (Case-studies 1-2) and optimize (Case study-3) biofuels production processes. This paper, therefore, represents a collection of the neural network applications fully developed during this PhD course. Besides the case studies reported in Papers 1-3, the modeling of anaerobic digestion of agro-food wastes was also reported. In the last case, a pure neural model was proposed to model the bioreactor behavior and to prove that the proposed model can be exploited so as to achieve a process optimization.

The contents of Paper 5 differ, to a certain extent, from those reported in the other papers belonging to this chapter; the attention was indeed focused on another worth-of-consideration biotechnological process, i.e. the hydrolysis of the biopolymers by means of immobilized enzymes. Unlike the other contributions, a pure first-principle model was chosen to describe the behavior of the immobilized enzyme, identifying if the system is actually controlled by the kinetics rather than by the transport phenomena occurring outside the biocatalyst. The possibility of developing a very general model, applicable to any kind of bioprocess, was actually beyond the scopes of the present work; from the obtained results it was, however, evident that the choice of the best modeling approach is strictly problem-dependent and always represents the results of the critical analysis of the particular process under study.

1.1 Paper 1: A hybrid neural approach to model batch fermentation of “ricotta cheese whey” to ethanol

In the present paper, a hybrid neural model was proposed to describe the RCW lab-scale fermentation . The mass balance equations describing the behavior of a batch reactor were written with reference to the most important species, i.e. lactose (S), ethanol (P) and biomass (B); for each of the species, the generation term was expressed by a one-parameter rate equation. Three neural networks were combined to the theoretical model so as to achieve the instantaneous estimation of the kinetic parameters and to obtain the actual time evolutions of S, P and B.

A hybrid neural approach to model batch fermentation of “ricotta cheese whey” to ethanol.

Alessandra Saraceno[1], Stefano Curcio, Vincenza Calabrò, Gabriele Iorio

Department of Engineering Modeling – University of Calabria

Via P. Bucci - Cubo 42/A - 87036 Arcavacata di Rende (CS) – ITALY

Abstract

In this work, the fermentation of “ricotta cheese whey” for the production of ethanol was simulated by means of a multiple Hybrid Neural Model (HNM), obtained by coupling neural network approach to mass balance equations for lactose (substrate), ethanol (product) and biomass. A HNM represents an alternative method that may allow predicting the behavior of complex systems, such as biotechnological processes, in a more efficient way. Some well-assessed phenomena, in fact, are described by a fundamental theoretical approach; some others, being very difficult to interpret, are analyzed by means of rather simple ‘‘cause-effect’’ models, based on artificial neural networks. The

[1] Corresponding author. E-mail: alessandra.saraceno@unical.it

experimental data, necessary to develop the model, were collected during batch fermentation runs. For all the proposed networks, the inputs were chosen as the operating variables with the highest influence on reaction rate. Simulation results showed the ability of the developed model to represent the process dynamics. The HNM was capable of an accurate representation of the system behavior by predicting biomass, lactose and ethanol concentration profiles with an average error percentage lower than 10%. Moreover, the hybrid approach showed the ability to limit error propagation into the models that can be caused by the purely black-box nature, typical of neural networks.

Keywords: grey-box models; artificial neural networks; batch fermentation; modeling

1. Introduction

Modeling of biotechnological processes represents a key issue to achieve proper design and control aimed at process optimization (Lubbert and Jorgensen, 2001).

Biochemical reactions actually involve many parallel-serial reaction steps and depend on several transport phenomena that may limit the observed reaction rates. Usually, the fundamental approach, largely considered as the most rigorous, cannot be applied in reaction kinetic modeling due to inherent non-linearity, lack of information, experimental inaccuracy, deviations from ideal conditions (Feyo de Azevedo et al., 1997).

On the contrary, black-box models, suggested by the empirical approach, suffer from a restricted validity domain depending on the range of data collected during the experiments.

A reasonable trade-off between theoretical and empirical approach is represented by hybrid modeling, leading to a "grey-box" model capable of good performance in terms of data interpolation and extrapolation. Hybrid model predictions are given as a combination of both a theoretical and a "pure" neural network approach, together concurring to the obtainment of system responses. The main advantage of hybrid modeling regards the possibility of describing some well-assessed phenomena by means of a fundamental theoretical approach, leaving the analysis of other aspects, very difficult to interpret and describe in a traditional way, to rather simple "cause-effect" models. Among these, Artificial Neural Networks (ANNs) were successfully used in bioreactor modeling (Feyo de Azevedo et al., 1997; James at al., 2002; Laursen et al., 2007; Simutis et al., 1995; Zorzetto et al., 2000).

ANNs consist of interconnected computational elements called neurons or nodes: each neuron receives input signals from the related units, elaborates these stimuli by an activation or transfer function and generates an output signal that can be transferred to other neurons.

Neurons are organized in a multi-layer structure, which allows obtaining the output signal starting from a definite set of the inputs (Zhang et al., 1998). Many different artificial neural network structures have been proposed but the most common is the multi-layer perceptron (MLP). With MLP structure the backpropagation training algorithm is usually used: the information about the performance error moves backwards from the output layer to the input layer according to a feedback procedure (Riedmiller, 1994).

When ANNs are utilized in a hybrid model, a very important step is identifying the respective domain of theoretical and empirical parts in such a way as to determine the model structure. In parallel model structure, the purpose of ANN is to compensate the error existing between the output data of the theoretical model and the experimental results. In serial model structure, ANN operates so as to predict the unknown parameters of the theoretical model. With reference to a kinetic study, the latter structure is more physically motivated than the former one since ANN, can operate as a kinetic parameters estimator (Agarwal, 1997; Kahrs and Marquardt, 2007; Klimasauskas, 1998; van Can et al., 1998).

Feyo de Azevedo et al. (1997) modelled the Baker's yeast production in a fed-batch fermenter comparing the hybrid approach to both the theoretical and the pure black-box ANN approach. In their work the biomass mass balance received the kinetic information from ANN that determined the biomass specific growth rate. One of the network input was represented by the actual value of biomass concentration and so the empirical and theoretical part of the model had to be solved simultaneously.

James et al. (2002), developed a grey-box soft-sensor for on-line estimation of biomass concentration during *Alcaligenes eutrophus* fed-batch fermentation. The authors realized a feed-forward neural network to evaluate the specific growth rate of biomass by available on-line measurements and the previous specific growth rate. As compared to either the pure neural network sensors or the linear approximations based sensors, the proposed hybrid solution provided better results.

Zorzetto et al. (2000) used artificial neural networks to make "less dark" black-box models of a batch beer fermentation. The authors proposed two hybrid models: the first-one, based on ANN, determined biomass specific growth rate from temperature and substrate concentrations; the second one, based on Monod kinetics and on neural network predictions, was used to determine the dependence on

temperature of model parameters. Even if the second model was “less black” than the first one, both of them exhibited similar performance.

Substrate and product concentrations cannot always be inferred from biomass owing to the variability in yield coefficients (James at al., 2002). In this case a substrate and product mass balance can be formulated on the basis of consumption and production rate equations, determined using ANN (Laursen et al., 2007).

Ricotta cheese whey, “scotta”, is a dairy industry waste characterized by a lactose content of about 45-50 g/l and a very low amount of proteins ranging from 0.22 – 0.24 % in weight. BOD reduction of “scotta” can be achieved, for instance, by alcoholic fermentation of lactose carried out by *Kluyveromyces Marxianus*. Even if several authors dealt with biotechnological utilization of cheese whey (Gonzàles Siso, 1996; Ozmihci and Kargi, 2006, 2007a, 2208b) no specific work exists about “Ricotta Cheese whey”. The aim of this paper was to propose a model that can describe batch fermentation of lactose in ethanol.

The hybrid neural approach was proposed as an alternative way to properly describe the fermentation progress, whereas the most common unstructured batch growth models turned out to be less accurate for this purpose. More specifically, a hybrid neural model was developed suggesting a grey-box structure that, as compared to similar studies available in the literature, has several advantages, namely a) the capability of predicting not only biomass concentration but substrate and product concentration profiles too; b) the ability of estimating difficult-to-measure quantities from easily measurable variables; c) a higher generality level that might be useful for the implementation of advanced control systems. For these reasons, the proposed model could be regarded as a general approach for the model batch fermentation processes so as to achieve an optimal process control. The proposed approach allowed fulfilling the model identification step in a very efficient way, thus overcoming the intrinsic limitations typical of biotechnological processes.

2. Model development

The proposed HNM consists of three models, characterized by a similar general structure, for the prediction of biomass, lactose and ethanol concentration profiles during fermentation. For the development of the HNMs a mass balance equation was written for each component in a batch reactor and an ANN was set up to evaluate the kinetic parameters actually necessary to solve the balance

equations. Some logic conditions, expressing the fulfilment of physical constraints, were also introduced into the model.

The three resulting grey-box models have the general form shown in Fig.1.

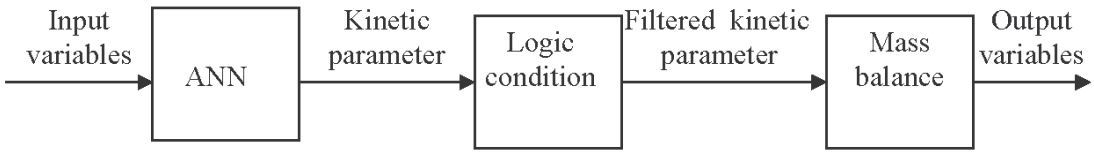

Fig. 1. General structure of the three hybrid models

To predict the current value of the kinetic parameter, a set of input variables were identified for each model, i.e.: temperature (T), pH (pH), reactor stirring rate (rpm), initial lactose concentration (C_{lac}^{0}) and reaction time (t). From a preliminary analysis it was showed that these variables, among all the parameters that can affect reaction progress, exhibited the highest influence on process performance.

Temperature and pH directly affect the microbial growth; as widely reported in the literature, optimal values of both temperature and pH exist and any deviation from these values may indeed result in a significant reduction of biomass growth (Bailey and Ollis, 1986). The stirring rate affects microbial growth since it is responsible for the concentration distribution inside the reactor, influences the rate of transport phenomena between the fermentation broth and the living cells and exerts a mechanical action on the biomass.

The initial lactose concentration (C_{lac}^{0}) determines the extent of biomass growth and if it is larger than a limit value, it can cause inhibition due to substrate excess. Finally, the reaction time is a measure of the reaction progress and can take into account different phenomena as, for instance, the existence of a lag phase (Bailey and Ollis, 1986).

No interaction between kinetic parameters and concentrations profiles was considered (such as in Monod kinetic model), with the result that concentrations do not appear among the input variables. The knowledge of fermentation initial conditions (C_{lac}^{0}) and of operating conditions (T, pH, rpm) was, therefore, considered sufficient to exhaustively describe the process evolution.

The kinetic parameters, evaluated using ANN, were subsequently processed by a logic condition that verified the agreement between the net output and some well-assessed process information. This

filtering function was aimed at the reduction of error propagation into the model due to the purely black-box nature of neural networks.

Finally, the filtered kinetic parameter was used in the mass balance to calculate the current concentration value.

An important consequence of the present modeling approach has to be put in evidence: difficult-to-measure quantities, such as concentrations, can be evaluated from easily measurable variables (T, pH, rpm, t) and initial condition (C_{lac}^{0}). These characteristics of the models can be exploited to infer on-line concentrations measurement during the control-phase of the reactor, without inserting any time delay into the control-loop (James et al., 2002).

The first modeling step consisted in describing biomass concentration profile. Lactose and ethanol concentration profiles were determined next using biomass concentration predictions.

2.1 Biomass concentration

The biomass mass balance in a batch reactor is described by the following differential equation:

$$\frac{dX}{dt} = \mu X \qquad 1$$

where, X is the biomass concentration, t the reaction time and μ the biomass specific growth rate.

With reference to the growth curve of microorganisms in a batch fermenter, it is worthwhile remarking that all the different phases, i.e. lag phase, exponential phase, stationary phase, decline phase, generally occur (Bailey and Ollis, 1986). Each one of these phases, however, is characterized by a different value of biomass specific growth rate. As a consequence of this behaviour, the μ term in Eq. 1 is a mathematical function that is intended to describe biomass growth throughout all fermentation process.

In this work, the determination of μ was performed by an ANN, called NN1, capable of predicting biomass growth rate as a function of fermentation operating conditions.

Since neural networks are data-driven models, it was necessary to determine the specific growth rate value in an as wide as possible range of operating conditions so to provide the net with proper input-output vectors as training points. To this aim, the experimental value of the specific growth rate was determined by experimental data. To guarantee a smooth first derivative for the biomass concentration

profile, cubic spline interpolation was preliminary performed. Eq. 1 was then approximated by Euler's discretization and the discretized form was used recursively to allow the biomass concentration prediction at time instant $t + \Delta t$, using the μ value provided by NN1. The value of the biomass concentration at time t=0 was supplied by the experimental data as an initial condition necessary to solve Eq.1.

The specific growth rate term of Eq. 1 is actually capable of describing the exponential and stationary phases of the biomass growth and, consequently, it can assume a positive or equal to zero value**.**

Nevertheless, since a black-box approach was utilized to evaluate the specific growth rate, any value of μ estimated as negative by ANN is set equal to zero by a logic condition.

2.2 Substrate concentration

Similarly to biomass, the substrate mass balance in batch reactor led to the following differential equation:

$$-\frac{dS}{dt} = qX \qquad 2$$

where, S is the substrate concentration and q the lactose consumption rate function. Eq. 2 provides lactose consumption rate as a function of biomass concentration only through the q term.

Eq.2 was approximated by Euler's discretization and the discretized form was used recursively to predict lactose concentration profile.

As well as for biomass concentration model, it was necessary to estimate lactose consumption rate, q. This was achieved by a second ANN, called NN2, capable of predicting q as a function of fermentation operating conditions. Substrate concentration at time t, S_t, was estimated from the already obtained model predictions, with the exception of the time instant $t = 0$, where a proper initial condition for substrate concentration was defined. A logic condition was introduced to filter NN2 outputs in order to improve model predictions. Considering that lactose concentration decreases during the reaction progress, the q term in Eq. 2 has to be always positive, or - at most - zero, as also suggested by analyzing the collected experimental data

It is worthwhile remarking that in Eq. 2 substrate consumption is due to biomass maintenance because a proportionality relation between lactose consumption rate $\left(-\frac{dS}{dt}\right)$ and biomass concentration in the fermentation broth (X) exists. Usually, in batch fermentation substrate consumption is related not only to biomass maintenance but also to biomass growth; according to this approach, Eq. 2 should actually be modified as:

$$-\frac{dS}{dt} = qX + \frac{1}{Y_G}\frac{dX}{dt} \qquad 3$$

where, Y_G is the so-called yield factor (Bailey and Ollis, 1986). Nevertheless, in order to describe the substrate profile by a grey-box model, Eq. 3 cannot be used, due to the difficulties of rearranging it in explicit form with respect to the kinetic parameters.

In addition, it is worthwhile observing that, usually, substrate consumption is related not only to biomass concentration but also to product formation. A kinetic model expressing this condition can be written as:

$$-\frac{dS}{dt} = \alpha X + \beta\frac{dP}{dt} \qquad 4$$

As it will be shown later, a simple kinetic model for product formation was chosen. This model related product formation only to biomass concentration through the kinetic parameter μ_p. Introducing this information in Eq. 4, it can be modified as follows:

$$-\frac{dS}{dt} = \alpha X + \beta\mu_P X = (\alpha + \beta\mu_P)X = qX \qquad 5$$

With reference to Eq.5 the lactose consumption rate q accounts for both biomass production and product formation.

2.3 Ethanol concentration

The ethanol mass balance in a batch reactor assumes the following form:

$$\frac{dP}{dt} = \mu_p X \qquad 6$$

where P is the product concentration and μ_P the product growth rate. A kinetic model depending on only one parameter was adopted for the same reasons already expressed about substrate consumption. As well as for biomass and lactose concentration profiles, Eq. 6 was approximated by Euler's discretization and the discretized form was used recursively to estimate ethanol concentration profile.

A third ANN, NN3, was trained to predict the μ_P value as a function of fermentation operating conditions. Considering that product concentration has to increase with respect to time, a logic condition was added to the model; therefore, any μ_P value returned by the neural network as negative, was set equal to zero.

3. Materials and Methods

3.1 Experimental design

The experimental data necessary to develop the hybrid models were collected from a set of anaerobic fermentations performed on "Ricotta cheese whey". According to the factorial design method (Box et al., 1978), the following variables and operating condition were chosen: 1) Temperature in the range 32- 40 °C; 2) pH in the range 4-6; 3) Stirring rate in the range 100-300 rpm; 4) Initial lactose concentration in the range 45-90 g/l. A total of 16 batch runs, having a duration of 18 hours with a sampling time of one hour, were therefore performed (Tab. 1) and a total of 912 experimental points, expressing the time evolutions of biomass, lactose and ethanol concentration, were collected during fermentations.

Test number	T [°C]	pH [-]	Agitation level [rpm]	C_{lat}^{0} [g/l]
1	40	6	300	90
2	40	4	100	90
3	32	6	300	45
4	40	6	100	45
5	32	6	100	90
6	32	4	300	90
7	40	4	300	45
8	32	4	100	45
9	40	4	100	45
10	40	6	300	45
11	40	4	300	90
12	32	6	100	45
13	32	4	300	45
14	32	4	100	90
15	40	6	100	90
16	32	6	300	90

Table 1. Batch fermentation operating conditions

Each fermentation test actually consisted of two steps: 1) the inoculum culture preparation; 2) the batch fermentation in a stirred anaerobic bioreactor.

3.2 Inoculum preparation

Kluyveromices Marxianus var. Marxianus obtained from Centraalbureau Voor Schimmelcultures (Holland) was used in all the fermentation experiments.

The inoculum culture was prepared putting a single yeast colony into 150 ml culture medium containing 50 g/l lactose, 10 g/l peptone, 5 g/l yeast extract (Fluka). The culture was kept in a 250 ml flask held in a temperature controlled bath with roto-translational external mixing (OLS 200, Grant), at 150 rpm and 37 °C for 12 h.

3.3 Batch fermentation

During each fermentation test one litre of ricotta cheese whey was fermented in a 2 l batch fermenter (*Z611020002,* Appikon) equipped with a temperature, pH, rpm controller (ADI 1030, Applikon). The duration of each run was 18 h from the addition of the inoculum culture into the bioreactor, sampling 2 ml of fermentation broth every hour. Ethanol and lactose concentrations were measured by HPLC technique with the detection of components achieved by a refractive index (RI 930, Jasco). The mobile phase was orto-phosphoric acid 1% (v/v) (Fluka), fed at a flow rate of 1 ml/min with 20 μl of fermentation broth injected into the instrument to perform each single analysis. The column was an Alltima Amino NH2 (Alltech). Biomass concentration analysis was carried out by Bactoscan (Foss).

3.4 Neural Network development

The above-described neural networks were developed by an iterative procedure implemented according to Matlab Neural Network Toolbox Ver. 4.0.1 (the Mathworks Inc., USA). The first step of the procedure consisted in determining the experimental values of μ, q_s, μ_p, by interpolating the collected experimental data by cubic splines. Subsequently, the experimental points relative to 15 of the 16 available runs were used to train/test the developed networks: the data points were randomly split into two groups, reserving 2/3 of data (570 points) to the training phase and remaining 1/3 (285 points) to test the neural networks. Finally, the three realized neural models were validated using a complete experiment (corresponding to 57 experimental points) never exploited during both the previous training/test phases. A multi-layer perceptron (MPL) feed-forward architecture with a pyramidal structure, having a decreasing number of neurons from input to output layer, was used. To train all the networks, thus estimating the weights and the bias of the networks, the Bayesian regularization was used (Demuth and Beale, 2000). The neuron transfer function was always the hyperbolic tangent except for the output layer where a linear transfer function was used; the choice of these transfer functions was supported by preliminary training tests.

To develop the ANNs, thus determining the number of nodes in each layer and the number of hidden layer, a trial-and-error procedure was implemented. A performance index, i.e. the percentage error defined in terms of each predicted ($C_{P,k}$) and measured ($C_{M,k}$) concentration value, was used to assess the ANNs reliability and, therefore, to choose the networks architecture:

$$\varepsilon\% = \frac{\left|C_{P,k} - C_{M,k}\right|}{\min(C_{M,k}, C_{P,k})} \cdot 100 \qquad (11)$$

In the present case, the convergence was achieved as soon as the average percentage error of each run, $\varepsilon_A\%$, calculated as $\varepsilon_A\% = \frac{\sum_{k=0}^{18} \varepsilon\%}{19}$, was lower than 10%.

The implemented iterative procedure can be schematized as reported in Fig. 2 where i is the generic network layer and n_i is the number of neurons in the i^{th} layer.

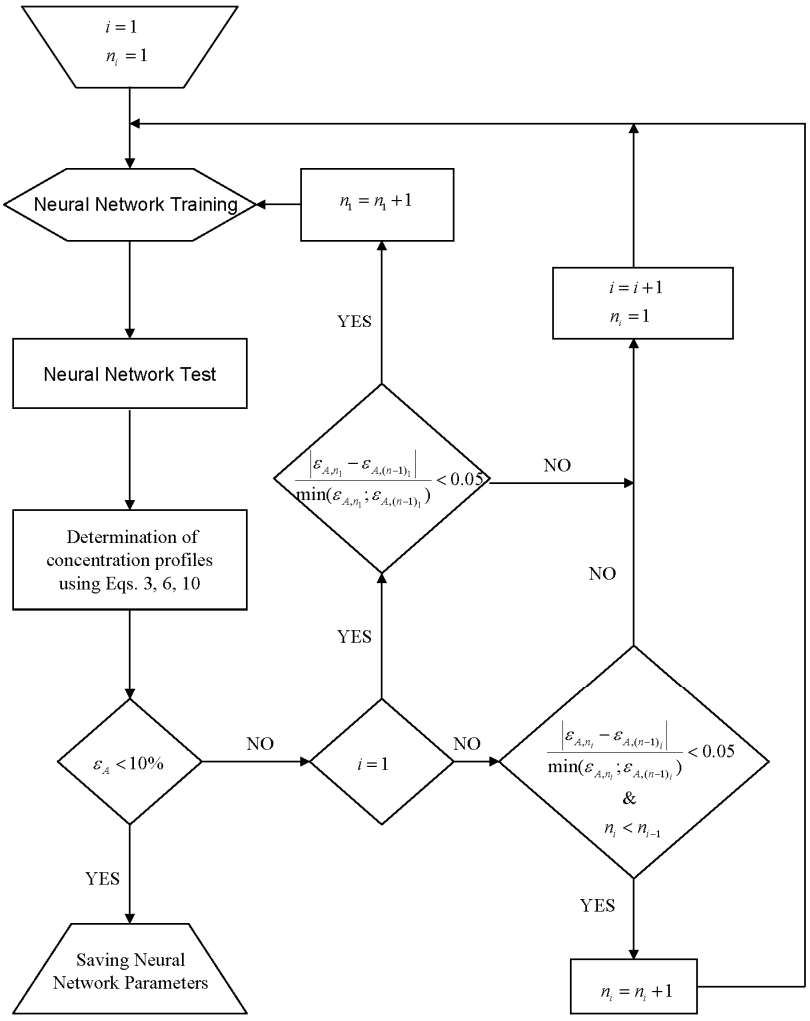

Fig. 2. Neural network realization procedure

Moreover, in order to avoid the development of very complex models that might increase the computational effort it was decided not to add another neuron in a generic layer only if a 5% reduction of ε_A % was actually attained.

4. Results and discussion

On the basis of the previous discussion, three hybrid neural models were developed with the aim of predicting biomass, lactose and ethanol concentration profiles during batch fermentation runs. Tab. 2 summarizes the architecture of the NN1, NN2, NN3 respectively, while, a typical network structure is shown in Fig. 3.

NN1	Layer	Neurons number	Activation function
	1st hidden layer	6	Hyperbolic tangent
	2nd Hidden layer	5	Hyperbolic tangent
	Output layer	1	Linear
NN2	Layer	Neurons number	Activation function
	1st hidden layer	10	Hyperbolic tangent
	2nd Hidden layer	3	Hyperbolic tangent
	Output layer	1	Linear
NN3	Layer	Neurons number	Activation function
	1st hidden layer	10	Hyperbolic tangent
	2nd Hidden layer	2	Hyperbolic tangent
	Output layer	1	Linear

Table 2. NN1, NN2, NN3 architecture

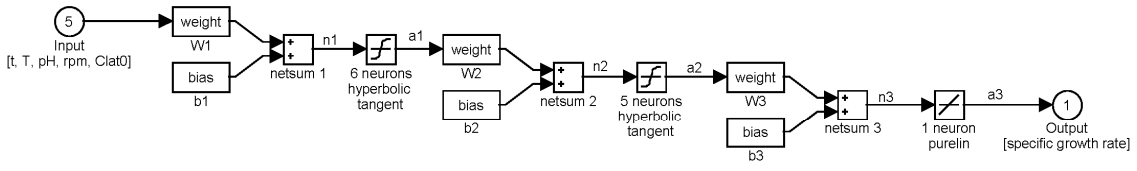

Fig. 3. NN1 architecture

A comparison between HNM predictions and the corresponding experimental data is reported in Fig.4; a remarkable agreement can be observed since the obtained straight line is characterized by unitary slope with a correlation coefficient of 0.999.

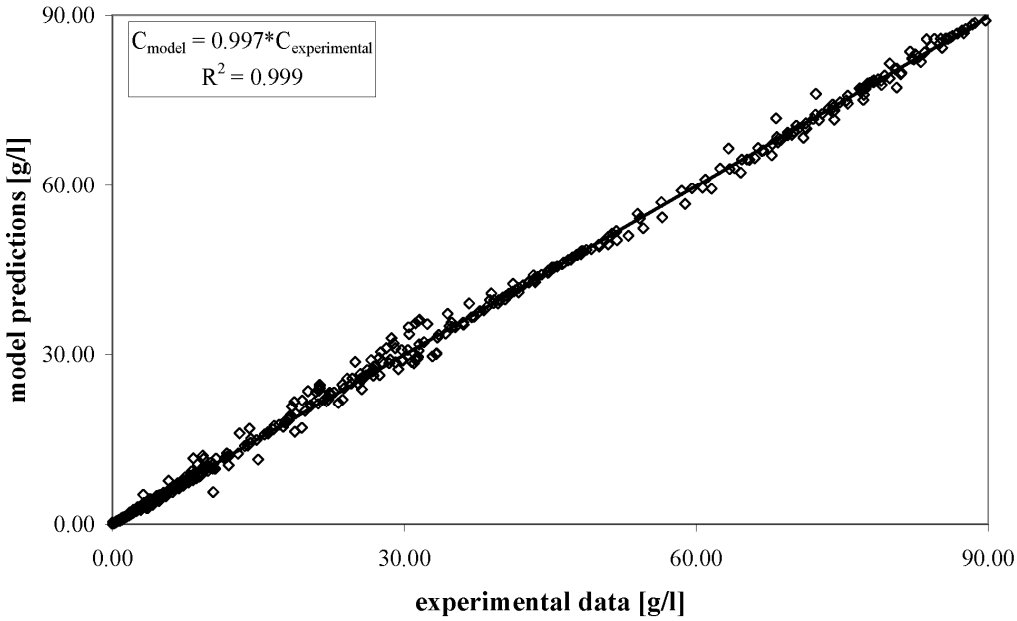

Fig. 4. Whole simulation results

Model	ε_A %
Biomass concentration	<3.7
Lactose concentration	<2.9
Ethanol concentration	<4.8

Table 3. Model performance

With reference to the data shown in Tab. 3, it was proved that the proposed approach gives satisfactory results since the developed hybrid models were characterized by an average percentage error much lower than 10% that represented a threshold limit assessing the reliability of HNMs predictions. It is worthwhile observing that the HNMs results, as reported in Fig.4, give a lower average percentage error as compared to the average error calculated on the basis of ANNs predictions. Even though the

developed HNMs were characterized by a sequential information transfer that might suggest an error propagation, an error dumping was, instead, observed. This confirms that hybrid models, based as they are on fundamental equations, perform better than the pure neural networks in interpreting the physical phenomena analysed in this paper and, more generally, the complex phenomena involved in biotechnological processes.

In Figs. 5-7 some typical profiles referred to biomass, lactose and ethanol concentrations, respectively, are shown; it is possible to notice that HNMs are capable of predicting both the concentration values and their time evolution with a remarkable agreement.

It is worthwhile remarking that the results shown in Figs. 5-7 compare HNMs predictions to the corresponding experimental values for which 2/3 of the available data were used to train the net and the remaining 1/3 to the test the model.

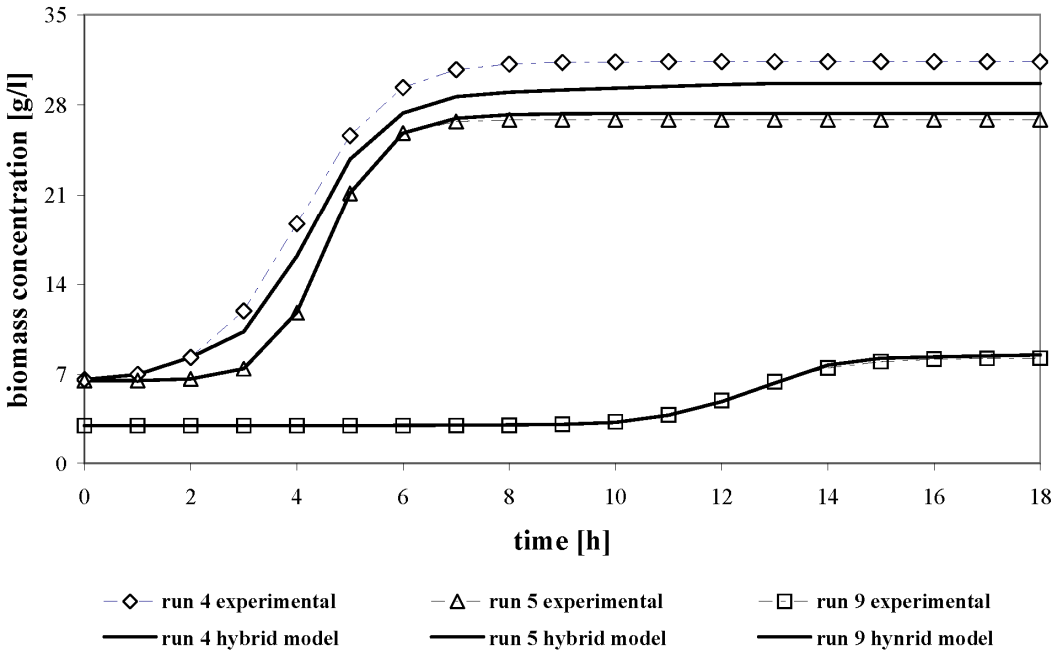

Fig. 5. Biomass concentration model: simulation results

With reference to Fig. 5, a general behaviour verified in all experimental runs, can be recognized: the temporal range in which biomass grew, was limited if compared to the observation time. As a consequence, the choice of Eq. 4 to relate substrate consumption only to biomass maintenance is

confirmed by the experimental evidence and it is probably responsible of the good performance of substrate concentration model.

The results reported in Figs. 6 and 7, relative to lactose and ethanol concentrations, were obtained after providing biomass concentration as calculated by biomass concentration model.

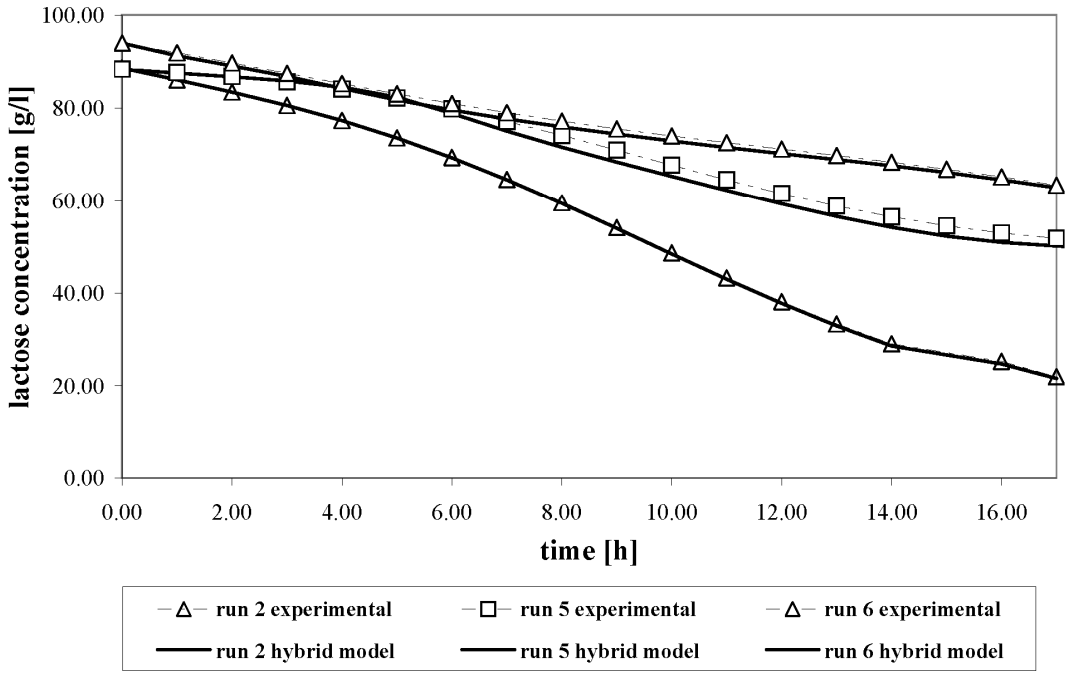

Fig. 6. Lactose concentration model: simulation results

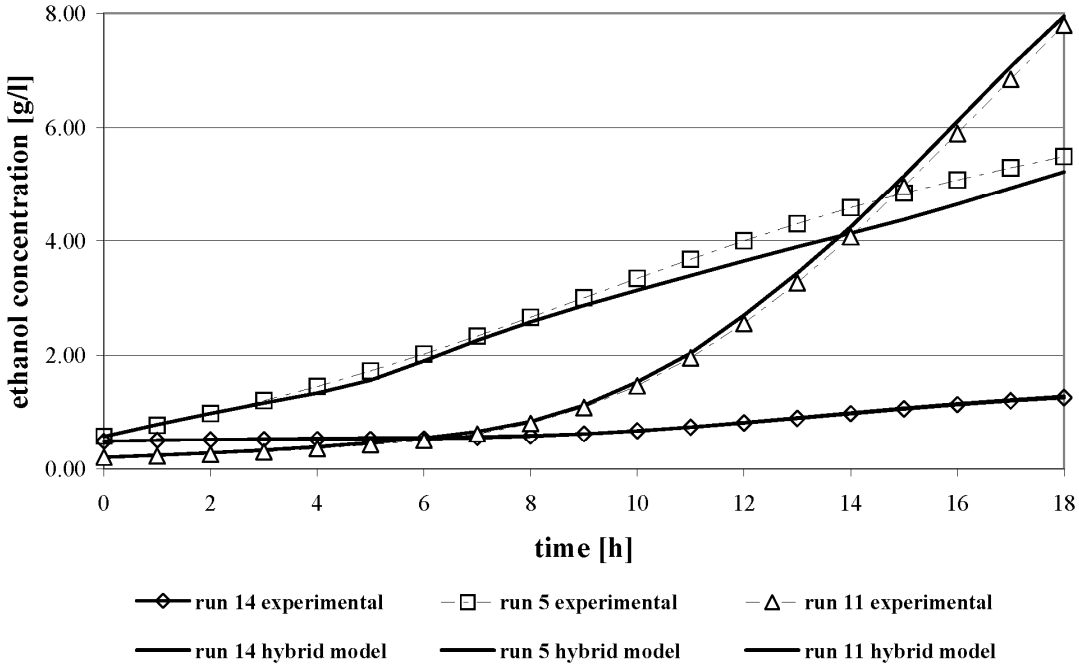

Fig. 7. Ethanol concentration model: simulation results

The choice of using a basically biased value and not an experimental data-set to estimate lactose and ethanol concentrations was aimed at testing the capability of the models to provide good simulation results, even if their inputs were bias affected. This capability of the lactose and ethanol concentration models was confirmed as suggested by Figs. 6 and 7.

Fig. 8 shows, instead, the simulation results relative to a complete experiment never exploited during both the learning and the test phases; this simulation represents, therefore, a general validation of the proposed model since it tests the HNMs' capability of properly predict the system behaviour even in operating condition never seen before.

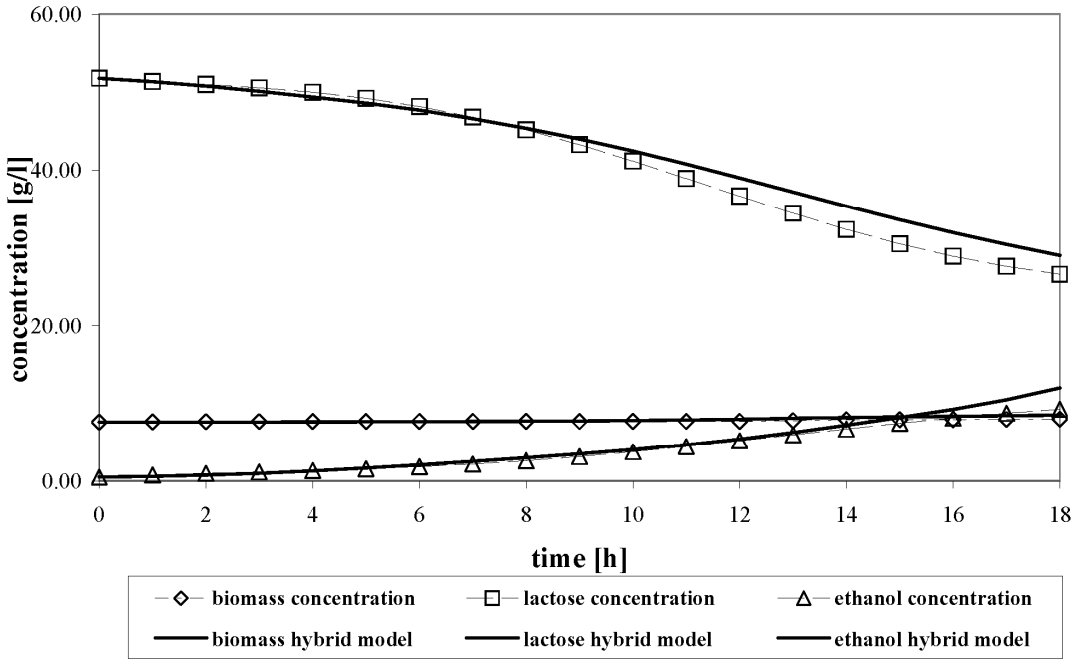

Fig. 8. Validation run

With reference to Fig.8, it should be emphasized how the hybrid model is capable of giving good simulation results even during validation; during validation, the model performance, measured in terms of $\varepsilon\%$, is comparable to that obtained with the experimental data used to perform the training and the test phases.

The results obtained during the validation phase show that neural networks training is not a passive phase in which the networks just learn in order to recognize the training points; instead, the networks are able of predicting the system behaviour even when it is operated in conditions never exploited before. This feature of the developed HNMs is particularly useful as far as process control is concerned. In fact, it is expected that HNMs, providing reliable predictions of system behaviour, may represent a necessary starting point for the implementation of advanced control systems to be used in biotechnological applications.

5. Conclusions

The multiple hybrid neural approach turned out to be a very efficient tool for the analysis and simulation of the “ricotta cheese whey” fermentation process and, more generally, of several complex

biotechnological processes that could be very difficult to interpret in a traditional way. On one hand, in fact, it allows to overcome the difficulties of a complex reaction mechanism, such as the whey fermentation and, on the other hand, to exploit all the available fundamental knowledge of this process in a synergistic manner. The choice to identify the unclear process aspects into the reaction kinetic and, consequently, to estimate the kinetic parameters using neural networks, resulted appropriate and capable to guarantee good simulation results. The realized model appears as a reliable instrument to predict system behaviour even in operating condition never exploited during the training phase. Moreover it is characterized by a high level of generality so that it can offer a general grey-box approach to model batch fermentation. The proposed model represents so far only the process identification step that plays an essential role in optimization, design and process control. A future development of this work could be the possibility to implement a hybrid neural network predictive control in which the model predicts process responses to potential control signals in such a way that proper control action can be undertaken to optimize future process performance.

References

Agarwal, M. (1997). Combining neural and conventional paradigms for modelling, prediction and control. Int. J. Syst. Sci., 28, 65-81.

Bailey, J.E., & Ollis, D.F. (1986). Biochemical Engineering Fundamentals. New York: McGraw-Hill Companies.

Box, G., Hunter, W., & Hunter, S. (1978). Statistics for Experimenters, An Introduction to Design, Data Analysis and Model Building. New York: John Wiley and Sons.

Demuth, H., & Beale, M. (2000). Neural Network Toolbox User's Guide. Natick: The MathWorks.

Feyo de Azevedo, S., Dahm, B., & Oliveira, F.R. (1997). Hybrid modelling of Biochemical Processes: A comparison with the conventional approach. Comput. Chem. Eng., 21, 751-756.

Gonzàles Siso, M. I. (1996). The biotechnological utilization of cheese whey: a review. Bioresour. Technol., 57, 1-11.

James, S., Legge, R., & Budman, H. (2002). Comparative study of black-box and hybrid estimation methods in fed-batch fermentation. J. Process Control, 12, 113-121.

Kahrs, O., & Marquardt, W. (2007). The validity domain of hybrid models and its application in process optimization. Chem. Eng. Process., 46, 1054-1066.

Klimasauskas, C.C. (1998). Hybrid modeling for robust nonlinear multivariable control. Isa Transactions, 37, 291-297.

Laursen, S. O., Webb, D., & Ramirez, W. F. (2007). Dynamic hybrid neural network model of an industrial fed-batch fermentation process to produce foreign protein. Comput. Chem. Eng., 31, 163-170.

Lubbert, A., & Jorgensen, S. B. (2001). Bioreactor performance: a more scientific approach for practice. J. Biotechnol., 85, 187-212.

Ozmihci, S., & Kargi, F. (2006). Utilization of cheese whey powder for ethanol fermentation: effects of operating parameters, Enzyme and Microbial Technol., 38, 711-718.

Ozmihci, S., & Kargi, F. (2007a). Kinetics of batch ethanol fermentation of cheese whey powder (CWP) solution as a function of substrate and yeast concentrations. Bioresour. Technol., 98, 2978-2984.

Ozmihci, S., & Kargi, F. (2007b). Effects of feed sugar concentration on continuous ethanol fermentation of cheese whey powder solution (CWP). Enzyme Microb. Technol., 41, 876-880.

Riedmiller, M. (1994). Advanced supervised learning in multi-layer perceptrons-From backpropagation to adaptive learning algorithms. Computer Standard & Interfaces, 15, 265-278.

Simutis, R., Dors, M., & Lubbert, A. (1995). Bioprocess optimization and control: Application of hybrid modelling. J. Biotechnol., 42, 285-290.

van Can, H.J.L., te brake, H.A.B., Dubbelman, S., Hellinga, C., Luyben, K. C. A. M., Heijnen, J. (1998) . Understanding and Applying the Extrapolation Properties of Serial Grey-Box models. AIChE J., 44, 1071-1089.

Zhang, G., Patuwo, B.E., Hu, M. J. (1998). Forecasting with Artificial Neural Network: the state of Art. Int. J. of Forecasting, 14, 35-62.

Zorzetto, L. F. M., Maciel Filho, R., & Wolf-Maciel, M.R. (2000). Process modelling development through artificial neural networks and hybrid models. Comput. Chem. Eng., 24, 1355-1360.

1.2 Paper 2: A comparison between different modeling techniques for the production of bio-ethanol from dairy industry wastes

The fermentation of Ricotta Cheese Whey was modeled by using different modeling techniques. In this paper, the performance of the HNM already presented in Paper 1, was compared with a) a pure neural model and b) a simple analytical model, which made use of properly defined yield factors to infer product and substrate concentrations. The three models were compared on the basis of the reliability of their predictions; actually, the HNMs provided the best results.

A comparison between different modeling techniques for the production of bio-ethanol from dairy industry wastes

Alessandra Saraceno, Sascha Sansonetti, Vincenza Calabrò, Gabriele Iorio, Stefano Curcio[2]

Department of Engineering Modeling-University of Calabria, via P. Bucci

cubo 42/A, Arcavacata di Rende 87036, Italy

Abstract

In the present work, the fermentation process aimed at obtaining bio-ethanol starting from ricotta cheese whey (RCW), a waste biomass rich in lactose, was simulated by both a pure neural network model (NM) and a multiple hybrid neural model (HNM). The simulation results showed that the developed HNM was capable of providing an accurate representation of the actual time evolution of lactose, ethanol and biomass concentrations even in conditions never exploited during model

[2] Corresponding author. Tel. +39 0984496711; fax: +39 0984494043.
E-mail: stefano.curcio@unical.it (S. Curcio)

development. HNM predictions indeed exhibited an average percentage error lower than 10%, as compared to the experimental data collected during RCW fermentation runs. The proposed methodology, leading to the formulation of a hybrid paradigm, may allow overcoming some of the inherent difficulties accompanying the development of reliable models that are called to describe the true behavior of biotechnological processes.

Keywords: Whey; Fermentation; Ethanol; Grey-box models; Artificial neural networks; Modelling.

1. Introduction

Fermentations are inherently un-steady state processes, usually performed as batch and fed-batch mode of operation. Significant variations of raw material properties and problems during bioreactor start-up are commonly observed and have to be tackled by proper control systems, which, therefore, are called to suppress the influence of external disturbances, to ensure the process stability and to optimize the process performance. The starting point for the implementation of any kind of automatic control is definitely represented by the availability of a predictive model of the process under study.

Most of the available models aimed at describing the fermentation process are based on the experimental measurement of extracellular metabolites concentrations, i.e. substrate(s), product(s) and biomass[1]. This modeling approach, however, is highly unstructured and precludes any interpretation of the actual cell physiology. The formulation of structured model, conversely, takes into account the microorganisms' metabolism and, therefore, the control and the regulatory mechanisms taking place in living cells, thus leading to a very complex reactions network, which requires a considerable computational effort[1,2]. Moreover, with the aim of validating a rigorous structured model, advanced analytical techniques are to be exploited so as to have an experimental evidence of the actual intracellular metabolism[1]. Lei et al.[4] developed a structured model for *Saccharomyces cerevisiae* focusing on both oxidative and oxido-reductive metabolism; on the basis of several assumptions regarding the abiotic and the biotic factors involved in the reaction , the authors defined a set of 12 reaction steps. For each of the steps a Michaelis Menten kinetics was assumed and, finally, 36 kinetics parameters were experimentally estimated. Garcıa-Ochoa et al.[5], developed a semi-structured model for xanthan production; the biomass growth was actually calculated by a not-structured model, namely a logistic function, but the product formation was described considering the cells metabolism, thus

leading to a final reaction mechanism that accounted also for intracellular species. In order to avoid any measurement of intracellular species, the assumption of a pseudo-steady state order for both ATP and Cofactor within the cell was formulated so as to identify three key-components, corresponding to each of the extracellular metabolites. From an accurate analysis of the available papers, it is evident that fully mechanistic models aimed at describing the fermentation process resulted in a series of complex reactions whose resolution either necessitates a set of simplifying hypotheses, which may not be applicable in several cases, or is too onerous and time consuming for practical purposes. An alternative approach to theoretical modeling was actually represented by black-box models (BBMs), which, however, do not make use of any transport equation that might help determining, on the basis of fundamental principles, the mutual relationships existing between the inputs and the outputs. Among BBMs, Artificial Neural Networks (ANNs) are noteworthy. ANNs are a data-driven method capable to learn from examples; no *a priori* knowledge of the process is therefore necessary for their definition. ANNs are composed of interconnected computational elements, called neurons; each neuron receives input signals from the related units, elaborates these stimuli by an activation function and, eventually, generates an output signal, which is transferred to other neurons.

A neural model is, generally, rather complicated, since it requires many different connections and, therefore, a great number of parameters to be estimated. Moreover, it is worthwhile observing that since extrapolation based on ANNs predictions is an unreliable procedure, it is often necessary to perform many different experiments in order to train the network in a range as wider as possible of significant situations[6]. Artificial neural networks allow reliably managing large sets of data and, generally, are capable of describing the actual input-output relationships even when trained with unreliable, missing or noisy data[7].

A reasonable trade-off between theoretical and empirical approaches is represented by hybrid modeling, leading to a so-called “grey-box” model, which allows predicting the behavior of complex systems in a more efficient way. Hybrid model predictions are indeed given as a combination of both theoretically based and “pure” neural network models, together concurring at the obtainment of system responses. The main advantage of a hybrid system is the possibility of describing some well-assessed phenomena by as simpler as possible theoretical relationships, leaving the analysis of other aspects, generally difficult to be interpreted, to rather straightforward neural models[8-11]. The neural network ability of properly managing unreliable or noisy data is strongly improved when it is inserted in a

hybrid structure. This is due to the theoretical part of the model that, among all the other tasks that it is called to accomplish, may perform as a filtering function that limits the error propagation throughout the system even when its inputs are perturbed.

When ANNs are utilized in a hybrid model, it is preliminary necessary to identify the respective domain of exploitation pertaining to either theoretical or empirical models in such a way as to decide which aspects of the process are to be described by a BBM and which ones by the fundamental relationships. Two kinds of HNMs can be generally defined depending on the interactions existing between the neural and the theoretical blocks. In a model based on a parallel architecture (Fig.1a), the inaccuracy in the predicted value from the fundamental part is minimized by the addition of the residuals calculated by the neural network[12]. In a model based on a serial architecture (Fig.1b) a process variable, which is difficult to measure, is estimated by a neural network and, then, fed as an input to the theoretical block[10].

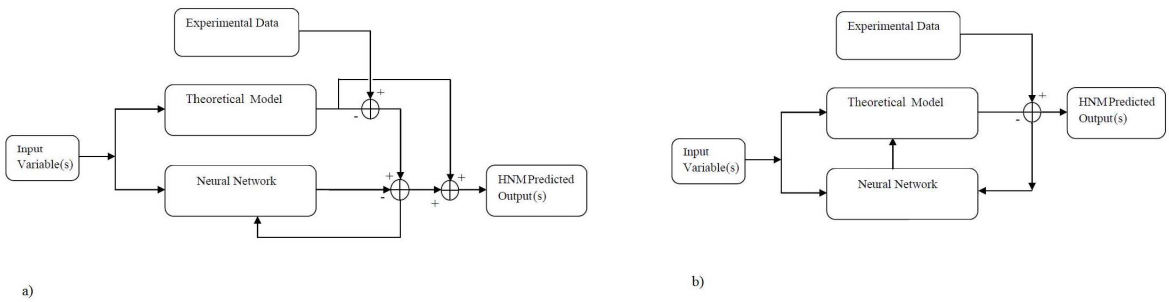

Fig. 1. HNM structures. a) Structure based on a parallel architecture; b) Structure based on a serial architecture

Even though hybrid neural models were, so far, not so common, the serial architecture was more popular in bioreactors modeling since it allows exploiting the ANN as an estimator of kinetic parameters[12-16].

Feyo de Azevedo et al.[3] compared the performance of hybrid and pure neural models in the case of Baker's yeast production achieved in a fed-batch fermenter. In their work, the theoretical part of hybrid model was represented by a mass balance equation written to describe the time evolution of biomass concentration, whereas the ANN part was appointed to determine the biomass specific growth rate on the basis of the calculated biomass concentration. James et al.[9] developed a grey-box soft-sensor in order to estimate biomass concentration during fed-batch fermentation of *Alcaligenes eutrophus*. Zorzetto et al.[17] proposed the application of two hybrid models to describe the batch fermentation of

beer. The first model, based on ANN, was formulated to determine the specific growth rate of biomass from temperature and substrate concentrations; the second one, based on the Monod's equation and on the predictions provided by the already-developed neural network, was used to calculate the dependence of model parameters on temperature.

The object of the present paper was to compare different paradigms aimed at modeling the batch fermentation of ricotta cheese whey (RCW), a high pollutant dairy waste, obtained as the main by-product in ricotta cheese production process[19]. RCW is mainly obtained in Italy but also in other countries belonging to the Mediterranean area. It is estimated that Italian production amounts to about 1.0 Mt of RCW per year, thus determining significant environmental problems related to its disposal[19]. Among all bio-fuels, bio-ethanol is definitely the most common. Nowadays, nearly all bio-ethanol, however, is obtained by fermentation of vegetable biomasses, essentially sugar cane and cereals, thus contributing to the observed increase of foodstuffs price. It is, therefore, necessary to identify alternative renewable and non-vegetable sources for bio-fuels production. RCW could potentially fit this requirement and may potentially represent an interesting fermentation substrate owing to its main characteristics, namely the relatively high content of lactose (5% w/w) that can be directly fermented to ethanol, and to its low cost, as determined by the fact that it is actually a waste[19-20]. The concentration profiles of lactose, of ethanol and of biomass characterizing the time evolution of RCW fermentation process were predicted both by a pure neural model and a multiple hybrid neural model, which was formulated accounting for the transient mass balance equations referred to the main components participating in the reaction. Finally, a simple analytical model composed by two kinetic equations was proposed to infer substrate and product concentration profiles directly from biomass predictions, as provided by the developed HNM. As compared to the studies already available in the literature, the novelty of this paper is represented by the development of a reliable multiple hybrid model, which allowed predicting the true behavior of a fermentation process aimed at the obtainment of a second-generation biofuel. It was intended, therefore, to show how the exploitation of process engineering tools and, particularly, of advanced modeling techniques represents a preliminary, fundamental step for any further investigation, e.g. process optimization, design of an efficient control system, about the process under study.

2. Materials and methods

Data-driven models are actually based on experimental data and are called to provide a reliable representation of the system behavior over an as wider as possible range of operating conditions. As a consequence, the utilization of well-assessed methods aimed at estimating the effects of process variables on system behavior is definitely essential when model identification is to be performed[21]. The experimental data necessary to develop the models whose performance was compared in the paper, were obtained from a set of anaerobic fermentations carried out on ricotta cheese whey. Each experimental run actually consisted of two subsequent steps: the inoculum culture preparation and the batch fermentation carried out in a stirred anaerobic bioreactor. *Kluyveromyces marxianus* (E.C. Hansen) Van der Walt *var. marxianus* (CBS 397) obtained from Centraalbureau Voor Schimmelcultures (Holland) was used in all the fermentation experiments. The inoculum culture was prepared adding a single yeast colony to 150 ml culture medium containing 50 g/l lactose, 10 g/l peptone, 5 g/l yeast extract (Fluka). The culture was kept at 37 °C for 12 hours in a 250 ml flask held in a temperature-controlled bath (OLS 200, Grant) with a roto-translational external mixing of 150 rpm.

During each fermentation test one liter of RCW was fermented in a 2 l batch fermenter (Z611020002, Applikon) equipped with temperature, pH, and rpm controllers (ADI 1030, Applikon). Two milliliters of fermentation broth were sampled every hour so as to measure the time evolution of ethanol and lactose concentrations. The analyses were performed injecting 20 μl of fermentation broth into a Jasco HPLC, equipped with a refractive index (RI 930, Jasco). The mobile phase was orto-phosphoric acid 1% (v/v) (Fluka), fed at a flow rate of 1 ml/min. The column was an Alltima Amino NH_2 (Alltech).

The time evolution of biomass concentration, instead, was measured by Bactoscan (Foss).The operating conditions and the process variables were chosen according to the factorial design method[22], on the basis of the indications obtained from both available literature information[23-24] and the results collected after a preliminary experimental analysis on RCW fermentation. In particular, temperature (T) ranged between 32 °C and 40 °C; pH was in the range 4-6; stirring rate (rpm) was varied between 100 and 300 rpm; lactose concentration (C^0_{lat}) was changed between 45 g/l and 90 g/l. As far as C^0_{lat} was concerned, it is worthwhile remarking that the chosen lower bound accounted for any possible lactose degradation due, for instance, to an improper storage of RCW; whereas, the chosen upper bound accounted for a possible pre-treatment of RCW aimed at increasing, for instance by ultrafiltration, the available lactose concentration. Actually, it should be observed that a higher

substrate concentration fed to the fermenter usually leads to a higher ethanol concentration in the stream flowing out the bioreactor. This determines a lower cost for ethanol purification and, therefore, an improved downstream processing. According to factorial design method, a total of 16 batch runs, lasting 18 hours each, was performed. With the aim of evaluating the performance of the developed models, an additional fermentation run (run N°17) was carried out under a set of operating conditions not belonging to that chosen to perform the experimental design. Tab.1 summarizes the conditions in which each experiment was performed. Considering that for each sample the concentration of lactose, of ethanol and of biomass was actually available, a total number of 969 experimental points was exploited to train, test and validate the performance of both the neural and the hybrid models developed in this paper.

Run N°	T [°C]	pH [-]	Agitation level [rpm]	C_{lat}^{0} [g/l]
1	40	6	300	90
2	40	4	100	90
3	32	6	300	45
4	40	6	100	45
5	32	6	100	90
6	32	4	300	90
7	40	4	300	45
8	32	4	100	45
9	40	4	100	45
10	40	6	300	45
11	40	4	300	90
12	32	6	100	45
13	32	4	300	45
14	32	4	100	90
15	40	6	100	90
16	32	6	300	90
17	37	5	300	50

Table 1. Batch fermentation operating conditions

3. Development of the models

3.1 Neural model development

In order to model the fermentation process of RCW, three neural networks, i.e. NM1, NM2 and NM3, aimed at predicting, respectively, the time evolution of lactose, ethanol and biomass concentrations, were developed.

To determine the networks structure, it was necessary to specify: a) the number of both input and output variables; b) the number of layer(s) composing the network; c) the number of neurons composing each layer; d) the activation function of each neuron. In the present case, all the proposed neural models were characterized by the same set of input variables: temperature (T), pH, reactor stirring rate (rpm), initial lactose concentration (C^0_{lat}) and reaction time (t). It was indeed observed that the above variables, among all the parameters that could affect the reaction progress, exhibited the highest influence on process performance. Each of the developed neural model had a single output, i.e. lactose, ethanol and biomass concentration, respectively, for NM1, NM2 and NM3. As far as the identification of neural networks architecture was concerned, both the number of hidden layers and the number of neurons comprised in each layer were determined according to a trial and error procedure, described in section 3.3.

3.2 Hybrid neural model development

The developed hybrid neural models consisted of a combination of a theoretical part, represented by a system of transient mass balance equations (Eqs.1) and of a rather simple neural model.

$$\begin{cases} \dfrac{dX}{dt} = \mu X \\ -\dfrac{dS}{dt} = qX \\ \dfrac{dP}{dt} = \mu_P X \end{cases} \tag{1}$$

where μ was the specific growth rate of biomass, q was the substrate consumption rate function and μ_p was the specific ethanol production rate. The theoretical model was aimed at predicting the concentrations of biomass (X), lactose (S) and ethanol (P), whereas the neural model was set up so as to estimate the parameters, μ, q *and* μ_p, necessary to determine the actual reactions rates.

Eqs.(1) were then approximated by the Euler's discretization and the discretized form was used recursively to determine the biomass, lactose and ethanol concentration values at the successive time step, $t+\Delta t$, on the basis of the knowledge already achieved at time t. The values of parameters μ, q *and* μ_p at time t, strictly necessary to solve the discretized form of the equations, were provided by three independent neural networks, namely HNM1, HNM2 and HNM3, estimating μ, q and μ_p, respectively.

The kinetic parameters were subsequently processed by some logic conditions (Eqs.2) that verified the physical reliability of networks outputs. In fact, it is expected that, during the fermentation runs, biomass and ethanol concentrations have to continuously grow, whereas lactose concentration has to monotonically decrease.

$$\begin{cases} if\ \ \mu < 0 \Rightarrow \mu = 0 \\ if\ \ q < 0 \Rightarrow q = 0 \\ if\ \ \mu_p < 0 \Rightarrow \mu_p = 0 \end{cases} \qquad (2)$$

The "filtered" values of parameters μ, q *and* μ_p were finally fed to the theoretical part of the hybrid model, thus allowing obtaining three "grey-box" models characterized by a serial architecture and having the general form shown in Fig. 2.

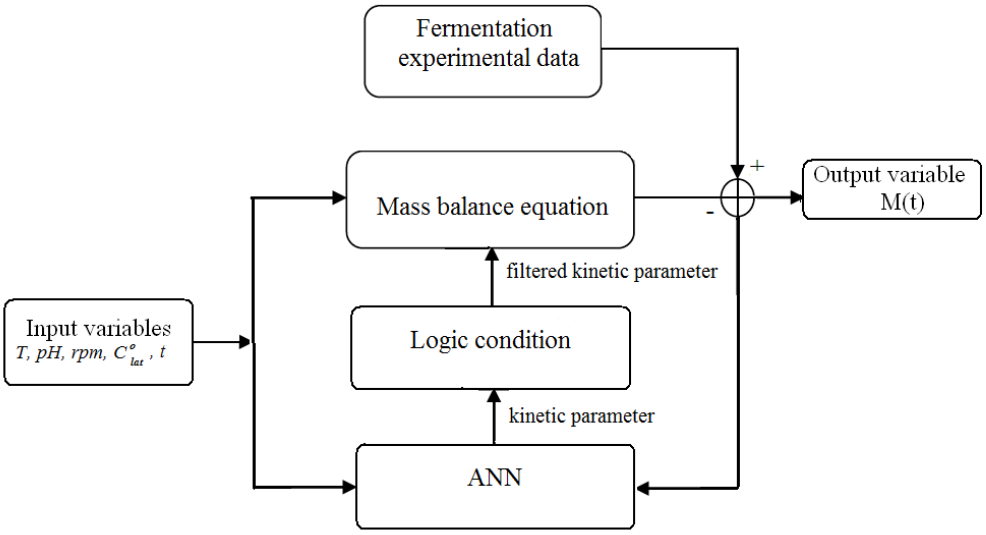

Fig.2. HNM general structure

The instantaneous value of biomass concentration was preliminarily estimated by HNM1. Then, the so-calculated *X(t)* was fed to HNM2 and HNM3 to determine, respectively, the time evolutions of both lactose and ethanol concentration. The choice of using the values of *X(t)* as given by the developed hybrid model, instead of the corresponding measured values, was aimed at testing the capability of the models to provide good simulation results, even if their inputs were bias affected.

3.3 Neural networks development

To identify the final architecture of both the pure neural models and the neural part of each HNMs, an iterative trial-and-error procedure was implemented in Matlab Neural Network Toolbox Ver. 4.0.1. The procedure was based on the definition of a performance index that allowed estimating the reliability of the simulation results. In the present paper, the percentage error, $\varepsilon\%$, between each value of concentration, C_p, as predicted by the model, and the corresponding measured value, C_m, was considered:

$$\varepsilon\% = \frac{\left|C_p - C_m\right|}{\min(C_p, C_m)} \cdot 100 \tag{3}$$

In particular, the convergence was considered to be achieved as soon as in a whole batch run the average value of ε % was lower than 10%. The implemented iterative procedure was schematically reported in Fig. 3, where i was the generic network layer and n_i was the number of neurons in the i^{th} layer.

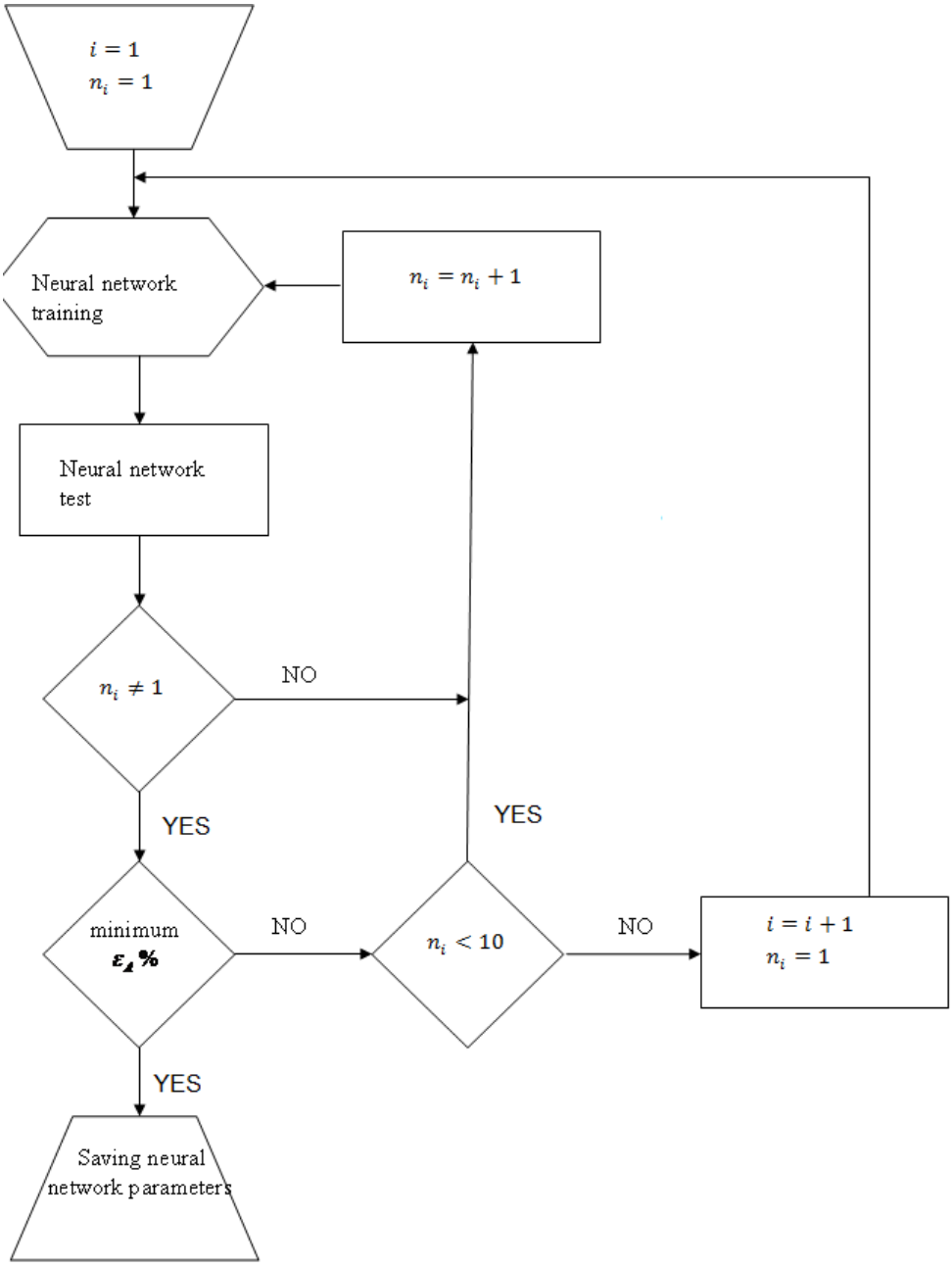

Fig. 3. Neural network realization procedure

As far as the pure neural model was concerned, only the concentration values collected during the batch fermentation experiments were actually exploited to train the networks; whereas for HNM development it was necessary to preliminarily determine the values of μ, q, μ_p by interpolating the collected experimental data. Of the considered 17 batch runs, 15 experiments were used to train and to

test the developed networks. The experimental data were randomly split into two groups, reserving 2/3 of data (570 points) to the training phase and the remaining 1/3 (285 points) to test neural networks predictions during their development. A multi-layer perceptron (MLP) feed-forward architecture was exploited to develop all the networks[8]; the networks weights and bias were estimated by the Levenberg-Marquardt algorithm with Bayesian regularization so as to avoid lengthy cross validation[25]. The neuron transfer function was chosen as the hyperbolic tangent for all the layers, except for the output layer where a linear transfer function was used; the choice of these transfer functions was actually supported by preliminary training tests.

On the basis of the above-described methodology, 6 neural networks were eventually obtained: 3 networks, actually represented the pure black-box models and 3 networks constituted the neural part of the developed HNMs. The predictions of each models were finally validated using two complete experiments (run N° 8 and run N° 17), corresponding to a total number of 114 points), which were never exploited either during the training or during the test phases. It is worthwhile remarking that run N° 17 was performed under a set of operating conditions not belonging to that defined by the experimental design.

3.4 Constant yields model

With the aim of strengthening the theoretical part of the proposed hybrid neural models, the possibility of inferring the concentration values of lactose and ethanol directly from the amount of biomass, as predicted by the hybrid model HNM1, was also evaluated. In particular, the substrate consumption rate, q, and the product growth rate, μ_p, of Eqs.1 were calculated by defining two yield coefficients, which were assumed constant throughout the fermentation progress. Actually, the assumption of constant yield factors was widely used to model biochemical reactors[26-29] and allowed obtaining two additional relationships having the following form:

$$\begin{cases} -\dfrac{dS}{dt} = \dfrac{1}{Y_{x/s}} \cdot \dfrac{dX}{dt} \\ \dfrac{dP}{dt} = Y_{p/s} \cdot \dfrac{1}{Y_{x/s}} \cdot \dfrac{dX}{dt} \end{cases} \quad with \quad \begin{cases} Y_{x/s} = \dfrac{\Delta X}{\Delta S} = \dfrac{X_{t=t_F} - X_{t=t_0}}{S_{t=t_0} - S_{t=t_F}} \\ Y_{P/S} = \dfrac{\Delta P}{\Delta S} = \dfrac{P_{t=t_F} - P_{t=t_0}}{S_{t=t_0} - S_{t=t_F}} \end{cases} \tag{4}$$

where $Y_{x/s}$ was the yield factor of biomass toward lactose, $Y_{p/s}$ was the yield factor of ethanol toward lactose, t_0 and t_F were the initial and the final time of biomass exponential growth rate, respectively. For each reaction run $Y_{x/s}$ and $Y_{p/s}$ were calculated as the arithmetic means of the experimental yield factors, as measured during the course of reaction.

This alternative approach to model substrate and product concentration profiles allowed replacing HNM2 and HNM3 with Eqs.4.

It is worthwhile observing that the proposed theoretical structure, although very common, is simpler than other available models, which allow a more precise description of the actual phenomena involved in fermentation at the expense, however, of a higher computational effort. The substitution of HNM2 and HNM3 with Eqs.4 has to be considered, according to authors' intention, as a way to reduce the black-box nature of the developed hybrid neural model, without significantly increasing the required computational effort. Any exploitation of more complicated theoretical model was far beyond the scopes of the present paper, which, instead, was aimed at proving that rather simple hybrid neural structures were capable of overcoming some of the inherent difficulties accompanying the rigorous modeling of biotechnological processes.

4. Results and discussion

Tab.2 summarizes the architecture of the networks developed according to the previously-described trial-and-error procedure.

Neural Network	Number of neurons 1st hidden layer	Number of neurons 2nd hidden layer	Number of neurons output layer
NM1	8	5	1
NM2	10	10	1
NM3	10	4	1
HNM1	6	5	1
HNM2	10	3	1
HNM3	10	2	1

Table 2. ANNs architecture

It can be observed that, due to the presence of the theoretical relationships as expressed by Eqs. 1, the architecture of the neural part of HNMs is simpler than that of the corresponding pure neural models.

Figs. 4a-4b show a comparison between the predictions provided by both pure neural model and hybrid neural model when the experimental points belong to the training/test dataset.

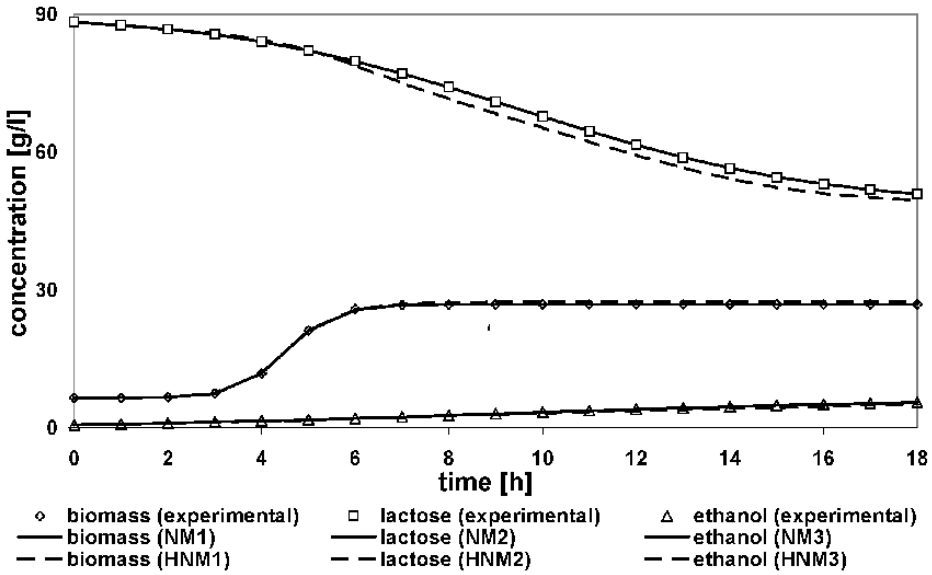

a)

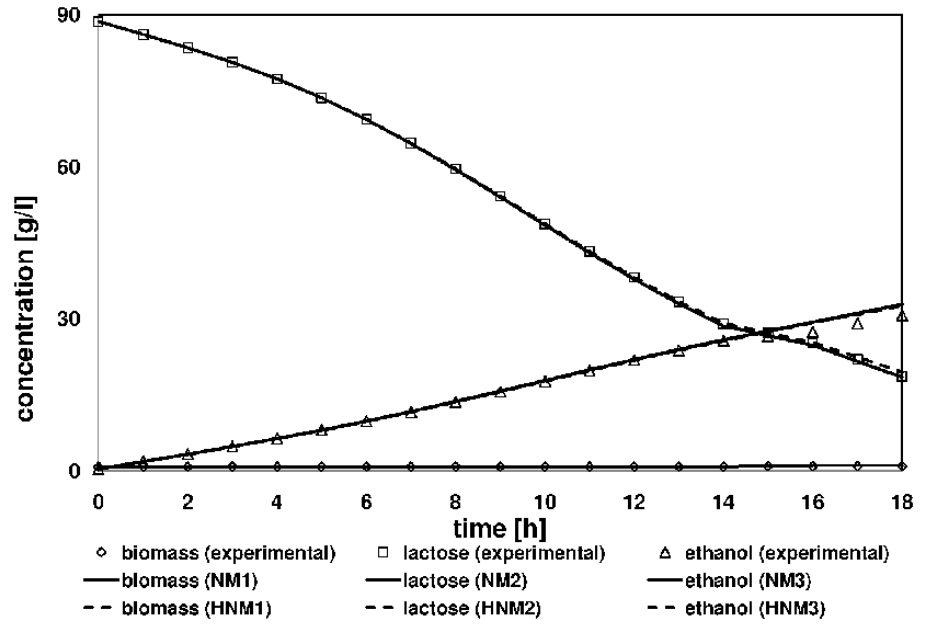

b)

Fig. 4. Predictions during training/test. a) run conditions: T=32°C, pH=6, rpm=100, C^0lat=90 g/l; b) run conditions: T=40°C, pH=4, rpm=100, C^0lat=90 g/l

In both cases, a remarkable agreement is actually observed throughout the considered time horizon. The average percentage error is much lower than 10% and both the models reproduce very well the actual time evolution of substrate, product and biomass concentrations measured during lab-scale fermentation performed on RCW. The performance of both the proposed models is very similar and the corresponding predictions tend to overlap.

Figs. 5a-5b show the behavior of both NMs and HNMs when they are called to reproduce the system behavior under a set of operating conditions never exploited before, thus performing the so-called model validation, e.g. a verification of the generalization capability of the models.

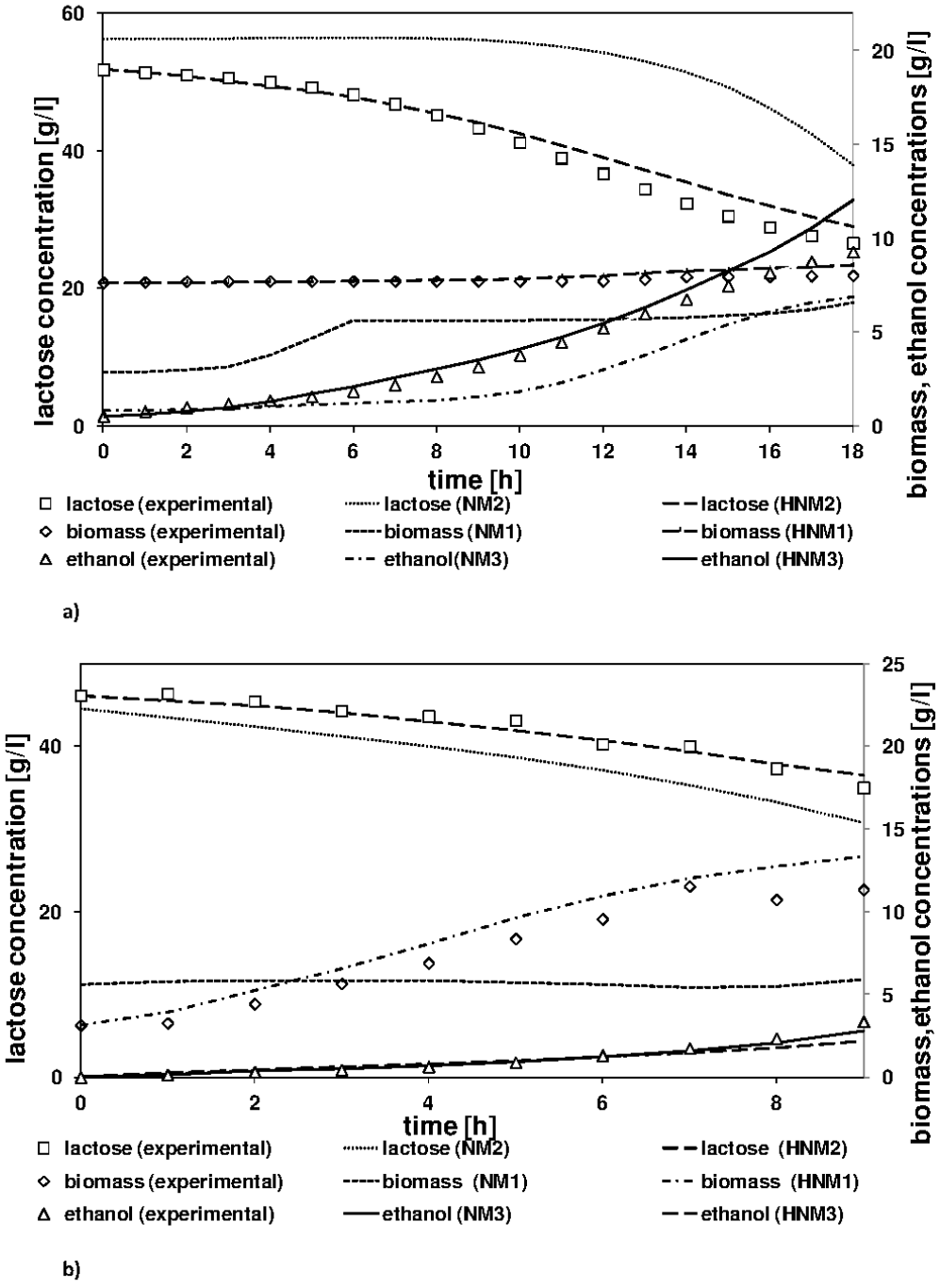

Fig. 5. Models validation. a) run conditions: T=32°C, pH=4, rpm=100, C^0lat =45 g/l ; b) run conditions: T=37°C, pH=5, rpm=300, C^0lat =50 g/l.

Actually, the predictions provided by NMs and HNMs are rather different; the hybrid models, in fact, performed very well in both the validation tests since the calculated values of percentage errors are comparable to those obtained during the training/test phases. These results indicate that hybrid models not only do recognize the training points, but the level of knowledge they have learnt during training allows them predicting the system behavior even when they are operated in unexploited conditions.

On the contrary, pure neural models fail to a large extent since their predictions, given as the time evolutions of biomass, lactose and ethanol concentrations, are characterized by an average percentage error of about 30%, with peak values, referred to lactose concentration (Fig.5a), as high as 60%. This result confirms that pure black-box models may provide reliable predictions strictly within their definition domain, whereas they become far less accurate when they are called to extrapolate.

Therefore, for the process under study, the combination of simple theoretical equations with straightforward neural models fairly widens the applicability of pure neural models even outside the training range, thus strengthening their performance. The theoretical part of HNMs, indeed, plays the role of filtering function with respect to the predictions of the neural part of HNMs, thus limiting the introduction and the propagation of errors, typical of a black-box model, and determining a significant improvement of model accuracy. This improvement is to be ascribed to the fact that the predicted kinetic constants are subsequently processed by the theoretical part of the model. This sequential transfer of signals, together with the chosen architecture, iteratively refines the estimation of the actual reaction rates. Therefore, also in conditions never exploited before, HNMs exhibit a higher reliability, as compared to a pure black-box models for which any prediction outside the training range definitely represents a mere extrapolation. Moreover, it is worthwhile remarking that the reported concentrations of both lactose and ethanol have been obtained using the estimation of biomass concentration, as provided by HNM1. The choice to feed HNM2 and HNM3 directly with the results provided by HNM1 instead with the actual experimental data, was actually aimed at testing the consistency of hybrid models predictions even if their inputs were bias affected.

After verifying the reliability of HNMs, the possibility of inferring lactose and ethanol concentration values, directly from HNM1 predictions by a set of properly defined yield factors, was also explored. The aim of this attempt was to strengthen the developed hybrid model by introducing two additional theoretical equations (Eqs. 4) that might replace the function of both HNM2 and HNM3, which, therefore, were dropped out. In other words, it was intended to verify the actual necessity of developing

HNM2 and HNM3, or, otherwise, if the prediction of lactose and ethanol concentrations could be calculated defining two yield coefficients that were actually assumed constant throughout the fermentation progress. Figs. 6a-b report a comparison, respectively for lactose and ethanol, between the predictions obtained by the present hybrid models and those calculated replacing HNM2 and HNM3 with Eqs. 4.

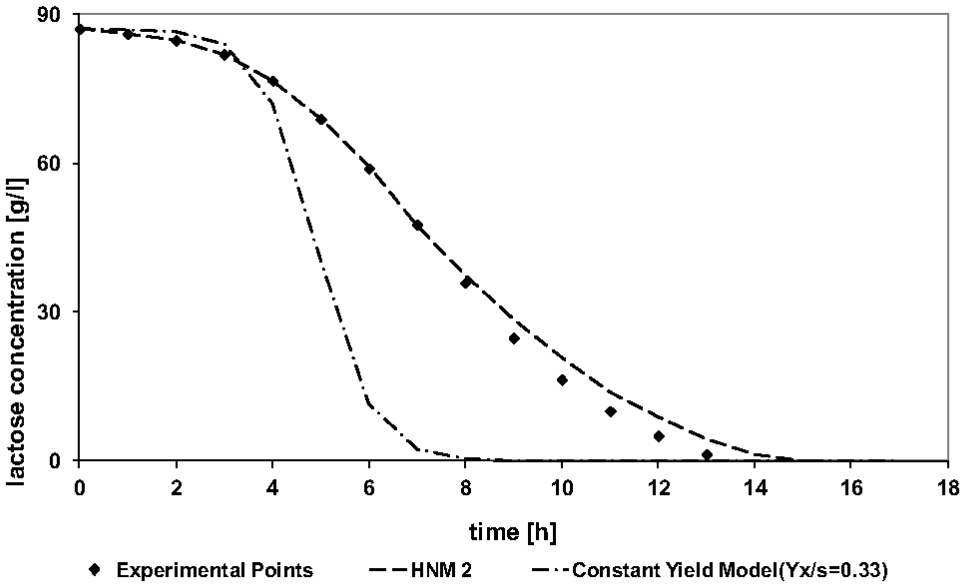

a)

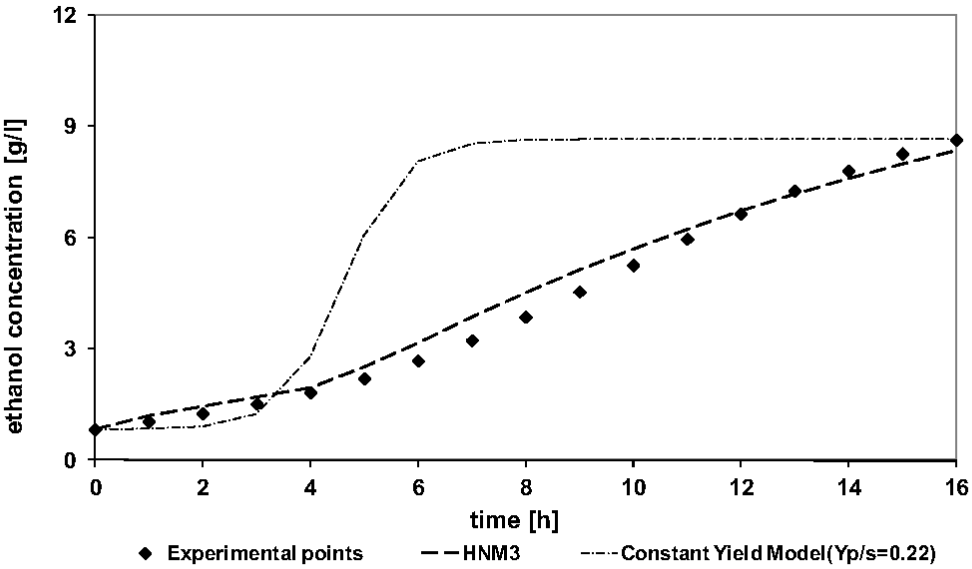

b)

Fig. 6. Yield factors models: a) comparison with HNM2 results; b) comparison with HNM3 results.

It can be observed that the assumption of constant yield factors, although widely exploited to describe the behavior of biochemical reactors, does not allow providing, in the present case, an accurate description of both lactose and ethanol concentration. This result can be interpreted observing that,

actually, for any given organism in any given medium there is no *a priori* certainty that yield factors keep constant during fermentation progress. It was, in fact, observed that variations of yield factor can be due to several phenomena, e.g. the assimilation into cell mass, the provision of energy for cell synthesis and the provision of energy for maintenance [26].

The possibility of exploiting Eqs. 4, therefore, has to be preliminarily verified depending on the characteristics of the particular reaction that is to be performed. In the present case, it was proved that the constant yield factors model, even if based on the same experimental data exploited to develop the hybrid neural models, was not applicable to predict the true time evolutions of lactose and ethanol concentrations on the basis of the sole knowledge of the amount of biomass formed during the fermentation progress.

5. Conclusions

In the present work a comparison among different modeling approaches aimed at predicting the behavior of RCW batch fermentation process was presented. The hybrid modeling approach showed better forecasting capability than the pure neural model proving that the proper coupling of the un-steady state mass

balance equations and of a neural model led to the definition of a very effective and versatile tool for the simulation of the process under study. The proposed hybrid approach could represent the basis to develop very robust and reliable models that might allow implementing either advanced control systems or novel optimization strategies particularly useful in biotechnological field.

References

1. Gombert, A.K., Nielsen, J., Current Opinion Biotech. 11(2000) 180.
2. Villanueva, M.A., Stuart, M.S., Jørgensen, S.B., Bioprocess Modelling for Learning Model Predictive Control (L-MPC), Computational Intelligence Techniques for Bioprocess Modelling, Supervision and Control, pp. 237-280, Springer-Verlag, Germany, 2009.
3. Feyo de Azevedo, S., Dahm, B., Oliveira, F.R., Comput. Chem. Eng. 21 (1997) 751.
4. Lei, F., Rotboll M., Joergensen S.B., J. of Biotech. 88 (2001) 205.
5. Garcia-Ochoa, F., Santos, V.E., Alcon A. Enz. Mic. Tech. 23 (1998) 75.
6. Zhang, G., Patuwo, B.E., Hu, M. J., Int. J. of Forecasting 14 (1998) 35.
7. Lee, E.W.M., Peng Lim, C., Yuen, R. K., Lo, S. M. IEEE Trans Syst Man Cybern 34 (2004).
8. Curcio, S., Aversa, M., Saraceno, A., Focus on Food Engineering, Nova Publishers, New York, 2010.
9. James, S., Legge, R., Budman, H., J Process. Control.12 (2002) 113.
10. Laursen, S. O, Webb, D., Ramirez, W. F., Comput. Chem. Eng. 31 (2007) 163.
11. Simutis, R., Dors, M., Lubbert, A., J. Biotechnol. 42 (1995) 285.
12. Kahrs, O., Marquardt, W. Chem. Eng. Process. 46 (2007) 1054.
13. Chen, L., Bernard, O., Bastin, G. and Angelow, P.,Control. Eng. Pract. 8 (2000) 821.
14. Agarwal, M., Int. J. Syst. Sci. 28 (1997) 65.
15. Klimasauskas, C.C., Isa Transactions 37 (1998) 291.
16. Van Can, H.J.L., Te brake, H. A.B., Dubbelman, S., Hellinga, C., Luyben, K. C. A. M., Heijnen, J., AIChE J. 44 (1998) 1071.
17. Zorzetto, L.F.M., Maciel Filho, R., Wolf-Maciel, M.R., Comput. Chem. Eng. 24 (2000) 1355.
18. Marwaha, S.S., Kennedy, J.F., Int. J. of Food. Sci. Technol. 23 (1988) 323.
19. Sansonetti, S., Curcio, S., Calabrò, V., Iorio, G., Biomass and Bioenerg. 12 (2009) 1687.
20. Sansonetti, S. G., Curcio, S., Calabro', V., Iorio, G., Chem. Eng. Trans. 20 (2010) 13.
21. Gregersen, L., Jorgensen, S.B., Chem. Eng. J. 75 (1999) 69.
22. Box, G., Hunter, W., Hunter, S., Statistics for Experimenters, an Introduction to Design, Data Analysis and Model Building, John Wiley and Sons, New York, 1978.
23. Ozmihci, S., Kargi, F.,. Bioresour. Technol. 98 (2007a) 2978.
24. Ozmihci, S., Kargi, F., Enzyme Microb. Technol. 41 (2007b) 876.

25. Demuth, H., Beale, M., Neural Network Toolbox User's Guide, The MathWorks, Natick, 2000.
26. Bailey, J.E., Ollis, D.F., Biochemical Engineering Fundamentals, McGraw-Hill Companies, New York, 1986.
27. Barba, D., Beolchini, F., Del Re, G., Di Giacomo, G., Vegliò, F., Process. Biochem. 36 (2001) 532.
28. Dochain, D., Perrier, M., Adv. in Biochem. Eng. 56 (1997) 149.
29. Luedeking, R., Piret, E.L., Biotechnol. and Bioeng. 67 (2000) 393.

1.3 Paper 3: Biodiesel production from waste oils by enzymatic trans-esterification: process modeling with hybrid neural model

In this paper a hybrid neural model was proposed to describe the kinetics of the trans-esterification of waste oils by lipase. A theoretical model previously developed by some of the authors of the present paper, was strongly improved by a properly trained neural network. The network was used to forecast the instantaneous value of product (ethyloleate) yield toward reactant (triglycerides) whereas, in the original version of the model, an empirical linear relationship was postulated between the concentrations of the two species. The reliability of the model predictions was testes on a real olive husk oil even if the model was built using experimental data obtained feeding the reactor with a simulating oil.

Biodiesel production from waste oils by enzymatic transesterification: process modeling with hybrid neural model

V. Calabro', S. Curcio, A. Saraceno, E. Ricca, M.G. De Paola , G. Iorio

Department of Engineering Modeling – University of Calabria

Via P. Bucci - Cubo 42/A - 87036 Arcavacata di Rende (CS) – ITALY

Abstract

In this paper an experimental and theoretical study of glycerides enzymatic trans-esterification aimedt biodiesel production has been performed.

The enzyme was Lipase from *Mucor Miehei*, immobilized on ionic exchange resin. This immobilized enzyme exhibited high catalytic specific surface and allowed an easy recover, regeneration and reutilization of the biocatalyst.

The source of glycerides was a simulating waste vegetable oil, i.e. a non-food competitive by-product, so as to reduce the pollution problems related to their treatment.

A mathematical hybrid model based on the combination both of a rigorous kinetic mechanism and of an Artificial Neural Network (ANN) has been formulated in order to determine the mutual relationships existing between the inputs, i.e. the feed composition and the most important operating conditions, and the outputs, i.e. the biodiesel composition and the reaction yield, of the process under study.

The developed hybrid model, therefore, incorporated both an *a priori* knowledge of the kinetics of enzymatic trans-esterification and an adaptive neural network aimed at identifying the difficult-to-model (uncertain) part of the process dynamics.

The effect of several process and operating conditions, i.e. the enzyme/substrate and the glycerides/alcohol feed mass ratios, the mixing rate and the medium of reaction, has been investigated in order to estimate the process performance. As compared to a previous study, the developed hybrid model exhibited more reliable predictions; its exploitation, in fact, could be extended well outside the range of the training data.

Keywords: Biodiesel, Lipase, Hybrid Neural Model (HNM), Kinetic, Artificial Neural Network ANN.

Introduction

Biodiesel is a mixture of alkyl esters and of fatty acids obtained from vegetal sources. As compared to petro-diesel, biodiesel shows a lower viscosity and it is less polluting as far as the production of CO_2 is concerned since it allows saving 2.4 – 3.2 kg of CO_2 per kg of fuel. Furthermore, it is biodegradable and, during the combustion, a reduced level of particulate, carbon monoxide and nitrogen oxides is produced.

Biodiesel can be produced from fatty acids of vegetal oils by catalytic or bio-catalytic trans-esterification of glycerides, performed in presence of short chain alcohols [1]. The transesterification reaction, i.e. the alcoholysis of triglyceride esters, results in a mixture of mono-alkyl esters and produces, as a byproduct, glycerol that has to be removed from the reaction mixture so as reduce the viscosity of the final product The transesterification process can be performed in different ways,

namely by an alkaline catalyst, by an acid catalyst or by a biocatalyst that could be entrapped in a proper support.

The enzymatic process offers some advantages, such as a higher yield and a better glycerol recovery, as well as the possibility of using, in the reaction mixture, free fatty acids oils that avoid the obtainment of saponification products [1-6]. Some additional advantages regard: a) the utilization of a rather low operating temperatures (up to 323 K); b) the re-esterification of free fatty acids achieved by lipase [7,8]; c) the absence of inhibition effects as determined by water; d) the rather high yield in esters that do not require a downstream purification process. If the enzymatic process is carried out, the improvement of enzyme thermal and mechanical stability is the most significant issue to profitably perform the process [7,8]. Research works actually focus on the identification of a proper immobilization technique as well as on the optimization of the reaction operating conditions. In both cases the kinetic mechanism of enzymatic transesterification should be understood [9].

The possibility to use waste or low quality vegetal oils in the biodiesel production represents a very interesting alternative since allows simultaneously achieving their valorisation and disposal .In a previous paper, [10] some of the authors of the present paper showed that transesterification, performed on two substrates by immobilized lipase, could reliably be described by a ping-pong bi-bi kinetic mechanism. The obtained theoretical predictions were indeed in good agreement with the experimental results. The kinetic analysis was carried out in order to investigate the effect of two key parameters, i.e. the reactants molar ratio and the enzyme/substrate ratio fed to a batch bioreactor. Another aspect not actually taken into consideration in the previous work was the water content of the reaction medium [9-13]. The possibility to perform the trans-esterification reaction even in presence of water is worthy of a detailed investigation since a real process aimed at biodiesel production could make use of either not anhydrous ethanol as a substrate or of low quality/reused vegetal oil that usually contain some amount of water. In another work [14], a factorial analysis was implemented to account for the mixing rate, the amount of enzyme and the reactants ratio fed to the bioreactor. The study was based on an experimental design and optimization aimed at understanding the effect of each significant parameters on the process performance, defined as either the final conversion or the final product concentration [15-16].

However, both the previous studies were based on some assumptions: the most important of which was the linear relationship, determined by analysing through a fitting procedure the whole set of

experimental data, existing between the reactants and the product concentrations [10]. A pure neural model actually does not make use of any transport equation that could help to determine, on the basis of fundamental principles, the mutual relationships existing between the inputs and the outputs of a definite process. ANNs, in fact, are data-driven models capable to learn from examples and represent a particularly useful tool when difficult-to-interpret phenomena are to be described. ANNs are composed of interconnected computational elements, called neurons or nodes. The neurons are combined so as to form one or more layers composing the network. In a multilayer network each neuron receives one or more inputs from other related units and, by means of an activation function, produces an output, i.e. a signal that is fed to the other nodes connected to it. To develop a neural model describing the behavior of a dynamic system it is preliminary necessary to perform the network training. This is generally achieved by the so-called supervised back-propagation learning technique, which is based on the knowledge of a reference output (target), represented - in most cases - by the experimental results obtained after a specific experimental protocol [17, 18]. Trained back-propagation networks are able to give reasonable responses when presented with inputs never exploited during the learning phase. This generalization property permits to train a network on a representative set of input/target pairs and get good results without training the network on all possible input/output couples. Many different artificial neural network structures were proposed but the most common was certainly the multi-layer perceptron (MLP). A MLP is composed by an input layer that receives the input information about the process, an output layer that produces the response(s) of the ANN and a certain number of hidden (intermediate) layers [19, 20]. The number of layers and the number of neurons in each layer is the result of a trial and error procedure whose convergence is achieved by minimizing a proper performance index.

One of the most interesting improvements of neural networks is, however, represented by the proper integration of theoretical and neural paradigms, thus realizing a so-called “grey-box” model (hybrid approach) usually capable of good performance in terms of both data interpolation and extrapolation. The main advantage of Hybrid Neural Models (HNMs) regards the possibility of describing some well-assessed phenomena by means of a theoretical approach, leaving the analysis of other aspects, more difficult to interpret and to describe in a fundamental way, to rather simple “cause-effect” models, such as neural networks [17-21]. The model resulting from the utilization of the hybrid neural paradigm allows to employ alternative and complementary source of knowledge, thus increasing model accuracy [22]; it is simpler, under a computational standpoint, than that provided by a fundamental theoretical approach; moreover, with reference to the pure black-box models, it gives the possibility to consider

one or more physical relationships that may help achieving a more precise knowledge of the actual system behaviour.

Starting from the results obtained in the above-described papers [10], where the actual influence of process and operating conditions on the bio-catalytic transesterification of waste oils was presented, it is intended in the present work to critically revise the methodology that brought the authors to assume a linear relationship between the reactants and the product concentrations. This is achieved by more accurate computational methods, which, based on Artificial Neural Networks, may allow estimating the complex relations existing between the process parameters and the true reaction pathway. In particular, it will be shown that hybrid neural approach can be successfully applied to model biotechnological processes and represents, in the case of bio-catalytic transesterification of oils, a powerful tool offering very precise predictions of the actual system behaviour over a wide range of process and operating conditions.

1.Kinetic and theoretical model

The reaction pattern of bio-catalytic transesterification of triolein in presence of ethanol was described in a previous paper as a sequence of three reactions in series, leading to the formation of one mole of ester for each step and the obtainment of glycerol only at the third step, when mono glycerides are actually converted, according to the following scheme [10].

$$\text{Triolein} + \text{Ethanol} \leftrightarrow \text{Diolein} + \text{EthylOleate}$$
$$\text{Diolein} + \text{Ethanol} \leftrightarrow \text{Monolein} + \text{EthylOleate}$$
$$\text{Monolein} + \text{Ethanol} \leftrightarrow \text{Glycerol} + \text{EthylOleate}$$

The proposed mechanism has been revised and simplified, considering triolein and ethanol as the substrates, ethyloleate, glycerol and the other glycerides (monolein and diolein) as the products. These glycerides are found, in fact, in the reaction mixture at the end of the bio-catalytic process. The complex kinetic mechanism was eventually described by a Ping-Pong Bi-Bi mechanism with ethanol inhibition and the King-Altman kinetics method, based on singling out geometrical rules that permits evaluating the concentrations of enzyme in all its complexes ([E], [e], [ES], [EP], etc.), was adopted.

By considering the actual rate of each elementary reaction, it was possible to formulate the overall kinetic rate equation, expressed as the disappearance of triolein [T], as follows:

$$-\frac{d[T]}{dt}=\frac{K_1[T][Et]-K_2[P][EO]}{K_3[T]+K_4[Et]+K_5[T][Et]+K_6[P]+K_7[EO]+K_8[P][EO]+K_9[T][P]+K_{10}[Et][EO]+K_{11}[Et]^2+K_{12}[Et][P]}\cdot[e_0] \quad (1)$$

where [T] represented the triolein concentration [mol/l]; [Et] was the ethanol concentration [mol/l]; [P] the overall concentration of glycerol, monolein and diolein [mol/l]; [EO] was the ethyloleate concentration [mol/l]; [e_0] the lipase concentration [g/l] K_i (i = 1..12) the kinetic constants to be estimated.

The analysis of the experimental data permitted simplifying the kinetic rate (eq. 1) as follows:

$$v_T=-\frac{d[T]}{dt}=\frac{\alpha\cdot[T]\cdot[Et]-\beta\cdot[P]\cdot[EO]}{[T]^2+\delta\cdot[T]+\varepsilon}\cdot[e_0] \quad (2)$$

where $\alpha,\beta,\delta,\varepsilon$, were kinetic constants, [T], [Et], [P], [EO] were triolein, ethanol, products (glycerides) and ethyleoleate concentration values, respectively.

A possible limitation of the above-described kinetic analysis is actually represented by the methodology adopted to express, on the basis of stoichiometry and semi-empirical correlations, the concentrations of products and ethanol as a function of triolein actual concentration [T] and of substrates initial concentrations [T_0] and [Et_0]:

$$\delta=\delta_1\cdot[Et_0]+\delta_0 \quad \varepsilon=\varepsilon_2^2\cdot[Et_0]^2+\varepsilon_1\cdot[Et_0]+\varepsilon_0 \quad (3)$$

$$[Et]=2.25\cdot([T]-[T_0])+[Et_0] \quad (4.a)$$

$$[EO]=-2.25\cdot([T]-[T_0]) \quad (4.b)$$

$$[P]=[T_0]-[T] \quad (4.c)$$

The linearity shown in Eqs.4a-4c, however, could be justified according to the following considerations: a) a highly specific 1, 3 lipase, as that exploited to perform the kinetic study, led to an ethyloleate/reacted triolein ratio of 2 to which an additional contribution of 0.25, due to acyl migration, is to be summed; b) the fitting of experimental data , as performed in the range of tested operating

conditions, was in good agreement with this assumption; c) the reliability of the predictions of the complete theoretical model, as given by Eqs. 2 and Eqs. 4a-4c, was demonstrated at different enzyme/substrate ratios and substrate/alcohol molar ratios as testified by the good agreement existing among predicted and experimental data.

In the present paper a completely different methodology aimed at determining the actual relationship existing among the concentrations of products and ethanol and the variables [T], [T_0] and [Et_0] is presented. The already-determined linear relationship between triolein and ethyl oleate, as provided by Eqs. 4a-4c, in principle, might not be accurately verified in some cases, especially when the concentrations of reactant(s) or of product(s) are low, i.e. at the beginning or at the end of the reaction. Product obtainment, in fact, exhibited in some circumstances an initial delay with reference to substrate consumption; a final decrease of product production rate as compared to substrate consumption rate was observed as well. An improper estimation of the actual substrate(s)-product(s) relationship, therefore, does lead to unfair predictions of the bio-catalytic reaction under study especially if it is considered that initial rate strongly affects the actual process dynamics, whereas the final values are critical when the reaction yield and the substrate conversion are to be calculated.

The methodology proposed in the present paper makes use of advanced computational models, based on Artificial Neural Networks, properly integrated with the already proposed kinetic mechanism so as to formulate an overall hybrid neural model, which is expected to provide more reliable predictions of the actual time-evolutions of substrate(s) and product(s) concentrations involved in the bio-catalytic transesterification process. It is worthwhile observing, however, that the validity of ping-pong bi-bi mechanism was definitely not in discussion; the simplified form expressed by Eq.2 will be hereafter exploited, since it permits reducing the model complexity, while ensuring an acceptable description of the overall system kinetics. In order to extend the validity of the approach proposed in the present paper, besides the already tested process and operating conditions [10, 14], the effect of both mixing conditions and medium composition has been elucidated as well.

Mixing rate in fact, plays a key role since it is responsible for the distribution of the enzyme in the reaction medium; actually, a low mixing rate would determine a non-homogeneous enzyme distribution and an increase of mass transfer resistances.

As regards the reaction medium, the attention was focussed to the utilization of hexane, as solvent; it is indeed expected a variation of the solubility of both alcohol and oil when the feed ratio hexane/triolein

is changed.

Furthermore, in order to allow a possible utilization on a pilot/industrial scale of either bioethanol or low quality oil, both presenting a certain amount of water, the effect of H_2O concentration was analysed too.

2.Hybrid neural model development

The inherent limitation of the previous theoretical model (TM) was the identification of an empirical linear correlation, obtained by interpolating the experimental data collected in specific operating conditions, existing between the instantaneous product concentration [EO] and the substrate instantaneous concentration [T]. However, some criticisms can be raised towards the previous approach: a) it was assumed that the instantaneous product concentration depended only on the instantaneous substrate concentration; therefore, the product yield did not depend on to the reaction operating conditions and on the feed ratios; b) an average best fitting coefficient, relating substrate and product concentrations was chosen to describe all the experimental runs used during model development; of course the selected value did not actually correspond to the best fitting coefficient for each experimental run; c) the chosen correlation, even if it provided rather good reproduction of the experimental data that allowed its determination, was characterized by a restricted validity domain and did not permit any extrapolation outside the range of tested operating conditions.

With the aim of widening the validity domain of the previously proposed TM, a hybrid neural model (HNM) was therefore developed.

With reference to the process at hand, the reaction mechanism and the relative kinetic equation were determined using a rigorous theoretical approach whereas the relation existing between substrate and product concentrations was determined on the basis of an Artificial Neural Network, properly trained by the experimental data obtained over a wide range of process and operating conditions. The theoretical part of the proposed HNM preserved the simplified kinetic equation proposed during TM development (Eq.2), but a neural network was exploited to predict ethyloleate concentration on the basis of both the substrate concentration values and the reaction operating conditions.

The [EO] concentration value was provided by the neural network whereas ethanol and reaction product concentration, [Et] and [P] respectively, were calculated as follows:

$$[P] = [T_0] - [T] \tag{4.c}$$

$$[Et] = [Et_0] - [EO] \quad (5)$$

After specifying the theoretical part of the model, the neural network input-output structure was determined. The neural network objective was to predict the product concentration: consequently the realized network was characterized by a single output variable, the Ethyloleate formation, expressed in terms of the concentration difference ([EO(t)]-[EO_0]).

In order to predict the neural network output variable, a set of significant input variables were considered on the basis of sensitivity analysis performed of the bio-catalytic process under study:

1) enzyme/triolein initial mass ratio ([e_0]/[t_0]);

2) ethanol/triolein initial molar ratio ([Et_0]/[T_0]);

3) initial water content of the reaction mixture ([W_0]);

4) agitation rate of the reactor (rpm);

5) triolein/hexane initial ratio ([T_0]/[Ex_0]);

6) triolein consumption, expressed in terms of concentration ([T_0]-[T(t)]).

These variables, among all the others that could affect the reaction progress, exhibited the highest influence on product formation.

The input-output structure of the HNM is synthesized in Fig.1.

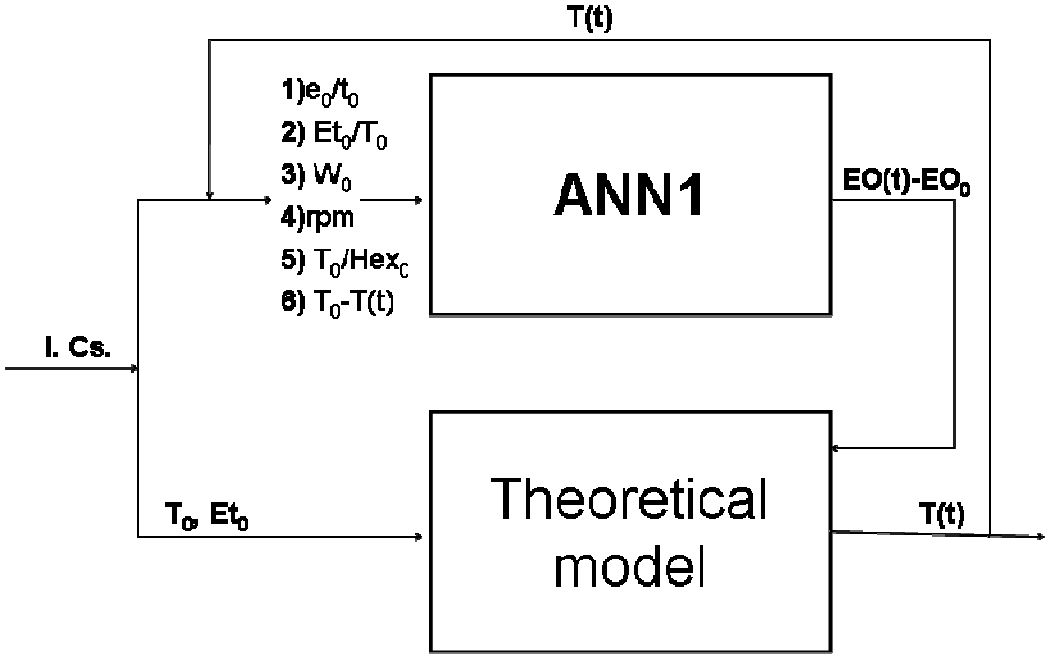

Figure 1. Input output structure of the HNM

The realized HNM is characterized by a parallel structure since a continuous recycle of a signal exists between the theoretical and neural parts of the model.

After specifying the input-output structure of the model, the neural network architecture was defined and the training procedure set-up. Considering the available set of experimental data that will be described in the following section, the experimental runs were split in two groups reserving 2/3 of reaction runs (runs n° 3-4-5-6-8-9), corresponding to 88 experimental points, to the training/test phases of the neural networks; the remaining 3 runs (runs n° 1-2-7), corresponding to 50 points, were used to validate the predictions of the developed ANN in a set of conditions never exploited neither during learning, nor during test.

A multi-layer perceptron (MLP) feed-forward architecture with a pyramidal structure having a decreasing number of neurons from the input to the output layer, was identified by Matlab Neural Network Toolbox (The Mathworks), Ver. 4.0.1. For the training of each tested network, by means of estimation of their weights and biases, the Bayesian regularization, which allows a significant improvement of ANN generalization, was used [24]. The neuron transfer function was a hyperbolic tangent for both input and hidden layers, whereas a linear transfer function was chosen for the output layer.

The choice of the "best" network architecture was achieved by a trial-and-error procedure, as suggested in the literature [25-28]; the number of both the hidden layers and the neurons belonging to each layer were determined through iterative cycles.

It was supposed that the convergence was achieved when, during the test/training phase, the percentage average error (calculated on the basis of the whole training/test dataset, eq. 6) between the predictions of neural model and the corresponding experimental points reached a minimum, set equal to 10%.

$$\left(\varepsilon_A\% = \frac{\left| EO(t)_{EXP} - EO(t)_{ANN} \right|}{EO(t)_{EXP}} \cdot 100 \right) \tag{6}$$

On the basis of the above-described iterative procedure a neural model, ANN, was eventually developed; it consisted of the following structure (Fig. 2):

- An input layer with 6 neurons;
- A first hidden layer with 10 neurons;

- A second hidden layer with 3 neurons:
- A single neuron output layer.

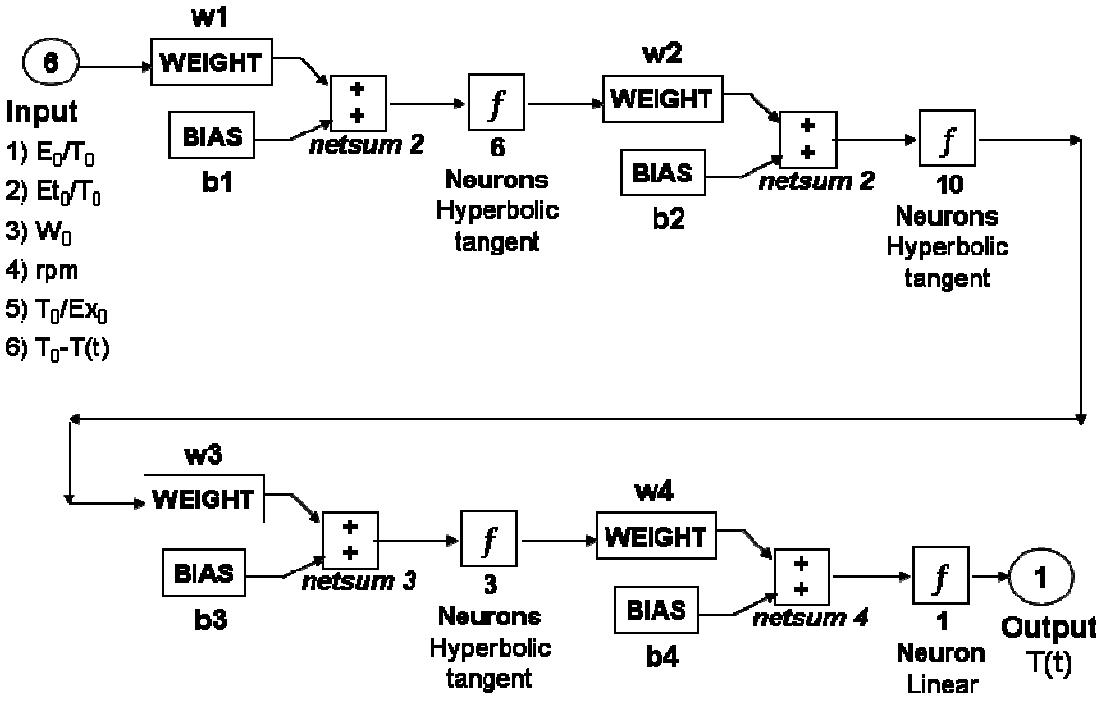

Figure 2. ANN1 structure

3.Materials and methods

Reactants

Simulating oil, having a 60% (w/w) of pure triolein, was used to perform the kinetic analysis. The remaining 40% of the mixture included fatty acid or mono and di-glycerides. To validate the model with a different substrate from the simulating oil, a single experimental run was conducted using very low quality olive husk oil whose composition in triolein (most relevant triglycerides in the husk oil) was equal to 60%.

Ethanol (99.8% grade) from Fluka was used as the secondary substrate; hexane (95% grade) from Fluka was the solvent, as suggested in the Literature [29]. Distillate water was employed to perform the tests in not anhydrous conditions.

HPLC grade acetone and acetonitrile, exploited for the analysis of samples, were supplied by Fluka.

Biocatalyst

The catalyst was Lipozyme_ MM IM (Novozymes, Denmark), a lipase from *Mucor miehei* immobilised on a macroporous particulate ion exchange resin. The diameter of the supporting particles ranged between 0.3 and 1.0 mm and their wet bulk density was 0.42 g/ml. The enzyme was highly 1,3 specific, with a Molecular Weight of 32 KDa and an activity of 37 U/g.

Experimental protocol

All the experiments were performed at an operating temperature of 37 °C and neutral pH by. a well mixed batch reactor having a volume of 125 ml. The reaction mixture was prepared according to the procedure reported in [10], so as to guarantee good mixing conditions.

Reaction samples of 200 μl were collected following the procedure reported in [10], ensuring not to have any catalyst in the sample and avoiding that the total amount of collected samples was 5% greater than the total volume.

The mass ratios enzyme/triolein [e_0/t_0] fed to the bioreactor were 1:8, 1:20, 1:30, the reactants molar ratios ethanol/triolein [Et_0/T_0] were 2:1, 2.5:1, 3:1, in anhydrous conditions and with simulating triolein/hexane feed mass ratio fixed to 1.4 (that corresponds to a molar ratio [Hex_0/T_0] =1.2). The feed volumetric ratio simulating oil with 60% triolein/hexane was 1:1; 4:1; 1:2, that corresponded to a mass feed ratio [s_0/hex_0] of 1.4, 5.61 and 0.7.

In order to verify the possibility of recovering and reusing the enzyme after the reaction runs, a proper procedure was followed. After a first reaction run conducted with fresh enzyme, the enzyme was recovered by filtration, washed three times with acetone, then dried at room temperature and reused for a new reaction run (Soumanou, 2003). The recovery/reuse procedure was conducted in two subsequent reaction runs.

As compared to the experimental data reported in [10], a new set of tests was performed in order to widen the applicability of the present methodology based on hybrid neural modelling and to improve the accuracy of the kinetic analysis.

In particular, some tests were carried out with 1 g of water, corresponding to a molar ratio water/ethanol [W_0]/[Et_0] equal to 1; whereas, the effect of stirring rate was ascertained using a twofold higher, as compared to the procedure reported in [10] stirring rate or even the absence of any mixing. Finally, with the aim to evaluate hybrid neural model performance if a real feedstock with impurities is fed to the reactor, a single experimental run was conducted using olive husk oil as a substrate. Tab.1 summarizes all the tested experimental conditions.

Run N°	Enzyme type	Oil type	$[e_0]/[t_0]$ [g/g]	$[Et_0]/[T_0]$ [moles/moles]	w_0 [g/l]	Stirring rate [-]	$[t_0/0.6]/[Hex_0]$ or $[s_0]/[Hex_0]$
1	Fresh	Simulating	1 : 8	2 : 1	1.0	1	1.4
2	Fresh	Simulating	1 : 8	2 : 1	0	1	1.4
3	Fresh	Simulating	1 : 8	2 : 1	0	2	1.4
4	Fresh	Simulating	1 : 8	2 : 1	0	0	1.4
5	Fresh	Simulating	1 : 8	2 : 1	0	1	5.61
6	Fresh	Simulating	1 : 20	2 : 1	0	1	1.4
7	Fresh	Simulating	1 : 20	2.5 : 1	0	1	1.4
8	Fresh	Simulating	1 : 20	3 : 1	0	1	1.4
9	Fresh	Simulating	1: 4	2 : 1	0	1	0.69
10	Reused (1^{st}cycle)	Simulating	1 : 8	2 : 1	0	1	1.4
11	Reused (2^{nd}cycle)	Simulating	1 : 8	2 : 1	0	1	1.4
12	Fresh	Husk oil	1 : 8	2 : 1	0	1	1.4

*$[s_0]$ represents the mass concentration of triolein simulating oil where pure triolein, named $[t_0]$ in [g/l], is at 60%.

Table 1. Set of experimental conditions and set of variables input of ANN1

Analytical methods

Concentrations of reactants, e.g. glycerides, and of product, i.e. ethyloleate, were quantitatively measured by a high performance liquid chromatography, HPLC (JASCO) under the following conditions: RI detector, eluent phase composition: acetone/acetonitrile 70/30 v/v, flow rate 1 ml/min, internal normalization as integration method. Prior to each analysis both the catalyst and the hexane were removed by centrifugation and by evaporation, respectively. Ethanol concentrations were not directly measured, but obtained assuming a 1:1 stoichiometric ratio with ethyl-oleate.

The utilized HLPC column was Alltech Adsorbosphere HS (C18) 5 μm, having a length of 250 mm

and an inlet diameter 4.6 mm; the column was provided with a 7.5 x 4.6 mm Alltech pre-column

4.Results and discussion

Experimental data have been elaborated to evaluate the kinetic rate as a function of triolein concentration as reported in the eq.2. The analysis of experimental data permits to approximate the concentration of products and ethanol as function of triolein actual concentration [T] and substrates initial concentrations [T_0] and [Et_0].

The experimental data of produced ethyl-oleate ([EO(t)]-[EO_0] = [EO]) vs. triolein consumption ([T_0]-[T]) were reported for each experiment carried out, in order to investigated the effect of each operating conditions on the neural network.

The results have been compared with those obtained in the previous model, where relationship was found linear with a coefficient equal to 2.25, as described by eq. 4.a and 4.b.

On the basis of the previous discussion, a neural network model (ANN1) and a multiple hybrid neural model HNM were realized.

Main objective of the neural network model ANN1 was to investigate about the relationship between the triolein consumption and Ethyl Oleate production. ANN1 was realised by using a random selection of the experimental data under different operating conditions, i.e. both the experimental data obtained in the present paper and those reported in literature [10]. Purpose of this analysis was to make a comparison between the two different approaches.

The results show how a neural model does not just learn in order to recognize the training points; instead, it is also able to predict the system behaviour even when it is operated in conditions unexploited during training phase.

On the basis of the ANN1 a preliminary comparison between experimental results and theoretical data, predicted with above theoretical TM and ANN1 models, was carried out. Such comparison has been carried out with all the results previously obtained in [10] as well as with the new ones: some of the results obtained have been shown in the Fig. 3, 4, 5.

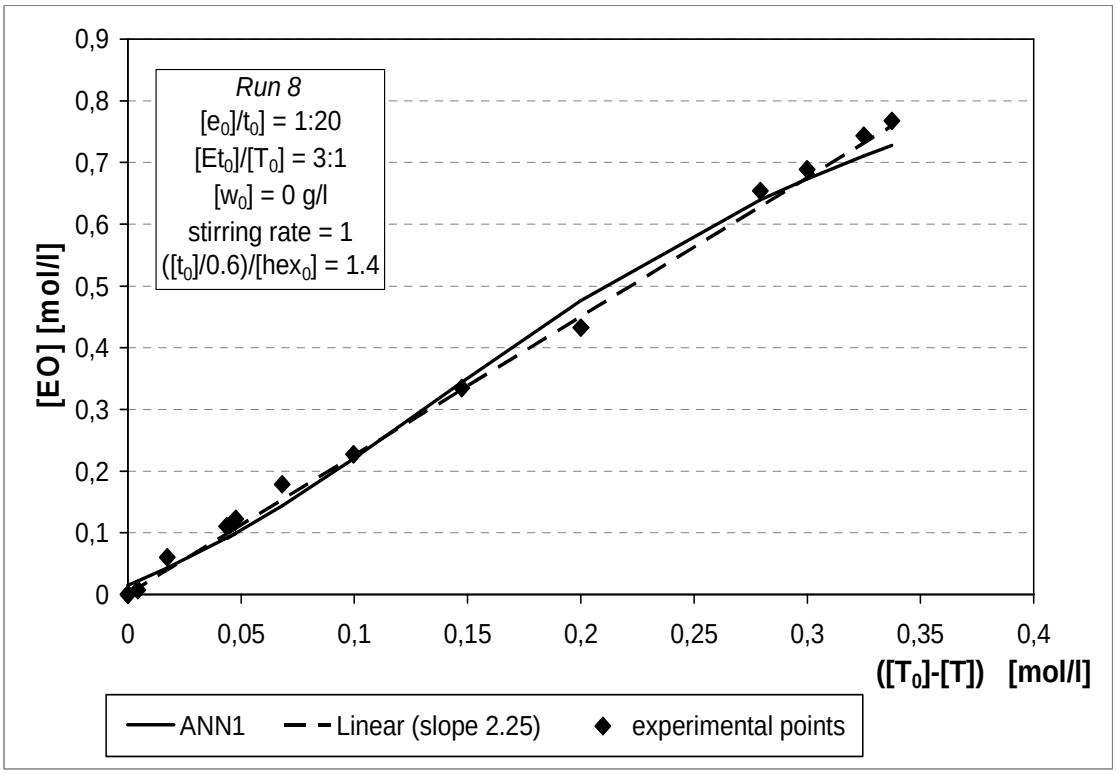

Figure 3. Comparison between experimental data, predictions with ANN1 and linear empirical correlation ([EO]=2.25*([T_0]-[T]), for the determination of the relationship between ethyl-oleate production and triolein consumption. Operating conditions as run 8 of table 1.

In Fig. 3 is reported an experimental run belonging to the previous paper, where operating conditions are corresponding to the run n° 8 that represents the typical results observed when the ANN1 has been applied to the experiments already reported in literature [10]. As it is possible to appreciate from the figure, experimental results show a linear behaviour, as evidenced with the TM and as well fit also by the ANN1.

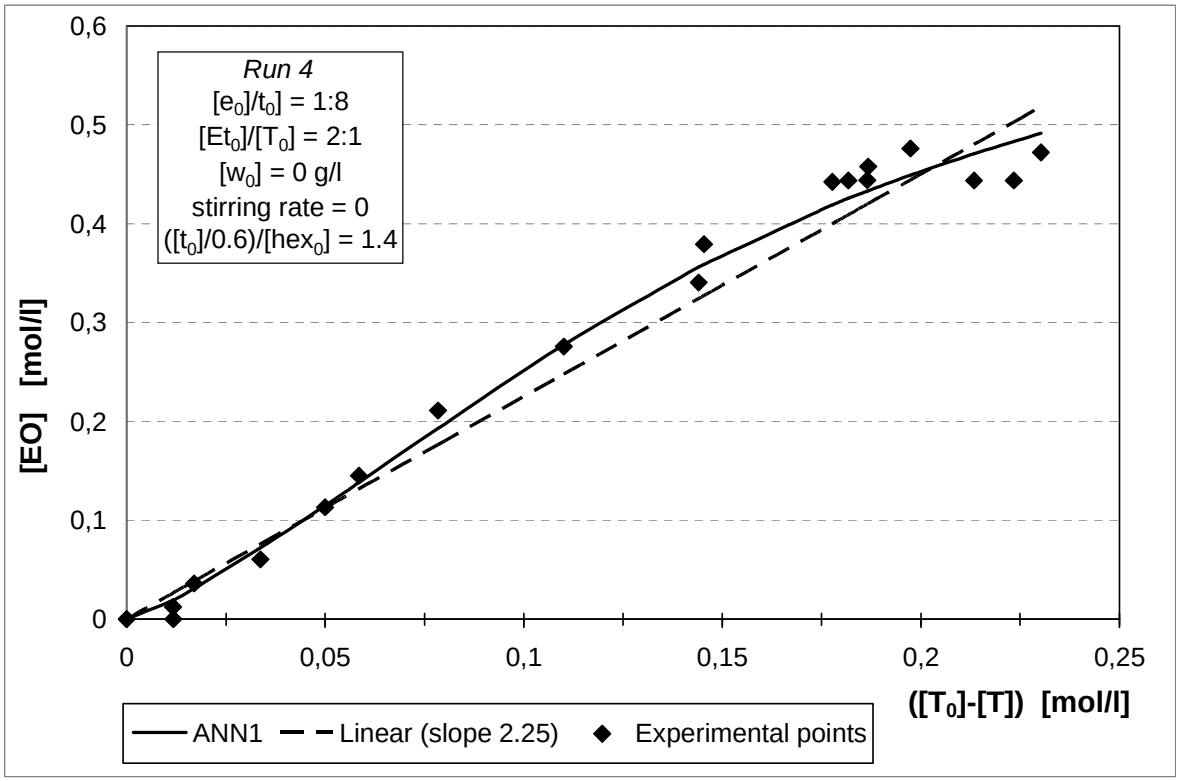

Figure 4. Comparison between experimental data, prediction with ANN1 and linear empirical correlation ([EO]=2.25*([T_0]-[T]), for the determination of the relationship between ethyloleate production and triolein consumption. Operating conditions as run 4 of table 1.

Fig, 4 and 5 are relative to the new data obtained and reported in the present paper. Fig. 4 is relative to the case where no stirring is carried out, at the operating conditions corresponding to run n° 4. Unlike the previous fig. 3, experimental data do not exhibit a definite linear behaviour, especially at the end of the reaction. As a consequence, the TM model, based only on a general linear equation with just one single coefficient, fails in well reproducing the experimental data. The ANN1, instead well fit all the set of experimental data.

This aspect is more evident in the next Fig. 5 relative to the run n° 5, where a different triolein/hexane ratio has been used.

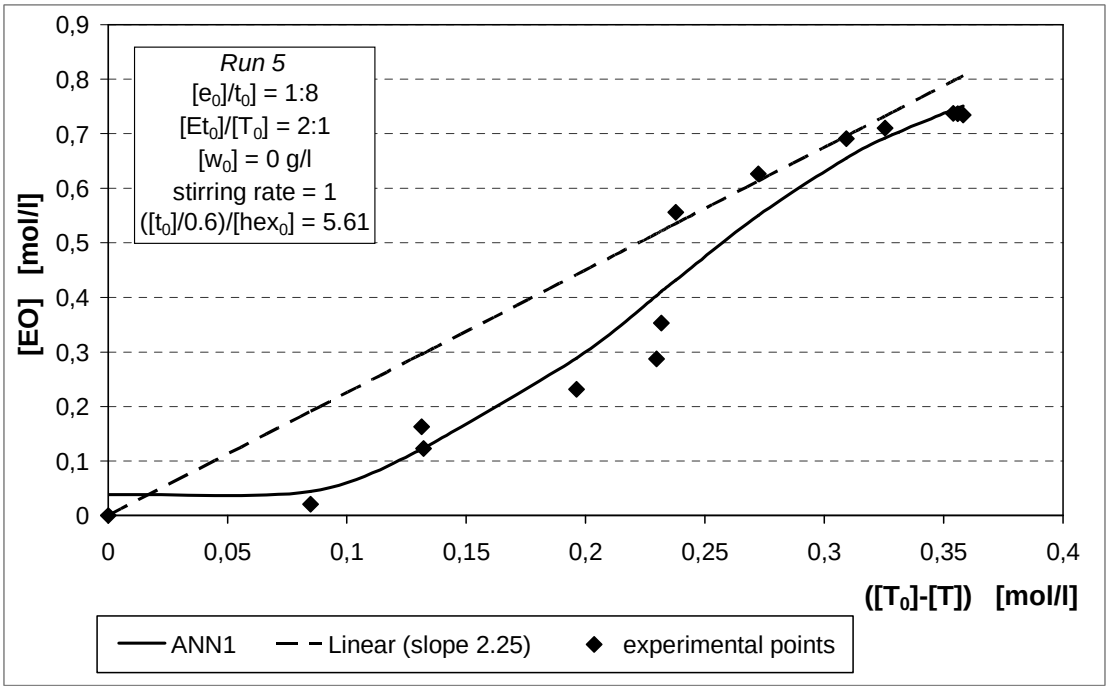

Figure 5. Comparison between experimental data, prediction with ANN1 and linear empirical correlation ([EO]=2.25*([T_0]-[T]), for the determination of the relationship between ethyloleate production and triolein consumption. Operating conditions as run 5 of table 1.

In this case a sigmoidal behaviour is observed and catched from the ANN1 where, instead linear prediction of TM is failing.

The deviation from linearity of experimental data might attributed to a relevant influence of the different conditions that have been applied: in particular the run n° 5, reported in fig. 5, is relative to a different solubility conditions due to the low amount of hexane in the reaction medium: in this case ethanol might affect enzyme stability, reducing its catalytic activity. By the same way data of Fig. 4, run n°4 without stirring, are affected by a not optimal enzyme distribution in the system.

It is evident that ANN1 is more able to understand the system behaviour when tested with experimental point that cannot be well fit with the simple linear relationship, eq. 4, as reported in the previous paper.

A general comment to the simulation results reported in Fig.3-5 can be stated. These figures testify how the proposed ANN1 is capable to describe with a remarkable agreement the relation existing between the triolein and ethyloleate concentrations in different operating conditions. ANN1 is actually able to predict the system behaviour both when experimental data are characterized by a linear behaviour and both when a significant deviation from linearity can be observed. On the other side,

the linear relation between substrate and ethanol concentration, that was proposed in a previous paper [14], even if well predicting system behaviour in specific operating condition, can not be considered a general relation applicable in all the operating conditions reported in Table.1. After conducting this comparison, we can conclude that the ANN1, using the run operating conditions as input variables, is capable to widen the applicability domain of the proposed kinetic model, being capable to adequately predict the system behaviour even with other operating variables are taken into considerations (water content, mixing rate, triolein /hexane feed ratio).

After validating the neural part of the model, the realized HHM was used in order to predict the system behaviour in terms of products and reagents concentration profiles.

As mentioned in HNM development paragraph, the kinetic model proposed, composed by the kinetic equation and the neural network, was tested on a batch reactor mass balance equation written with reference to triolein. The results obtained are reported in the following Fig 6-9.

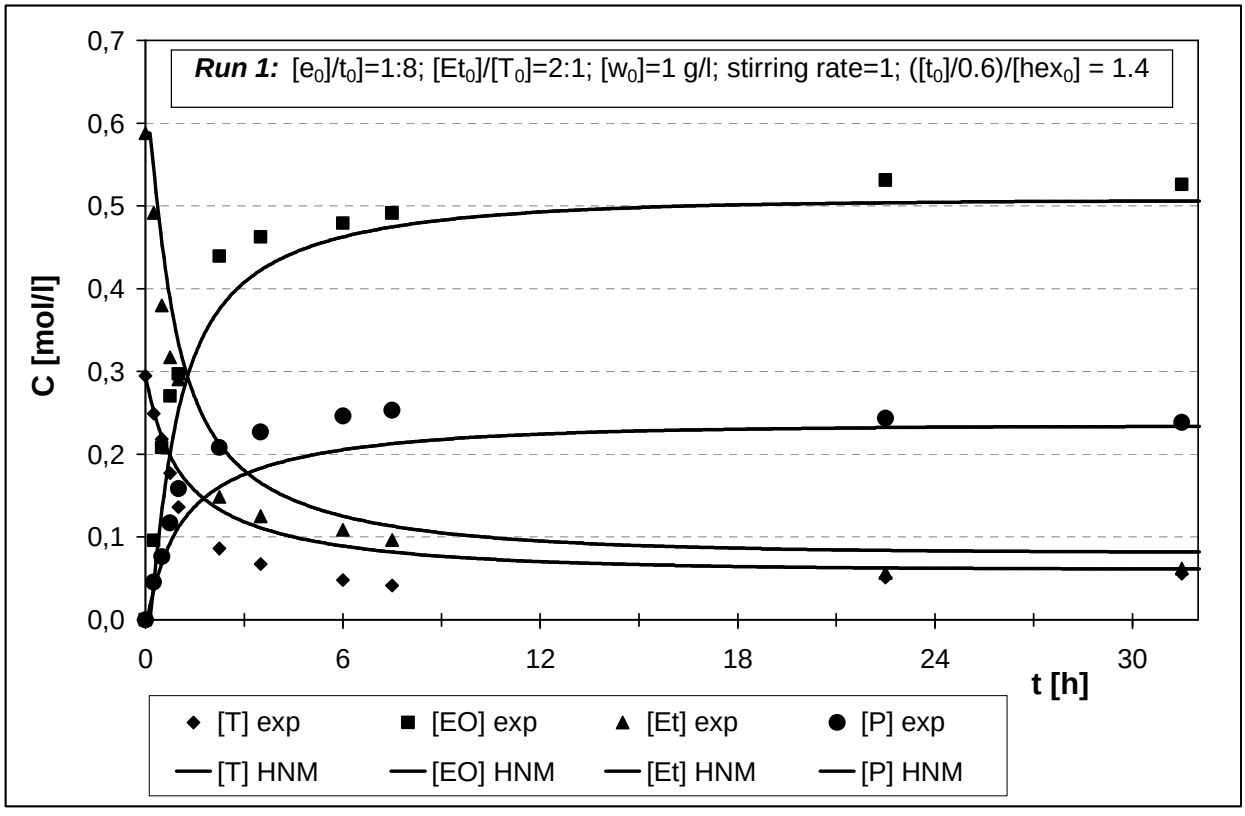

Figure 6. Comparison between experimental data and predicted value with Hybrid Neural Model, HNM. Operating conditions as run 1of table 1.

Fig. 6 reports the experimental data and the simulation results relative to run n° 1. This experimental run, belonging to the new experiments datasets, is the only one run conducted in not anhydrous conditions. Observing Fig. 6 it should be noted that a significant agreement exists between experimental points and the simulation results: the HNM is in particular, capable to predict the product and substrate plateau value with a remarkable agreement. It should be noted that, due to the ANN1 structure, the HNM is capable to take into consideration the not anhydrous conditions of the present experimental run thus amplifying the spectrum of the operating conditions that can be exploited by the model. This represents a strong improvement with reference to the TM that was not capable to distinguish two experimental runs characterized by a different water content, since this variable was not taken into consideration during TM development.

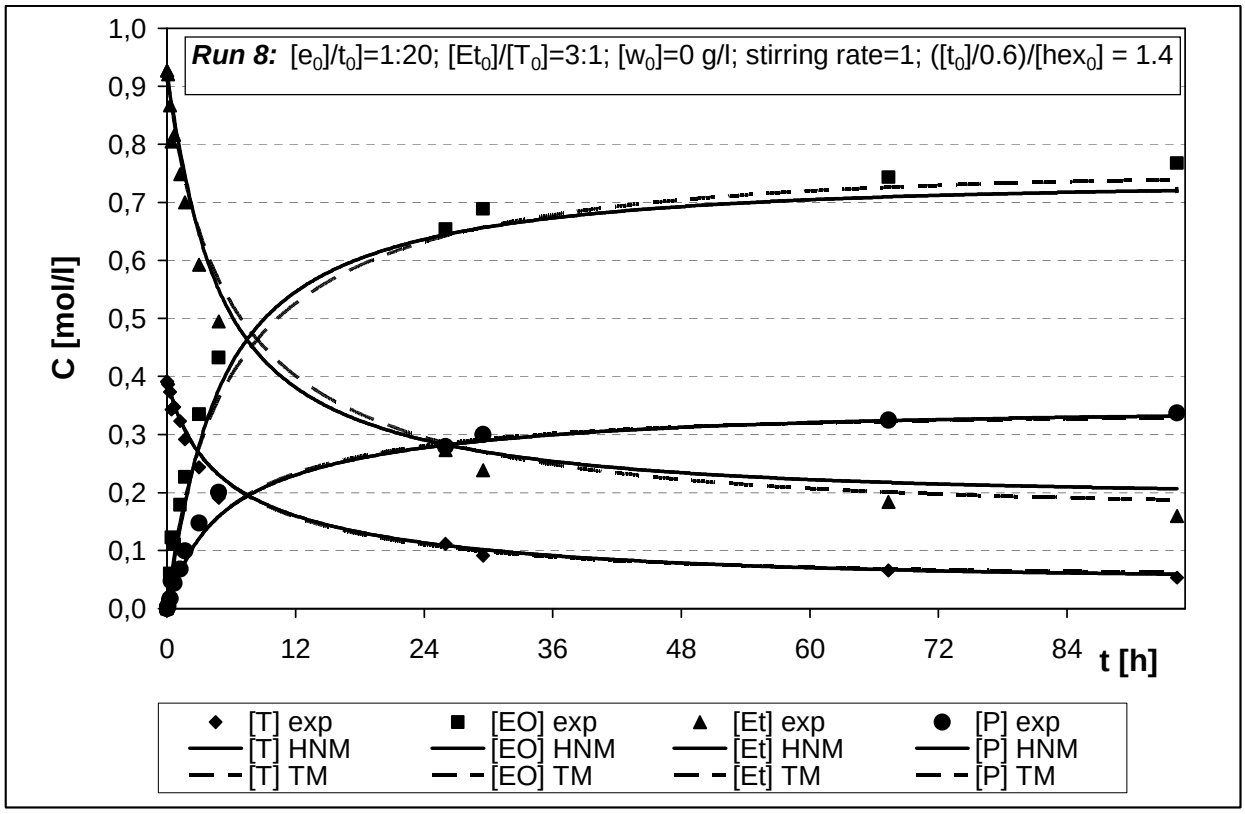

Figure 7. Comparison between experimental data and predicted value with both Hybrid Neural Model, HNM, and Theoretical Model TM. Operating conditions as run 8 of table 1.

In fig. 7 the TM and HNM simulation results relative to run n° 8 are reported. In this case the reaction has been followed for long time in order to verify the stability of the bioconversion and of the enzyme.

As previously observed, this run was characterized by a strongly linearity between experimental substrate and product concentrations and, in this case, the TM and the ANN1 furnished similar results. The same situation is advisable in the simulation results relative to the product and substrate concentrations. Indeed, in this case the simulation results relative to the TM and the HNM tended to mingle: both model were capable to pointly predict the concentrations profiles with a high accuracy level being capable to well fit experimental data both in terms of dynamic and plateau values.

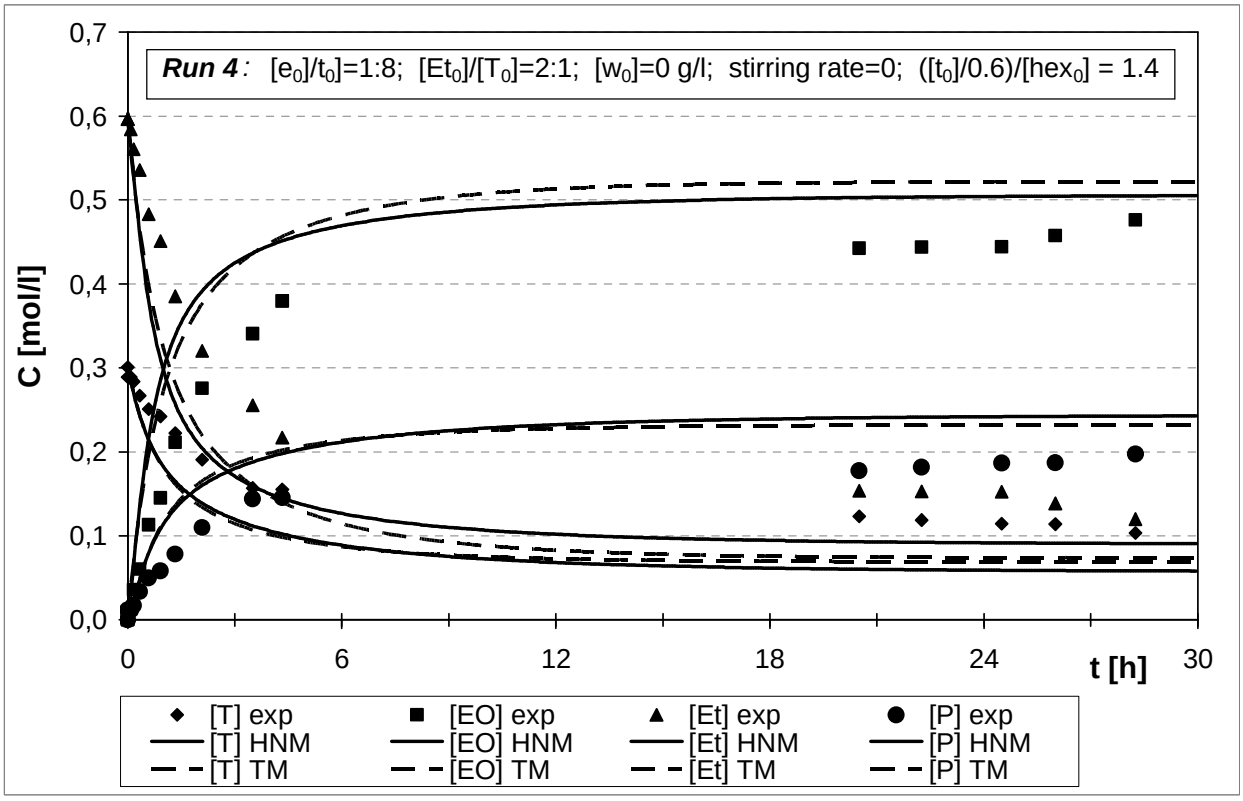

Figure 8. Comparison between experimental data and predicted value with both Hybrid Neural Model, HNM, and Theoretical Model, TM. Operating conditions as run 4 of table 1.

Fig.8 reports the simulation results relative to run n° 4, carried out until the plateau is reached. Run n° 4 was characterized by the absence of stirring, that means a worst enzyme distribution in the batch and, probably, a significant effect of mass transfer resistance, [28]. Despite of these limits, HNM is more able then TM to reproduce the experimental data and, in particular, to predict the final value that might be reached.

Same consideration might be done for the fig.9 where the simulation results relative to run n° 5 are reported. As it was previously observed, this experimental run showed a strong deviation from linear conditions and consequently, using a linear relation in order to predict product concentration on the basis of the substrate concentration, would lead to inaccurate predictions. Comparing the results obtained in terms of concentration profile, we expect that, using the TM, a substantial error existed in predicting ethyloleate concentration values. The experimental evidence confirms this expectance, indeed a strong improvement in predicting ethyloleate plateau value can be registered predicting the concentration profiles by means of the HNM instead of the TM.

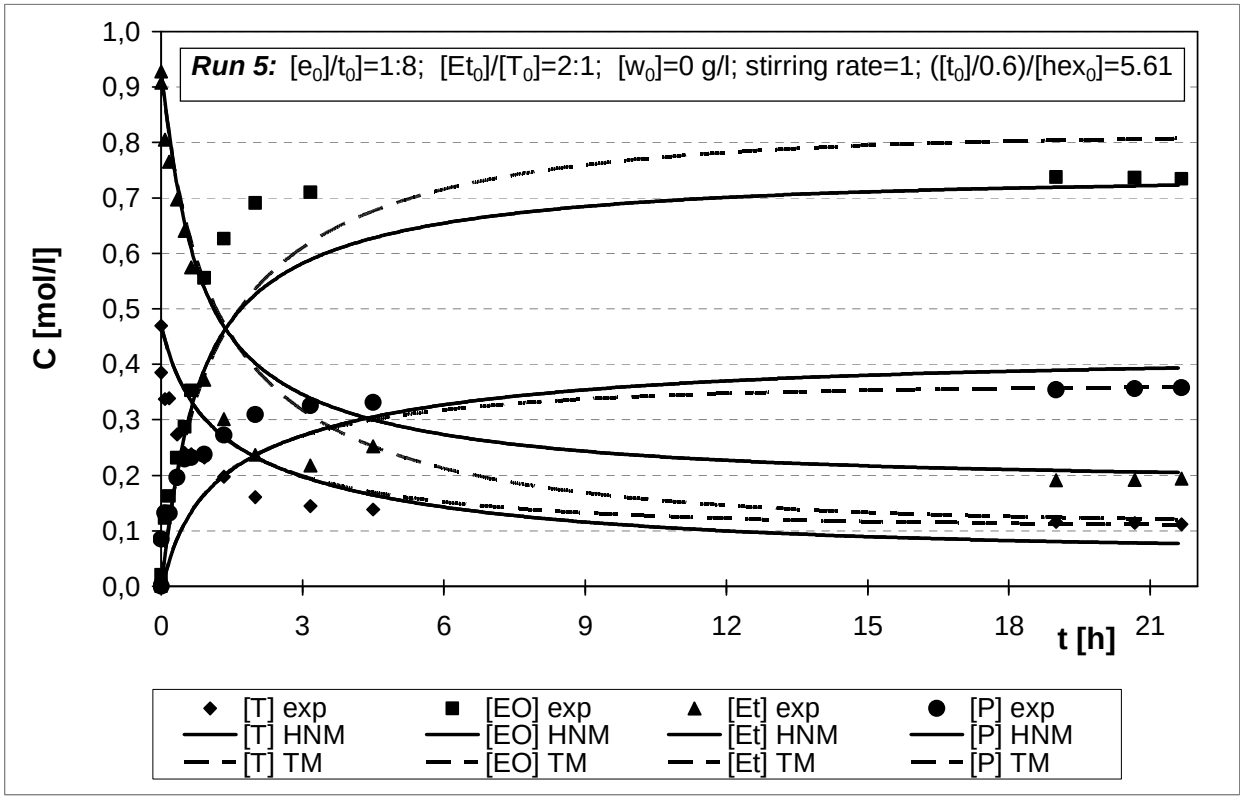

Figure 9. Comparison between experimental data and predicted value with both Hybrid Neural Model, HNM, and Theoretical Model, TM. Operating conditions as run 5 of table 1.

From Fig.9 it should be noted that, at the beginning of the reaction run, both TM and HNM were characterized by a certain inaccuracy level and both model tended to underestimate the ethyloleate concentration value. However, the TM, being a best fitting model, in the second part of the reaction run

tended to overestimate the ethyloleate concentration thus resulting in worst performance on the ethyloleate plateau value prediction. On the contrary, HNM, being not based on a simple experimental data interpolation, is capable to furnish an accurate ethyloleate plateau prediction.

5.Model exploitation

After stating the better forecasting capability of the HNM if compared to the TM, in the present paragraph some possible applications of the proposed model are reported. In particular the realized model was used to forecast the system behavior if the enzymatic reaction was carried out using: a) reused enzyme instead of fresh enzyme; b) a real olive husk oil as a substrate instead of a simulating oil. Both these conditions represent a general validation for the proposed model since it is called to predict the system behaviour under operating conditions (in terms of substrate and enzyme kinds) never seen during model development.

As concerns the experimental runs conducted with reused instead of fresh enzyme, run N°10 and N°11 (Tab.1), the same operating conditions of run N°2 were adopted. During the reaction and the recovery phases, enzyme deactivation takes place and with the aim to predict the process behaviour by means of the HNM, it is necessary to estimate the amount of active enzyme at the beginning of each subsequent enzyme reuse. The residual activity of the enzyme can be expressed as a function of time according to a first order model having the following form:

$$e_a(t) = e_a^0 \exp(-k_d t) \tag{7}$$

where $e_a(t)$ is the active enzyme at time t, e_a^0 is the fresh enzyme activity and k_d is the deactivation constant. On the basis of the reaction initial velocity registered during runs N° 2, 10 and 11, the parameter k_d was estimated and the active enzyme amount at the beginning of reaction runs N° 10 and 11 was calculated (Tab.2).

Run N°	$\frac{e_a(t)}{e_a^0}$ [-]	e_a [g/l]
2	1.000	34.4
10	0.535	18.4
11	0.391	13.5

Table 2. Enzyme activity during subsequent use

The information about the initial active enzyme concentration of experimental runs N°10 and 11 allowed calculating the HNM input variables and the obtained simulation results are reported in Fig. 10.

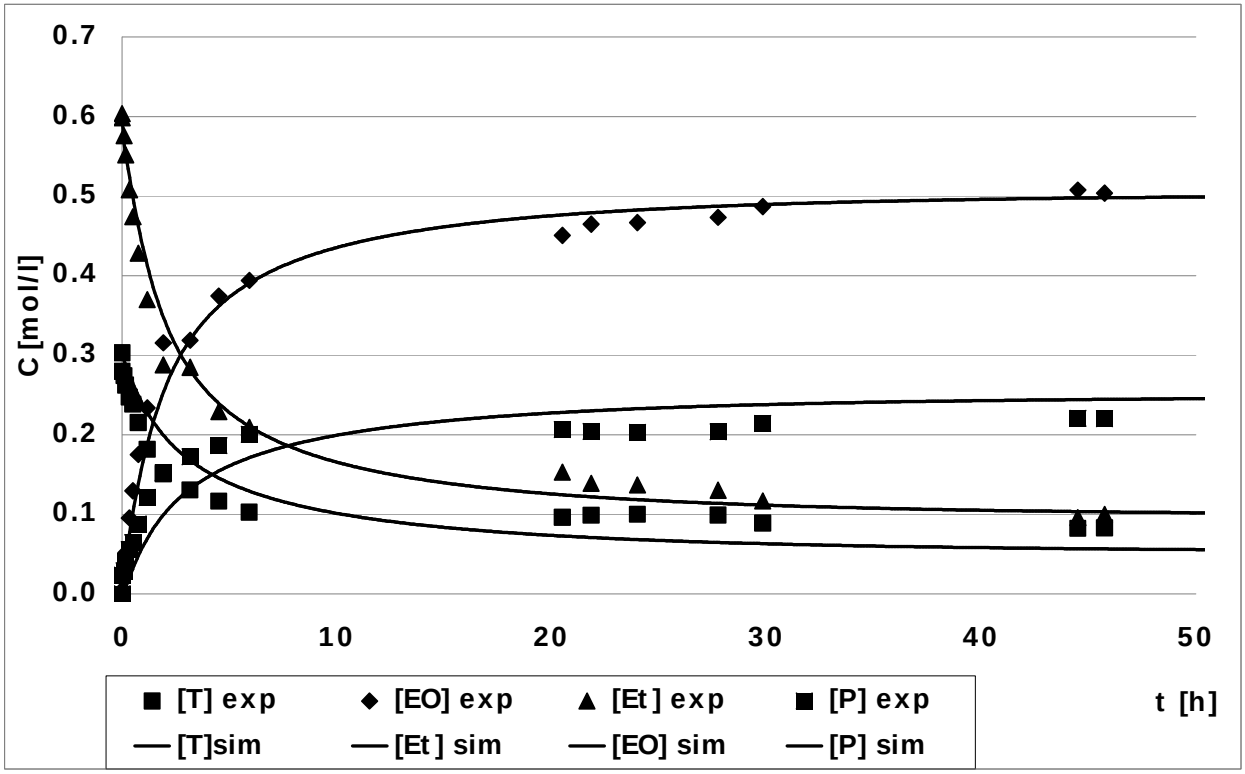

Figure 10. Comparison between experimental data and predicted value with HNM. Operating conditions as run 11 of table 1.

As it is possible to appreciate from this figure, relative to the 2nd reusing cycle, the HNM is capable to predict the experimental data with a very high reliability level, reaching a performance that is comparable to that achieved during the model development phase. This result testify how the proposed model is a very versatile tool, that being based on a proper choice of input variables, when the value of these input variables changes, it can forecast the process behaviour with a remarkable agreement.

The same approach was followed when the HNM was called to predict the enzyme kinetics in the case of a real olive husk oil used as a substrate instead of a simulating oil. This time the HNM input variable that had to take into account the variation of the substrate was the triolein initial concentration, T_0. The olive husk oil is a very complex mixture of triglycerides, each one being involved in the

transesterification reaction. Under the modeling point of view these component were assimilated to the triolein and their cumulative concentration was set for T_0 for the reaction run N°12. The simulation results obtained are reported in Fig. 11.

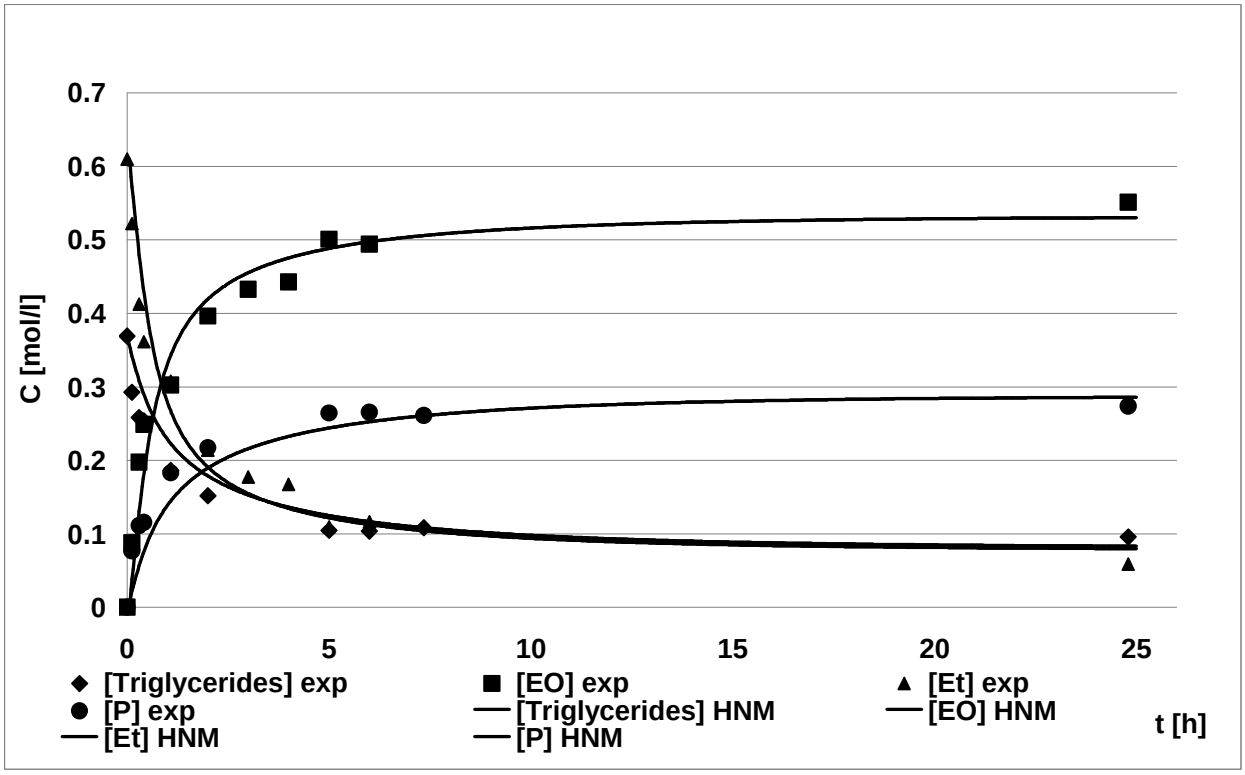

Figure 11. Comparison between experimental data and predicted value with HNM. Operating conditions as run 12 of table 1.

Again the results obtained are very satisfying since the HNM predicts the experimental data with a remarkable agreement. These results pointed out how the model can be used to forecast the enzymatic kinetics under operating conditions significantly different from those exploited during model set-up and even in this case, the model shows an high robustness and flexibility.

6.Conclusion

This result shows how neural models do not just learn in order to recognize the training points; instead, the models are also able to predict the system behaviour even when they are operated in conditions unexploited during training phase. Moreover, the results obtained in this paper, indicate how the introduction of theoretical information into black-box models can lead to a more robust modeling

approach; indeed the results obtained during the model exploitation phase, testify the model reliability during two kind of situation not taken into consideration during the model set-up but very interesting under an industrial standpoint. i.e. a) enzyme recovery and reuse and b) feedstock characterized by a variable composition.HNM permits to better describe and predicted system behaviour in a wide range of operating conditions where ANN is more able to find the correlations between the variables taking into account all the effects. Furthermore HNM should be better used in order to realise a control system for the process, where operating conditions might be choose as manipulating variables and yield or conversion might be used as output variables. This methodology offers very interesting opportunity for the kinetic study of bioconversion, where some effects are sometime not evident or they are difficult to introduce into rigorous kinetic model. Furthermore the use of ANN and of the fundamental equations in the HNM permits to reduce the calculus time.

Reference

[1] Fukuda H, Kondo A, Noda H. Biodiesel fuel production by trans-esterification of oils. J Biosci Bioeng 2001; 92:405-416.

[2] Ma F, Hanna MA. Biodiesel production: a review. Bioresour Technol 1999; 70: 1-15.

[3] Freedman B, Pryde EH, Mounts TL. Variables affecting the yields of fatty esters from trans-esterified vegetable oils. J Am Oil Chem Soc 1984; 61: 1638-1643.

[4] Srivastava A, Prasad R. Triglycerides-based diesel fuels. Renew Sus Energ Rev 2000; 4: 111-133.

[5] Formo MW. Ester reactions of fatty materials. J Am Oil Chem Soc 1954; 31: 548-559.

[6] Freedman B, Butterfield RO, Pryde EH. Transesterification kinetics of soybean oil. J Am Oil Chem Soc 1986; 63: 1375-1380.

[7] Ban K., Kaieda M., Matsumoto T., Kondo A., Fukuda H. Whole cell biocatalyst for biodiesel fuel production utilizing Rhizopus oryzae cells immobilized within biomass support particles. Biochem. Eng. J., 2001, 8, 39-43.

[8] Ban K., Hama S., Nishizuka K., Kaieda M., Matsumoto T., Kondo A., Noda H., Fukuda H. Reapeated use of whole cell biocatalysts immobilized within biomass support particles for biodiesel

fuel production. J. Mol. Catal. B: Enz., 2002, 19.

[9] Al-Zuhair S. Production of biodiesel by lipase-catalyzed transesterification of vegetable oils: a kinetic study. Biotechnol Prog , 2005; 21: 1442-1448.

[10] Calabro' V. , Ricca E. , De Paola M. G. , Curcio S. , Iorio G., Kinetics of enzymatic trans-esterification of glycerides for biodiesel production. Bioprocess and Biosystems Engineering, 2009, 33, 701-710, --DOI 10.1007/s00449-009-0392-z.

[11] Kaieda M, Samukawa T, Matsumoto T, Ban K, Kondo A, Shimada Y, Noda H, Nomoto F, Ohtsuka K, Izumoto E, Fukuda H. Biodiesel fuel production from plant oil catalyzed by *Rhizopus oryzae* lipase in a water-containing system without an organic solvent. J Biosci Bioeng 1999; 88: 627-631.

[12] Al-Zuhair S, Ling FW, Jun LS. Proposed kinetic mechanism of the production of biodiesel from palm oil using lipase. Process Biochem., 2007; 42: 951–960.

[13] Kaieda M, Samukawa T, Kondo A, Fukuda H. Effect of methanol and water contents on production of biodiesel fuel from plant oil catalyzed by various lipases in a solvent-free system. J Biosci Bioeng, 2001; 91: 12-15.

[14] De Paola M. G. , Ricca E. , Calabro' V. , Curcio S. , Iorio G., Factor analysis of transesterification reaction of waste oil for biodiesel production. Bioresource Technology , 2009, Vol. 100, n. 21, pp. 5126-5131, ISSN: 0960-8524.

[15] Hari Krishna, S., Sattur, A.P., Karanth, N.G., Lipase-catalyzed synthesis of isoamyl isobutyrate-optimization using a central composite rotatable design. Proc. Biochem, 2001; 37: 9–16.

[16] Vicente, D.G., Coteron, A., Martinez, M., Aracil, J., Application of the factor design of experiments and response surface methodology to optimize biodiesel production. Ind. Crops Prod., 1998; 8: 29–35.

[17] Reilly, D.L; Cooper, L.N. An overview of neural networks: early models to real world systems. In: Zornetzer, S.F.; Davis, J. L.; Lau, C. (Eds), An Introduction to neural and Electronic Networks. Academic Press, New York, 1990, 227-248.

[18] Zhang, G.; Patuwo, B.E.; Hu, M. J. Forecasting with Artificial Neural Network: the state of Art, Int. J. of Forecasting 1998; 14: 35-62.

[19] Roy, A.; Kim, L.S.; Mukhopadhyay, S. A polynomial time algorithm for the construction and training of a class of multilayer perceptron. Neural Networks 1993; 6: 535-545.

[20] Wang, Z.; Massimo, C.D.; Tham, M.T.; Morris, A.J. A procedure for determining the topology of multilayer feed-forward neural networks. Neural Network 1994; 7 (2): 291-300.

[21] Murata, N.; Yoshizawa, S.; Amari, S. Network information criterion determining the number of hidden units for an artificial neural network model. IEEE transaction on Neural Networks 1994; 5 (6): 865-872.

[22] Oliveira R. Combining first principles modelling and artificial neural networks: a general framework. Comp. Chem Eng. 2004; 28: 755-766.

[23] Al-Zuhair S, Dowaidar A, Kamal H. Dynamic modeling of biodiesel production from simulated waste cooking oil using immobilized lipase Biochem Eng J 2009; 44: 256–262.

[24] Demuth, H.; Beale, M. Neural Network Toolbox User's Guide. Natick, The MathWorks, 2000.

[25] Saraceno, A., Curcio, S., Calabrò, V., Iorio, G. A hybrid neural approach to model batch fermentation of "ricotta cheese whey" to ethanol. Computers and Chemical Engineering. 2010, 34 (10), 1590

[26] Curcio, S., Scilingo, G., Calabrò, V., Iorio, G. Ultrafiltration of BSA in pulsating conditions: An artificial neural networks approach. Journal of Membrane Science. 2005; 246 (2): 235-247

[27] Curcio, S., Calabrò, V., Iorio, G. Reduction and control of flux decline in cross-flow membrane processes modeled by artificial neural networks. Journal of Membrane Science. 2006, 286 (1-2), pp. 125-132.

[28] Curcio S. , Aversa M. , Saraceno A., Advanced modeling of food convective drying: a comparative study among fundamental, artificial neural networks and hybrid approaches, in Food Engineering. Cap. 14, (2010), Ed. Brendan C. Siegler, Nova Science Publishers, Inc.USA, ISBN code: 978-1-61728-913-2

[29] Nelson LA, Foglia A, Marmer WN. Lipase-catalyzed production of biodiesel. J Am Oil Chem Soc 1996; 73: 1191-1195.

1.4 Paper 4: how hybrid neural model might help on the optimization of biofuels product

In this paper it was showed how neural models can be used to model and optimize biofuels production processes. Three different case studies were analyzed; for two of them an hybrid neural model was proposed to describe the reaction kinetics whereas, in the case of anaerobic digestion of agro-food wastes, due to the high complexity of the tested system, a pure neural model was set-up to predict the behavior of a pilot-scale fermenter. On the basis of an optimization protocol, an improved feeding strategy of waste biomass was identified so as to maximize the biogas productivity.

How hybrid neural model might help on the optimization of biofuels product

Alessandra Saraceno, Stefano Curcio, Vincenza Calabrò

Department of Engineering Modeling – University of Calabria

Via P. Bucci - Cubo 42/A - 87036 Arcavacata di Rende (CS) – ITALY

Abstract

The aim of this paper was showing how artificial neural networks could by applied in modeling and optimization of biofuel production processes. In bioprocesses the use of biocatalysts, like enzymes or whole cells, usually requires a detailed analysis of kinetics and mass transfer phenomena difficult to be achieved using a pure theoretical approach. Artificial neural networks (ANNs) are black-box models that may be used in bioprocess modeling both realizing pure empirical models and hybrid neural models (HNMs), i.e. a combination between pure black-box and theoretical models. In this paper three case-studies were reported referring to biodiesel, bioethanol and biogas production starting from agro-industrial wastes. When a partial knowledge of the process at hand was available, a hybrid neural approach was applied (case-study 1-2), whereas when the complexity of the analyzed phenomena did not allow any reliable theoretical analysis, a pure black-box model was developed (case-study 3). In

case-study 3, the possibility to incorporate the realized model in an optimization procedure was shown as well.

The obtained results testify the effectiveness of neural networks in bioprocess modeling and optimization and suggested the exploitation of ANNs that represent a very flexible tools to describe bioconversion and bioreactors systems.

Keywords: biofuel, bioethanol, biodiesel, biogas, modelling.

1.Introduction

In bioconversion processes design, the modeling step plays a key role being preliminary to both optimization and control. In particular, the kinetic analysis of this kind of processes, which make use of enzymes or whole cells as catalysts, is rather complex due to the presence of parallel-serial reaction sets and simultaneous mass transfer phenomena. This aspect is particularly accentuated in fermentation processes where the objective product is only one of the products of the microorganism metabolic path. Moreover, when the bioconversion is carried out on industrial or agro-industrial waste products, such as in the case of second generation biofuels, the kinetic analysis results even more complex due to the presence of contaminants that may interfere with bio-catalysts during the reaction progress. Nevertheless, the possibility to convert industrial wastes into valuable products represents a very challenging task since it allows their disposal and also their valorization.

Many alternatives exist to model the reaction kinetics of bioprocesses. The first one is choosing a theoretical approach that, making use of conservation laws, leads to a first principle model; however, due to the high complexity of the phenomena under study, many (strong) simplifying hypothesis are usually necessary to achieve the description of the process. An alternative to the theoretical approach is the empirical one that leads to a black-box model. The main limit of this solution is represented by the restricted validity domain of the resulting model corresponding to the data on which the model was actually built on. Finally, an arrangement between the two above-mentioned approaches is represented by a hybrid model, consisting of a combination of both theoretical and empirical models. In this case, the well assessed aspects of the process can be modeled by a theoretical approach whereas the difficult-to-interpret aspects can be described using a black-box approach.

Artificial Neural Networks (ANNs) are black-box structures that may be used in bio-reactor modeling,

thus achieving an empirical model that can also be exploited, in a simplified form, to develop a hybrid neural model (HNM). A pure neural model actually does not make use of any transport equation that could help to determine, on the basis of fundamental principles, the mutual relationships existing between the inputs and the outputs of a definite process. ANNs, in fact, are data-driven models capable to learn from examples and particularly useful when no a priori knowledge exists about the process. Under a computational point of view ANNs are composed of interconnected elements, called neurons or nodes. The neurons are combined so as to form one or more layers composing the network. In a multilayer network each neuron receives one or more inputs from other related units and, by means of an activation function, produces an output, i.e. a signal fed to the other nodes connected to it. When ANNs are utilized in a hybrid model, a very important step is identifying the respective domain of theoretical and empirical parts so as to decide which aspects of the process are to be described by a black-box model and which ones by fundamental equations. Two kinds of HNMs can be generally defined depending on the interactions existing between the neural and the theoretical blocks. In a model based on a parallel architecture the inaccuracy in the predicted value from the fundamental part is minimized by the addition of the residuals calculated by the neural network. In a model based on a serial architecture a process variable, which is difficult to measure, is estimated by a neural network and, then, fed as an input to the theoretical block.

In the present paper three case-studies were analyzed with the aim to show how ANNs, in some cases combined with theoretical equations, can be used to model (Case-studies 1-2) and optimize (Case study-3) biofuel production processes. Case-study 1 concerns the exploitation of hybrid neural paradigm to the kinetic modeling of an enzymatic process, i.e. the biodiesel production starting from waste oils. Case-study 2 deals with the kinetic modeling of a fermentation process, thus a process catalyzed by living micro-organism, i.e. the ricotta cheese whey fermentation aimed at bioethanol production. Case-study 3 consists in the application of ANNs to the modeling of the anaerobic digestion of agro-food wastes aimed at biogas production, that is a fermentative process using a micro-organisms complex. In this last case-study a possible model exploitation for process optimization purposes is also shown.

2.Case-studies description

In this paragraph the key features of the analyzed bio-processes are reported with reference to the corresponding case-study

2.1Case-study 1: biodiesel production via glycerides enzymatic trans-esterification

In Case-study 1 the kinetic analysis of the glycerides enzymatic trans-esterification was performed. Trans-esterification consists in the alcoholysis of triglyceric esters and results in a mixture of mono-alkyl esters and glycerol.

The reaction path can be schematized as follows:

$$\text{Triglycerides} + \text{Ethanol} \leftrightarrow \text{Diglycerides} + \text{Ethyloleate}$$
$$\text{Diglycerides} + \text{Ethanol} \leftrightarrow \text{Monoglycerides} + \text{Ethyloleate}$$
$$\text{Monoglycerides} + \text{Ethanol} \leftrightarrow \text{Glycerol} + \text{Ethyloleate} \quad (1)$$

where the ethyloleate represents the objective product, i.e. the main biodiesel constituent.

The kinetic modeling of the trans-esterification reaction was performed developing a HNM. The experimental data necessary to build the model were collected during batch experimental runs: a mixture simulating the waste oil was used as a source of glycerides and ethanol was used to perform the alcoholysis; the enzyme was Lipase from Mucor Miehei, immobilized on ionic exchange resin [6].

2.2 Case-study 2: bioethanol production via Ricotta Cheese whey fermentation

In Case-study 2 the fermentation of “Ricotta cheese whey” to ethanol was analyzed.

Ricotta cheese whey (RCW) is a high pollutant dairy waste obtained as the main by-product in ricotta cheese production process. The high lactose concentration in RCW (about 50 g/l) suggests the possibility to convert this sugar into ethanol using a fermentative path. Lactose fermentation can be summarized as follows:

$$\text{Lactose} + \text{Water} \leftrightarrow \text{Ethanol} + \text{Carbon Dioxide} \quad (2)$$

It should be underlined that the above written equation represents a strong simplification of the reaction mechanism since the transformation of sugars into ethanol by a fermentative path is the results of many parallel-serial reaction steps. Even in this case a HNM was realized with the aim of describing the

reaction kinetics. The experimental points used to set-up the model were collected during the lab scale RCW fermentation. The microorganism used to carry out the reaction reported in Eq.2 was the *Kluyveromices Marxianus var. Marxianus* [7].

2.3 Case-study 3: biogas production via anaerobic digestion

In Case-study 3 the anaerobic digestion of agro-industrial wastes to produce biogas was taken into consideration.

During the anaerobic digestion, the organic matter is bio-degraded in absence of dissolved oxygen by means of a microorganism complex; the main product of this process is a gas mixture mainly consisting of methane (50-60%) and carbon dioxide (30-40%). The source of organic matter can be the manure, i.e. a classic digestion process, or the manure with one or more co-substrate(s), i.e. a co-digestion process [8].

In this paper the manure/orange juice waste (OJW) co-digestion process was analyzed with the aim of finding the optimal ratio of the two substrates that should be fed to the fermenter and of identifying a proper feed-strategy for the fermenter. As compared to the processes analyzed in Case-studies 1-2, the case-study 3 resulted much more complex, since the substrate is a solid-like mixture composed by many compounds (identified as organic matter) and many metabolic paths take place (a microorganism complex was used).

Due to the complexity of the analyzed process, a pure ANNs model was realized to accomplish the process modeling step; subsequently, using the realized model, an optimization framework based on ANNs was applied.

3.Materials and methods

In this paragraph it is reported the experimental procedure followed to collect the experimental data in the three case-studies.

3.1Case-study 1: trans-esterification reactions.

The experimental runs were performed using a simulating oil as a substrate: the 60% (w/w) of the oil was triolein (triglyceride); the remaining 40% were fatty acid or mono and di-glycerides. The second reagent was ethanol at 99.8% (Fluka). Hexane (95% grade, Fluka) was the solvent when anhydrous

condition were required; distillate water was instead exploited in not anhydrous conditions.

The catalyst was a lipase from *Mucor miehei* (Lipozyme by Novozymes). immobilised on a macroporous ion exchange resin in particulate form (characteristic diameter ranging between 0.3 and 1.0 mm).

All the experimental runs were carried out using a well mixed 125 ml batch reactor; the operating temperature was 37°C and the pH was 7. The batch runs were designed varying the following variables: 1) the mass feed ratio enzyme/triolein (e_0/t_0); 2) the reactants molar ratios ethanol/triolein (Et_0/T_0); 3) the mass of water fed to the bioreactor (W_0); 4) the stirring rate (ω) with three characteristic level (0-1-2); 5) the mass feed ratio simulating oil /hexane (s_0/Hex_0).

The operating conditions of all the performed experimental runs are summarized in Table I.

Table I: Case-study 1 batch runs experimental conditions

Run N°	e_0/t_0 [g/g]	Et_0/T_0 [mol/mol]	W_0 [g/l]	ω [level]	s_0/Hex_0 [g/g]
1	1:8	2:1	1.0	1	1.4
2	1: 8	2:1	0	1	1.4
3	1:8	2:1	0	2	1.4
4	1:8	2:1	0	0	1.4
5	1:8	2:1	0	1	5.61
6	1:20	2:1	0	1	1.4
7	1:20	2.5:1	0	1	1.4
8	1:20	3:1	0	1	1.4
9	1:4	2:1	0	1	0.69

In all the exploited experimental conditions the reaction progress was monitored in terms of reactants and products concentrations using high performance liquid chromatography, HPLC (JASCO).

3.2Case-study 2: RCW fermentation

In Case-study 2, the experimental data necessary to develop the HNM were collected from a set of anaerobic fermentations performed on RCW. Each fermentation test actually consisted of two steps:

the inoculum culture preparation and the batch fermentation in a stirred anaerobic bioreactor.

The inoculum culture was prepared putting a single yeast colony (*Kluyveromices Marxianus var. Marxianus*, Centraalbureau Voor Schimmelcultures, Holland) into 150 ml of culture medium. The medium composition was: 50 g/l lactose, 10 g/l peptone, 5 g/l yeast extract (Fluka). The culture was kept in a 250 ml flask held in a temperature controlled bath with roto-translational external mixing (OLS 200, Grant), at 150 rpm and 37 °C for 12 h. During each fermentation test one litre of ricotta cheese whey was fermented in a 2 l batch fermenter (*Z611020002,* Appikon) equipped with a controller of temperature, pH and rpm controller (ADI 1030, Applikon). The duration of each run was 18 h from the addition of the inoculum culture into the bioreactor.

The fermentation runs experimental condition were designed according to the factorial design method [9]. The following variables and operating condition were chosen: 1) temperature (T) in the range 32-40 °C; 2) pH in the range 4-6; 3) stirring rate (ω) in the range 100-300 rpm; 4) initial substrate (lactose) concentration (S_0) in the range 45-90 g/l. Applying the two levels factorial experimental design, the extreme values of the variables characteristics ranges were chosen to set the batch runs experimental conditions. A total of 16 batch runs were performed and are summarized in Table II.

Table II**: Case-study 2 fermentation runs experimental conditions**

Run N°	T [°C]	pH [-]	ω [rpm]	S_0 [g/l]
1	40	6	300	90
2	40	4	100	90
3	32	6	300	45
4	40	6	100	45
5	32	6	100	90
6	32	4	300	90
7	40	4	300	45
8	32	4	100	45
9	40	4	100	45
10	40	6	300	45
11	40	4	300	90

12	32	6	100	45
13	32	4	300	45
14	32	4	100	90
15	40	6	100	90
16	32	6	300	90

The fermentations progress was followed in terms of lactose, ethanol and biomass concentration profiles. Lactose and ethanol concentration measurement was performed by HPLC with the detection of components achieved by a refractive index (RI 930, Jasco). Biomass concentration analysis was carried out by Bactoscan (Foss).

3.3 Case-study 3: anaerobic digestion reactions

The anaerobic digestion reactions were carried out on a pilot scale batch reactor. The reactor had a volume of 23.7 l and was filled with 15 l of mixture manure / OJW; the remaining 8.7 l of reactor were intended for the biogas produced during the reaction.

The experimental runs operating conditions were designed so as to test 5 different initial manure / OJW feed ratios (Table III). Each reaction run had a duration of 28 days.

Table III: **Case-study 3 anaerobic digestion experimental conditions**

Run N°	Manure [mass %]	OJW [mass %]
1	100	0
2	95	5
3	90	10
4	85	15
5	50	50

The charged matrix was characterized in terms of initial chemical oxygen demand (COD_0), pH_0, and initial carbon/nitrogen ratio $(C/N)_0$ of the organic matter.

The reaction progress was followed measuring, once a day, the methane concentration (objective

product), the COD and the pH. As stated in paragraph 2, during anaerobic digestion, the methane production is the result of a reaction path. Contrary to Case-study 1-2, in case-study 3 it was not possible to identify a single substrate whose concentration could be directly related to methane production. As a consequence, the COD measurement was considered as an inferential measurement of the overall substrates concentration.

4.Model development

4.1 Case-study 1: trans-esterification kinetic model

The kinetics of the trans-esterification reactions reported in Eq.1 was modeled using a HNM. Some of the authors of the present contribution developed, for the reaction at hand a first principle kinetic model based on a Ping-Pong Bi-Bi mechanism with ethanol inhibition [6]. Applying the King-Altman kinetics method the following triolein consumption rate was obtained:

$$-r_T = -\frac{d[T]}{dt} = \frac{\alpha \cdot [T] \cdot [Et] - \beta \cdot [P] \cdot [EO]}{[T]^2 + \delta \cdot [T] + \varepsilon} \cdot [e_0] \quad (3)$$

where $-r_T$ was triolein consumption rate, [P] was the overall products concentration (glycerol, monolein and diolein), [EO] was the ethyloleate concentration and α, β, γ and ε were kinetic constants. The concentrations of ethyloleate, ethanol and products were expressed as a function of triolein actual concentration [T] and of substrates initial concentrations [T_0] and [Et_0].

$$\begin{aligned} [EO] &= -2.25 \cdot ([T] - [T_0]) \\ [Et] &= -[EO] + [Et_0] = 2.25 \cdot ([T] - [T_0]) + [Et_0] \\ [P] &= [T_0] - [T] \end{aligned} \quad (4)$$

In the previous study, the correlation existing between [EO] and [T] (Eqs. 4) was empirically determined on the basis of a linear fitting of the experimental data. With the aim to overcome the inherent limit of already proposed theoretical model a HNM was realized, hereafter referred as HNM1. The reaction mechanism and the relative kinetic equation were determined using a rigorous theoretical approach whereas the relation existing between substrate and product concentrations was determined using an ANN, hereafter called ANN1. In particular, the neural network predicted the ethyloleate

concentration as a function of triolein concentration and reaction initial conditions (I.Cs). The HNM1 structure is reported in Fig.1.

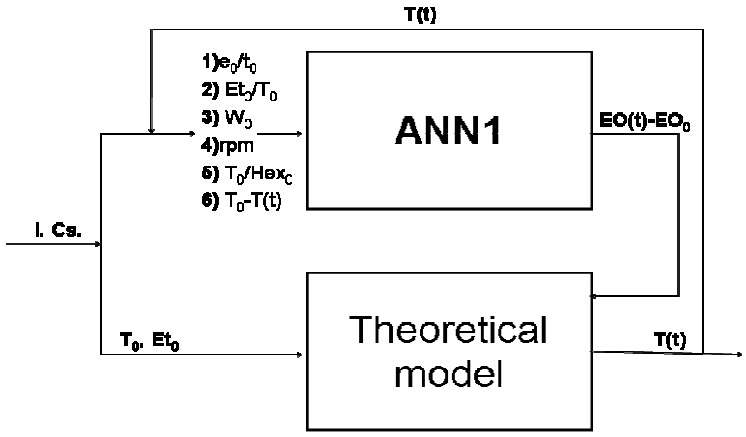

Figure 1: **HNM1 structure**

With reference to ANN1 block in Figure 1 it is possible to identify the input/output variables of the neural network.

After defining the input/output structure of the network, the neural network architecture was defined and the ANN training procedure set up. The available experimental runs (Table I) were split in two groups reserving 2/3 of reaction runs, 88 experimental points, to the training/test phases of the neural networks and the remaining 3 runs, 50 points, to validate the predictions of the developed ANN1. A multi-layer perceptron (MLP) feed-forward architecture with a pyramidal structure was chosen using Matlab Neural Network Toolbox (The Mathworks), Ver. 4.0.1. The choice of the "best" network structure, i.e. the number of hidden layers and number of neurons in each layer, was achieved by a trial-and-error procedure.

The resulting structure of ANN1 consisted of:

- An input layer with 6 neurons;
- A first hidden layer with 10 neurons;
- A second hidden layer with 3 neurons:
- A single neuron output layer.

The neurons transfer function characterizing input and hidden layers was the hyperbolic tangent; the single neuron output layer was instead characterized by a linear transfer function [10].

4.2 Case-study 2: RCW fermentation kinetic model

In Case-study 2, three HNMs were developed for the prediction of biomass (HNM2), lactose (HNM3) and ethanol (HNM4) concentration profiles during fermentation. The three HNMs were characterized by the same general structure: for each considered component a mass balance equation was written in a batch reactor, i.e. the theoretical part of the model; the kinetic parameter actually necessary to solve the balance equations was estimated using an ANN.

The mass balance equations written with reference to biomass (X), lactose (S) and ethanol (P) in a batch reactor assumed the following form:

$$\begin{cases} \dfrac{dX}{dt} = \mu X \\ -\dfrac{dS}{dt} = qX \\ \dfrac{dP}{dt} = \mu_P X \end{cases} \tag{5}$$

where μ was the specific growth rate of biomass, q was the lactose consumption rate function, μp was the product growth rate.

Eqs.5 were solved applying the Euler's discretization to determine biomass, lactose and ethanol concentration value at time t+Δt, on the basis of the knowledge already achieved at time t. To solve the discretized form of Eqs. 5, the time-dependent values of the kinetic parameters were provided by three independent neural networks, namely ANN2, ANN3 and ANN4, which were called on to predict μ, q and μp, respectively.

The kinetic parameters predicted by the neural network were processed by the following logic conditions:

$$\begin{cases} if \ \ \mu < 0 \Rightarrow \mu = 0 \\ if \ \ q < 0 \Rightarrow q = 0 \\ if \ \mu_p < 0 \Rightarrow \mu_p = 0 \end{cases} \tag{6}$$

The logic conditions verified the physical reliability of the ANNs prediction. HNM2-3-4 structure is schematized in Fig.2.

In Fig.2 the input/output structure of ANN2, ANN3 and ANN4 could be deduced: the three neural networks received the same input variables (i.e. T, pH, ω, S0, and the batch time, t) and produced respectively μ, q and μp as output variables.

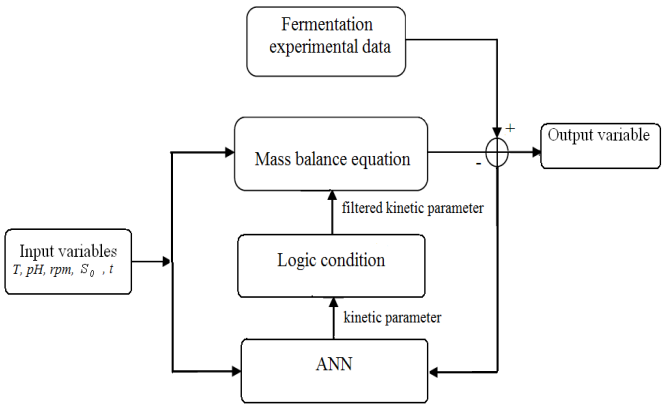

Figure 2: **RCW HNM2, HNM3 and HNM4 structure**

To develop the ANNs structure, the same procedure illustrated in the case of trans-esterification reaction was followed. The resulting structure of the ANNs is schematized in Table IV [7].

Table IV: **ANN2,ANN3, ANN4 structures.**

Neural Network	Input layer [neurons]	1st hidden layer [neurons]	2nd hidden layer [neurons]	Output Layer [neuron]
ANN2	5	6	5	1
ANN3	5	10	3	1
ANN4	5	10	2	1

The neurons transfer function characterizing input and hidden layers was the hyperbolic tangent;

the single neuron output layer was characterized by a linear transfer function.

4.3 Case-study 3: anaerobic digestion optimization

As mentioned in the previous paragraph, due to high complexity of the anaerobic digestion process, a pure neural model (ANN5) was developed to describe the process. The cumulative productivity of methane from the pilot-scale digester was chosen as ANN5 output variable. The chosen input variables were: 1) OJW mass percentage, 2) pH, 3) initial chemical oxygen demand (COD0), 4) carbon-nitrogen initial ratio ((C/N)0) of the mixture fed to the digester and 5) the batch time, t. The resulting structure of ANN5 consisted of:

- An input layer with 5 neurons (hyperbolic tangent transfer function);
- A first hidden layer with 5 neurons(hyperbolic tangent transfer function);
- A second hidden layer with 2 neurons (hyperbolic tangent transfer function):
- A single neuron (linear transfer function) output layer.

After defining ANN5 structure, the black-box model was used to optimize the operation of feeding the fermenter . The objective function was methane cumulative concentration at the end of fermentation process; the variable that had to be optimized was the OJW mass percentage into the reaction mixture.

The procedure followed to optimize the digester can be schematized into the following steps :

1) the batch time, i.e. 28 days, was divided in three time periods: I) days 1-9; II) days 10-19; III) days 20-28;

2) at the beginning of each individuated time period, it was supposed the possibility to change the reaction mixture composition to the following discrete OJW mass percentage 0-10-15-20%;

3) a grid of possible reaction progresses was obtained on the basis of the different OJW mass percentages that were set at the beginning of each time period (64 possible scenarios);

4) the value of the objective function was calculated using ANN5 for each possible scenario identified at point 3 of the procedure;

4) the scenario capable of guaranteeing the maximization of the objective function was chosen as the optimal solution.

5.Results and discussion

5.1 Results relative to Case-study 1

In Fig. 3 the comparison between the experimental points and the prediction provided by ANN1 is reported. From this figure, it can be noted that the experimental points do not show a linear trend, as it was supposed in the previously proposed theoretical model. On the contrary, a sigmoidal behavior can be recognized. Consequently, the ANN1 is much more reliable of predicting the actual relationship existing between ethyloleate and triolein concentrations than a pure linear correlation.

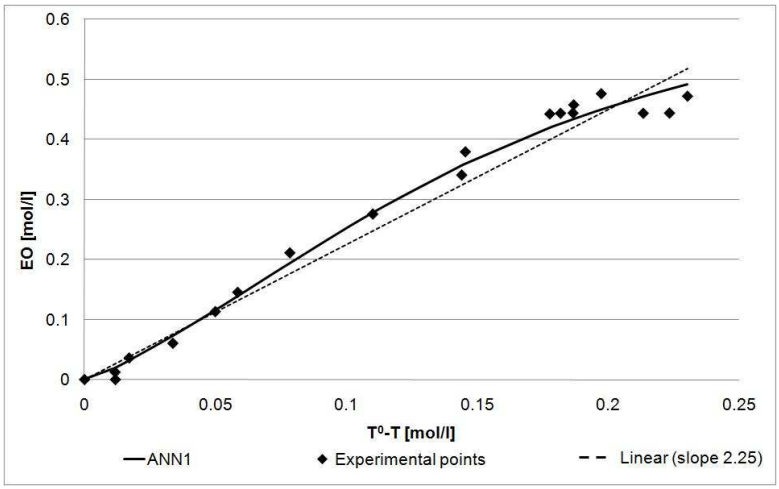

Figure 3: **Experimental points and ANN1 model prediction relative to Run 4 of Table I.**

After estimating the relation existing between [EO] and [T], HNM1 allows predicting the concentration profiles of all the reacting species. Fig. 4 reports the experimental data and the simulation results relative to Run N° 1. This experimental run, is the only run performed in not anhydrous conditions. Observing Fig. 4 it can be noted that a significant agreement exists between experimental points and the simulation results: the HNM is capable of predicting the product and substrate plateau values with a remarkable agreement.

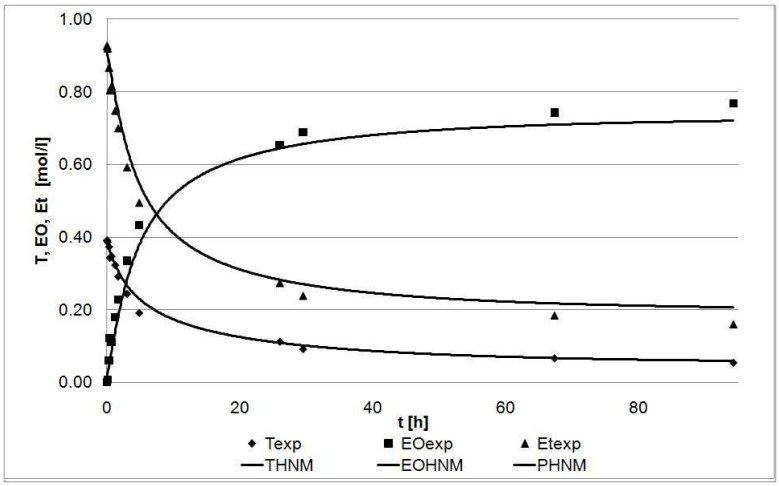

Figure 4: **HNM1 Prediction in terms of reacting species concentration.**

Similar results to those shown in Fig. 3 and Fig. 4 were obtained in the other exploited experimental conditions (data not shown). It is worthwhile remarking that the HNM1 was obtained on the basis of experimental points performed on a simulating oil. With to aim to test the generalization capability of HNM1, the model was used to predict the trans-esterification evolution when a real husk olive oil was used. The results obtained are reported in Fig. 5.

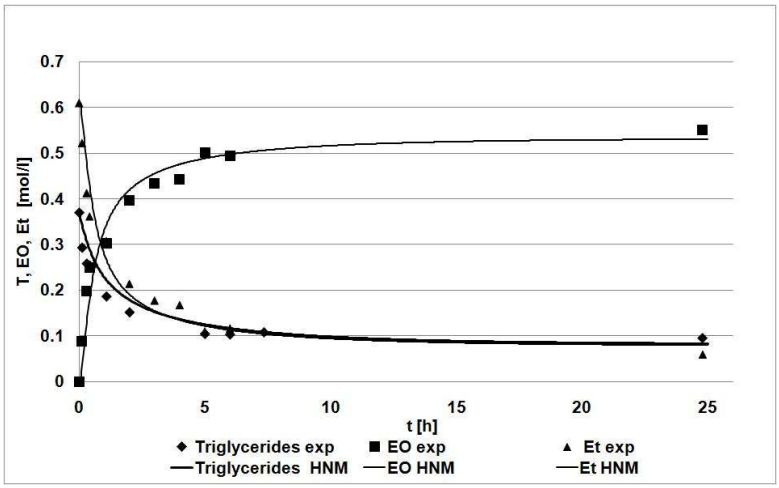

Figure 5: **Experimental points and HNM1 model prediction. Trans-esterification of a real waste oil.**

In this case the triglycerides concentration is reported in spite of triolein concentration. The results shown in Fig. 5 are very satisfying, since they prove that HNM1 not only learns so as to recognize the training points, but it is also able to predict the system behavior even when operated in conditions never exploited during training phase.

5.2 Results relative to Case-study 1

In this paragraph the results obtained applying the HNM approach to the RCW fermentation process are discussed. In particular, in Fig. 6, a whole fermentation run is shown in terms of biomass, lactose and ethanol concentration profiles In this figure both the experimental points and the HNM2, HNM3, HNM4 model predictions are reported. From Fig. 6 it is possible to state that all the realized HNMs are characterized by a high reliability. Indeed, the three models are capable to predict the experimental points with an average percentage error always lower than 10%

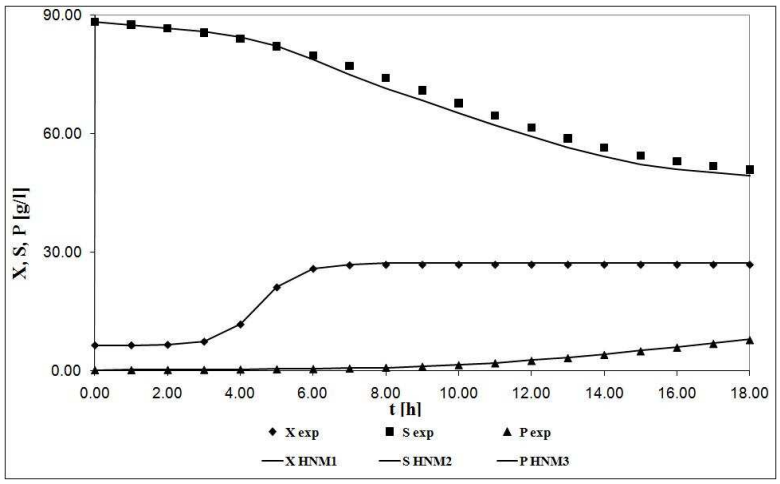

Figure 6: **Experimental points and HNM2. HNM3 and HNM4 model predictions.**

However, it is necessary to remark that the experimental points reported in Fig. 6 are all relative to the training/test dataset: as a consequence, a high performance of the developed models is expected in these conditions. Fig. 7 shows, instead, the simulation results relative to a complete experimental run never exploited during the training/test phases; this simulation represents, therefore, a general validation of the proposed model since it tests the HNMs' capability of properly predict the system

behaviour even in operating condition never seen before

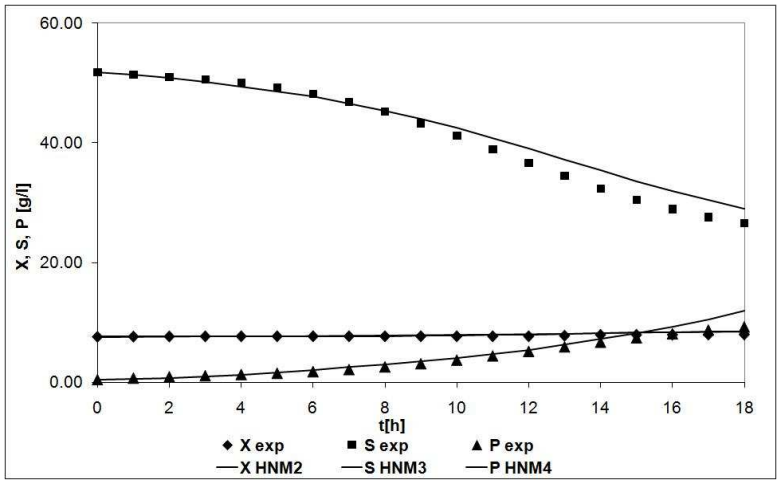

Figure 7: **Simulation results relative to validation phase.**

With reference to Fig. 7, it is worthwhile observing that the hybrid model is capable of providing reliable predictions even during validation; during validation, the model performance, measured in terms of percentage error is comparable to that obtained with the experimental data used to perform the training and the test phases.

The results of the Case-study 2 confirm those ones relative to Case-study 1. In both the case-studies it was shown that neural networks, when integrated in a hybrid structure, not only learn so as to recognize the training points, but are also able of predicting the system behavior even when operated in conditions never exploited before.

These features of the developed HNMs are particularly useful as far as process optimization and control are concerned; indeed, after properly accomplishing the model identification step, the obtained model can be properly integrated both in an optimization procedure and in an advanced control scheme.

5.3 Results relative to Case-study 3

The capability of the realized model ANN5 to predict the anaerobic digestion progress was evaluated both on experimental runs used during the model building (training/test phases) and during the validation phase.

In Fig. 8 the results relative to training/test phases are reported. As expected, a very good agreement between experimental points and model predictions exists.

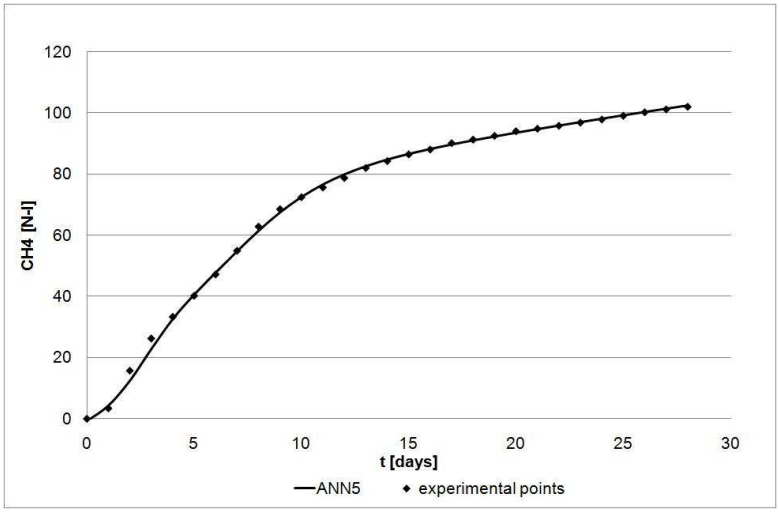

Figure 8: **Experimental points and ANN5 model predictions. Training/test phase**

On the other side, in Fig. 9 the simulation results relative to an experimental run not used during model development phase is reported. Actually, a significant worsening of model performance is observed during validation phase. This effect should be ascribed to the pure black-box nature of the model chosen to describe the anaerobic digestion. However, due to the difficulty in theoretically describing the process at hand, the pure black-box performance can be considered rather satisfying. Indeed, even if characterized by a lower accuracy during validation, the model was capable to predict the main features of the methane cumulative curve.

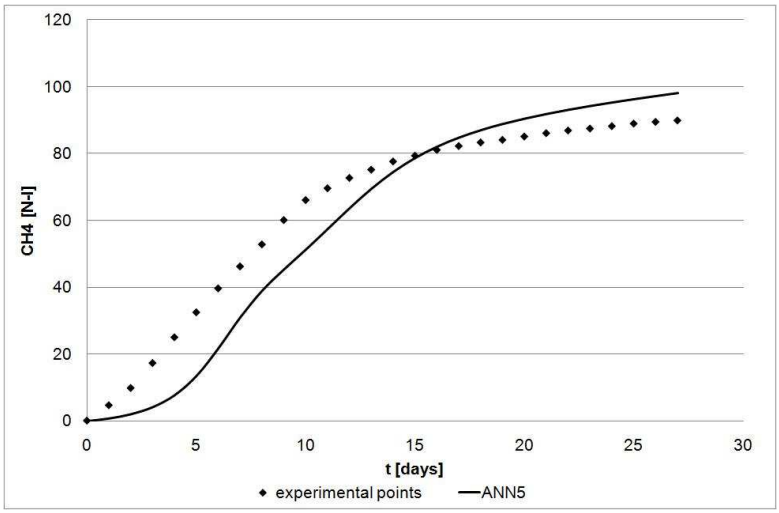

Figure 9: **Experimental points and ANN5 model predictions. Validation phase.**

After the modeling step, the optimization procedure was set-up. As mentioned in the model development paragraph, 64 digestion possible scenarios were simulated.

Some of the obtained scenarios are reported so as to show the procedure followed in process optimization. In particular, in Fig. 10 the discontinuous curve represents the methane cumulative curve that would have been obtained if the animal dejection/OJW ratio was not varied during the reaction progress.

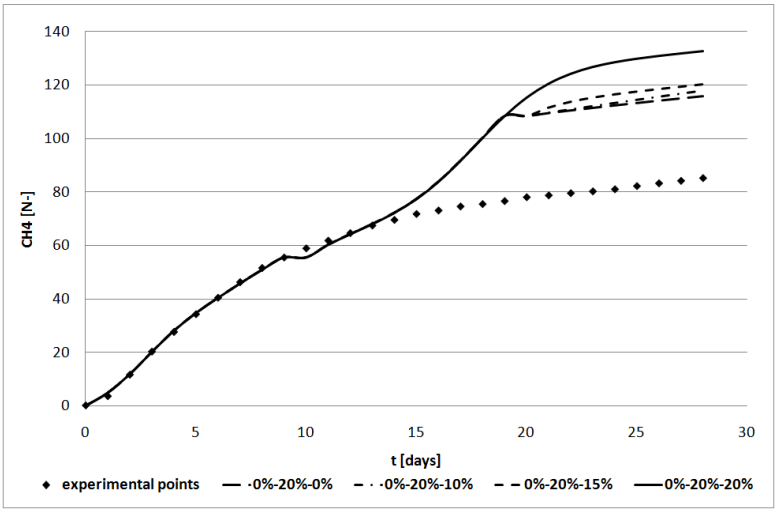

Figure 10: **Some possible scenarios obtained during the optimization phase**

If animal dejection/OJW ratio is varied, a significant improvement in the objective function is therefore observed.

The optimal scenario was obtained when the OJW was kept constant during the digestion progress and equal to 20% w/w.

6.Conclusions

In this paper it was shown how ANNs, both in a pure black-box and in a hybrid model could be very useful in modeling and optimizing bioprocesses. If a partial theoretical knowledge of the analyzed process exists, the ANN can be incorporated in a hybrid structure so that the theoretical and the black-box part of the model can work in a synergistic manner (Case-study 1-2). On the basis of the results showed in this paper, this approach turned out to be very efficient and can be adapted to the analyzed processes on the basis of their intrinsic characteristics and of the information actually available. When the analyzed process is so complex that a proper theoretical analysis cannot be performed (or could be cumbersome and time consuming), a pure back-box model can be exploited to model the process (Case-study 3).

The HNMs realized in Case-studies 1-2 and the pure ANN realized in Case-study 3 were characterized by a good forecasting capability. After the model identification step, in the case of Case-study 3 a possible model exploitation was showed. The obtained results proved that if the model is properly inserted in an optimization algorithm it could be very effective and may significantly reduce the experimental effort.

References

[1]L .Gregersen, S.B. Jorgensen, Supervision of fed-batch fermentations. Chemical Engineering Journal, (1999), 75, pag. 69.

[2]J.E. Bailey, J.E. Ollis, Biochemical Engineering Fundamentals, (1986), McGraw-Hill Companies; New York.

[3]S. Feyo de Azevedo, B. Dahm & F.R Oliveira, Hybrid modelling of Biochemical Processes: A comparison with the conventional approach, Computer and. Chemical Engineering, (1997), 21,

pag.751.

[4]G. Zhang, B.E. Patuwo, M.J. Hu, Forecasting with Artificial Neural Network: the state of Art, Int J of Forecasting, (1998), 14, pag. 35.

[5]M. Agarwal, Combining neural and conventional paradigms for modelling, prediction and control, International Journal of System Science, (1997). 28, pag. 65.

[6]V. Calabro', E. Ricca, M. G. De Paola, S. Curcio, G. Iorio, Kinetics of enzymatic trans-esterification of glycerides for biodiesel production, Bioprocess and Biosystems Engineering, (2009), 33, pag.701.

[7]A. Saraceno, S. Curcio, V. Calabrò, G.Iorio, A hybrid neural approach to model batch fermentation of "ricotta cheese whey" to ethanol, Computer and chemical engineering, (2009), 34, 10, pag. 1590.

[8]S. Curcio, V. Calabrò, M. Aversa, E. Ricca, S. Sansonetti, G. Iorio, Production Of Biogas With Bioconversion Of Organic Solid Waste (Manure) And Food Industry Waste, Journal of Biotechnology, (2010), pag. 165.

[9]G. Box, , W. Hunter, S. Hunter, Statistics for Experimenters, An Introduction to Design, Data Analysis and Model Building, (1978), John Wiley and Sons, New York.

[10] V. Calabro', S. Curcio, A. Saraceno, E. Ricca, M.G. De Paola, G. Iorio, Biodiesel production from waste oils by enzymatic transesterification: process optimization with hybrid neural model, Journal of Biotechnology (2010), 150, pag. 371

1.5 A mass transport/kinetic model for the description of inulin hydrolysis by immobilized enzyme

In this paper, a pure theoretical model was proposed to describe the inulin enzymatic hydrolysis by means of inulinase immobilized in a proper support. The intrinsic kinetics of the immobilized enzyme was analyzed by observing the enzyme behavior under a set of experimental conditions that allows neglecting the mass transport limitations; subsequently, the mass transport limitations were evaluated by means of a proper semi-empirical correlation. The framework proposed to describe the inulin hydrolysis is characterized by a high generality level and, applying the proper modifications, can be used to model other kinds of polysaccharides hydrolysis as well.

A mass transport/kinetic model for the description of inulin hydrolysis by immobilized inulinase

Alessandra Saraceno, Emanuele Ricca[3], Stefano Curcio, Vincenza Calabrò, Gabriele Iorio

Department of Engineering Modeling – University of Calabria

Via P. Bucci - Cubo 42/A - 87036 Arcavacata di Rende (CS) – ITALY

Abstract

In this paper a mass transport/kinetic model is proposed with the aim to describe the enzymatic hydrolysis of inulin catalyzed by immobilized inulinase. The proposed model takes into consideration both kinetic and mass transfer phenomena involved in the reaction and quantifies their relative relevance according to the evaluation of the effectiveness factor. As a polysaccharide, the inulin main characteristic is its polymeric nature that implies an inherent variability of the molecular weight and polydispersity; focusing on this aspect, the model is able to predict the effect of molecular weight both

[3] Corresponding author. E-mail: emanuele.ricca@unical.it

on the enzyme intrinsic kinetics and on mass transfer. The obtained experimental results testify a high reliability of the model that is able to predict the system behavior in a wide range of operating conditions; moreover, the model predictions confirmed the effective relevance of the molecular weight on the observed reaction rate. Even if developed with reference to the inulin hydrolysis, the model is the result of a general approach that, after the proper modifications, could be applied for modeling other polysaccharides hydrolysis.
Keywords: biopolymers, enzyme, kinetics, mass transfer, biocatalysis.

1.Introduction

Biocatalysts and, more specifically, immobilized enzymes are used in a wide range of processes typical of food, pharmaceutical and textile industry. Associated to enzyme immobilization there is a number of advantages and disadvantages that must be taken into account from case to case. As a consequence of immobilization, enzyme catalytic activity usually decreases: immobilization procedure may cause enzyme disfiguration and micro-environmental effects due to interaction of the support with the enzyme-substrate system (Khorasheh et al., 2002). This results in a change in the enzymatic reaction mechanism and, contextually, a strong increase in mass transport limitation is registered (Garcia et al., 2000). As a consequence, the kinetic behavior of the immobilized enzyme can be different from that exhibited by native enzyme (Kamin and Wilson, 1980; Kheirolomoom et al., 2001; Seong et al., 2003). On the other hand, immobilization allows to conduct enzymatic reactions in a continuous reactor, making the catalyst recovery and its reutilization an easier task, and to adopt specific reactor configurations such as packed-bed or fluidized-bed reactors. In addition, immobilization can preserve the catalyst from mechanical stress thus guaranteeing performance, stability and constant product characteristics (Bailey and Ollis, 1986). However, in immobilized enzyme reacting systems, the overall rate of the process depends on both the chemical reaction kinetics and the solid-liquid mass transfer processes (Pangarkar et al., 2002) due to inherent serial nature of these phenomena (Martin et al., 2008; Yankov, 2003).

The enzymatic hydrolysis of inulin by means of the inulinase enzyme is a valid alternative for the production of fructose (Ricca et al., 2007, 2009a). In a previous work, some of the authors of the present paper developed a kinetic model capable to describe the native enzyme enzymatic hydrolysis taking into consideration some of the main difficulties related to the peculiar characteristics of the

substrate-enzyme system (Ricca et al., 2009b). In a subsequent paper inulinase enzyme was covalently immobilized on Sepabeads ® and its activity was tested (Basso et al. 2010).

The present paper deals with inulin hydrolysis catalyzed by inulinase enzyme chemically immobilized on the external surface of spherical beads. As a polymeric substrate, inulin inherent characteristics are the variability of the molecular weight, MW, (or, equivalently, of the degree of polymerization, DP) and polydispersity. These features influence transport phenomena and kinetics involved in enzymatic catalysis: indeed, each inulin molecule diffuses from the reaction medium to the catalyst and reacts on the catalyst surface depending on its own molecular weight. Moreover this MW spectrum changes all along the reaction progress.

The aim of the present paper is to establish the convenience of using immobilized enzymes for inulin hydrolysis. In this process, the mass transport limitations are considered a crucial feature and investigated on an experimental basis in order to establish the process feasibility.

To clarify the phenomena involved in the analyzed reaction, a fundamental modeling of the biocatalytic kinetics is provided and the real effect of mass transport on overall kinetics is quantified. The model allows to determine the drawbacks deriving from mass transport limitations and to establish to what extent they could be counterbalanced by the above described advantages of immobilization.

2.Materials and methods

2.1 Design of experiments

The experimental runs were designed to test the immobilized enzyme performance activity and stability. To test the enzyme activity the quantification of both enzyme intrinsic kinetics and mass transfer resistances was accomplished. The enzyme intrinsic kinetics was observed in the reaction limited regime (RLR), i.e. the experimental runs were conducted under experimental conditions of negligible diffusive resistances. The preliminary identification of both RLR and diffusion limited regime (DLR) was performed analyzing the batch runs summarized in Tab. 2a; these experiments were conducted applying the initial velocity method (Levenspiel, 1972).

	Operating conditions			
	T [°C]	$e_{a,0}$ [kg/m^3]	S_0^0 [kg/m^3]	n [rps]
RLR and DLR identification	40	1.0	8.1	2-5-8.3-11.7-13.3-18.3
	50	1.0	8.1	11.7-13.3-18.3
	60	1.0	8.1	11.7-13.3-18.3

Tab. 2a. RLR and DLR identification: initial velocity batch runs experimental conditions

The range for the changes of the variables reported in Tab. 2a were defined according to the following criteria. The temperature range, pH and substrate initial concentration values were chosen according to the previous literature works dealing with the inulin enzymatic hydrolysis (Ettalibi & Baratti, 1990; Ricca et al., 2009b; Zittan, 1981). The initial concentration of supported enzyme was set equal to 1kg/m^3; this concentration value guaranteed the complete enzyme suspension within the reaction medium in all the exploited experimental conditions. The stirring rate was varied in the range 2-18.3 rps; actually, it was observed that below 2 rps, the reacting mixture was not well mixed; whereas, above 18.3 rps the enzyme stuck at the reactor walls.

With reference to Tab.2a, for each chosen operating temperature several batch runs were performed under constant enzyme and substrate initial concentrations and changing the reactor stirring rate that was increased until a constant reaction rate region was found. This region actually corresponds to a process whose rate is limited by the kinetics (Satterfield, 1969). First of all, the RLR was identified at 40°C (stirring rate higher than 11.7 rps); then, the validity of the same stirring rate range was verified at the temperatures of 50 and 60°C.

In the identified RLR, the influence of substrate concentration and temperature on the reaction rate was investigated conducting experimental batch runs at the operating conditions reported in Tab. 2b. Even in this case, the batch runs were conducted according to the initial velocity method.

	Operating conditions			
	T [°C]	$e_{a,0}$ [kg/m^3]	S_0^0 [kg/m^3]	n [rps]
S_0^0 and T dependence	40	1.0	4.9-6.5-8.1-12.15	13.3
	50	1.0	4.9-6.5-8.1-12.15	13.3
	60	1.0	4.9-6.5-8.1-12.15-12.15-20.3-32.4 48.8	13.3

Tab. 2b. Initial velocity batch runs experimental conditions: substrate concentration and temperature dependence of reaction rate

The substrate concentration range exploited in the experiments of Tab.2b was chosen to guarantee the inulin solubility at each temperature.

Enzyme stability was investigated in terms of activity decay as a function of temperature. At each investigated temperature, once chosen the values of enzyme and substrate concentrations, the enzyme was used in subsequent batch runs: the followed experimental procedure is described in more detail in section 2.2 and the corresponding experimental conditions are reported in Tab 2.c.

	Operating conditions			
	T [°C]	$e_{a,0}$ [kg/m^3]	S_0^0 [kg/m^3]	N [rps]
Thermal deactivation tests	40	5.0	8.1	5.0
	50	5.0	8.1	5.0
	60	5.0	8.1	5.0

Tab. 2c. Batch runs experimental conditions: Enzyme activity thermal decay

The stirring rate of the experiments of Tab.2c was chosen to minimize the enzyme mechanical stress.

The importance of mass transfer on the process observed rate was evaluated from initial velocity experiments conducted in the pre-identified DLR (Tab.2d).

	Operating conditions			
	T [°C]	$e_{a,0}$ [kg/m^3]	S_0^0 [kg/m^3]	n [rps]
Mass transport limitations	50	1.0	8.1	2-5-8.3-11.7-13.3-18.3

Tab. 2d. Evaluation of mass transfer resistance effects

All the reaction runs reported in Tab. 2a-d were conducted following the initial velocity method thus giving only a partial description of the enzyme behavior: to extend the validity of the kinetic analysis, time course tests were conducted in both the control regimes, DLR and RLR(Tab 2e).

		Operating conditions			
		T [°C]	$e_{a,0}$ [kg/m^3]	S_0^0 [kg/m^3]	n [rps]
MW dependent model validation	RLR	50	1.0	4.9	13.3
		50	1.0	6.5	13.3
		50	1.0	8.1	13.3
		60	1.0	12.2	13.3
		60	1.0	20.3	13.3
		60	1.0	32.4	13.3
	DLR	40	1.0	8.1	2

Tab. 2e. Experimental conditions in time course batch runs

The time course tests allowed to evaluate all the time dependent effects, i.e. the enzyme thermal and shear stress deactivation and the molecular weight decrease during the reaction course; both these aspects should affect significantly the transport phenomena and the kinetics.

The immobilized enzyme behavior, described by experiments of Tab.2a-e, was compared with that of the native enzyme so as to test the profitability of the inulinase immobilization. The native enzyme kinetic behavior was derived as a reference by the work of Ricca et al. (2009a).

2.2 Experimental procedure

2.2.1 Experiments conducted using native enzyme

Inulin extracted from chicory roots (average DP = 28) was used as substrate (Sigma-Aldrich, Italy).

The enzyme was the commercial liquid Fructozyme LTM ,(r = 1.13 g/mL) kindly provided by Novozymes A/S (Denmark) with a declared activity of 2000 U/g.

The initial velocity tests were conducted in a batch reactor with a reaction volume of 100 mL, held in a temperature-controlled bath with roto-translational external mixing (OLS, Grant). The reaction time was chosen to keep conversions lower than 8%. The enzyme concentration was 550 U/L, pH 5.0. The range of temperature values considered was 40–60 °C. Inulin concentrations were investigated in the range of 3–60 g/L.

The concentrations of the reaction products, i.e. fructose and glucose, were determined by HPLC (Jasco,) equipped with a refractive index detector (RI 930, Jasco). The mobile phase was orthophosphoric acid/water 0.1% (v/v) (Fluka), fed at a flow rate of 1 ml/min; the column was a Supelcogel C-610H (Sigma-Aldrich) (2009a).

2.2.2 Experiments conducted using immobilized enzyme

Inulinase enzyme was immobilized on Sepabeads (Basso et al., 2010) (Mitsubishi, Italy), kindly provided by Sprin Technologies (Italy). The enzyme was covalently bonded to the support and a series of tests was performed on the supernatant in order to verify that no enzyme leakage occurred during reaction and sampling (data not shown).

The experiments of Tabs. 2a-e were carried out according to the following procedure. The same inulin powder described in paragraph 2.2.1 was initially dissolved in an acetate buffer solution (acetic acid-sodium acetate 0.2 M, pH 5) prepared using reagent grade chemicals (Sigma-Aldrich). Inulin was added to the buffer solution and heated up to the reaction temperature; in the meantime, the enzyme was mixed with a certain volume of buffer and gradually acclimatized from 4°C (storage temperature) to the reaction temperature. When both enzyme and substrate mixtures reached the reaction

temperature they were mixed together in the bioreactor and the reaction started: the total reaction volume was equal to $2 \cdot 10^{-4}$ m^3 for each experiment. The batch reaction runs were performed in a $5 \cdot 10^{-4}$ m^3 batch fermenter (Autoclavable fermenter, Biotron), consisting of a glass vessel with a six-blade impeller, equipped with temperature, pH and mixing rate digital controllers (ADI 1030, Applikon). The reaction progress was monitored sampling $1.2 \cdot 10^{-6}$ m^3 of the reaction medium at fixed time intervals by means of a syringe equipped with a $90 \cdot 10^{-6}$ m filter that allowed retaining all the supported enzyme, thus stopping the reaction course.

In the initial velocity tests (Tab 2.a,b,d), the duration of each batch run and the sampling interval were chosen so as to keep inulin conversion well lower than 8%.

In complete time course tests (Tab. 2d), the reaction progress was followed for 420 minutes, sampling 8 times at 0, 10, 15, 30, 60, 120, 240 and 420 minutes.

In order to investigate the enzyme deactivation, an experimental procedure aimed at the enzyme separation and at its reusing in subsequent reaction cycles was developed. For each set of experimental conditions reported in Tab. 2c, five reaction cycles of 24 hours each were performed adding inulin powder at the end of each cycle. The reaction progress was monitored and the initial velocity was registered for each reaction run. The residual enzymatic activity was eventually evaluated starting from the calculated initial velocity corresponding to each reaction cycle.

The same analytical techniques described in paragraph 2.2.1 were used to determine the products concentration.

3. Model development

To interpret and predict the true behavior of the system under study, a comprehensive fundamental model, accounting for the importance of both mass transfer phenomena and kinetics, was formulated. In a previous paper, Ricca et al. (2009a) demonstrated the reliability of Michaelis-Menten model to describe the kinetic behavior of native inulinase during initial velocity tests.

To develop the present theoretical model, it was assumed that Michaelis-Menten kinetic equation could be exploited to describe the dependence of reaction rate on inulin concentration also with inulinase covalently bound to Sepabeads surface. The Michaelis-Menten kinetic parameters, k_2 and K_m, were expressed as functions of operating temperature according to an Arrhenius-type equation (Ricca et al., 2009a). In addition, due to the polymeric nature of the substrate and to the enzyme-substrate complex

affinity, it was assumed that the Michelis constant, K_m, depended also on the inulin molecular weight according to a the relationship reported in Eq.2 (Ricca et al, 2011).

$$\boldsymbol{k_2 = k_{2,0} e^{-\frac{E_{a,2}}{RT}}} \quad \text{Eq. 1}$$

$$K_m = K_{m,0} e^{-\frac{E_{a,m}}{RT}} \cdot MW^{0.376} \quad \text{Eq. 2}$$

Finally, the residual activity of the enzyme, e_a, was expressed as a function of time according to a first order deactivation model in the following form:

$$\boldsymbol{e_a = e_a^0 \exp(-k_d t)} \quad \text{Eq. 3}$$

The kinetic parameter k_d was related to the operating temperature according to Arrhenius equation:

$$k_d = k_{d,0} \exp\left(\frac{-E_{a,d}}{RT}\right) \quad \text{Eq. 4}$$

As a result, the proposed kinetic model had the following form:

$$-\frac{dS_0}{dt} = \frac{k_{2,0} e^{-\frac{E_{a,2}}{RT}} e_a^0 \exp\left[-k_{d,0} \exp\left(\frac{-E_{a,d}}{RT}\right) t\right] S_0}{K_{m,0} \cdot e^{-\frac{E_{a,m}}{RT}} \cdot MW^{0.376} + S_0} \quad \text{Eq. 5}$$

Actually, Eq. 5 is capable of describing the true system behavior only when the process rate is controlled by kinetics and the resistance to mass transfer occurring outside the biocatalyst is negligible. In real cases, a concentration gradient between the bulk and the catalyst surface does exist and has to be accounted for in order to properly estimate the overall process rate. According to *Nernst diffusion layer* theory (Bailey and Ollis, 1986), it can be assumed that this concentration gradient is confined within a stagnant film surrounding the catalyst. Therefore, the mass flux, N_s, reaching by diffusion the catalyst surface can be expressed as:

$$\boldsymbol{N_s = k_s (S_0 - S)} \quad \text{Eq.6}$$

On biocatalyst surface, where no accumulation occurs, the mass flux of substrate is equal to the rate of substrate consumption, r_s, referred to the unit surface of supported biocatalyst:

$$\boldsymbol{k_s (S_0 - S) = -r_s} \quad \text{Eq.7}$$

r_s, however, can be expressed according to the Michaelis Menten equation, which, with reference to the whole reactor volume, has the following form:

$$k_s(S_0 - S)a_b = k_c(S_0 - S) = \frac{V_{max}S}{K_m + S} \quad \text{Eq.8}$$

The solution of Eq.8 provides the dependence of substrate concentration on biocatalyst surface, S, on both kinetic parameters and mass transfer coefficient.

The following set of dimensionless variables is introduced:

i. $x = \frac{S}{S_0}$, dimensionless substrate concentration;

ii. $\chi = \frac{K_m}{S_0}$, reciprocal of the saturation ratio;

iii. $Da = \frac{V_{max}}{k_c S_0}$, Damkoehler number, comparing the maximum reaction rate to the maximum mass transfer achievable in the film surrounding the biocatalyst

Using these dimensionless variables, Eq.8 can be rewritten in a dimensionless form as:

$$\frac{1 - x}{Da} = \frac{x}{\chi + x} \quad \text{Eq.9}$$

The solution of Eq. 9 provides the dependence of dimensionless substrate concentration x, upon χ and Da, i.e. $x = f(\chi, Da)$.

The influence of external mass transport resistance on the observed reaction rates was finally estimated by means of effectiveness factor, η, defined as the ratio between the observed reaction rate and the reaction rate that would be obtained with no mass-transfer resistance (Kheirolomoon et al., 2002; Levenspiel, 1972; Satterfield, 1969). In the present case, the effectiveness factor was expressed, according to Eq. 9, as:

$$\eta = \frac{\frac{x}{\chi + x}}{\frac{1}{\chi + 1}} = \eta(\chi, Da) \quad \text{Eq.10}$$

In determining the effectiveness factor, the estimation of the mass transfer coefficient actually represented a preliminary step. Boon-Long et al. (1978) proposed a synthetic classification of all the variables affecting mass transfer in a baffled vessel equipped with a six-bladed disc turbine (the standard laboratory system used to estimate mass transfer coefficient). They found that the effect of: 1) the geometry of the vessel-turbine system; 2) the properties of solid particles; 3) the properties of the liquid medium, e.g. density and viscosity, 4) the dynamic conditions used to guarantee the suspension of the solid particles, could be expressed as a unique semi-empirical correlation relating the Sherwood number, *Sh*, to a set of proper variables:

$$Sh = f\left(\mathrm{Re}, \frac{T}{d}, Ga, Sc, U, Mv\right) \qquad \text{Eq. 11}$$

The available correlations usually assume a simplified form, known as the Froessling's equation:

$$Sh = A + B\,\mathrm{Re}_p^n\,Sc^m \qquad \text{Eq. 12}$$

that can be considered as a particular case of Eq. 11.

In the present work, the correlation proposed by Levins, 1969:

$$Sh = 2 + 0.44 \cdot \mathrm{Re}^{0.504} \cdot Sc^{0.385} \qquad \text{Eq. 13}$$

i.e.

$$\frac{kc * d_p}{D} = 2 + 0.44 * \left(\frac{n \cdot d^2}{v}\right)^{0.504} \left(\frac{v}{D}\right)^{0.385} \qquad \text{Eq. 14}$$

was exploited to estimate the mass transfer coefficient. Eq. 14 was chosen since it is based on the application of Kolmogoroff's theory of local isotropic turbulence, one of the most used theory to explain the mechanism of particle-liquid mass transfer in agitated vessels.

The diffusion coefficient, *D*, appearing both in the Sherwood and in the Schmidt numbers was expressed as a function of both the substrate molecular weight and the reaction temperature.

For linear polymers and, in particular, for fructo-oligosaccharides, like inulin, Viel et al. (2003) proposed the following relationship:

$$D \propto MW^{-0.5} \qquad \text{Eq. 15}$$

Starting from a known value of diffusion coefficient value, D_{MW_1}, at a specific molecular weight value, MW_1, the unknown diffusion coefficient, D_{MW} at a generic molecular weight, MW, was, therefore, calculated as:

$$\frac{D_{MW}}{D_{MW_1}} = \left(\frac{MW_1}{MW} \right)^{0.5} \quad \text{Eq. 1}$$

As far as the dependence of D on temperature was concerned, the Stokes –Einstein equation, relating the diffusion coefficient to the properties of the solute-solvent system, was adopted:

$$D = \frac{kT}{6\pi r \mu} \quad \text{Eq. 1}$$

The applicability of this correlation to macromolecular system was widely verified by Viel et al. (2003), Pluen et al. (1999), Schimpf et al.(1987).

Before formulating the complete model accounting for both mass transfer and kinetics, it is worthwhile discussing about the effect of inulin molecular weight on the actual process rate. At the beginning of a specific reaction run, inulin is characterized by a definite spectrum of MWs, expressed in terms of a mean value and a variance; both these parameters, however, are subjected to a change as the reaction progresses. As a consequence, both the Michaelis constant and the diffusion coefficient at a specific reaction time should be calculated as average values considering the actual evolution of molecular weights spectrum. This procedure, even if rigorous, is cumbersome and time consuming since it would require the determination of the true molecular weights spectrum at each reaction time. To simplify the numerical complexity of the model, it would be desirable that the Michaelis constant and the diffusion coefficient could be expressed as a function of the average value of molecular weights spectrum only.

With this aim, it was assumed that the molecular weight of the considered inulin (DP = 28) could be represented as a log-normal distribution (Tomasik, 2003). Under this hypothesis, the true Michaelis constant, $K_{m|distributionMW}$, could be easily calculated and its value compared to that, $K_{m|averageMW}$, estimated considering only the average value of inulin molecular weight corresponding to the same DP of 28. Actually, the calculated value of percentage error between $K_{m|distributionMW}$ and $K_{m|averageMW}$ was lower than 6%. The same procedure was adopted to estimate the diffusion coefficient, D; in this case, the calculated value of the percentage error between $D_{|distributionMW}$ and $D_{|averageMW}$ was lower than 3.5% due to the milder dependence of diffusion coefficient on inulin molecular weight. The rigorous

estimation of the dependence of both K_m and D on substrate MW was, therefore, simplified considering two relationships that were expressed in terms of the average value of inulin molecular weight, $\overline{MW}$, and not of its distribution:

$$K_m \propto \overline{MW}^{\,0.376} \qquad \frac{D_{\overline{MW}(t)}}{D_{MW_1}} = \left(\frac{MW_1}{\overline{MW}(t)} \right)^{0.5} \qquad \text{Eq. 18}$$

On the basis of the above discussion, Eq. 5 was rewritten to account also for the effect of external mass transfer resistance as:

$$-\frac{dS_0}{dt} = \eta(\chi, Da) \cdot \frac{k_{2,0} e^{-\frac{E_{a,2}}{RT}} e_a^0 \exp\left[-k_{d,0} \exp\left(\frac{-E_{a,d}}{RT} \right) t \right] S_0}{K_{m,0} \cdot e^{-\frac{E_{a,m}}{RT}} \cdot MW^{0.376} + S_0} \qquad \text{Eq. 19}$$

Eq. 19 was numerically solved by a Runge-Kutta 7th-8th order implemented in Maple.

4.Results and discussion

The behavior of the immobilized enzyme was initially compared to that of the native enzyme. To properly perform this comparison, two batch reaction runs were carried out at the same operating conditions and using the same protein loading. The reactions were followed until the charged substrate was completely converted and the obtained results are summarized in Fig.1. As expected, the immobilized enzyme was characterized by a lower activity as compared to native enzyme: the complete substrate conversion was indeed achieved in a batch time of 4.5 hours and of 5.5 h, respectively with native and immobilized enzyme. Actually immobilization was responsible for a certain activity loss of the enzyme; at each sampling time, in fact, the native enzyme exhibited a higher conversion . However this effect becomes less significant at higher values of substrate conversion. In particular, the target of complete conversion, at the operating condition reported in Fig.1, was reached in 4.5 hours using native enzyme; at the same batch time the immobilized enzyme was capable to convert the 95% of the substrate thus not determining a significant loss of performance.

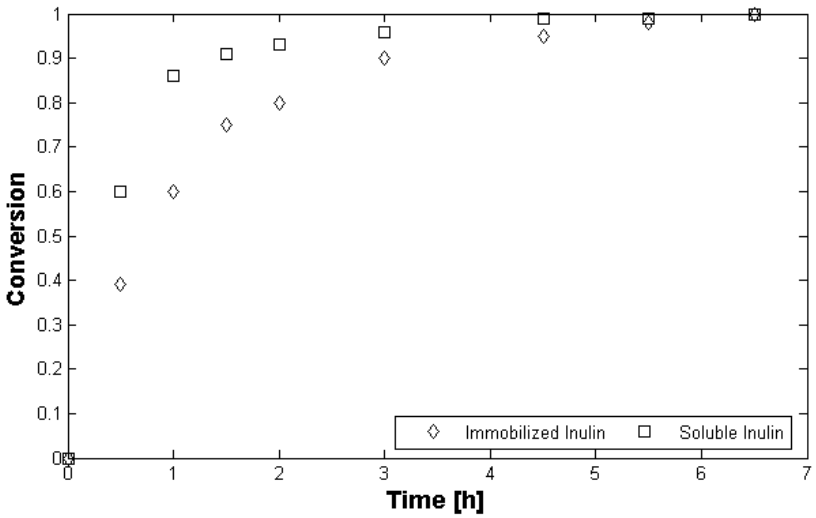

Fig. 1 Immobilized vs. Soluble on the same protein loading basis. S_0=9g/l, DP=6.4, E_0=2.84 $mg_{protein}$/l

The behavior of the present form of immobilized inulinase was, therefore, worth to be investigated more in detail so as to characterize its kinetics in as wider as possible range of operating conditions. The first step of this kinetic characterizations was represented by the identification of the DLR and RLR , according to the procedure described in section 2.1.The obtained results are reported in Fig.2 showing the observed reaction rate as a function of stirring velocity, the remaining operating conditions being kept constant.

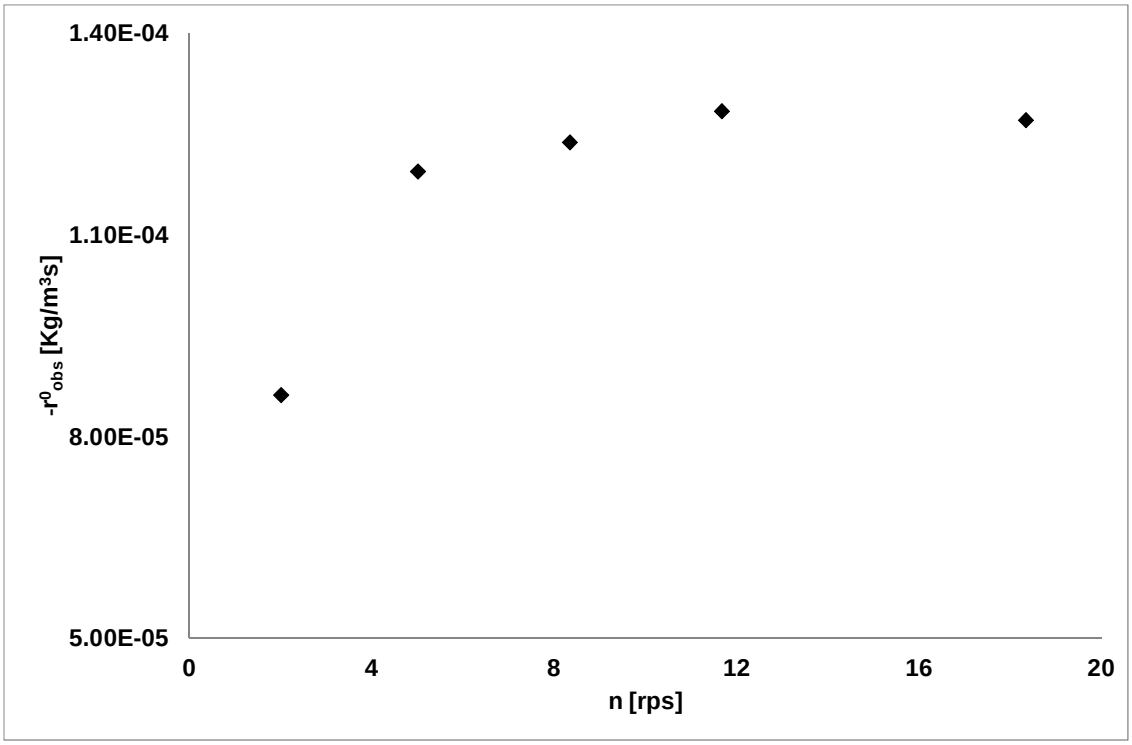

Fig.2. RLR and DLR identification at T=40°C.

The reaction limited regime could be actually identified from the plateau set in the range of 11.7-16.7 rps. A gradual increase of stirring rate does indeed determine a progressive decrease of mass transfer resistances outside the immobilized enzyme, so that, at a certain point, the observed reaction rate equals the intrinsic reaction rate. It is worthwhile remarking that the achievement of a constant reaction rate is to be ascribed to the effect of stirring rate on system behavior since the performed initial velocity tests allow actually excluding any enzyme deactivation.

The operating conditions identifying the reaction/diffusion limited regime should be determined at each operating temperature, which, all the other process parameters being fixed, determines the actual controlling regime. It was therefore verified if the stirring rate range identified at T=40°C could guarantee a reaction limited regime at T= 50 °C and at 60°C as well. The obtained results showed that, in the range 11.7-16.7 rps, the observed reaction rate values did not change between 50°C and 60°C.

Starting from the above-described results, it can be asserted that: a) stirring rate values higher than 11.7 rps make the process rate controlled by kinetics; in these conditions the intrinsic kinetic model can be, therefore, validated; b) when the stirring rate is lower than 11.7 rps, both kinetics and mass transfer

contributions are to be considered in order to correctly estimate the observed reaction rate.

The Michaelis Menten kinetic model was validated in the case of an operating stirring rate of 13.3 rps, verifying the dependence of the intrinsic reaction rate on some key factors for the process under study, namely the substrate concentration and the operating temperature.

The dependence of reaction rate on substrate initial concentration was investigated by the initial velocities method, performing the batch runs summarized in Tab. 2a. In Fig. 3 the experimental results obtained at the temperature of 40°C are reported. The initial reaction rate corresponding to each investigated value of substrate initial concentration was determined applying the differential method of data analysis (Levenspiel,1972);

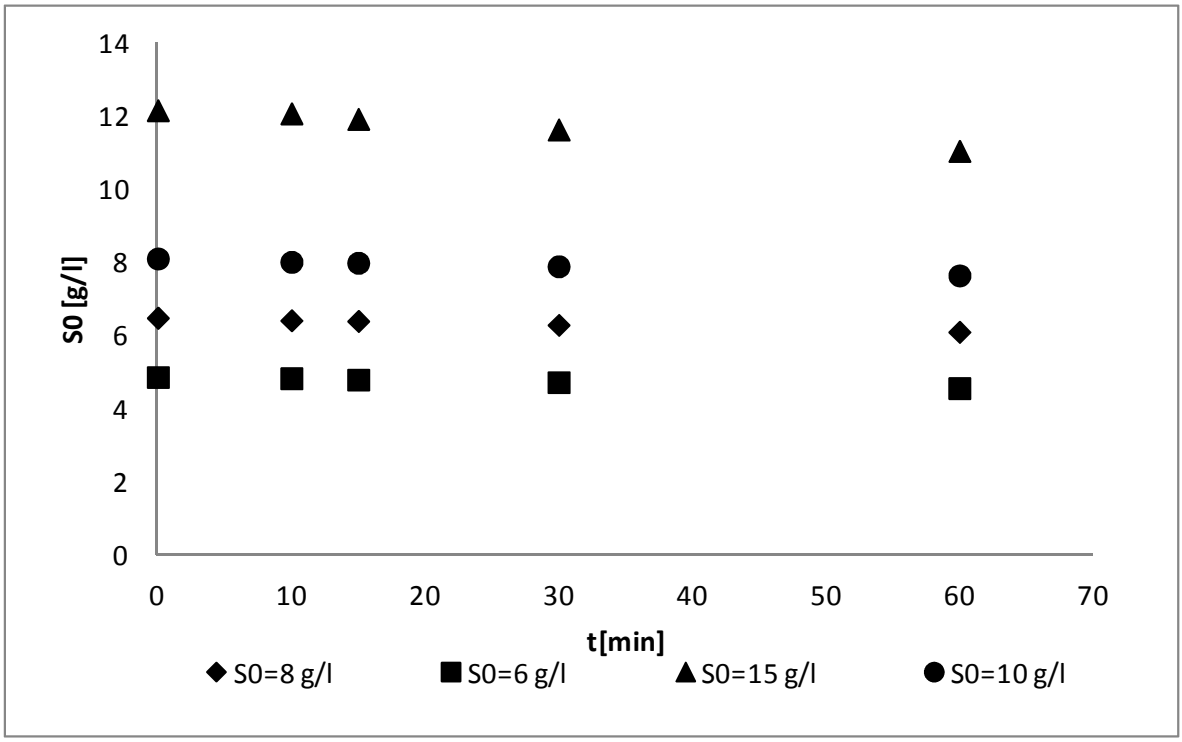

Fig.3 Initial velocity tests at T=40°C.

the validity of Michaelis-Menten model was then verified according to the double reciprocal Lineweaver-Burk (DRLB) plot. Fig.4 shows the DRLB plot obtained at the three exploited temperatures. Actually, the Michelis Menten model can be considered as appropriate to interpret the system behavior, as demonstrated by the remarkable agreement existing with the collected

experimental data and by the high value of R^2= 0.992. Similar results were obtained also at the other two operating temperatures (T = 50°C and T = 60°C) .

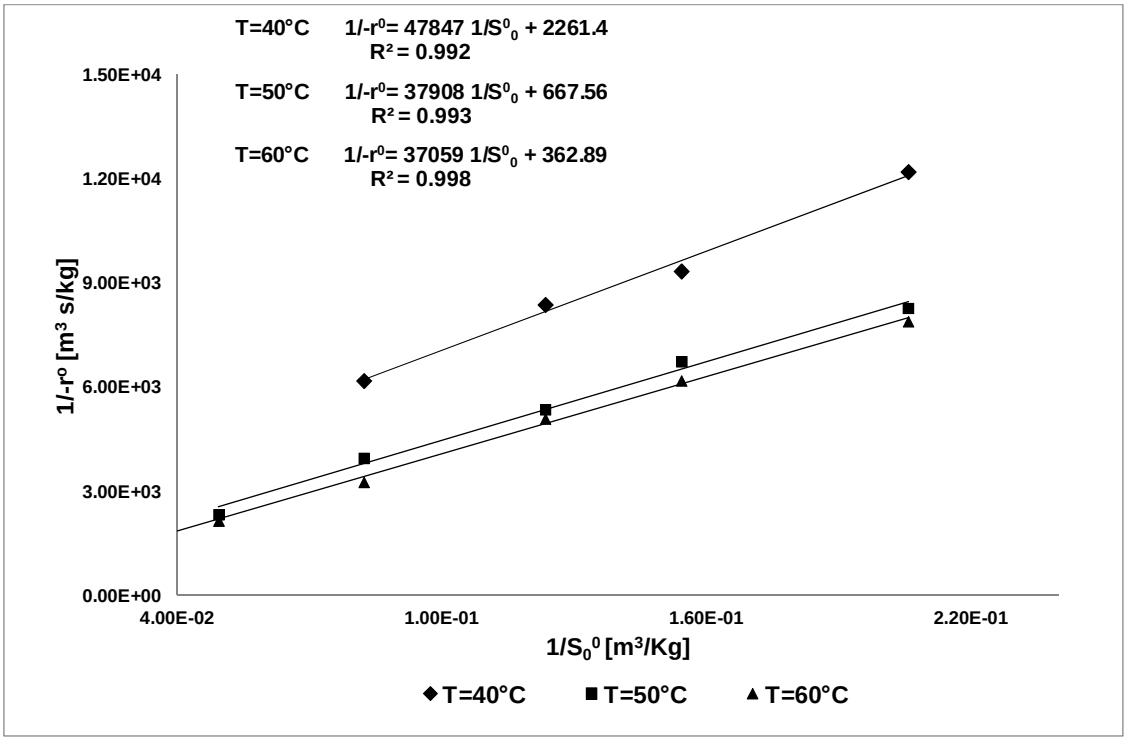

Fig.4. Lineweaver-Burk plots

The corresponding Michaelis-Menten model kinetic parameters were reported in Tab. 3 together with the values that, exploiting an Arrhenius model, allow expressing both k_2 and K_m as a function of the operating temperature.

T [°C]	K_m [kg_{sub}/m^3]	V_{max} [kg_{sub}/m^3 s]
40	21.2	$4.42\ 10^{-4}$
50	56.8	$1.5\ 10^{-3}$
60	102	$2.75\ 10^{-3}$

Kinetic parameter	$E_{a,i}$ [J/mol]	$\ln k_o$
k_2[kg_{sub}/kg_{enz} s]	$7.95\ 10^4$	22.9
$K_m \left(\frac{kg_{sub}}{m^3_{reactor}}\right)$	6.84 E+04	26.2

Tab. 3. Kinetic parameters values.

As far as the enzyme thermal deactivation was concerned, the results obtained according to the procedure described in section 2.2.2, suggested, as expected, that thermal deactivation occurred to a very limited extent in the considered time window (till t = 420 min) even when an operating temperature of 60 °C was chosen to perform the experimental runs. Therefore, the active enzyme concentration was hereafter considered constant and equal to enzyme initial concentration. This assumption was already proved by Ricca et al. (2009a), who found that, after 200 minutes and at an operating temperature of 60°C, enzyme in its native form did actually lose 42 % of its initial activity, whereas immobilized enzyme did not show any appreciable activity decay. This result confirms once again that the immobilization significantly improves the enzyme stability, thus counterbalancing the activity reduction that, as compared to native enzyme, was frequently observed.

On the basis of the previous considerations, the predictions of the theoretical model already described in section 3 were compared with the experimental data collected during the time course tests reported in Tab.2e. The considered tests gave a precise indication of the actual time evolution of inulin molecular weight and of the influence of this parameter on both kinetics and mass transfer.

The model validation as a function of substrate initial concentrations is reported in Figs. 5-6, respectively for an operating temperature of 50 °C and of 60°C. The reported comparisons were obtained under a set of operating conditions resulting in a kinetically controlled process rate, i.e. when, due to the negligibility of mass transfer limitations, the effectiveness factor reaches a unity value and only the effect of MW variation on kinetics could actually be appreciated. An almost perfect agreement between the experimental data and the model predictions was observed, thus confirming the model reliability in predicting the time evolution of substrate and its effect on kinetics.

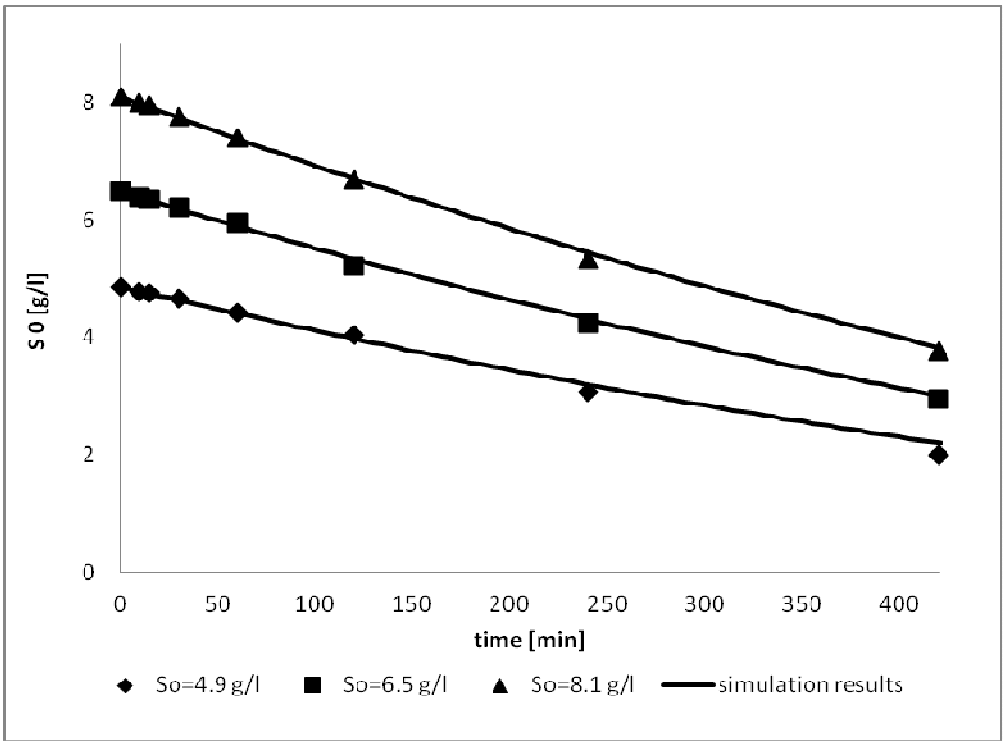

Fig.5. Simulation results and experimental points. Operating conditions: T=50°C; n=13.3 rps.

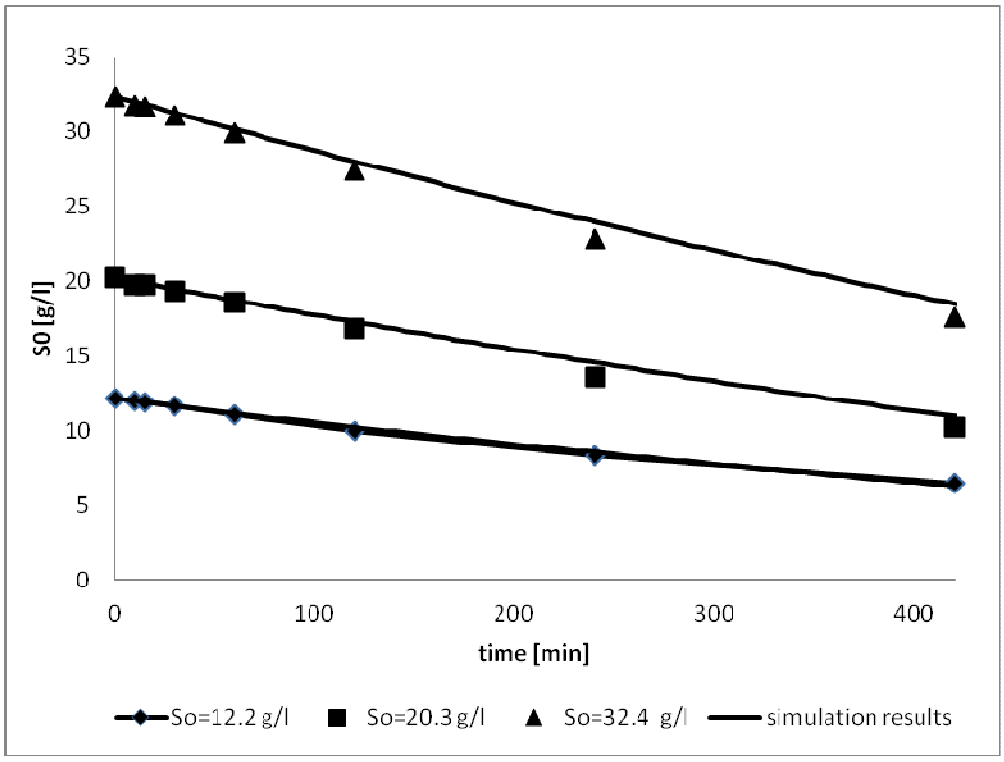

Fig.6. Simulation results and experimental points. Operating conditions: T=60°C; n=13.3 rps.

With the aim of widening the model validity domain, its forecasting ability was tested even during a time course batch run characterized by an average value of effectiveness factor significantly lower than unity, with significant mass transfer limitations. The comparison between model predictions and experimental data obtained at two different values of operating temperature are reported in Fig. 7.

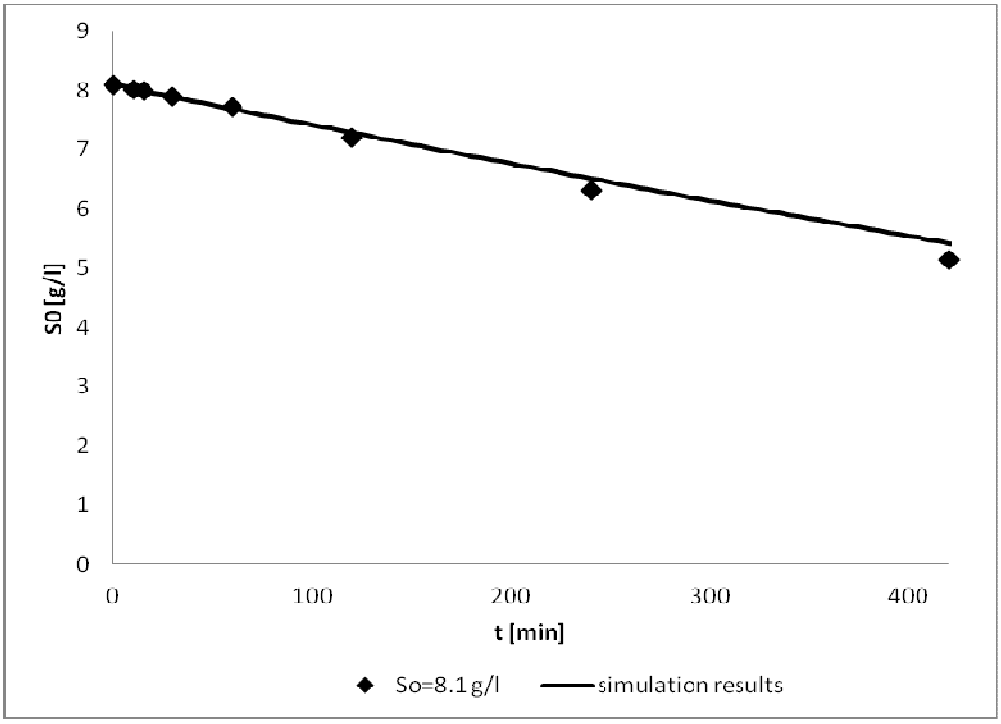

Fig.7. Simulation results and experimental points. Operating conditions: T=40°C; n=2 rps.

The model capability of predicting the observed system behavior is confirmed, as demonstrated by the remarkable agreement existing between the experimental points and the simulation results. Moreover it is worthwhile remarking that, in all the tested cases, the model prediction never overestimated the actual time evolutions of substrate concentration thus definitely validating the assumption of enzyme decay negligibility.

5.Conclusions

A theoretical and experimental analysis of inulin hydrolysis by immobilized enzyme was presented. The enzyme performance was tested in a range of process conditions having a physical significance,

showing that the model performance resulted very satisfying in all the experimental conditions exploited during both the model development phase and during its validation, thus testifying a proper assemblage of all the modeling components expected to converge in the complete model; moreover the model is capable to disentangle and to quantify all the phenomena affecting the observed reaction rate thus allowing a deep interpretation of the phenomena taking place during the reaction.

Even if developed for the specific case of inulin enzymatic hydrolysis, the proposed model was developed following a procedure intentionally kept general so as that, with a proper estimation of the kinetic parameters, it could be applied for modeling the enzymatic hydrolysis of different polysaccharides.

List of symbols

D	diffusion coefficient, $\left(\frac{m^2}{s}\right)$
Da	Damkoehler number, [-]
d_p	enzyme support diameter, [m]
e_a	enzyme concentration, $\left(\frac{Kg_{catalyst}}{m^3_{reactor}}\right)$
e^0_a	initial enzyme concentration, $\left(\frac{Kg_{catalyst}}{m^3_{reactor}}\right)$
$E_{a,2}$	activation energy for the kinetic parameter $k_{2,}$ $\left(\frac{J}{mol}\right)$
$E_{a,2}$	activation energy for the kinetic parameter $k_{d,}$ $\left(\frac{J}{mol}\right)$
$E_{a,m}$	activation energy for the kinetic parameter $\frac{K_m}{MW}$, $\left(\frac{J}{mol}\right)$
g	gravity acceleration $\left(\frac{m}{s^2}\right)$
Ga	$\left(\frac{g \cdot L^3 \cdot \rho^2}{\mu^2}\right)$ Galileo number, [-] where L is the characteristic length.

k	*Boltzman* constant, $\left(\frac{J}{K}\right)$
k_2	Kinetic constant of the Michaelis Menten equation, $\left(\frac{Kg_{substrate}}{m^3_{reactor} \cdot Kg_{catalyst}}\right)$
$k_{2,0}$	k_2 pre-exponential factor, $\left(\frac{Kg_{substrate}}{m^3_{reactor} \cdot Kg_{catalyst}}\right)$
k_c	mass transport coefficient $\left(\frac{1}{s}\right)$
k_d	deactivation constant $\left(\frac{1}{s}\right)$
$k_{d,o}$	k_d pre-exponential factor $\left(\frac{1}{s}\right)$
K_m	Michealis constant, $\left(\frac{kg_{substrate}}{m^3_{reactor}}\right)$
$K_{m,0}$	K_m pre-exponential factor, $\left(\frac{kg_{substrate}}{m^3_{reactor} Da}\right)$
k_s	mass transport coefficient, $\left(\frac{m^3_{reactor}}{s \cdot m^2_{catayst}}\right)$
Mv	$\left(\frac{\rho_s - \rho}{\rho}\right)$, density group, [-]
MW	Substrate molecular weight, [Da]
n	mixing rate (rps)
N_s	mass flux per unit time and area, $\left(\frac{mol}{s \cdot m^2_{catalyst}}\right)$
R	universal gas constant, $\left(\frac{J}{mol \cdot K}\right)$
r	
Re	Reynolds number, [-]

r_s	rate of substrate consumption, $\left(\frac{mol}{s \cdot m^2_{catalyst}}\right)$
S	substrate concentration at the solid-liquid interface, $\left(\frac{Kg_{substrate}}{m^3_{reactor}}\right)$
Sc	$\left(\frac{\mu \cdot D}{\rho}\right)$ Schmidt number, [-]
Sh	Sherwood number, [-]
S_o	substrate concentration in the bulk fluid, $\left(\frac{Kg_{substrate}}{m^3_{reactor}}\right)$
S_0^0	initial substrate concentration in the bulk fluid, $\left(\frac{Kg_{substrate}}{m^3_{reactor}}\right)$
T	temperature, [°C]
U	Solid concentration, $\left(\frac{Kg}{m^3}\right)$
V_{max}	maximum rate of substrate consumption, $\left(\frac{Kg_{substrste}}{s \cdot m^3_{reactor}}\right)$
χ	inverse of the saturation ratio, [-]
x	Dimensionless substrate concentration, [-]
η	Effectiveness factor, [-]
μ	fluid viscosity $[Pa \cdot s]$
ρ	fluid density $\left(\frac{kg}{m^3}\right)$
υ	cinematic viscosity $\left(\frac{m^2}{s}\right)$

References

Bailey, J. E. and Ollis, D. F., 1986. Biochemical Engineering Fundamentals, McGraw-Hill Book Co., Singapore.

Basso, A., Spizzo, P., Ferrario, Knapic, L., Savko, N., Braiuca, P., Ebert, C., Ricca, E., Calabrò, V.,

Gardossi, L. Endo- and Exo-Inulinases: Enzyme-Substrate Interaction and Rational Immobilization. Biotechnol. Prog., 2010, Vol. 26, No. 2

Boon-Long, S., Laguerie, C., Couderc J. P., 1978. Mass transfer from suspended solids to a liquid in agitated vessels. Chemical Engineering Science 33, 813-819

Ettalibi, M. and Baratti, J. C., 1990. Molecular and kinetic properties of Aspergillus ficuum inulinase. Agric. Biol. Chem. 54, 61–68

Garcia, T., Coteron. A., Martinez, M., Aracil, J., 2002. Kinetic model for the esterification of oleic acid and cetyl alcohol using an immobilized lipase as catalyst. Chemical Engineering Science 55, 1411-1423

Kamin, R. A., Wilson, G. S., 1980. Rotating ring-disk enzyme electrode for biocatalysis kinetic studies and characterization of the immobilized enzyme layer. Analytical Chemistry 52: 1198-1205.

Kheirolomoom, A., Khorasheh, F., Fazelinia, H., 2004. Influence of external mass transfer limitation on apparent kinetic parameters of penicillin G. acylase immobilized on nonporous ultrafine silica particles. Journal of Bioscience and Bioengineering, 93: 125-129.

Khorashes, F., Kheirolomoom, A., Mirashghi, S., 2002. Application of an Optimization Algorithm for Estimating Intrinsic Kinetic Parameters of Immobilized Enzymes. Journal of Bioscience and Bioengineering 94(1), 1-7.

Levenspiel, O., 1972. Ingegneria delle reazioni chimiche, Ambrosiana, Milano.

Levins D. M., Glastobyry, J. R., 1969. Application of Kolmogoroff's theory to particle-liquid mass transfer in agitated vessels. Chemical Engineering science 27, 537-543

Martin, M., Montes, F. J., Galan, M. A., 2008. Bubbling process in stirred tank reactors II: Agitator effect on the mass transfer rates. Chemical Engineering Science 63, 3223-3234.

Pangarkar, V. G.,Yawalkar, A. A., Sharma, M. M., Beenackers, A. A., 2002. Particle-Liquid Mass Transfer Coefficient in Two/Three-Phase Stirred Tank Reactors. Industrial and Engineering. Chemical. Research 41, 4141-4167.

Pluen, A., Netti, P. A., Jain, R. K., Berk, D. A., 1999. Diffusion of macromolecules in agarose gels: Comparison of Linear and globular configurations. Biophysical Journal 77, 542-552.

Ricca, E., Calabrò, V., Curcio, S., Iorio, G., 2007. The state of the art in the production of fructose from inulin enzymatic hydrolysis. Critical Reviews in Biotechnology 27, 129-145.

Ricca, E., Curcio, S., Calabrò, V., Iorio, G., 2009a. Optimization of inulin hydrolysis by inulinase accounting for enzyme time-and-temperature dependent deactivation. Biochemical Engineering Journal 48, 81-86.

Ricca, E., Calabrò, V., Curcio, S., Iorio G., 2009b. Fructose production by chicory inulin enzymatic hydrolysis: A kinetic study and reaction mechanism. Process Biochemistry 44, 466-470.

Ricca, E., Curcio, S., Calabrò, V., Iorio, G., 2011. Inulin properties effect on the rate of Hydrolysis by immobilized inulinases. Personal communication

Satterfield, C., 1969. Mass transfer in heterogeneous catalysis, the MIT press, Boston.

Schimpf, M. E., Giddings, J. C., 1987. Characterization of thermal diffusion in polymer solutions by thermal field-flow fractionation: effects of molecular weight and branching. Macromolecules, 20, 1561-1563.

Seong, G. H., Heo, J., Crooks, R. M., 2003. Measurement of enzyme kinetics using a continuous-flow microfluidic system. Analytical Chemistry 75, 3161-3167.

Tomasik P, 2003. Chemical and functional properties of food saccharides. CRC press, USA.

Viel, S., Capitani, D., Mannina, L., Segre, A. L., 2003. Diffusion-ordered NMR spectroscopy: A versatile tool for the molecular weight determination of uncharged polysaccharides. Biomacromolecules 4, 1843-1847.

Yankov, D., 2004. Diffusion of glucose and maltose in polyacrylamide gel. Enzyme and Microbial Technology 34, 603-610.

Zittan, L. 1981. Enzymatic hydrolysis of inulin-an alternative way to fructose production. Starch. 33, 373–377.

CHAPTER 2

MODELING OF FOOD-INDUSTRY PROCESSES

Introduction

In this chapter the papers dealing with modeling of food-industry processes are sequentially reported as:

Paper 6: *Advanced modeling of food convective drying: a comparative study among fundamental, artificial neural networks and hybrid approaches* published in *Food Engineering*, Eds. Brendan-Siegler, Nova Publisher, 2010.

Paper 7: *Advanced modeling of food convective drying: artificial neural networks and hybrid approaches*, published on *Food and Bioprocess Technology*, DOI 10.1007/s11947-010-0477-3.

Paper 8: *A theoretical model for the control of color degradation and microbial spoilage occurring in food convective drying.* Submitted for an oral presentation to the 20th International Congress of Chemical and Process Engineering, CHISA 2012, Prague.

Drying is a typical food-industry process aimed at food preservation. Drying has to be performed under strictly controlled conditions since the resulting food characteristics must respect the safety standards imposed by the regulations. Moreover, the control of the process strongly influences the quality of the final product and consequently its success in the market. Within this frame, modeling actually represents the first, but necessary, step that allows optimizing and controlling food drying process.

During food drying, the reduction of food water content is achieved by exposing the food to dry and warm air: a simultaneous mass and heat transfer is achieved and the actual rates of these transport phenomena depend on both temperature and concentration differences between food material and air, as well as on the air velocity. The fundamental modeling of drying consists in the formulation of

transport models aimed at analyzing the simultaneous transfer of momentum, of heat and of water (both as vapour and as liquid), occurring in air as well as in food; under a mathematical point of view, these models result in a complex system of unsteady-state, non-linear partial differential equations that have to be solved by means of numerical methods, thus implying a high computation effort. For this reason the possibility to describe the drying process by using neural networks was exploited in paper 6 and 7.

In paper 6, four different modeling approaches for drying kinetics were reported. Being a book contribution, the authors' aim was to propose a range of model possibilities for drying kinetics giving a detailed analysis of all the presented approaches and highlighting, for each of them, all the advantages and the drawbacks.

In paper 7, a comparison between the neural and the hybrid models was performed so as to describe the so-called drying kinetics. The performance of both the models was tested with reference to two different vegetables and two different food geometries, showing that the predictions provided by the developed hybrid neural models were more reliable than those given by a pure neural network model.

Paper 8 is an extended abstract submitted to CHISA 2012. The aim of the work was to propose a control strategy to improve food drying process; in particular, choosing as reference parameters the microbial spoilage and the colour degradation, the optimal trajectory of drying operating conditions should be identified and, subsequently, followed by a proper defined control system. A first-principle model for the drying process was developed with the aim to relate the reference parameters to the drying operating conditions; it will be used to test different control strategies on the drying process.

2.1 Paper 6. Advanced modeling of food convective drying: a comparative study among fundamental, artificial neural networks and hybrid approaches

In this contribution, four different modeling approaches were compared in describing drying kinetics. After a description of the phenomena involved in food drying, the formulation of each of the analyzed approaches was reported. The comparison among the four developed models was performed on the basis of the agreement between the model predictions and the experimental points obtained during lab-scale convective drying of slab-shaped carrots. The obtained results confirmed the reliability of hybrid neural models, developed as a combination of an ANN with a very simple analytical model, and suggested a possible exploitation of HNM for process optimization and control applications.

Advanced Modeling of Food Convective Drying: A Comparative Study Among Fundamental, Artificial Neural Networks and Hybrid Approaches

Stefano Curcio[4], Maria Aversa[5] and Alessandra Saraceno[6]

Department of Engineering Modeling – University of Calabria

Via P. Bucci - Cubo 42/A - 87036 Arcavacata di Rende (CS) – ITALY

Mathematical modeling represents an effective support to design and control industrial processes. Different approaches can be used to develop reliable models aimed at investigating how system responses may change, with time, under the influence of both external disturbances and manipulated variables. In the present chapter, it will be shown how various kinds of advanced models, based either on fundamental, or on artificial neural networks or on hybrid modeling, can be used to predict the behavior of a typical industrial process: the convective drying of food. The main aims of convective

[4] Email: stefano.curcio@unical.it
[5] Email: maria.aversa@unical.it
[6] Email: alessandra.saraceno@unical.it

drying are a decrease of food water content and an increase of its temperature; both the above effects improve food preservation since microbial spoilage is favored by low temperature and high moisture content. Drying does actually preserve foods by decreasing water activity, thus stopping the micro-organisms growth. If food drying is performed in uncontrolled conditions, the level of water content could be not sufficiently low to stop the activity of micro-organisms, which continue proliferating. The starting point of any kind of automatic control is definitely represented by the availability of a predictive model of the process under study.

Fundamental or theoretical modeling is based on the formulation of transport models analyzing the simultaneous transfer of momentum, of heat and of water (both as vapor and as liquid), occurring in air as well as in food. An exhaustive analysis of all the complex transport phenomena involved in drying process, however, is rather onerous and time consuming for practical purposes, since the resulting system of non-linear partial differential equations can only be solved by means of numerical methods. Moreover, some physical transformations involved in drying process are not yet completely understood and, therefore, are very difficult to interpret by proper mathematical relationships. For the above reasons, several simplified approaches have been proposed to describe food convective drying.

On the other hand, a model based on Artificial Neural Networks (ANNs) does not make use of any transport equation that could help to determine, on the basis of fundamental principles, the mutual relationships existing between the inputs and the outputs. ANNs, in fact, are a data-driven method capable to learn from examples and represent a particularly useful tool to describe tough phenomena since no *a priori* knowledge is required. ANNs are composed of interconnected computational elements, called neurons or nodes. Each neuron receives input signals from the related units, elaborates these stimuli by an activation or transfer function and, eventually, generates an output signal, which is transferred to other neurons. A neural model is, generally, rather complicated, since it requires a large number of connections and, therefore, a great number of parameters that are to be estimated. Moreover, it is worthwhile observing that since extrapolation based on ANN predictions is an unreliable procedure, it is often necessary to perform many different experiments in order to train the network in a range as wider as possible of practical situations.

A good trade-off between a theoretical and a “pure” neural network approach is represented by hybrid modeling, which allows predicting the behavior of complex systems, in a more efficient way. Hybrid model predictions are indeed given as a combination of both theoretical and “pure” neural network

models, together concurring in the obtainment of system responses. The main advantage of a hybrid system regards the possibility to describe some well-assessed phenomena by means of a quite simple fundamental approach. Some others, that could be very difficult to interpret, are, instead, described by rather straightforward “cause-effect” models, based on ANN.

1.1 Models Formulation

1.1.1 Fundamental Modeling

When dry and warm air flows around a moist and cold food sample, a simultaneous transfer of both heat and water occurs. Heat is transferred from air to the material; water is transported from the food core, then to its surface and, eventually, to air. The rates of heat and mass transfer depend on both temperature and concentration differences and, also, on air velocity field. Convective drying is definitely the most common method for food preservation, so several different approaches were proposed to model this process. The models available in the open literature may be subdivided in two categories: simplified and complex approaches. The latter are based on the formulation of transport models analyzing the simultaneous transfer of momentum, of heat and of water (both as vapor and as liquid), occurring in air as well as in food; the former, instead, are quite simple and are based either on simplification hypotheses, not applicable in several real cases, or on the utilization of empirical correlations, necessary to estimate - by means of a set of transport coefficients – the heat and water fluxes at food-air interface(s). On developing fundamental models aimed at predicting the convective drying behavior, the solid foods are, generally, regarded as porous hygroscopic materials containing a great amount of physically bound water [1]. Hygroscopic materials are characterized by a limit moisture content below which internal vapor pressure, expressed in terms of both moisture content and temperature, is lower than that of liquid water at the same temperature [2]. Unbound water, on the other hand, exerts its full vapor pressure and is mostly held in the voids of the solid. Water removal from hygroscopic substances is a rather complex phenomenon, since both unbound and bound water are actually to be transported; in fact, once unbound water has been removed, a significant amount of bound water may still be present. Generally, bound water is removed by progressive vaporization within the solid matrix, followed by diffusion and pressure driven transport of water vapor through the solid [1]. An exhaustive analysis of all the complex transport phenomena involved in the drying

process was regarded as being too onerous and time consuming for practical purposes [3]. For this reason, many simplified approaches were proposed to model either the moisture transport only [4-6] or the simultaneous transfer of heat and moisture occurring during food drying [7, 8], even accounting for the variation of physicochemical properties of the food material [9]. The simultaneous presence of both liquid water and vapor within the solid makes drying modeling even more difficult [10]. Datta and his coworkers have already presented detailed and general multiphase models describing different heat and mass transfer processes in foods (convective heating, baking, frying, microwave heating, etc.) for which internal evaporation may play a significant role [1, 11-15]. Attention in Datta's papers, however, was focused on the formulation of transport models analyzing only food behavior; the transport phenomena occurring at food-air interfaces were described in terms of heat and mass transfer coefficients, estimated from the available literature data. To a certain extent, this might limit the model accuracy since, as reported in the literature [16, 17], even small errors in the estimation of transfer coefficients could lead to large deviations between predicted and real values, thus determining inappropriate equipment design or severe processing problems. In general, it would be advisable to account also for the transport phenomena occurring in the drying air in order to estimate the actual transport rates at the food/air interfaces without resorting to any empirical correlation [18, 19]. This is particularly necessary when food shape is not regular or it even changes with time because of, for instance, shrinkage. In a previous paper [18], some of the authors of this contribution actually formulated a complete theoretical model describing convective food drying. The model accounted for the simultaneous transfer of momentum, heat and mass in air as well as of heat and mass transfer within the food; the attention, however, was focused on the analysis of those cases characterized by very weak inner evaporation, which, therefore, was neglected. Moisture transport inside the food was modeled referring to an effective diffusion coefficient that did not make any distinction between the transport of liquid water, usually expressed in terms of a capillary diffusion coefficient, and that of vapor, expressed by a molecular diffusion coefficient [1]. In a subsequent improvement [20], another model was developed so to simulate drying behavior also when inner evaporation could not be neglected and a unique mass balance equation, expressing the transport of total moisture in food, was actually inadequate to describe properly the process. In particular, a multiphase approach, based on the conservation of both liquid water and vapor, was adopted. Moreover, the turbulent momentum transfer of drying air, considered as a gas mixture owing to its relative humidity always different from zero,

was described by the k-ω model [21], which – as compared to the k-ε model used in [18] – allowed improving the model predictions, especially in the boundary layer developing close to the food surfaces. The k-ω approach does, indeed, have several advantages that are related to its higher accuracy in boundary layer modeling, to the easier integration due to a proper definition of a viscous sub-layer and to the more accurate description of the transition occurring close to the solid boundaries [21]. Both the general transport models [18 and 20] led to a rather complicated system of unsteady partial differential equations whose solution, performed by the Finite Elements Method, allowed predicting the drying behavior of foods available in all shapes and over a wide range of process and fluid-dynamic conditions.

Both the mathematical and the numerical complications involved in the solution of a complete and general model, as those presented in [18] and in [20], may suggest developing, however, much simpler models.

To allow an appropriate comparison among the different approaches presented in the present contribution, a transport model describing the simultaneous bi-dimensional heat and moisture transfer occurring within the food sample only will be formulated so to analyze the influence of some of the most important operating variables on carrots drying rate [22]. In the following, the main assumptions and the mathematical equations used to model, by a simplified fundamental approach, the unsteady-state behavior of a convective dryer will be shown. It was supposed that drying air was continuously supplied to the dryer inlet section and flowed around the food in the axial direction (y), parallel to its main dimension (Figure 1**)**. Heat and mass transfer resistance were assumed negligible across the net on which the vegetable was placed [23-24]. On the basis of the above hypothesis, the system under investigation could be considered as a classical symmetric one; a symmetry axis, in fact, might be identified and only half of the original domain was taken in consideration. Moreover, any possible variation occurring with reference to the spatial coordinate *z* was assumed not relevant for the present study. This allowed analyzing a 2D geometry so that food sample could be considered as a slab. Each dependent variable was expressed as a function of two spatial coordinates, *x* and *y*, and of time, *t*.

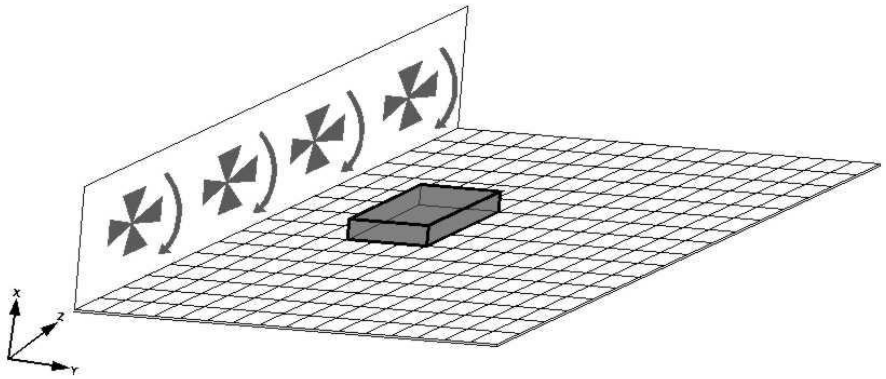

Figure 1. Schematic representation of the dryer under study.

The model accounted for the variation of air and food physical properties, defined in terms of the local values of temperature and of moisture content. As far as the food sample was concerned, a continuum approach was chosen; it was supposed, in fact, that the actual multiphase hygroscopic porous medium could be replaced by a fictitious continuum, any point of which had variables and parameters, which were continuous functions of point spatial coordinates and of time. Convective contributions in the transport equations written for the food were neglected, assuming weak inner evaporation. Therefore, heat and mass transfer in the product occurred only by conduction and diffusion, respectively. Shrinkage effects were assumed negligible in the range of average moisture content taken in consideration.

On the basis of the above discussion, water and heat transfers occurring during food drying process were modeled by the unsteady state mass and energy balances, respectively, whereas evaporation, occurring at air-food interfaces only, was considered by defining a proper set of boundary conditions expressed in terms of heat and mass transfer coefficients estimated by the semi-empirical correlations available in the literature [25].

The energy balance in the solid, based on the Fourier's law, led to

$$\rho C_p \, \partial T / \partial t = \underline{\nabla} \bullet \left(k_{eff} \, \underline{\nabla} T \right) \tag{1}$$

where ρ was the food density, C_p was its heat capacity, T was the temperature, t was the time and k_{eff} the effective thermal conductivity of food.

The mass balance, based on the Fick's law, led to:

$$\partial C / \partial t = \underline{\nabla} \bullet \left(D_{eff} \underline{\nabla} C \right) \tag{2}$$

where C was the water concentration in food and D_{eff} the effective diffusion coefficient of water in food. The subscript *eff* represented the condition that food transport properties were evaluated as effective indexes, thus accounting for a possible combination of different transport mechanisms occurring in the food.

Supposing that the above material parameters and transport properties (ρ, C_p, k_{eff}, D_{eff}), in the most general case, depended on the local values of food moisture content and of temperature, Eqs. 2-3 formed a system of unsteady, non-linear partial differential equations (PDEs). The expressions of ρ, C_p, k_{eff}, D_{eff}, as derived by Ruiz-López, Córdova, Rodríguez-Jimenes, García-Alvarado [26] in the case of carrot slices, were used.

Table 1. Correlations used to estimate carrots properties [26]

$\rho = 440 + 90 \cdot X$	[Kg/m^3]
$C_p = 1750 + 2345 \cdot \left(X / 1 + X \right)$	[J/(Kg K)]
$k_{eff} = 0.49 - 0.443 \cdot \exp(-0.206 \cdot X)$	[W/(m K)]
$D_{eff} = 2.8527 \cdot 10^{-10} \exp(0.2283369 \cdot X)$	[m^2/s]

The initial conditions were straightforward since it was assumed that before drying process actually began (t = 0), food moisture content and its temperature had definite values, i.e. C_0 and T_0, that were specified before performing each simulation.

The boundary conditions relative to Eq. 2, applied to each external surface of the food sample, where no accumulation occurred, expressed the physical condition that the heat transported by convection from air to food was partially used to raise sample temperature by conduction and partially to allow free water evaporation:

$$h(T_{db} - T_s) = -\underline{n} \bullet \left(-k_{eff}\, \underline{\nabla} T\right) - \lambda \cdot N_s \qquad (3)$$

where λ was the latent heat of vaporization for water, N_s was the diffusive flux of water at the food surface, h was the heat transfer coefficient, T_{db} was air dry bulb temperature, T_s was the temperature at the food surface; $\underline{n}$ was a generic unity vector normal to the surface.

The boundary conditions relative to Eq. 3, applied to each external surface of food sample, where no accumulation occurred, expressed the balance between the diffusive flux of liquid water transported from the product core to the surface and the flux of vapor that left the food surface and was transferred to the drying air:

$$-\underline{n} \bullet \left(-D_{eff}\, \underline{\nabla} C\right) = k_c \left(C_i - C_{gb}\right) \qquad (4)$$

where k_c was the mass transfer coefficient, C_{gb} was the bulk concentration of water in air, C_i was the water concentration evaluated in gaseous phase at the food/air interface.

An equilibrium relationship between the water concentration in the air and the water concentration on the food surfaces actually exposed to the drying air, was also formulated [27]:

$$\gamma_w\, x_w\, f_w = \hat{\phi}_w\, y_w\, p \qquad (5)$$

The superscripts *v* and *l* (vapor and liquid, respectively) were omitted with the understanding that γ_w, the activity coefficient of water and f_w , the fugacity of water, were referred to the liquid phase; $\hat{\phi}_w$, the fugacity coefficient of water, was instead referred to the vapor phase. x_w and y_w were the molar fractions of water in food and in air, respectively, p was the pressure within the drying chamber. The fugacity of water was expressed by:

$$f_w = \phi_w^{sat}\, P_w^{sat} \exp\left[\frac{V_w\left(p - P_w^{sat}\right)}{RT}\right] \tag{6}$$

where P_w^{sat} was the vapor pressure of water, expressed in terms of the local values of temperature; the exponential term reported in eq. 6 is known as the Poynting factor.
Introducing the quantity Φ_w:

$$\Phi_w = \frac{\hat{\phi}_w}{\phi_w^{sat}} \exp\left[-\frac{V_w\left(p - P_w^{sat}\right)}{RT}\right] \tag{7}$$

The following relationship was obtained:

$$\gamma_w\, x_w\, P_w^{sat} = \Phi_w\, y_w\, p \tag{8}$$

At low pressures (up to at least 1 bar), vapor phase usually approximated ideal gases ($\hat{\phi}_w = \phi_w^{sat} = 1$) and the Poynting factor differed from unity by only a few parts per thousand; moreover, the values of $\hat{\phi}_w$ and ϕ_w^{sat} differed significantly less from each other than from unity and their influence in Eq. 8 tended to cancel. Thus, the assumption that $\Phi_w = 1$ introduced a little error for low-pressure vapor-liquid-equilibrium (VLE) and allowed simplifying Eq. 8 to:

$$\gamma_w\, x_w\, P_w^{sat} = y_w\, p \tag{9}$$

It is worthwhile observing that in hygroscopic materials, like most of the foods, the parameter γ_w accounts for the effects related to the amount of physically bound water so it is usually expressed as a function of both food moisture content and of its temperature [26]. Once the activity coefficient was known for the particular food under examination, Eq. 9 allowed calculating the molar fraction of water in the vapor phase and, therefore, the value of C_i appearing at the right-hand side of the above Eq. 5.

As it will be specified in the following, heat and mass transfer coefficients were estimated on the basis of the well-known semi-empirical correlations (Figure2, Table 2) expressing the dependence of Nusselt number upon Reynolds and Prandtl numbers and, by means of the Chilton-Colburn analogy, of Sherwood number on Reynolds and Schmidt numbers, respectively [25]. The above described fundamental model made use of three different correlations, one for each of the surfaces exposed to drying air, to evaluate the local values of heat transfer coefficients from the Nusselt number, *Nu*, expressed in terms of characteristic Reynolds, **Re**, Prandtl, **Pr**, and Grashof, ***Gr***, numbers [25, 28].

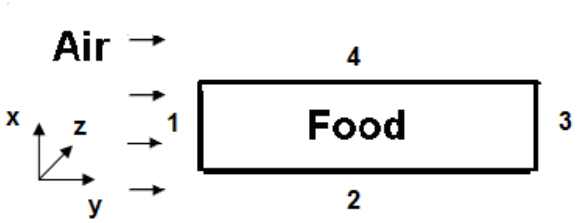

Figure 2. Schematic representation of the carrots sample.

Table 2. Semi-empirical correlations used to estimate heat transfer coefficients on each food surface

Boundary	Semi-empirical relationship	Definition of dimensionless numbers
Impact surface (identified as boundary 1)	$Nu_x = 0.25\,\mathrm{Re}_x^{0.588}\,\mathrm{Pr}^{1/3}$	$Nu_x = h_{x\|1} \cdot x / k_a$; $\mathrm{Re}_x = \rho_a \cdot u_0 \cdot x / \eta_a$
Surface parallel to air flow (identified as boundaries 2 and 4)	$Nu_y = 0.648\,\mathrm{Re}_y^{0.5}\,\mathrm{Pr}^{1/3}$	$Nu_y = h_{y\|2,4} \cdot y / k_a$; $\mathrm{Re}_y = \rho_a \cdot u_0 \cdot y / \eta_a$
Rear surface (identified as boundary 3)	$Nu_x = 0.59\,(\mathrm{Pr} \cdot Gr_x)^{1/4}$	$Nu_x = h_{x\|3} \cdot x / k_a$; $Gr_x = x^3 \cdot \rho_a \cdot g \cdot \Delta\rho_a / \eta_a^2$

The Prandtl number was defined as $\mathrm{Pr} = {C_{pa} \cdot \eta_a}/{k_a}$. In the previous relationships, *x* and *y* defined the local position on each of the food surfaces; $h_{(x,y)|i}$, characterized by a numeric subscript (*i*) corresponding to each boundary, was the local value of heat transfer coefficient; u_0 was air velocity at the inlet section of the drier; *g* was the acceleration of gravity. All the physical and transport properties defining each dimensionless number were evaluated at film conditions (the subscript *f* was omitted). It is worthwhile observing that, as far as the rear face of food sample was concerned, the Nusselt number was actually expressed in terms of the Grashof number since it was supposed that air circulation in proximity to boundary 4 was so limited that free convection prevailed over forced convection. Once the heat transfer coefficients was estimated, the Chilton-Colburn analogy was used to calculate the mass transfer coefficients referred to each corresponding boundary [25].

1.1.2 Thin-layer Model

Other kinds of simplified approaches were proposed in the literature to model the drying process of vegetables. Among these models, the so-called *thin-layer equation* [29-32] is actually the most common. The *thin-layer equation* is based on the assumption that moisture decrease is proportional to the instantaneous difference between material moisture content (assumed uniform within the food) and the moisture content in equilibrium with drying air. In addition, the model assumes a uniform temperature distribution within the food sample. The above assumptions led to a unique equation modeling the drying behavior:

$$\frac{dX}{dt} = k \cdot \left(X - X_e\right) \tag{10}$$

where *X* ($\mathrm{Kg}_{\mathrm{water}}$ / $\mathrm{Kg}_{\mathrm{dry\ solid}}$) was the food moisture content on a dry basis, X_e was the moisture content in equilibrium with drying air and *t* was the drying time. The parameter *k* was the so-called *drying constant* and represented a measure of drying process rate; it is a function of material moisture content, of the product size, of the uniform temperature distribution developing in the food and, finally, of air characteristics, i.e. its humidity, temperature and velocity. Several thin-layer models were proposed [32], differing from each other for the number of parameters to be estimated. In the case of Eq. 10, also

known as the “Newton’s model”, only one parameter was considered. Integrating Eq. 10, the following relationship, resulting in an exponential equation according to a pseudo-first order reaction kinetics [29, 33], was obtained:

$$\frac{(X - X_e)}{(X_o - X_e)} = \exp(-k \cdot t) \tag{11}$$

where X_o (Kg $_{water}$ / Kg $_{dry\ solid}$) was the initial moisture content evaluated at t=0. The Newton’s model is usually used by fitting the experimental data, expressed as the time evolution of food moisture content on a dry basis, thus estimating the k value. Because of its main features, the procedure can be applied only when a series of measurements has been actually obtained for a particular drying experiment, whereas it is meaningless when no experimental data exist.

1.1.3 Artificial Neural Network (ANN) Model

Artificial neural networks (ANNs) are a data-driven method capable to learn from examples capturing the functional relationships existing between the input(s) and the output(s). This feature makes ANNs a particularly useful tool to model phenomena difficult to be described by a model-based approach because no a priori knowledge is required. ANNs are composed of interconnected computational elements called neurons or nodes. Each neuron receives input signals from the related units, elaborates these stimuli by an activation or transfer function and generates an output signal that can be transferred to other neurons. Any kind of differentiable mathematical function could be used as neuron activation function, but the most common, due to their forecasting capability, are the sigmoid logistic function, the hyperbolic tangent function and the linear function. Even if the prediction of each single neuron could be imperfect and bias-affected, the outcome of the interconnection(s) among neurons is a computational tool capable to learn from examples and to provide accurate predictions even with examples never seen before [34]. Neurons are organized in a multi-layer structure which allows obtaining the output(s) signal starting from a definite set of the input(s). The interconnection between the nodes takes place by means of a weight, a constant that reflects the strength of the connection that is responsible for the signal propagation. Many different artificial neural network structures were proposed but the most common is the multi-layer perceptron (MLP). A MLP is composed by an input layer that receives the input information about the process, an output layer that produces the

response(s) of the neural network and a certain number of hidden (intermediate) layers that are located between the input and the output layers [35].

To determine the network structure, it is necessary to specify the following information [35]: a) the number of both input and output variables; b) the number of layer (s); c) the number of neurons comprised in each layer; d) the activation function of each neuron. The number of input and output variables is problem-dependent since it is related, respectively, to the number of independent and dependent variables of the problem under consideration. On the contrary, the number of layers and the number of neurons in each layer is the result of an optimization process. Even if several methods were proposed to accomplish this task [36-38], a general procedure was not yet proposed and the network architecture is usually determined according to heuristic guidelines and trial and error procedures. After determining the network architecture, to complete the network definition, it is necessary to perform the so-called neural network training. During the training phase the network learns how to correlate the input to the output variables. More specifically, the network is submitted to a certain number of input and output data and, according to an error minimization algorithm, it changes the network weights values that could be considered as the key elements in which the network knowledge is stored [39]. Only a certain number of the available experimental points are used during the training phase; the remaining experimental points are used during a post-training analysis, called the test phase. During the test phase, the neural network is called to predict the output values corresponding to an input combination never exploited before and, therefore, a set of experimental points that do not belong to the training set. Even if the test phase is a post-training analysis only, it usually plays a fundamental role in the ANN architecture definition; in fact, the convergence of the above-mentioned trial-and-error procedure is usually considered achieved with reference to a performance index just based on test points. The test phase of the network is usually performed in the definition domain in which the training procedure was achieved. As a matter of fact, the forecasting capability of the neural networks outside this definition range cannot be guaranteed; due to the intrinsic black-box nature of neural networks models, the validity domain does indeed strictly depends on the range of data used in model definition [40]. Another kind of post-training analysis about neural network performance, it is the so-called validation phase. Similarly to the test phase, the network is called to predict the experimental points excluded from both the training and the test sets; unlike test phase, the evaluation of model prediction reliability does not influence the definition of neural network architecture.

Some authors developed ANNs models to describe the drying process of different vegetables: carrots [41], ginseng [42], tomato [43], cassava and mango [44]. In the present contribution the forecasting capability of neural networks was utilized so as to predict the time evolution of carrots drying. A preliminary theoretical analysis of the process was carried out with the aim of choosing the input and the output variables that resulted as the most representative of process dynamics. This step holds a fundamental position in neural network definition owing to the black-box nature of neural modeling. The output variables, in fact, should be sufficient to exhaustively describe the process dynamics as well as the input variables should be sufficient to properly predict the time evolution of the chosen output variables.

Drying processes are aimed at water removal from a matrix and, as a consequence, the variable chosen as the neural network output was the moisture content of the carrot sample; actually, the time evolution of dimensionless moisture content, *M(t)*, was considered as more representative of process behavior and, therefore, of major interest as far as drying modeling was concerned:

$$M(t)=\frac{X(t)-X_e}{X_o-X_e} \tag{12}$$

The choice to use a dimensionless form of carrots moisture content was taken so to allow an easy comparison between neural network and thin-layer model predictions. Moreover, by definition, at the beginning of each drying run *M (t=0)* had a value of 1, independently on the sample chosen to perform the experiment.

1.1.4 Hybrid neural model (HNM)

In the previous sections, different alternative modeling approaches of food convective drying were presented showing that the dynamics of the same process can indeed be described in a completely different way. The existence of so many modeling alternatives is due to the intrinsic complexity of the drying phenomenon that involves, from a physical standpoint, a simultaneous transfer of heat and of water (both as liquid and as vapor) taking place by convection, conduction and diffusion.

Theoretical models describe the process dynamics by means of a fundamental approach that usually

results in coupled nonlinear partial differential equations and, as a consequence, in numerical simulations that are time consuming and difficult to be incorporated in an on-line control software.

On the other side, black-box models are able to describe only the input-output dynamics of the process without accounting for any physical relationship characteristic of the system under consideration. Empirical models can approximate the drying kinetics by several line segments, high order polynomials and neural networks: the common characteristic of these models is that they have a narrower validity range but require only a limited number of simple arithmetic operations [45].

A reasonable trade-off between theoretical and empirical approach is represented by hybrid modeling, leading to a so-called "grey-box" model capable of good performance in terms of data interpolation and extrapolation. Hybrid model predictions are given as a combination of both a theoretical and a "pure" neural network approach, together concurring to the obtainment of system responses. The main advantage of hybrid modeling regards the possibility of describing some well-assessed phenomena by means of a theoretical approach, leaving the analysis of other aspects, very difficult to interpret and describe in a fundamental way, to rather simple "cause-effect" models [40, 46-49]. Two kinds of HNMs can be generally defined depending on the interactions existing between the neural and the theoretical blocks. In a model based on a parallel architecture (Figure 3) the inaccuracy in the predicted value from the fundamental part is minimized by the addition of the residuals calculated by the neural network. In a model based on a series architecture (Figure 4) a process variable, which is difficult to measure, is estimated by a neural network and, then, fed to the theoretical block as an input to it. Finally, the output coming out from the fundamental part is checked with the experimental value for convergence.

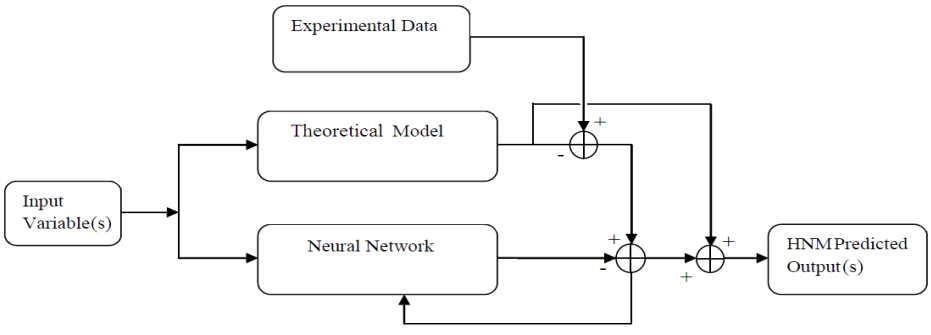

Figure 3. HNM structure based on a parallel architecture.

Even if the hybrid neural approach is, in principle, characterized by a higher generalization capability than artificial neural networks, no specific work dealing with food drying modeling by HNM has been published in the literature.

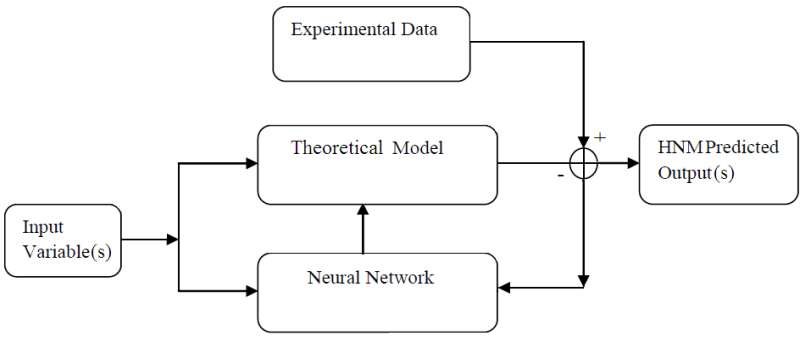

Figure 4. HNM structure based on a serial architecture.

1.2 Models Implementation

1.2.1 Theoretical Model Development

The above-described theoretical model leading to a system of unsteady non-linear partial differential equations (Eqs. 2-3) was solved by the Finite Elements Method (FEM) developed by the commercial package Comsol Multiphysics 3.4. The domain corresponding to food sample was discretized into 3550 triangular finite elements with a thicker mesh close to the boundaries actually exposed to the drying air. The total number of degrees of freedom was equal to about 15000. On a dual core personal computer running under Linux, a typical drying process duration of 5 hours was simulated, on average, in about 2 minutes, using the time-dependent nonlinear direct solver already implemented in the Comsol package. It is worthwhile remarking that the proposed model does not need any parameters adjustment or experimental data from drying experiments. Only the relationships expressing both

physical and transport properties as a function of food temperature and moisture content and the specification of a set of input variables that can be varied within a definite range of physical significance are actually necessary to simulate food drying behavior at different operating conditions.

1.2.2 Experimental Runs

In order to develop the ANN, the hybrid and the thin-layer models, several experiments of carrots drying were performed. Carrot samples of different dimensions were dried by air in a lab-scale convective dryer (Memmert Universal Dryer model UFP 400). The carrots, bought in a local market, were cut in slab shapes. The slab side (L) had an initial value of 30 mm. Three different values of initial slab thickness (d), i.e. 5, 10 and 15mm, were chosen to perform the present experimental analysis thus leading to a total number of three kinds of food samples. For each sample the weight was monitored, with respect to time, by a precision balance (Mettler AE 160), with an accuracy of ± 0.0001 g. The lab-scale dryer allowed monitoring air temperature, by a Dostmann electronic Precision Measuring Instrument (P 655), its humidity (by a rh 071073 probe) and the inlet velocity, by a H 113828 probe. The convective flow of drying air was obtained by a line of fans placed along the edge of dryer internal tray. Two values of air velocities, i.e. 2.8 and 2.2 m/s, and three values of air dry bulb temperature, i.e. 50˚C, 70˚C, 85˚C, were chosen; air absolute humidity, was kept constant throughout all the experiments and equal to 10.32 g water/m^3 dry air. The food samples were placed on a wide-mesh perforated tray. The dryer characteristics allowed analyzing six samples at the same time. Food weight was periodically measured during each experiment; each test was repeated twice to ascertain its reproducibility. The difference between instantaneous food weight and dry solid weight allowed evaluating the total amount of water contained in food. The operating conditions chosen to perform the present experimental analysis are summarized in Table 3.

Table 3. Operating conditions of the experimental analysis

	d = 5mm	d = 10mm	d = 15mm
Air conditions (uo, T)	Run N°	Run N°	Run N°
2.2m/s, 50°C	1	7	13
2.8m/s, 50°C	2	8	14
2.2m/s, 70°C	3	9	15
2.8m/s, 70°C	4	10	16
2.2m/s, 85°C	5	11	17
2.8m/s, 85°C	6	12	18

1.2.3 Thin Layer Model Development

To utilize the thin-layer model (Eq. 10) the experimental results corresponding to each of the performed runs (Table 3) were fitted so as to estimate the drying constant *k*. A commercial curve fitting software package was used to accomplish this task and to calculate all the parameters having a statistical significance. To calculate the moisture content in equilibrium with drying air, X_e, the psychrometric diagram was used. For the fixed value of air absolute humidity in which all the experiments were performed, the X_e values were equal to 0.02014, 0.0094, 0.00576 for the runs performed at an operating temperature of 50, 70 and 85° C, respectively.

1.2.4 ANN Model Development

With the aim to predict the time evolution of carrots moisture content, a set of significant input variables, i.e. the drying time (t), the dry bulb temperature (T_{db}), the air velocity (u_o), the characteristic sample size (d) and the relative humidity (U_r), was identified. From a preliminary sensitivity analysis it was showed that the above variables, among all the parameters that could affect the drying progress, exhibited the highest influence on the transport phenomena involved in the process and, therefore, on its performance. The input-output structure of the developed neural model is reported in Figure 5.

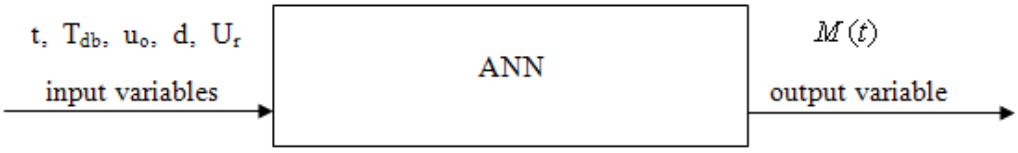

Figure 5. Neural model structure.

After specifying the input-output structure of the model, the neural network architecture was defined and the training procedure was set-up: the experimental points relative to the 18 drying runs, were randomly split into three groups, reserving 2/3 of data (12 runs) to the training phase, 1/6 of the remaining data (3 runs) were used to test the predictions of the neural network during its development, whereas the residual 3 runs were used to validate the ANN predictions in three conditions never exploited neither during learning, nor during test. A multi-layer perceptron (MPL) feed-forward architecture with a pyramidal structure, having a decreasing number of neurons from input to output layer, was developed and implemented by Matlab Neural Network Toolbox, Ver. 4.0.1. To train each of the tested networks, thus estimating their weights and their biases, the Bayesian regularization was used [39]. The neuron transfer function was a hyperbolic tangent for both input and intermediate layers, whereas a linear transfer function was chosen for the output layer.

The choice of the “best” network architecture was realized by a trial-and-error procedure as it is suggested in the literature [50, 51]. The number of hidden levels and the number of neurons belonging to every single layer were determined through iterative cycles according to the block diagram shown in Figure 6.

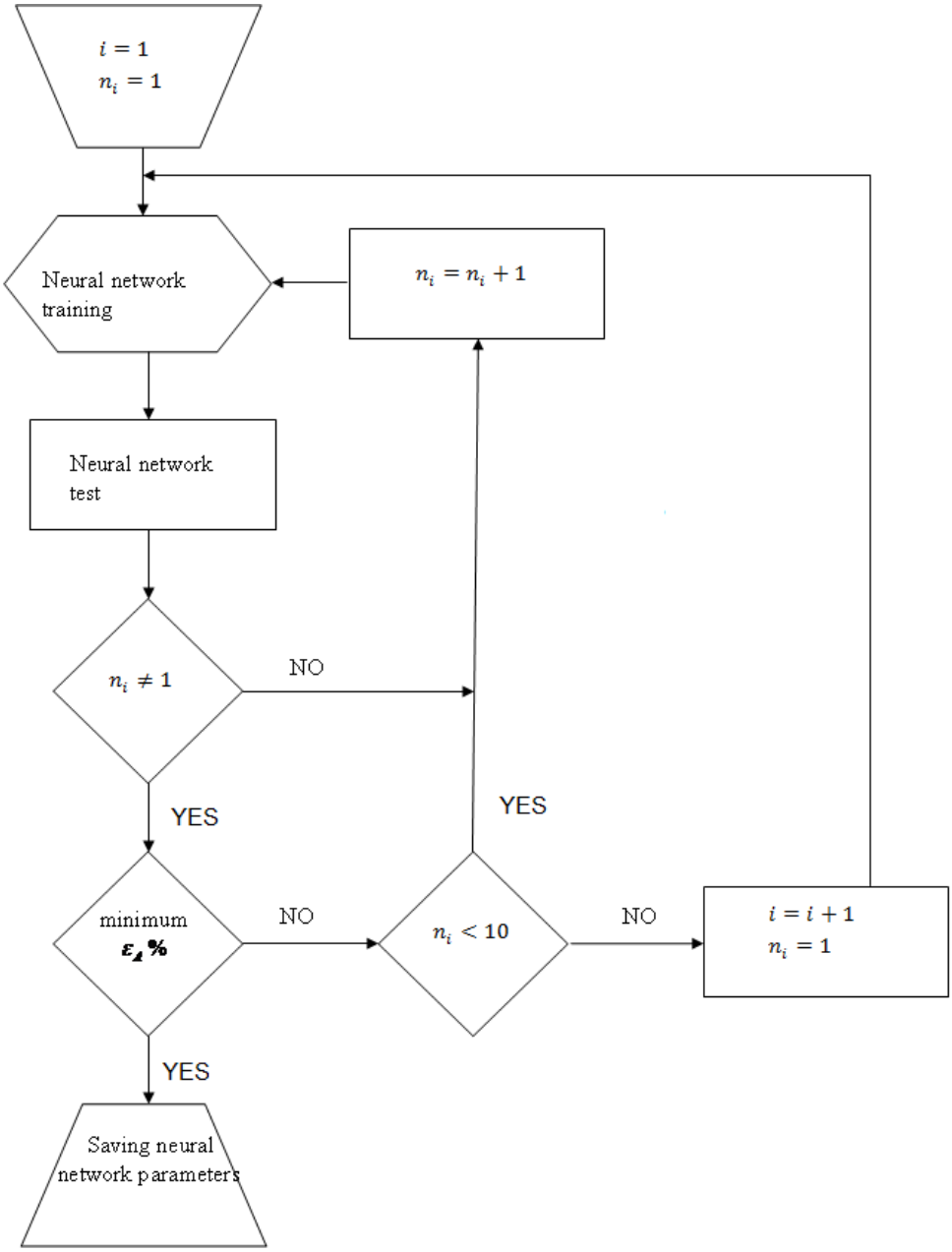

(i: generic hidden layer, n_i: number of neurons in the i^{th} layer)

Figure 6. Algorithm for ANN development.

It was supposed that the procedure convergence was achieved when, during the test phase, the percentage average error (calculated on the basis of the whole test dataset) between the predictions of the neural model and the corresponding experimental points,

$\left(\varepsilon_A\% = \frac{\left| M(t)_{\exp} - M(t)_{ANN1} \right|}{\min(M(t)_{\exp} - M(t)_{ANN1})} \cdot 100 \right)$ reached a minimum, set equal to 10%. On the basis of the above-described iterative procedure a neural model, ANN1, was eventually developed; it consisted of three different layers, according to a rather simple architecture (Figure7):

- An input layer with five neurons;
- A single hidden layer containing two neurons;
- A single neuron output layer.

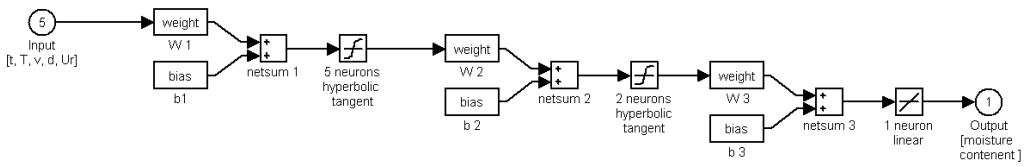

Figure 7. ANN1 structure.

The training procedure reached convergence within 196 epochs, i.e. the number of iteration of the back-propagation algorithm; the sum of squared errors (SSE) registered during the training phase was equal to $4.9 \cdot 10^{-2}$.

1.2.5 Hybrid Neural Model Development

The choice to model the drying process by means of a hybrid neural model HNM could be considered as a consequence of a critical analysis of the other approaches (theoretical and empirical) presented in the previous sections to model convective drying of foods. This analysis showed the inherent limits of both theoretical and empirical models in describing vegetables drying. Theoretical models, in fact, implied the utilization of rather complicated numerical methods, whereas “cause-effect” models did not make use of any fundamental equation that, instead, might be helpful to achieve a more precise knowledge of the dynamic process under study. On developing the “theoretical” part of a HNM, in

general, it should be advisable to adopt rather simple equation(s) so as to avoid the introduction of additional difficulties related to the solution of the equations. On the basis of the above consideration, the HNM was realized coupling a rather simple theoretical relationship, as represented by the solution of thin-layer model (Eq. 12) and a neural network aimed at determining, by the estimation of a model parameter (the drying constant *k*), the relationship between the process rate and the operating variables influencing drying behavior. Finally, the chosen model architecture was a classical serial model structure (Figure 8).

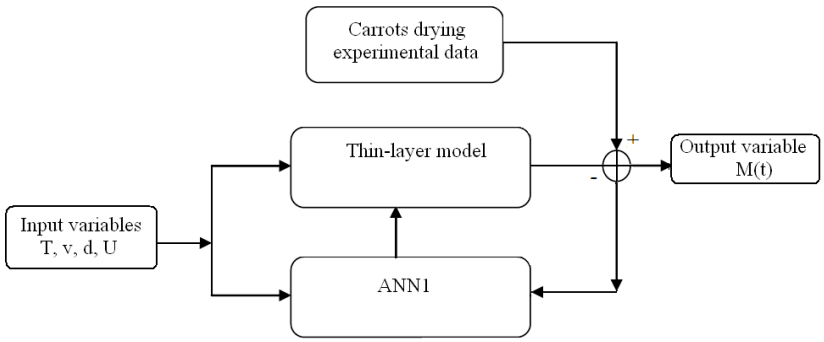

Figure 8. Hybrid neural model structure.

Having determined the general architecture of the HNM, the inputs to the neural block were specified. It is worthwhile evidencing that, with respect to the pure neural model, it was not necessary to input the process time, since the thin-layer model is capable of calculating, once the *k* parameter has been estimated by the neural network, the time evolution of food moisture content. Actually, on developing a pure neural model referred to an intrinsic transient process, it was necessary to explicitly feed the network with an array of process times that permitted calculating how food moisture content (the network response) changed with time under the influence of the operating variables. On the contrary, in the HNM, the time-dependency was directly provided by the theoretical part of the model, i.e. by the solution (Eq. 11) of the ordinary differential equation represented by Eq. 10. On the basis of the above considerations, it is expected, therefore, that the neural model architecture contained in the HNM is

much simpler than that of pure neural model, thus achieving a significant reduction of simulation time. Another interesting improvement related to the formulation of the present hybrid approach concerned the actual role played by the drying constant *k*, i.e. an ignorance parameter in which to include everything that might be difficult to express by proper mathematical relationships. Comparing the pure neural model and the hybrid neural model structures, it is worthwhile noting that the role played by the neural network is certainly less important in hybrid modeling, according to the initial statement that hybrid models are to provide a "less-dark" description of physical phenomena. Moreover, the theoretical part of the hybrid model plays a sort of filter function with respect to neural network model prediction; the estimated values of *k*, in fact, are used in the integration of Newton equation and, therefore, it is expected that the predictions errors due to the pure black-box nature of the model are limited.

After the HNM definition, it was necessary to define the neural part of the model, thus specifying the neural network architecture and set-up the training procedure. Similarly to the pure neural model, the experimental points relative to the 18 drying runs, were randomly split into three groups, reserving 2/3 of data (12 runs) to the training phase, 1/6 of the remaining data (3 runs) were used to test the predictions of the HNM during its development, whereas the residual 3 runs were used to validate the hybrid neural model predictions in three conditions never exploited neither during learning, nor during test.

In order to allow a proper comparison between different approaches, the runs chosen for both the test and the validation phases of the hybrid model were the same of those used to develop the pure neural model. A MLP feed-forward architecture was used and the same transfer functions and the training procedure described in the previous section to develop ANN1 were utilized. A second neural network, ANN2, was finally achieved; ANN2, which – as expected - is more slender than ANN1, had the following characteristics (Figure 9):

- An input layer with two neurons and a hyperbolic tangent transfer function;
- A single neuron output layer with a linear transfer function.

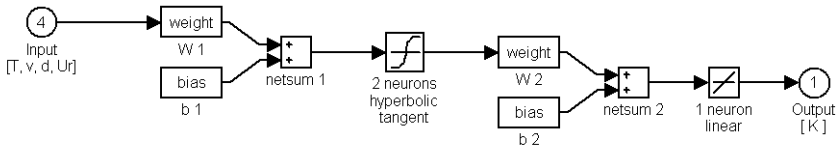

Figure 9. ANN2 structure .

1.3 Comparison of Models Performance

All the developed models were tested in the experimental conditions summarized in Table 3 to verify the reliability of their predictions and to compare their performance. Before analyzing some of the most interesting results, it is worthwhile remarking the main differences existing among thin-layer, fundamental and ANN models. Actually, any fundamental model requires a deep knowledge of the transport phenomena occurring in the process, whereas both the thin–layer and ANN models require a great number of experimental data to achieve a higher accuracy. Both physical modeling and experimental tests are highly time-consuming; nevertheless, physical modeling is generally more complex than the experimental procedure. In most cases, also a fundamental approach requires a set of experimental data; in particular, both the physical and the transport properties of foods, necessary to solve the heat and mass balance equations, are very difficult to estimate and are available only for certain types of foods. A fundamental model is capable to describe the profiles of moisture content developing in food as a function of space coordinates, thus allowing determining, for instance, if the local moisture content is still so high to promote microbial spoilage. Thin-layer and ANN models are capable to predict the time-evolution of average moisture content, since the collected experimental results usually do not provide any information about temperature and moisture content distributions. A complete analysis of the transport phenomena occurring in food is very difficult to be modeled by a fundamental approach due to the structural and thermodynamic modifications, not yet fully understood, involved in food drying; for this reason, ANN and thin-layer models represent an attractive alternative since they require a series of accurate experimental tests that can be obtained much more easily than an accurate and comprehensive physical and mathematical modeling.

The results obtained during the fitting procedure, obtained using the thin-layer model, are summarized

in Table 4, where, as well as the *k* values relative to each experimental run, the most meaningful statistical parameter are reported.

The very high value of r^2 coefficient indicates a very good agreement between the Newton's model and the experimental drying curves. For all the experiments an increase in drying constant value is observed, as both air temperature and its velocity increase and food characteristic dimension decreases. This last effect is to be ascribed to three main factors occurring at lower thickness: the shorter path through which water is transported within the solid matter; the increased exposed surface per unit volume; the decrease of both internal and external mass transfer resistances [52].

Figs. 9.1, 9.2 and 9.3 show, in some typical conditions, the drying curves obtained using three of the proposed models (the HNM performance will be analyzed more in detail afterwards). As far as ANN model is concerned, the predictions shown in Figs. 9.1, 9.2 and 9.3 are referred to some experiments belonging to the training, the test and the validation datasets, respectively. It is worthwhile noting that fundamental model exhibits a lower accuracy with respect to thin-layer approach that, instead, gives more reliable predictions.

Table 4. Results of drying curves fitting procedure using Newton model

	T= 5mm				T = 10mm				T = 15mm			
Air conditions (u, Ta)	r^2	K [1/min]	K Standard Error	Test N°	r^2	K [1/min]	K Standard Error	Test N°	r^2	K [1/min]	K Standard Error	Test N°
2.8m/s, 85°C	0.987	3.84E-02	0.00193	6	0.992	1.84E-02	0.000467	12	0.993	1.33E-02	0.000248	18
2.8m/s, 70°C	0.994	2.85E-02	0.001121	4	0.999	1.20E-02	0.000151	10	0.99	8.30E-03	0.000192	16
2.8m/s, 50°C	0.978	1.45E-02	0.000827	2	0.995	7.90E-03	0.000149	8	0.988	5.88E-03	0.000124	14
2.2m/s, 85°C	0.991	2.93E-02	0.001076	5	0.995	1.34E-02	0.000222	11	0.999	9.17E-03	6.01E-05	17
2.2m/s, 70°C	0.995	2.06E-02	0.000623	3	0.996	1.02E-02	0.000194	9	0.995	7.17E-03	0.000109	15
2.2m/s, 50°C	0.988	1.00E-02	0.000366	1	0.984	6.00E-03	0.000171	7	0.997	4.36E-03	4.05E-05	13

As a general comment, it should be observed that the formulated theoretical model was a rather simple one that estimated the transfer rates at the food/air interface by a set of semi-empirical correlations, thus not accounting for the actual influence on drying rate of air velocity field developing in the drying chamber. Moreover, the proposed simplified fundamental model was based on a unique mass balance equation, expressing the transport of total moisture in food, thus not accounting for the actual transport of water both as liquid and as vapour. As far as the ANN model predictions are concerned, it can be observed that when the experimental data belong to the training set (Figure 9.1) ANN gives a very good representation of the actual time evolution of drying process. When, instead, the experimental data belong to the test set (Figure 9.2) and the neural network is called to predict a condition never exploited during the training process, but actually used to achieve the final network architecture, a lower accuracy of ANN model is observed with maximum relative errors between ANN predictions and experimental data of about 10%. Finally, when the experimental data belong to the validation set (Figure 9.3), i.e. to an input combination definitely unknown to the network, an even lower accuracy of ANN model is observed with relative errors between ANN predictions and experimental data reaching at most 40 %. Thin-layer model, as already reported in Table 4, gives always very good performance since it actually represents a best-fitting procedure (actually based on a simple theoretical model) of existing experimental data; however, it is worthwhile remarking that, due to its main features, thin layer model cannot be absolutely applied to any situation never exploited during the experimental tests.

From this preliminary analysis, it is possible to derive some interesting considerations. A) The theoretical model should be as accurate as possible to provide reliable predictions; even small errors in the estimation of transfer coefficients lead to huge deviations between estimated and real values of temperature and moisture content, thus determining an unfair design of drying equipments or severe problems during food processing. Since the developed theoretical model did not depend on any adjustable parameter, it was capable of estimating drying behavior over a wide range of operating conditions. However, the formulation of so many simplification hypotheses, necessary to reduce the numerical complications and to achieve the PDEs solution in a reasonable time so as to allow the incorporation of the model in an on-line control system, determined significant discrepancies between the theoretical predictions and the measured data. B) The developed neural network model gave very accurate predictions of actual system behavior when it was tested within the range used for training. However, ANN model exhibited worse performance when it was called to interpret the time evolution of drying process in conditions never exploited during the learning phase (test and validation), thus proving that extrapolation based on neural model predictions is definitely unreliable when it is performed outside the training range. C) The thin layer model

offered very precise predictions, but represents an invalid and an inapplicable procedure in those cases in which no experimental data is actually available since it cannot allow the estimation of drying constant, *k*; however, due to its "semi-theoretical" nature, thin layer model may provide useful indications about the time dependency of food moisture content.

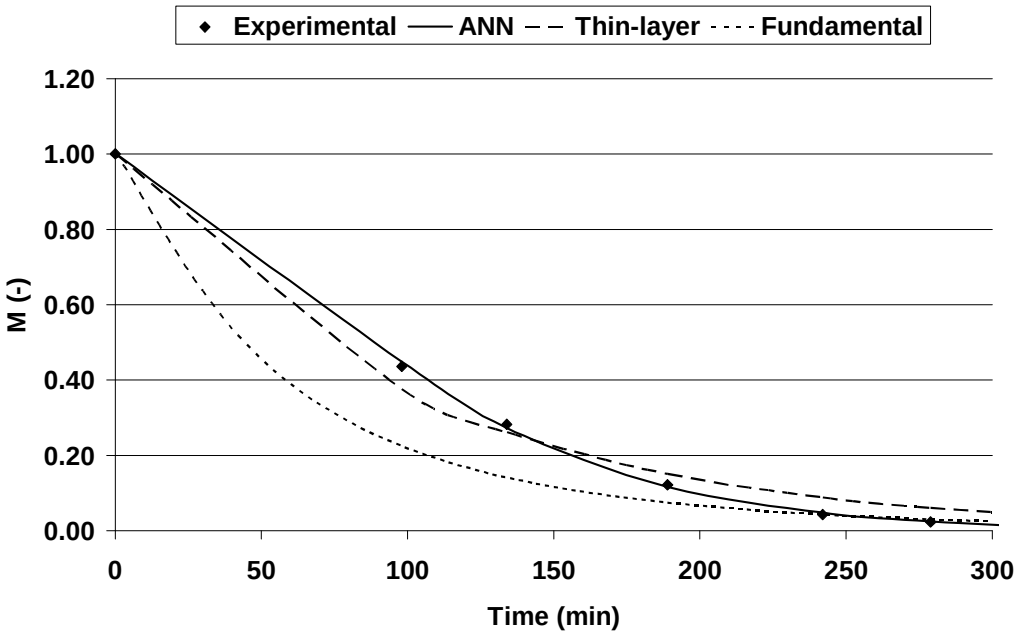

Figure 9.1. Simulation results relative to run N°1 (training phase). Operating conditions: T=50; v_0=2,2; d=5 mm.

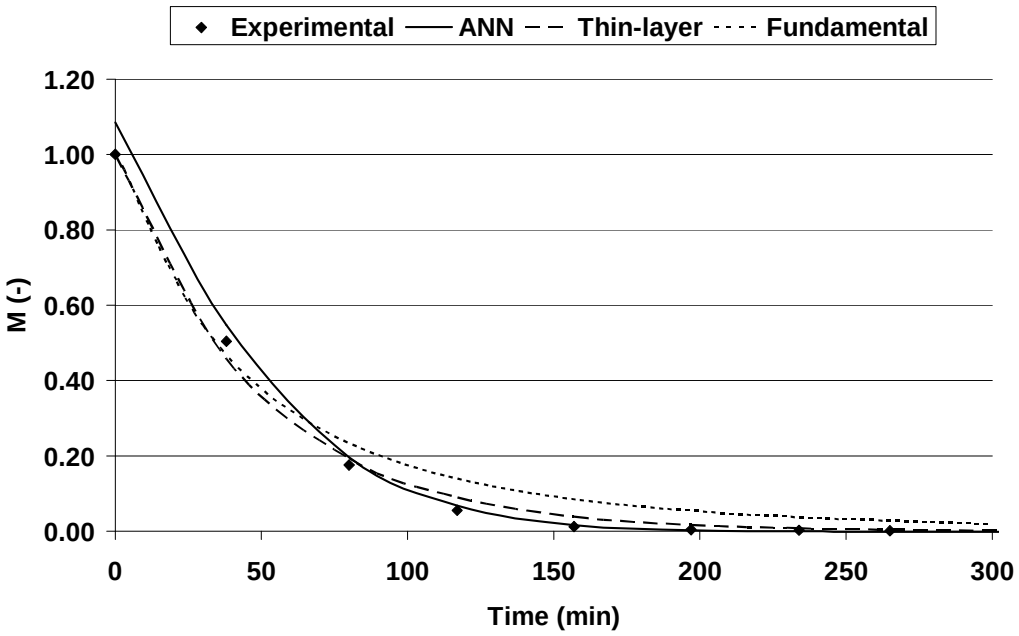

Figure 9.2. Simulation results relative to run N° 3 (test phase). Operating conditions: T=70; v_0=2,2; d=10 mm.

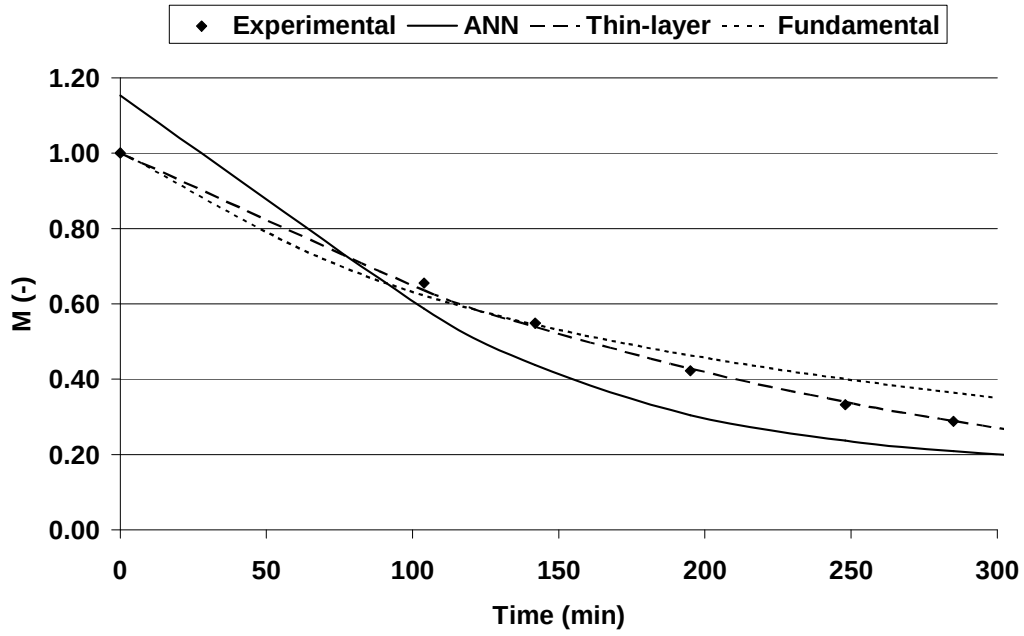

Figure 9.3. Simulation results relative to run N° 13 (validation phase). Operating conditions: T=50; v_0=2,2; d=15 mm.

As described in the previous sections, a Hybrid Neural Model (HNM) may, in principle, combine the best features of the above-described models. For instance, it could allow extending the applicability of thin-layer model on the basis of the learning ability provided by an artificial neural network model, which operates as a parameter(s) estimator and allows evaluating, by means of drying constant, a series of complex phenomena difficult to be expressed by proper mathematical relationships.

Figure 10 shows a comparison between HNM predictions, considering only the points belonging to both test and validation datasets and the corresponding experimental results, expressed in terms of dimensionless moisture content M(t) (Eq. 12). It is worthwhile observing that the neural part of the hybrid model (ANN2) was used so as to predict the values of drying constant, *k*, in situations never exploited during the training phase. The choice to refer to test and validation datasets is due to the necessity of evaluating the forecasting capability of HNM model in those situations in which ANN1 showed rather unreliable predictions, with relative errors reaching about 40 %.

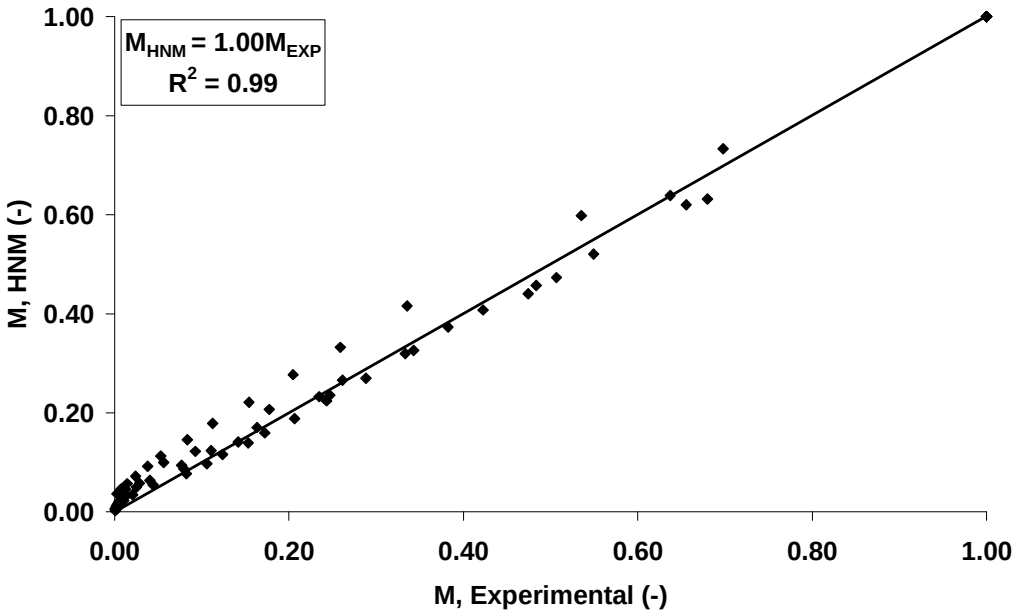

Figure 10. HNM performance.

A remarkable agreement between the model predictions and the experimental points can be observed since a straight line characterized by unitary slope and a nil intercept was used to fit the data with a very high correlation coefficient, $R^2 = 0.99$.

Figs. 11.1-11.3 show a comparison, expressed as the time evolution of dimensionless moisture content, between HNM and ANN1 model predictions during both test and validation phases. From Figure 11.1, obtained considering a set of experimental points belonging to the test dataset, it can be observed that both the models performance is comparable since HNM and ANN predictions are in good agreement with the experimental data. This behavior is to be ascribed to the trial and error procedure used to define ANN1 and ANN2 architectures and, in particular, to the control performed on percentage error even during the test phase. However, HNM is more accurate in predicting the system behavior at the beginning of drying process due to its semi-theoretical nature that does indeed require the precise knowledge of an initial condition, which has to be fixed before each HNM simulation is performed.

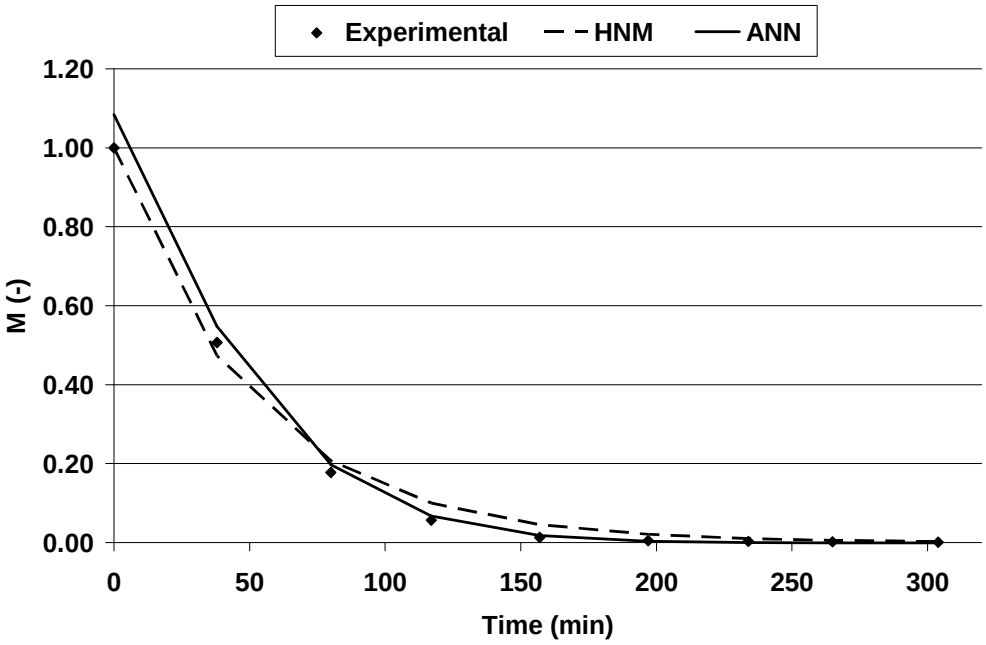

Figure 11.1. Comparison between HNM and ANN model (test phase). Run N°3: T=70; v_0=2,2; d=5 mm.

Figs. 11.2-11.3 show a comparison between HNM and ANN model performance in two typical situations, belonging to the validation dataset and, therefore, definitely never exploited during the training phase by both ANN1 and ANN2. Actually, the behavior of the two models is rather different since HNM shows excellent prediction ability, comparable to that obtained during the test phase, whereas the pure ANN model is not capable to accurately reproduce the measured decrease of carrots moisture content.

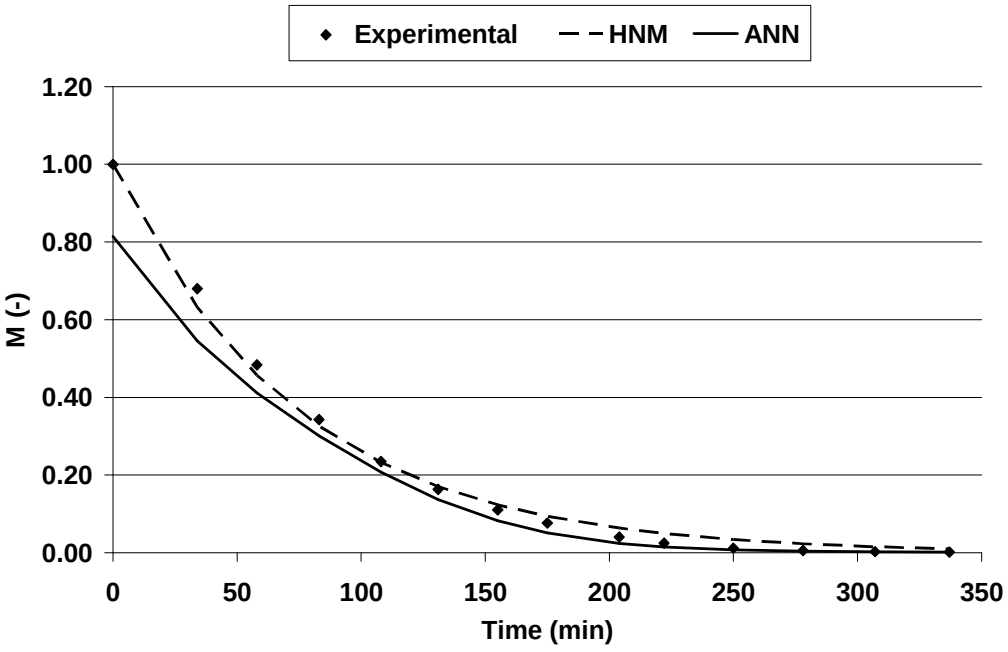

Figure 11.2. Comparison between HNM and ANN model (validation phase). Run N°11: T=85; v_0=2,2; d=10 mm.

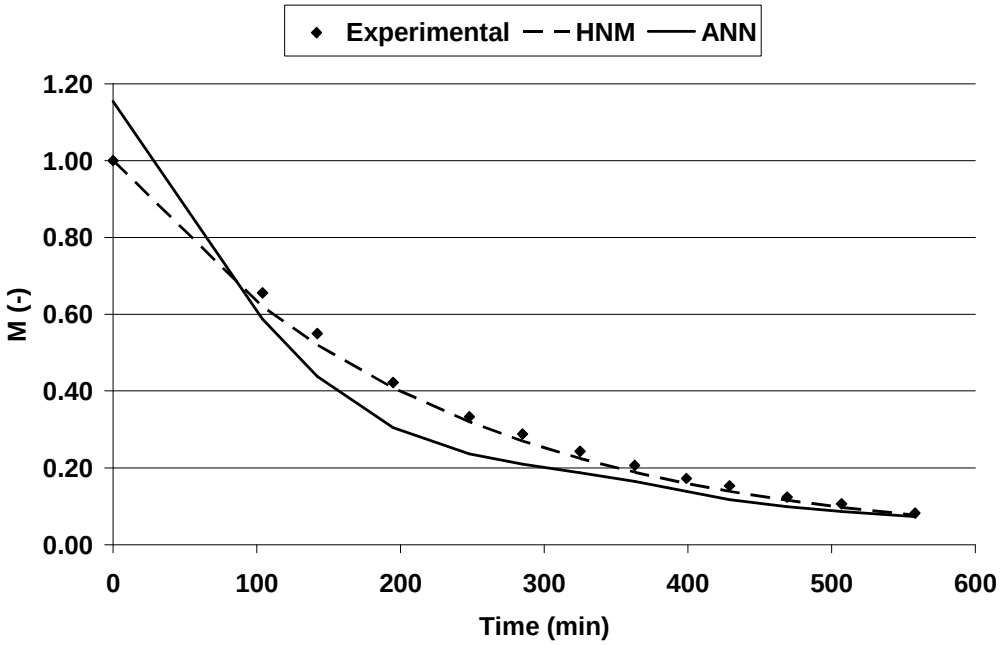

Figure 11.3. Comparison between HNM and ANN model (validation phase). Run N°13: T=50; v_0=2,2; d=15 mm.

As a matter of fact, the proposed HNM is characterized by a high level of reliability and, therefore, represents a powerful tool that, as compared to all the other models described in the present contribution, allows obtaining very precise predictions of the actual system behavior in all the tested conditions. The obtained results demonstrate that the combination of an even simple theoretical model with a straightforward neural model consisting of three neurons only is capable to fairly widen the applicability of pure neural models outside the training range, thus strengthening the model performance. The theoretical part of HNM does indeed play a role of filtering function with respect to ANN2 model predictions, thus limiting the errors introduction typical of a black-box model and determining a generalized improvement of model performance. On the contrary, the inherent data-based nature of pure artificial neural networks is responsible for a narrower validity of ANN models that, actually, makes any extrapolation outside the training range improper and uncertain.

1.4 Concluding Remarks

In the present contribution different approaches of food convective drying modeling were presented and critically analyzed with the aim of describing the advantages and the drawbacks of each of them. Theoretical modelling, in principle, could predict the drying behavior of foods available in all shapes and over a wide range of process and fluid-dynamic conditions. However, when a

fundamental model was based, as in the present case, on a great number of simplification hypotheses, significant discrepancies between the theoretical predictions and the measured data were generally observed. Among the straightforward theoretical models, it was showed that the thin-layer model provided useful and accurate indications about the time evolution of food moisture content, even though it did not allow any generalization being inapplicable when no experimental data were actually available.

On the other side, the developed neural network model reproduced very well the actual system behavior when the inputs combination belonged to the chosen training range, but it was characterized by unfair predictions when it was tested with a set of experimental points never exploited during network development (validation points). The hybrid paradigm, as proposed in the present contribution, was characterized by a high level of reliability and represented a powerful tool offering very precise predictions of the actual system behavior. The obtained results demonstrated that the proper combination of an even simple theoretical model with a straightforward neural model was capable to fairly widen the applicability of pure neural models outside the training range, thus allowing the utilization of HNM for process optimization purposes and for the implementation of efficient on-line control applications.

1.5 References

[1] Datta, A. K. Porous media approaches to studying simultaneous heat and mass transfer in food processes. I: Problem formulations. Journal of Food Engineering, 2007, 80, 80-95.

[2] McCabe W. L.; Smith J. C.; Harriot P. Unit operations of chemical engineering; McGraw-Hill Int.; Singapore, 1985.

[3] Wang, W.; Chen, G.; Mujumdar, A.S. Physical Interpretation of Solids Drying: An Overview on Mathematical Modeling Research. Drying Technology 2007, 25, 659–668.

[4] Chin, S. K.; Law, C. L.; Supramaniam, C. V.; Cheng, P. G. Thin-Layer Drying Characteristics and Quality Evaluation of Air-Dried Ganoderma Tsugae Murrill. Drying Technology, 2009, 27, 975–984.

[5] Bon, J.; Rossello, C.; Femenia, A.; Eim, V.; Simal, S. Mathematical Modeling of Drying Kinetics for Apricots: Influence of the External Resistance to Mass Transfer. Drying Technology, 2007, 25, 1829–1835.

[6] Arrieche L. S.; Sartori, D. J. M. Fluid Flow Effect and Mechanical Interactions during Drying of a Deformable Food Model. Drying Technology 2008, 26, 54–63.

[7] Zuniga, R.; Rouaud, O.; Boillereaux, L.; Havet, M. Conjugate Heat and Moisture Transfer During a Dynamic Thermal Treatment of Food. Drying Technology 2007, 25,1411–1419.

[8] Rahman, S. M. A.; Islam, M. R.; Mujumdar, A. S. A Study of Coupled Heat and Mass Transfer in Composite Food Products during Convective Drying. Drying Technology, 2007, 25, 1359–1368.

[9] Pakowski, Z.; Adamski, A. The Comparison of Two Models of Convective Drying of Shrinking Materials Using Apple Tissue as an Example. Drying Technology, 2007, 25, 1139–1147.
[10] [10] Chen, X. D. Moisture Diffusivity in Food and Biological Materials. Drying Technology, 2007, 25, 1203–1213.
[11] Datta, A. K. Porous media approaches to studying simultaneous heat and mass transfer in food processes. II: Property data and representative results. Journal of Food Engineering, 2007, 80, 96-110.
[12] Zhang J.; Datta A. K. Some considerations in modeling of moisture transport in heating of hygroscopic materials. Drying Technology 2004, 22 (8), 1983-2008.
[13] Ni H.; Datta A. K. Heat and moisture transfer in baking of potato slabs. Drying Technology, 1999, 17 (10), 2069-2092.
[14] Ni, H.; Datta, A. K.; Torrance, K. E. Moisture transport in intensive microwave heating of wet materials: a multiphase porous media model. International Journal of Heat and Mass Transfer, 1999, 42, 1501–1512.
[15] Zhang, J.; Datta, A. K.; Mukherjee, S. Transport processes and large deformation during baking of bread. AIChE Journal 2005, 51(9), 2569–2580.
[16] Kondjoyan, A.; Boisson, H.C. Comparison of Calculated and Experimental Heat transfer Coefficients at the Surface of Circular Cylinders Placed in a Turbulent Cross-flow of Air. Journal of Food Engineering, 1997, 34, 123-143.
[17] Verbdryer, P.; Nicolaï, B. M.; Scheerlinck, N.; De Baerdemaeker, J. The Local Surface Heat Transfer Coefficient in Thermal Food Process Calculations: A CFD Approach. Journal of Food Engineering, 1997, 33, 15-35.
[18] Curcio S.; Aversa M.; Calabro` V.; Iorio G. Simulation of food drying: FEM analysis and experimental validation, Journal of Food Engineering 2008, 87, 541–553
[19] Marra F.; De Bonis M. V.; Ruocco G. Combined microwaves and convection heating: a conjugate approach, Journal of Food Engineering 2009, doi: 10.1016/j.jfoodeng.2009.09.012.
[20] Curcio S., A multiphase model to analyze transport phenomena in food drying processes, Drying Technology, 2010, in press.
[21] Wilcox, D.C. Turbulence Modeling for CFD, 2nd Ed.; DCW Industries Inc., 2004.
[22] Aversa, M.; Curcio, S.;Calabrò, V.; Iorio, G. An analysis of the transport phenomena occurring during food drying process. Journal of Food Engineering 2007, 78 (3), 922-932.
[23] Thorvaldsson, K.; Janestad, H. A Model for Simultaneous Heat, Water and Vapour Diffusion. Journal of Food Engineering, 1999, 40, 167-172.
[24] Viollaz, P.E.;Rovedo, C.O. A Drying Model for Three-Dimensional Shrinking Bodies. Journal of Food Engineering, 2002, 52, 149-153.
[25] [25] Perry, R.H.;Green, D. Perry's Chemical Engineers' Handbook. Mc Graw-Hill, New York.
[26] Ruiz-López, I.I.; Córdova, A.V.; Rodríguez-Jimenes, G.C.; García-Alvarado, M.A. Moisture and Temperature Evolution During Food Drying: Effect of Variable Properties. Journal of Food Engineering, 2004, 63, 117-124.
[27] Smith, J.M. Van Ness, H.C.; Abbott, M.M. Chemical Engineering Thermodynamics IV edition. McGraw-Hill, New York.
[28] Welty, J. R.; Wicks, C. E.; Wilson, R. E.; Rorrer, G. Fundamentals of Momentum, Heat and Mass Transfer (IV edition). John Wiley & Sons., New York, 2001.
[29] Ertekin, C.; Yaldiz, O. Drying Of Eggplant And Selection of a Suitable Thin Layer Drying Model. Journal of Food Engineering, 2004, 63, 349-359.
[30] Doymaz, İ.Convective Air Drying Characteristics of Thin Layer Carrots. Journal of Food Engineering, 2004, 61, 359-364.

[31] Krokida, M.K.; Karathanos, V.T.; Maroulis, Z.B.; Marinos-Kouris, D. Drying Kinetics of Burdens Vegetables. Journal of Food Engineering 2003, 59, 391-403.
[32] Akpinar, E. K.; Bicer, Y; Yildiz, C. Thin layer drying of red pepper. Journal of Food Engineering, 2003, 59, 99–104.
[33] Senadeera, W.; Bhandari, B.R.; Young, G.; Wijesinghe B. Influence of shapes of selected vegetable materials on drying kinetics during fluidized bed drying. Journal of Food Engineering, 2003, 58, 277-283.
[34] Reilly, D.L; Cooper, L.N. An overview of neural networks: early models to real world systems. In: Zornetzer, S.F.; Davis, J. L.; Lau, C. (Eds), An Introduction to neural and Electronic Networks. Academic Press, New York, 1990, 227-248.
[35] Zhang, G.; Patuwo, B.E.; Hu, M. J. Forecasting with Artificial Neural Network: the state of Art, Int. J. of Forecasting, 1998, 14, 35-62.
[36] Roy, A.; Kim, L.S.; Mukhopadhyay, S. A polynomial time algorithm for the construction and training of a class of multilayer perceptron. Neural Networks 1993, 6, 535-545.
[37] Wang, Z.; Massimo, C.D.; Tham, M.T.; Morris, A.J. A procedure for determining the topology of multilayer feed-forward neural networks. Neural Network, 1994, 7 (2), 291-300.
[38] Murata, N.; Yoshizawa, S.; Amari, S. Network information criterion determining the number of hidden units for an artificial neural network model. IEEE transaction on Neural Networks, 1994, 5 (6), 865-872.
[39] Demuth, H.; Beale, M. Neural Network Toolbox User's Guide. Natick, The MathWorks, 2000.
[40] van Can, H.J.L.; te brake, H.A.B.; Dubbelman, S.; Hellinga, C.; Luyben, K. C. A. M. Heijnen, J.. Understanding and Applying the Extrapolation Properties of Serial Grey-Box models. AIChE J. 1998, 44, 1071-1089.
[41] Erenturk, S.;Erenturk, K. Comparison of genetic algorithm and neural network approaches for the drying process of carrots. Journal of Food Engineering, 2007, 78, 905-912.
[42] Martynenko A.I.;Simon X. Yang.Biologically Inspired Neural Computation for Ginseng Drying Rate. Biosystems Engineering, 20069, 5 (3), 385–396.
[43] Movagharnejad, K.; Nikzad, M. Modeling of tomato drying using artificial neural network. Computers and Electronics in Agriculture, 2007, 59, 78–85.
[44] Hernàndez-Pèrez, J.A.; Garcia-Alvarado, M.A.; Trystram, G.; Heyd, B. Neural networks for the heat and mass transfer prediction during drying of cassava and mango, Innovative Food Science and Emerging Technologies, (2004), 5, 57–64.
[45] Hernàndez-Pèrez, J.A.; Garcia-Alvarado, M.A.; Trystram, G.; Heyd, B. Application of an Artificial Neural Network for Moisture transfer prediction considering Shrinnkage during drying of foodstuffs. In: Welti-Chanes, J.;Vélez-Ruiz, J.F.; Barbosa-Cànovas, G.V. (Eds.). Transport Phenomena in Food Processing, CRC press, 2003, 183-197.
[46] Agarwal, M. Combining neural and conventional paradigms for modelling, prediction and control. Int. J. Syst. Sci. 1997, 28, 65-81.
[47] Psichogios, D. D.; Ungar, L.H. A hybrid neural network-First principle approach to process modeling. AIChE J.1992, 38 (10), 1499-1511.
[48] Curcio, S., Calabrò, V., Iorio, G. Reduction and control of flux decline in cross-flow membrane processes modeled by artificial neural networks and hybrid systems. Desalination. 2009, 236 (1-3), 234-243
[49] Saraceno, A., Curcio, S., Calabrò, V., Iorio, G. A hybrid neural approach to model batch fermentation of "ricotta cheese whey" to ethanol. Computers and Chemical Engineering. 2009, in press.

[50] Curcio, S., Scilingo, G., Calabrò, V., Iorio, G. Ultrafiltration of BSA in pulsating conditions: An artificial neural networks approach. Journal of Membrane Science. 2005, 246 (2), 235-247
[51] Curcio, S., Calabrò, V., Iorio, G. Reduction and control of flux decline in cross-flow membrane processes modeled by artificial neural networks. Journal of Membrane Science. 2006, 286 (1-2), pp. 125-132
[52] Bird, R.B.; Stewart, W. E.; Lightfoot, E. N. Fenomeni di trasporto. Ambrosiana, Milano, 1979.

2.2 Paper 7. Advanced modeling of food convective drying: artificial neural networks and hybrid approaches

In this paper, the convective drying of food was described by means of three different approaches, i.e. simplified thin-layer model, a pure Artificial Neural Network model and Hybrid Neural Model. The models predictions were compared to the experimental data collected during lab-scale convective drying tests. The experimental tests were performed with two different vegetables, shaped both as cylinder and slab samples and in different drying conditions, obtained changing either the velocity or temperature of the drying air. The HNM was characterized by a higher reliability since provided very precise predictions during both the training/test phase and the validation performed with a series of experimental data never exploited during model development.

Advanced modeling of food convective drying: a comparison between artificial neural networks and hybrid approaches

Alessandra Saraceno, Maria Aversa, Stefano Curcio*
Department of Engineering Modeling, via P. Bucci, cubo 39/c
University of Calabria, 87036 Rende, Italy.
*Corresponding author: tel. +39 0984 496711; fax: +39 0984 494043.
alessandra.saraceno@unical.it; maria.aversa@unical.it; stefano.curcio@unical.it;

Abstract

In the present paper, three different approaches are proposed to model the convective drying of food. The performance of thin layer, pure neural network and hybrid neural model is compared in a wide range of operating conditions, with two different vegetables, available either as cylinders or as slabs with different characteristic dimensions. It was found that the thin layer model was adequate to describe food drying behavior but it could be applied only as a fitting procedure. Pure neural models gave accurate predictions in some situations, but exhibited poor performance when tested outside the range of operating conditions exploited during their development. Finally, it was shown

that hybrid neural models, formulated as a combination of both theoretical and neural network models, are capable of offering the most accurate predictions of system behavior with average relative errors never exceeding 10%, even in operating conditions unexploited during the definition of the neural part of the model. The results obtained proved that the hybrid neural paradigm is a novel and efficient modeling technique that could be used successfully in food processing, thus allowing drying process optimization to be achieved and efficient and fast on-line controllers to be implemented.

Keywords: Vegetables drying, models formulation, computational tools.

1.Introduction

Convective drying occurs when warm dry air flows around cold moist food samples. A simultaneous transfer of both heat and water takes place so that heat is transported from the air to the material, whereas water is transported from the food core, then to its surface and, eventually, to the air (Pilatowski et al., 2010; Marquez & de Michelis, 2009; Lopez et al., 2009). Different approaches were proposed to predict the behavior of convective drying by either simplified or complex models. The latter are based on the rigorous analysis of the transport phenomena (momentum, heat and water, both as vapor and as liquid), occurring in air as well as in food (Curcio et al., 2008; Curcio, 2010; Curcio et al. 2010; Datta, 2007a; Datta, 2007b; Ni & Datta, 1999; Zhang & Datta, 2004; Zhang et al., 2005). The formulation of such theoretical models, however, results in coupled nonlinear partial differential equations that can be solved by cumbersome numerical methods, which are time consuming and difficult to incorporate in on-line control devices.

The simplified models, instead, do not pose numerical difficulties but are based on a series of simplification hypotheses that limit their application to a reduced number of real cases, and/or on the utilization of empirical correlations, which are necessary to estimate the heat and water fluxes at food-air interface(s) by means of proper transport coefficients (Arrieche and Sartori, 2008; Bon et al., 2007; Chin et al., 2009; Kondjoyan & Boisson, 1997; Rahman et al., 2007; Verbdryer et al., 1997; Zuniga et al. 2007).

Among simplified models, the so-called *thin-layer equation* (Akpinar et al. 2003; Doymaz, 2004; Ertekin & Yaldiz, 2004; Krokida et al., 2003; Shittu & Raji., 2008; Uribe et al., 2009; Uribe et al. 2010) is actually one of the most common. The *thin-layer equation* is based on two main assumptions: a) the moisture decrease is proportional to the instantaneous difference between material moisture content (assumed uniform within the food) and the moisture content in equilibrium with the drying air; b) the temperature distribution within the food sample is uniform.

The above assumptions lead to a unique ordinary differential equation, the so-called Newton's model, expressing the time evolution of food moisture content through a *drying constant* (k), i.e. a parameter which is to be estimated by fitting the collected experimental data of sample moisture content versus time. The *thin-layer equation*, therefore, has a definite limitation: it can be applied only when a series of measurements has been actually obtained for a specific drying experiment, whereas it is meaningless when there is no experimental data.

An alternative approach to both complex and simplified modeling is represented by black-box models and, more specifically, by artificial neural networks (ANNs). ANNs are a data-driven method capable of learning from examples capturing the functional relationships between the input(s) and the output(s). This characteristic makes ANNs a valuable computational tool in those cases in which it is necessary to model phenomena difficult to describe with a traditional, fundamental approach since no *a priori* knowledge of process main features is actually required. ANNs are composed of interconnected computational elements called neurons or nodes. The neurons are combined so as to form one or more layers composing the network. In a multilayer network each neuron receives one or more inputs from other related units and, by means of an activation function, produces an output, i.e. a signal that is fed to the other nodes connected to it. To develop a neural model, describing the behavior of a dynamic system, it is necessary to perform the network training beforehand. This is generally achieved by the so-called supervised back-propagation learning technique, which is based on the knowledge of a reference output (target), represented - in most cases - by the experimental results obtained after a specific experimental protocol (Reilly & Cooper, 1990; Zhang et al., 1998). Trained back-propagation networks are able to give reasonable responses when presented with inputs never exploited during the learning phase. This generalization property permits a network to be trained on a representative set of input/target pairs and to obtain good results without training the network on all possible input/output couples. Many different artificial neural network structures were proposed but the most common was certainly the multi-layer perceptron (MLP). An MLP is composed of an input layer that receives the input information about the process, an output layer that produces the response(s) of the ANN and a certain number of hidden (intermediate) layers (Zhang et al., 1998; Demuth & Beale, 2000). The number of layers and the number of neurons in each layer is the result of a trial and error procedure whose convergence is achieved by minimizing a proper performance index.

The neural network approach is relatively common in food technology and it was applied to different processes involving heat and mass transport phenomena, such as extraction using supercritical carbon dioxide (Mitra et al, 2008), osmotic dehydration (Fathi et al., 2009),

radiofrequency and microwave processes (Boyaci et al., 2008). Moreover, neural networks were applied in food quality monitoring (Dehghani et al. 2009; Klaypradit et al., 2010).

As far as vegetables drying is concerned, some authors developed ANNs models to describe the drying process of different vegetables: i.e. carrots (Erenturk & Erenturk, 2007), ginseng (Martynenko & Yang, 2006), tomato (Movagharnejad & Nikzad, 2007), cassava and mango (Hernàndez-Pèrez et al., 2004), grain (Liu et al., 2007), *Echinacea Angustifolia* (Erenturk et al., 2005), rice (Zhang et al. 2002).

One of the most interesting improvements of neural networks is the proper integration of theoretical and neural paradigms, thus realizing a so-called "grey-box" model (hybrid approach) usually capable of good performance in terms of data interpolation and extrapolation. The main advantage of hybrid neural models (HNMs) regards the possibility of describing some well-assessed phenomena by means of a theoretical approach, leaving the analysis of other aspects, more difficult to interpret and to describe in a fundamental way, to rather simple "cause-effect" models, such as neural networks (Agarwal, 1997; Curcio et al., 2009; Patnaik, 2010; Psichogios and Ungar, 1992; Saraceno et al., 2010; van Can et al., 1998). The model resulting from the utilization of a hybrid neural paradigm is simpler, from a computational standpoint, than that provided by the theoretical approach; moreover, with reference to the pure black-box models, it gives the possibility of considering one or more physical relationships that may help achieving a more precise knowledge of system behavior. Even if the hybrid neural approach is, in principle, characterized by a higher generalization capability than pure neural network models, no specific work has been published in the literature dealing with food drying modeling by HNM.

In the present paper, different approaches are exploited to model the convective drying of two vegetables, i.e. potatoes and carrots. The performance of thin layer, pure neural network and hybrid neural modeling is compared in a wide range of situations, showing that hybrid neural modeling has several advantages, if compared to both thin-layer and neural models. The main aim of the present paper is, therefore, to prove that a novel and efficient modeling technique, i.e. the hybrid paradigm, can be successfully applied to food processing and be a powerful tool offering very precise predictions of the actual system behavior.

2.Materials and Methods

Potatoes and carrots were purchased from the local market. They were cut by proper tools that allowed obtaining either cylinders or slabs shapes. The cylinders had a fixed length of 3 ± 0.01 cm and a diameter (d) that was chosen in the range 0.5 - 1.5 ± 0.01 cm; the slabs had two identical sides, 3 ± 0.01 cm long, and a thickness (□) that was chosen in the range 0.5 - 1.5 ± 0.01 cm. The above dimensions were measured by a vernier caliper providing a precision of 0.02 mm. Some

fragments, collected randomly from either the same potato or the same carrot used to perform the experiments, were utilized to measure beforehand the initial moisture content of each sample by an electronic moisture analyzer. The drying experiments were performed in a lab-scale convective oven (Universal Oven model UFP 400, Memmert GmbH, Germany), equipped with a stainless steel wide-mesh net where each sample was placed. To determine the time evolution of food average moisture content, weight losses were measured, at given time intervals, by a precision balance (AE 160, Mettler Toledo, Switzerland), providing an accuracy of ± 0.0001 g. The lab-scale oven allowed monitoring air temperature, by a Precision Measuring Instrument (P 655, Dostmann electronic GmbH, Germany), its humidity, by a rh 071073 probe (Dostmann electronic GmbH, Germany) and the inlet velocity, by a H 113828 probe (Dostmann electronic GmbH, Germany). The convective flow of drying air was obtained by a line of fans placed along the edge of the internal oven tray; air entered the drier in the axial direction and flowed parallel to the food sample axis. Different operating conditions were chosen; however, only the experimental results collected at three different air temperatures (323 K, 343 K and 358 K) and at two different inlet velocities (2.2 m/s and 2.8 m/s) will be considered in the following. All the experiments had a total duration of five hours at most and were performed at a constant value of air absolute humidity, Y, equal to 10.32 g water/m^3 dry air. With the aim of evaluating the performance of the developed models in a set of operating conditions definitely external to the range reported in Tab. 1, two additional drying runs, namely Extrapolation Run 1 and Extrapolation Run 2, were performed and hereafter considered. Extrapolation Run 1 was performed in the following operating conditions: T= 318 K; v=2.7 m/s; Y= 9.5 g water/m^3 dry air; d=9 mm. Extrapolation Run 2 was performed in the following operating conditions: T= 318 K; v=3 m/s; Y=9.0 g water/m^3 dry air; d=9 mm.

	d or δ = 5mm	**d or δ = 10mm**	**d or δ = 15mm**
Air conditions (v, T)	**Run N°**	**Run N°**	**Run N°**
2.2m/s, 50°C	1	7	13
2.8m/s, 50°C	2	8	14
2.2m/s, 70°C	3	9	15
2.8m/s, 70°C	4	10	16
2.2m/s, 85°C	5	11	17
2.8m/s, 85°C	6	12	18

Tab.1. Operating conditions chosen to perform the experimental analysis.

3.Statistical analysis

Each experiment was repeated twice. The statistical analysis was performed using Statgraphics V 7.0 software (Statistical Graphics, Englewood Cliffs, NJ, USA) and the level of statistical significance was $p < 0.05$. The effectiveness of the proposed mathematical models was evaluated by the determination coefficient (R^2) and the percentage error between predicted and experimental points.

4.Models development

4.1Thin-layer model implementation

Newton's model could be expressed as:

$$\frac{dX}{dt} = k \cdot (X - X_e) \qquad 1$$

where X ($Kg_{water} / Kg_{dry\ solid}$) is the food moisture content on a dry basis, X_e is the moisture content in equilibrium with drying air and t is the drying time. The parameter k is the so-called *drying constant* and represents a measure of the drying process rate; it is a function of the material moisture content, of the product size, of the uniform temperature distribution developing in the food and, finally, of air characteristics, i.e. its humidity, temperature and velocity.

Integrating Eq. 1, the following relationship, resulting in an exponential equation according to a pseudo-first order reaction kinetics (Zhang et al., 2002) is obtained:

$$\frac{(X - X_e)}{(X_o - X_e)} = \exp(-k \cdot t) \qquad 2$$

where X_o ($Kg_{water} / Kg_{dry\ solid}$) is the initial moisture content evaluated at t=0.

The experimental results providing the time-evolutions of food moisture content corresponding to each of the performed runs (Tab. 1) were fitted by the integrated form of Newton's model (Eq. 2) so as to estimate the drying constant k. A commercial curve fitting software package was used to accomplish this task and to calculate all the parameters with statistical significance. To determine the moisture content in equilibrium with the drying air, X_e, the psychrometric diagram combined to a set of empirical correlations available in the literature were used (Lewiki, 2000; Datta, 2007a).

4.2 ANN model development

A preliminary analysis of the process was carried out with the aim of choosing the input and the output variables that resulted as the most representative of process dynamics. The variable chosen

as the neural network output was the dimensionless moisture content of the food sample, M(t), which was considered of major interest as far as drying modeling is concerned:

$$M(t)=\frac{X(t)-X_e}{X_o-X_e} \quad (3)$$

With the aim of predicting the time evolution of the food moisture content, a set of significant input variables, i.e. the drying time (t), the dry bulb temperature (T), the air velocity (v), its relative humidity (Ur) and the characteristic sample size (d or □), was identified. From a preliminary sensitivity analysis it was shown that the above variables, among all the parameters that could affect the drying progress, exhibited the highest influence on the transport phenomena involved in the process and, therefore, on its performance.

After specifying the input-output structure of the model, the neural network architecture was to be defined and the training procedure set-up. Considering the drying process of slab-shaped carrots, regarded hereafter as a kind of reference case, the available 198 experimental points, relative to the 18 runs already presented in Tab.1, were randomly split into three groups, reserving 2/3 of drying runs, corresponding to 132 experimental points, to the training phase, 1/6 of the remaining runs, corresponding to 33 points, were used to test the predictions of the neural network during its development, whereas the residual 3 runs, i.e. 33 points, were used to validate the predictions of the developed ANN in a set of conditions never exploited neither during learning, nor during test. Finally, two other experimental drying runs were reserved to an additional validation phase performed to analyze the performance of the developed ANNs when they were called on to predict the drying behavior under operating conditions chosen outside the ranges reported in Tab.1.

A multi-layer perceptron (MLP) feed-forward architecture with a pyramidal structure, with a decreasing number of neurons from the input to the output layer, was identified by Matlab Neural Network Toolbox (The Mathworks), Ver. 4.0.1. To train each of the tested networks, thus estimating their weights and biases, the Bayesian regularization, allowing a significant improvement of ANNs generalization, was used (Demuth & Beale, 2000). The neuron transfer function was a hyperbolic tangent for both input and intermediate layers, whereas a linear transfer function was chosen for the output layer.

The choice of the “best” network architecture was made by a trial-and-error procedure, as suggested in the literature (Saraceno et al., 2010; Curcio et al., 2005; Curcio et al., 2006). The number of hidden layers and the number of neurons belonging to each single layer were determined through iterative cycles according to the block diagram shown in Fig. 1.

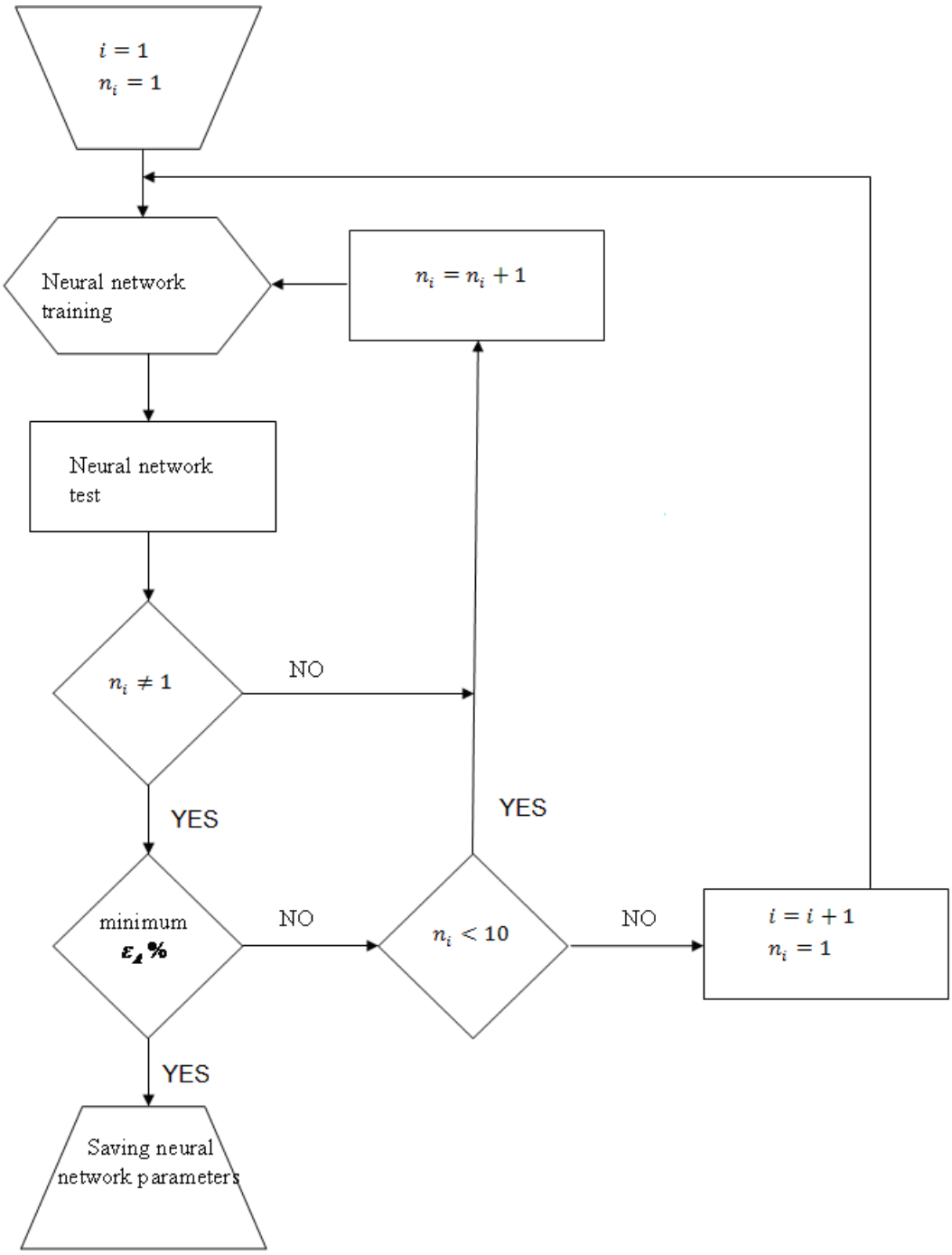

Fig. 1. Algorithm for ANN development (i: generic layer, n_i: number of neurons in the i^{th} layer).

It was supposed that the convergence was achieved when, during the test phase, the percentage average error (calculated on the basis of the whole test dataset) between the predictions of neural model and the corresponding experimental points (Eq.3) reached a minimum, set equal to 10%.

$$\left(\varepsilon_A\% = \frac{\left| M(t)_{EXP} - M(t)_{ANN,test} \right|}{\text{minimum}(M(t)_{EXP}, M(t)_{ANN,test})} \cdot 100 \right) \quad 4$$

On the basis of the above-described iterative procedure a neural model, ANN1, was eventually developed; it consisted of the following structure (Fig. 2):

- A first hidden layer with five neurons;
- A second hidden layer with two neurons;
- A single neuron output layer.

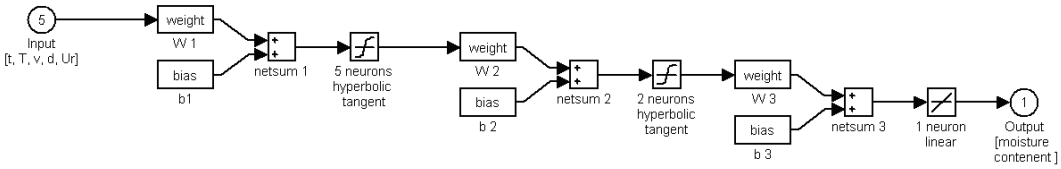

Fig. 2. ANN1 structure.

The training procedure reached convergence within 196 epochs, i.e. the number of iteration of the back-propagation algorithm; the sum of squared errors (SSE) during the training phase was equal to $4.9 \cdot 10^{-2}$.

The procedure described to determine the neural network architecture in the case of slabshaped carrots was utilized also in the case of cylindrical carrots samples and of slab-shaped potatoes samples, thus allowing two additional neural models to be obtained, called ANN2 and ANN3, respectively. Both ANN2 and ANN3 models were characterized by the same architecture as ANN1.

4.3Hybrid neural model development

The choice to model the drying process by means of a hybrid neural model (HNM), e.g. a model consisting of both a theoretical and a neural part together concurring at the obtaining of system responses, was determined by a critical analysis of purely “cause-effect” models. Neural models, in fact, did not make use of any fundamental equation that, instead, might be helpful to achieve a more precise knowledge of the dynamic process under study.

With the aim of reducing the mathematical complexity of the hybrid neural model, the “theoretical” part of the present HNM was represented by the thin layer model that, as reported in the literature, is usually considered as adequate to describe properly the time-evolution of vegetables moisture content during the convective drying process.

The proposed HNM was, therefore, realized coupling a rather simple theoretical relationship, as represented by the solution of thin-layer model (Eq. 2), to a neural network aimed at determining the drying constant *k* on the basis of the influence exerted by the operating variables on process

performance. The chosen architecture of the hybrid neural model can be classified as a classical serial model structure.

Having determined the general architecture of HNM, the inputs to the neural block had to be specified. The same input variables used to set-up the pure neural model were chosen, except for the process time, *t*. On developing the pure neural model described in the previous section, it was necessary explicitly to input *t* so as to calculate how food moisture content (the network response) changed with time under the influence of the operating variables. In the case of HNM, the solution (Eq. 2) to Newton's model directly provided the time-dependency of food dimensionless moisture content (Eq. 3). As a consequence, in the present formulation of HNM, the neural part of the model operated as an estimator of *k*, i.e. an ignorance parameter in which to include everything that might be difficult to express by proper mathematical relationships.

It is worthwhile observing that, owing to the serial structure of the HNM, the theoretical part of the proposed HNM is a sort of filter function with respect to the neural network model prediction: the estimated values of *k*, in fact, were used in the integration of Newton's equation.

After the HNM definition, it was necessary to define the neural part of the model, thus specifying its neural network architecture and setting-up the training procedure. Similarly to the pure neural model, the experimental points relative to the 18 drying runs, were randomly split into three groups; 2/3 of data, corresponding to 132 experimental points, were reserved to the training phase, 1/6 of the remaining data, i.e. 33 points, were used to test the predictions of the HNM during its development and the residual 3 runs, corresponding to 33 points, allowed the validation of hybrid neural model predictions in three conditions never exploited either during learning, or during the test. Analogously to the definition of the pure neural model, two additional drying runs were reserved to analyze the performance of the developed HNMs when the chosen combination of operating conditions was outside the ranges reported in Tab.1. In order to allow a proper comparison between the proposed different approaches, the runs used to test and to validate the predictions of hybrid and neural models for carrots and potatoes, both available as cylinders and slabs, were the same.

An MLP feed-forward architecture was used to estimate the parameter *k*. The same transfer functions and the training procedure described in the previous section to develop ANN1 were utilized too. A neural network, HNN1, representing the neural part of the hybrid model predicting the performance of slab-shaped carrots (HNM1), was finally achieved; owing to the introduction of a theoretical part into the model, HNN1 was more slender than ANN1, thus achieving a significant reduction of simulation time. It was composed of:

- A single hidden layer with two neurons and a hyperbolic tangent transfer function;

- A single neuron output layer with a linear transfer function.

The chosen hybrid model structure and HNN1 architecture are summarized in Fig. 3.

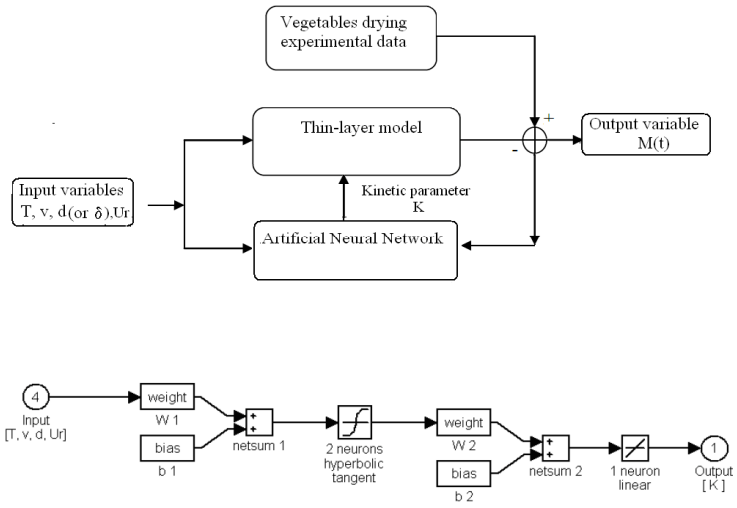

Fig. 3. Hybrid neural model structure and HNN1 structure.

As in the previous case, two additional hybrid models, called HNM2 and HNM3, were developed to predict the drying behavior of cylindrical carrot samples and of slab-shaped potatoes, respectively. Both the models were characterized by the serial structure already reported in Fig. 3; moreover, also the neural part of the two models, called HNN2 and HNN3, was the same as HNN1 (Fig. 3).

5.Results and Discussion

All the developed models described in the previous sections were tested in the experimental conditions summarized in Tab.1 to verify the reliability of their predictions and to compare their performance.

For all the experiments an increase in drying constant value was observed, as both air temperature and its velocity increased and characteristic dimension of the food decreased (Tab.2).

The latter effect can be ascribed to three main factors occurring at lower thickness: the shorter path

Table 2 Results of drying curves fitting procedure using the Newton's model (slab-shaped carrots)

Air conditions (v, T)	δ=5 mm						δ=10 mm						δ=15 mm					
	R^2	k [1/min]	k, SE	95% confidence limits		Test N°	R^2	k [1/min]	k, SE	95% confidence limits		Test N°	R^2	k [1/min]	k SE	95% confidence limits		Test N°
2.8 m/s, 85 °C	0.987	3.84E–02	1.93E–03	3.44E–02	4.25E–02	6	0.992	1.84E–02	4.67E–04	1.75E–02	1.94E–02	12	0.993	1.33E–02	2.48E–04	1.28E–02	1.38E–02	18
2.8 m/s, 70 °C	0.994	2.85E–02	1.12E–03	2.62E–02	3.09E–02	4	0.999	1.20E–02	1.51E–04	1.25E–02	1.31E–02	10	0.99	8.30E–03	1.92E–04	7.91E–03	8.71E–03	16
2.8 m/s, 50 °C	0.978	1.45E–02	8.27E–04	1.28E–02	1.63E–02	2	0.995	7.90E–03	1.49E–04	7.64E–03	8.26E–03	8	0.988	5.88E–03	1.24E–04	5.62E–03	6.14E–03	14
2.2 m/s, 85 °C	0.991	2.93E–02	1.08 E-3	2.71E–02	3.16E–02	5	0.995	1.34E–02	2.22E–04	1.29E–02	1.38E–02	11	0.999	9.17E–03	6.01E–05	9.05E–03	9.29E–03	17
2.2 m/s, 70 °C	0.995	2.06E–02	6.23E–04	1.93E–02	2.19E–02	3	0.996	1.02E–02	1.94E–04	9.82E–03	1.06E–02	9	0.995	7.17E–03	1.09 E-04	6.94E–03	7.39E–03	15
2.2 m/s, 50 °C	0.988	1.00E–02	3.66E–04	9.31E–03	1.08E–02	1	0.984	6.00E–03	1.71E–04	5.69E–03	6.40E–03	7	0.997	4.36E–03	4.05E–05	4.27E–03	4.44E–03	13

through which water was transported within the solid matter; the increased exposed surface per unit volume; the decrease of external mass transfer resistances (Bird et al.). The performance of Newton's model was similar in the case of both cylindrical carrots and slab-shaped potatoes but the results were not reported for the sake of conciseness.

In the following figures model predictions and experimental points are reported: as regards experimental points, in several cases the calculated standard deviation was even lower than 1% of the mean value itself and the error bars tended to mingle with the reported symbols.

Figs. 4 and 5 compared the drying curves obtained using the thin-layer and ANN models in the case of slab-shaped carrot samples

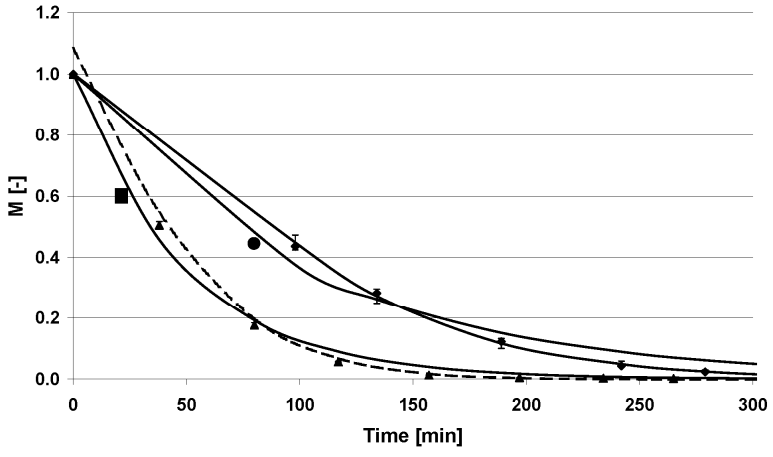

Fig. 4. Simulation results relative to slab-shaped carrots.

Training phase (Run 1): ◆ Experimental1 Run1; —— ANN1 Run 1; —●— Thin-layer Run 1.

Test phase (Run 3): ▲ Experimental1 Run 3; — – ANN1 Run 3; —■— Thin-layer Run 3.

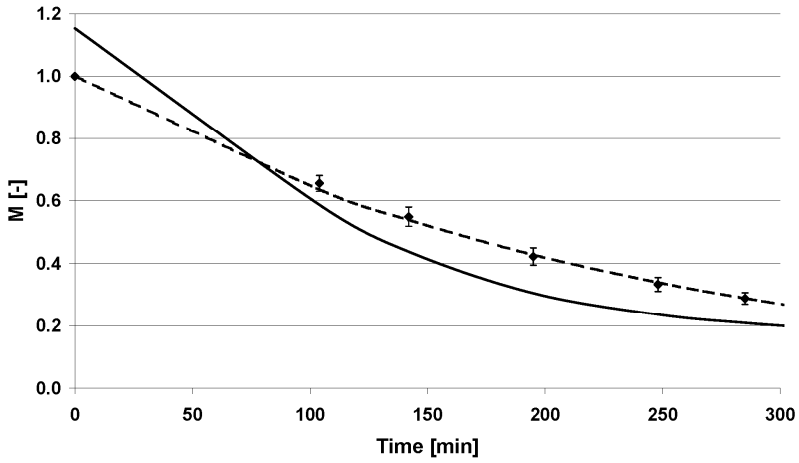

Fig. 5. Simulation results relative to slab-shaped carrots.

Validation phase (Run 13): ◆ Experimental1 Run 13; ——ANN1 Run 13; - - -Thin layer Run 13.

The predictions of the neural model were referred to three typical situations namely: the training (Fig. 4, Run1), the test (Fig. 4, Run3) and the validation (Fig. 5) phases; these runs were chosen since they were representative of models predictions in each of the considered datasets. Similar results were, in fact, obtained also for all the other runs, not shown for the sake of brevity.

It could be observed that when the experimental data belonged to the training set, ANN gave a very good representation of the actual time evolution of the drying process. When, instead, the experimental data referred to the test set and the neural network was called to predict a condition never exploited during the training process, but actually used to achieve the final network architecture, a lower accuracy was observed with maximum relative errors of about 10% between the ANN predictions and the experimental data. Finally, when the experimental data referred to the validation set, i.e. to an input combination definitely unknown to the network, an even lower accuracy of ANN model was observed with relative errors between the ANN predictions and experimental data reaching at most 40%. On the other hand, the thin-layer model, exhibited a rather good performance since it is a best-fitting procedure (actually based on a simple theoretical model) of existing experimental data; however, it is worth remarking that, owing to its main features, the thin layer model definitely cannot be applied to any situation never exploited during the experimental tests.

The comparisons between the pure neural network and thin-layer model in the case of cylindrical carrots and of slab-shaped potatoes are shown in Fig. 6, reporting the ANN predictions in conditions referring to the validation phase; also in these cases a low reliability of pure neural network model was observed.

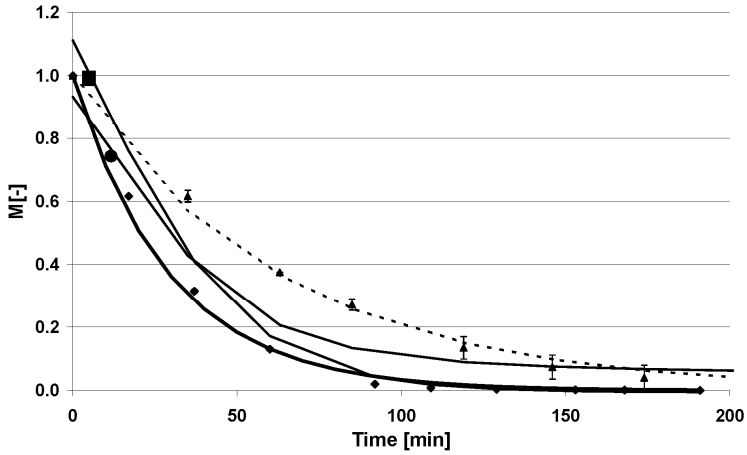

Fig. 6. Simulation results relative to validation phase.

Cylindrical carrots (Run 12): ◆ Experimental2 Run 12; —— Thin-layer Run 12; ■— ANN2 Run 12. Slab-shaped potatoes (Run 2): ▲ Experimental3 Run2; - - - Thin-layer Run 2; ●— ANN3 Run 2.

Starting from the previous analysis, some interesting considerations can be made:

A) The developed neural network models gave very accurate predictions of actual system behavior when tested within the range used for training. However, ANN models exhibited worse performance when they were called upon to interpret the time evolution of the drying process in conditions never exploited before, thus proving that extrapolation based on neural model predictions was definitely unreliable (Kahrs & Marquardt, 2007).

B) The thin-layer model offered very precise predictions, but is an inapplicable methodology in those cases in which no experimental data is actually available, since it could not allow estimation of the drying constant, *k*; however, owing to its "semi-theoretical" nature, the thin layer model might provide useful indications about the time evolution of the food moisture content.

As described in the previous sections, a Hybrid Neural Model might, in principle, combine the best features of the above-described models; HNM could indeed allow-the applicability of the thin-layer model to be extended on the basis of the learning ability provided by an artificial neural network model. In the following, the predictions of the developed hybrid neural models will be compared to the experimental points referring only to the test and the validation datasets, in order to evaluate the forecasting capability of HNM in situations, in which the pure artificial neural network model showed unreliable predictions, with relative errors reaching about 40%.

Fig. 7 showed a comparison between HNM1 and ANN1 during the test phase; actually, the performance of both the models was comparable since HNM1 and ANN1 predictions were in good agreement with the experimental data. However, the hybrid neural model was more accurate in

predicting the system behavior at the beginning of the drying process: this property can be ascribed to the semi-theoretical nature of HNM which indeed required the definition of a specific initial condition, before performing each simulation.

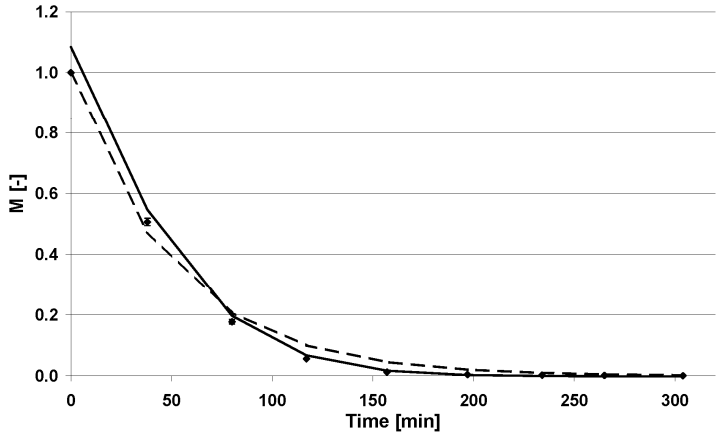

Fig. 7. Comparison between HNM1 and ANN1 models relative to slab-shaped carrots.

Test phase (run 3): ◆ Experimental1 Run3; — — HNM1 Run 3; ANN1 Run 3.

Fig. 8 showed a comparison between HNM1 and ANN1 model performance in two typical situations referring to the validation dataset.

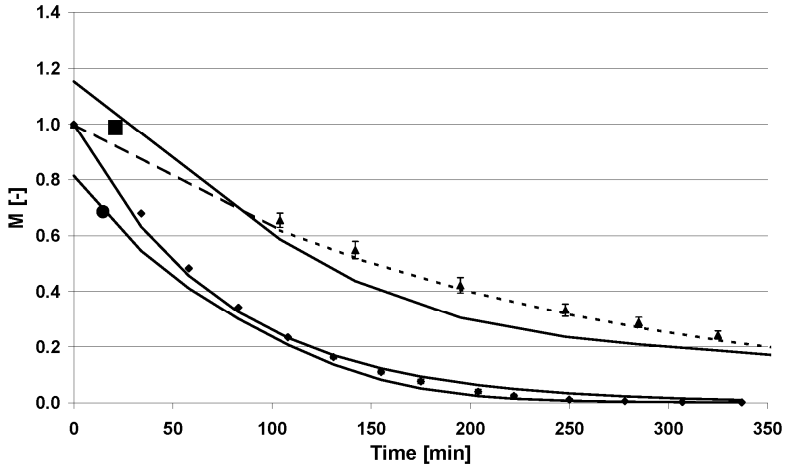

Fig. 8. Comparison between HNM1 and ANN1 predictions relative to slab-shaped carrot.

Validation phase (Run 11): ◆ Experimental1 Run 11; —— HNM1 Run 11; —●— ANN1 Run 11. Validation phase (Run 13): ▲ Experimental1 Run 13; - - - HNM1 Run 13; —■— ANN1 Run 13.

Actually, the two models exhibited a rather different behavior since HNM1 was characterized by an excellent prediction ability, comparable to that obtained during the test phase; it could be observed that the average relative error between the hybrid neural model predictions and the corresponding

experimental points never exceeded 10%. ANN1, instead, was not capable of accurately reproducing the measured decrease of carrots moisture content.

A similar behavior was observed on comparing the performance of the pure neural network and of the hybrid neural models in the case of cylindrical carrots and of slab-shaped potatoes samples (Fig. 9); also in these cases hybrid neural models predictions showed a good agreement with the experimental results belonging to the validation dataset and the average relative error was very low and, once again, always lower than 10%.

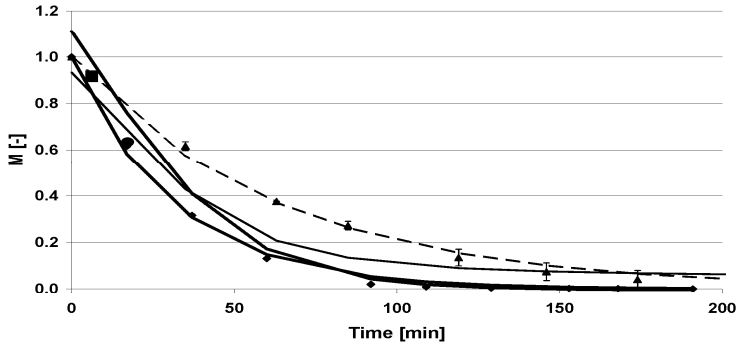

Fig. 9. Simulation results relative to cylindrical carrots and of slab-shaped potatoes: comparison between HNM and ANN models.

Validation phase (Run 12): ◆ Experimental2 Run 12; —— HNM2 Run 12; ■— ANN2 Run 12. Validation phase (Run 2): ▲ Experimental3 Run2; - - - HNM3 Run 2; ●— ANN3 Run 2.

In order to widen the validity domain of the proposed hybrid neural model, two additional validation tests, “Extrapolation Run 1” and “Extrapolation Run 2” were performed with the aim of analyzing the performance of the developed models in a more challenging situation, i.e. when they were called on to predict the drying behavior under a set of operating conditions chosen outside the ranges reported in Tab.1 and exploited during the training or the test phases.

Fig. 10-11 compared the performance of both ANN and HNM models in the case of dryed cylindrical-shaped carrots; similar results were actually obtained either for slab-shaped carrots or cylindrical-shaped potatoes (data not shown).

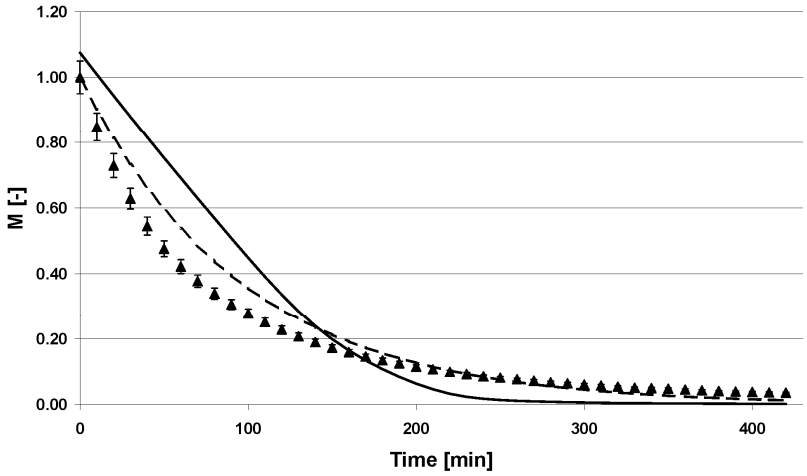

Fig. 10. Simulation results relative to Extrapolation Run 1. Operating conditions: T= 318 K; v=2.7 m/s; Y = 9.5g water/m^3 dry air; d=9 mm.

▲ Extrapolation Run 1; ——ANN2 Extrapolation Run 1; – – HNM2 Extrapolation Run1.

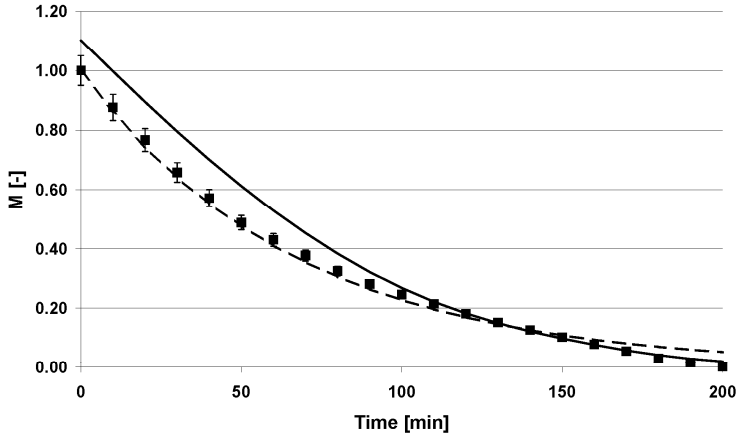

Fig. 11. Simulation results relative to Extrapolation Run 2. Operating conditions: T= 318 K; v=3 m/s; Y = 9.0 g water/m^3 dry air; d=9 mm.

■ Extrapolation Run 2; —— ANN2 Extrapolation Run 2; – – HNM2 extrapolation Run2.

It could be observed that HNM predictions were much more reliable than ANN, thus confirming that HNM reproduced the actual system behavior very well even if air temperature, air velocity and its relative humidity were chosen outside the ranges exploited to determine the drying constant, *k*. The proposed HNM approach, therefore, is a powerful and versatile computational tool that is capable of offering very accurate predictions of actual system behavior in a rather wide range of operating conditions, either changing the type of vegetable or its shape. The obtained results

demonstrated that the combination of even a simple theoretical model with a straightforward neural model, consisting of only two neurons in the hidden layer, might fairly widen the applicability of pure neural models even outside the training range, thus strengthening the model performance. The theoretical part of HNMs indeed played the role of filtering function with respect to the predictions of the neural part of hybrid models, thus limiting the introduction and the propagation of errors, typical of a black-box model, and determining an improvement of model accuracy. It is worth remarking that the inherent data-based nature of pure artificial neural networks was, instead, responsible for a narrower validity of ANN models that, actually, makes any extrapolation outside the training range improper and uncertain.

6.Conclusions

In the present contribution different approaches to modeling food convective drying are presented and analyzed with the aim of proposing the most appropriate method to predict process performance. The *thin-layer* model provided useful and accurate indications about the time evolution of food moisture content, even though it did not allow any generalization, since it was inapplicable when no experimental data were actually available. This characteristic of the thin-layer model definitely narrowed its applicability field.

On the other hand, the developed neural network models reproduced the actual system behavior very well when the inputs combination belonged to the chosen training-test dataset, providing a maximum relative error never exceeding 10% as compared to the collected experimental points. However, the ANNs were characterized by unfair predictions when their performance was tested with reference to a set of experimental points never exploited during the network development (validation points).

The hybrid paradigm, as proposed in the present contribution, was instead characterized by a high level of reliability and is a powerful tool offering very precise predictions, not only during the training and test phases, but, especially, during the validation phase. Moreover, the HNMs, owing to their theoretical nature, could be used even in extrapolation, a typical domain that is generally precluded to pure neural models. The results obtained demonstrated that the proper combination of even a simple theoretical model with a straightforward neural model was capable of fairly widening the applicability of pure neural models outside the training range. The generalization capability of HNMs was proved over a wide range of operating conditions, with two different kinds of vegetables, available either as cylinders or as slabs with different characteristic dimensions. The proposed HNMs, owing to their performance, may be used to achieve drying process optimization and to implement efficient and fast on-line controllers.

Acknowledgments

This work was supported by: the Food Science & Engineering Interdepartmental Center of the University of Calabria and L.I.P.A.C., Calabrian Laboratory of Food Process Engineering (Regione Calabria APQ-Ricerca Scientica e Innovazione Tecnologica- I atto Integrativo, Azione 2-Laboratori Pubblici di Ricerca "Mission oriented" Interfiliera).

References

Agarwal M (1997) Combining neural and conventional paradigms for modelling, prediction and control. International Journal of System Science, 28, 65-81.

Akpinar EK, Bicer Y & Yildiz C (2003) Thin layer drying of red pepper. Journal of Food Engineering, 59, 99-104.

Arrieche LS & Sartori DJM (2008) Fluid Flow Effect and Mechanical Interactions during Drying of a Deformable Food Model. Drying Technology, 26, 54-63.

Bird RB, Stewart W & Lightfoot EN (1979) Fenomeni di trasporto. Ambrosiana, Milano, Italy.

Bon J, Rossello C, Femenia A, Eim V & Simal S (2007) Mathematical Modeling of Drying Kinetics for Apricots: Influence of the External Resistance to Mass Transfer. Drying Technology, 25, 1829-1835.

Boyaci IH, Sumnu G & Sakiyan O (2009) Estimation of dielectric properties of cakes based on porosity, moisture content, and formulations using statistical methods and artificial neural networks. Food and Bioprocess Technology, 2, 353-360.

Chin SK, Law CL, Supramaniam CV & Cheng PG (2009) Thin-Layer Drying Characteristics and Quality Evaluation of Air-Dried Ganoderma Tsugae Murrill. Drying Technology, 27, 975-984.

Curcio S, Scilingo G, Calabrò V & Iorio G (2005) Ultrafiltration of BSA in pulsating conditions: An artificial neural networks approach. Journal of Membrane Science, 246 (2), 235-247.

Curcio S, Calabrò V & Iorio G (2006) Reduction and control of flux decline in cross-flow membrane processes modeled by artificial neural networks. Journal of Membrane Science, 286 (1-2), 125-132.

Curcio S, Aversa M, Calabro` V & Iorio G (2008) Simulation of food drying: FEM analysis and experimental validation. Journal of Food Engineering, 87, 541-553.

Curcio S, Calabrò V & Iorio G (2009) Reduction and control of flux decline in cross-flow membrane processes modeled by artificial neural networks and hybrid systems. Desalination, 236 (1-3), 234-243.

Curcio S (2010) A multiphase model to analyze transport phenomena in food drying processes. Drying Technology, 28 (6), 773 — 785.

Curcio S, Aversa M & Saraceno A (2010) Advanced Modeling of Food Convective Drying: A Comparative Study among Fundamental, Artificial Neural Networks and Hybrid Approaches. In: Siegler BC editor Food Engineering. Nova Publishers, New York, USA.

Datta AK (2007a) Porous media approaches to studying simultaneous heat and mass transfer in food processes. I: Problem formulations. Journal of Food Engineering, 80, 80-95.

Datta AK (2007b) Porous media approaches to studying simultaneous heat and mass transfer in food processes. II: Property data and representative results. Journal of Food Engineering, 80, 96-110.

Dehghani AA, Mohammadi ZB, Maghsoudlou Y & Mahoonak AS (2009) Intelligent estimation of the canola oil stability using artificial neural network. Food and Bioprocess Technology, (in press), DOI 10.1007/s11947-009-0314-8.

Demuth H & Beale M (2000) Neural Network Toolbox User's Guide. Natick, The MathWorks.

Doymaz İ (2004) Convective Air Drying Characteristics of Thin Layer Carrots. Journal of Food Engineering, 61, 359-364.

Erenturk K, Erenturk S & Tabil L (2005) A comparative study for the estimation of dynamical drying behavior of Echinacea angustifolia: regression analysis and neural network. Computers and electronics in agriculture, 45, 71-90.

Erenturk S & Erenturk K (2007) Comparison of genetic algorithm and neural network approaches for the drying process of carrots. Journal of Food Engineering, 78, 905-912.

Ertekin C & Yaldiz O (2004) Drying Of Eggplant And Selection of a Suitable Thin Layer Drying Model. Journal of Food Engineering, 63, 349-359.

Fathi M, Mohebbi M & Razavi SMA (2009) Application of image analysis and artificial neural network to predict mass transfer kinetics and colour changes of osmotically dehydrated kiwifruit. Food and Bioprocess Technology, (in press), DOI 10.1007/s11947-009-0222-y.

Hernàndez-Pèrez JA, Garcia-Alvarado MA, Trystram G & Heyd B (2004) Neural networks for the heat and mass transfer prediction during drying of cassava and mango. Innovative Food Science and Emerging Technologies, 5, 57-64.

Kahrs O & Marquardt W (2007) The validity domain of hybrid models and its application in process optimization. Chemical Enginering Processes, 46, 1054-1066.

Klaypradit W, Kerdpiboon S & Singh RK (2010) Application of artificial neural network to predict the oxidation of Menhaden fish oil obtained from Fourier transform infrared spectroscopy method. Food and Bioprocess Technology, (in press), DOI 10.1007/s11947-010-0386-s.

Kondjoyan A & Boisson H C (1997) Comparison of Calculated and Experimental Heat transfer Coefficients at the Surface of Circular Cylinders Placed in a Turbulent Cross-flow of Air. Journal of Food Engineering, 34, 123-143.

Krokida MK, Karathanos VT, Maroulis ZB & Marinos-Kouris D (2003) Drying Kinetics of Burdens Vegetables. Journal of Food Engineering, 59, 391-403.

Lewiki PP (2000) Raoult's law based food water sorption isotherm. Journal of Food Engineering, 43, 31-40.

Liu X, Chen X, Wu W & Peng G (2007) A neural network for predicting moisture content of grain drying process using genetic algorithm. Food Control, 18, 928–933.

Lopez J, Uribe E, Vega-Galvez, Miranda M, Vergara J, Gonzales E & Di Scala K (2010) Effect of air temperature on drying kinetics, vitamine c, antioxidant activity, total phenolic content, non-enzymatic browning and firmness of blueberries variety O'Neill. Food and Bioprocess Technology, 3(5), 772-777.

Marquez CA & de Michelis A (2009) Comparison of drying kinetics for small fruits with and without particle shrinkage considerations, Food and Bioprocess Technology, (in press), DOI 10.1007/s11947-009-0218-7.

Martynenko AI & Simon X Yang (2006) Biologically Inspired Neural Computation for Ginseng Drying Rate. Biosystems Engineering, 5(3), 385-396.

Mitra P, Barman PC & Chang KS (2008) Coumarin Extraction from Cuscuta Reflexa using supercritical fluid carbon dioxide and development of an artificial neural network model to predict the coumarin yield. Food and Bioprocess Technology, (in press), DOI 10.1007/s11947-008-0179-2.

Movagharnejad K & Nikzad M (2007) Modeling of tomato drying using artificial neural network. Computers and Electronics in Agriculture, 59, 78-85.

Ni H & Datta AK (1999) Heat and moisture transfer in baking of potato slabs. Drying Technology, 17(10), 2069-2092.

Ni H, Datta AK & Torrance KE (1999) Moisture transport in intensive microwave heating of wet materials: a multiphase porous media model. International Journal of Heat and Mass Transfer, 42, 1501-1512.

Patnaik PR (2010) Design consideration in hybrid neural optimization of fed-batch fermentation for PHB production by Ralstonia eutropha. Food and Bioprocess Technology, 3, 213-225.

Pilatowski I, Mounir S, Haddad J, Thai Cong D & Allaf K (2010) The instant controlled pressure drop process as a new post-harvesting treatment of paddy rice: impacts on drying kinetics and

end product attributes. Food and Bioprocess Technology, (in press), DOI 10.1007/s11947-010-0332-6.

Psichogios DD & Ungar LH (1992) A hybrid neural network-First principle approach to process modeling. AIChE Journal, 38 (10), 1499-1511.

Rahman SMA, Islam MR & Mujumdar AS (2007) A Study of Coupled Heat and Mass Transfer in Composite Food Products during Convective Drying. Drying Technology, 25, 1359-1368.

Reilly DL & Cooper LN (1990) An overview of neural networks: early models to real world systems. In: Zornetzer S.F, Davis J L, Lau C (Eds) An Introduction to neural and Electronic Networks. Academic Press, New York, 227-248.

Saraceno A, Curcio S, Calabrò V & Iorio G (2010) A hybrid neural approach to model batch fermentation of "ricotta cheese whey" to ethanol. Computers and Chemical Engineering, 34, 1590-1596.

Shittu TA & Raji AO (2008) Thin Layer Drying of African Breadfruits (Treculia Africana) Seeds: Modeling and Rehydration capacity. Food and Bioprocess Technology, (in press), DOI 10.1007/s11947-008-0161-z.

van Can HJL, te brake HAB, Dubbelman S, Hellinga C, Luyben KCAM & Heijnen J (1998) Understanding and Applying the Extrapolation Properties of Serial Grey-Box models. AIChE Journal, 44, 1071-1089.

Uribe E, Vega-Galvez A, Di Scala K, Oyanadel R, Torrico J S & Miranda M (2009) Characteristics of convective drying of Pepino fruits (Solanum Muricatum Ait.): Application of Weibull distribution. Food and Bioprocess Technology, (in press), DOI 10.1007-009-0230-y.

Uribe E, Miranda M, Vega-Galvez A, Quispe I, Claveria R & Di Scala K (2010) Mass transport modelling during the osmotic dehydration of Jumbo Squid (Dosidicus gigas): influence of temperature on diffusion coefficients and kinetic parameters. Food and Bioprocess Technology, (in press), DOI 10.1007/s-010-0336-2.

Verbdryer P, Nicolaï BM, Scheerlinck N & De Baerdemaeker J (1997) The Local Surface Heat Transfer Coefficient in Thermal Food Process Calculations: A CFD Approach. Journal of Food Engineering, 33, 15-35.

Zhang G, Patuwo BE & Hu MJ (1998) Forecasting with Artificial Neural Network: the state of Art. International Journal of Forecasting, 14, 35-62.

Zhang J & Datta AK (2004) Some considerations in modeling of moisture transport in heating of hygroscopic materials. Drying Technology, 22 (8), 1983-2008.

Zhang J, Datta AK & Mukherjee S (2005) Transport processes and large deformation during baking of bread. AIChE Journal, 51(9), 2569-2580.

Zhang Q, Yang S, Mittal G & Yi S (2002) Prediction of Performance Indices and Optimal Parameters of Rough Rice Drying using Neural Networks, Biosystems Engineering, 83(3), 281–290.

Zuniga R, Rouaud O, Boillereaux L & Havet M (2007) Conjugate Heat and Moisture Transfer During a Dynamic Thermal Treatment of Food. Drying Technology, 25, 1411-1419.

2.3 Paper 8. A theoretical model for the control of color degradation and microbial spoilage occurring in food convective drying.

The aim of this work is to investigate the possibility to control the color degradation and the bacterial spoilage during potatoes drying by means of different control schemes. In particular, to compare the performance of different control strategies, a model of the controlled process is necessary and it was developed using a theoretical approach. The developed model was capable to depict the bacterial spoilage and the color degradation as a function of drying conditions.

A theoretical model for the control of color degradation and microbial spoilage occurring in food convective drying.

Alessandra Saraceno, Maria Aversa, Stefano Curcio[7]

Department of Engineering Modeling – University of Calabria

Via P. Bucci - Cubo 42/A - 87036 Arcavacata di Rende (CS) – ITALY

Abstract

The aim of this work was the development of a control strategy aimed at improving food drying process. In particular, it was intended to determine, on the basis of an accurate transport model, the effect of operating conditions both on the color degradation, chosen as a reference quality parameter, and on the microbial spoilage occurring during potatoes drying. It is well known, in fact, that the exploitation of drastic operating conditions improves food safety, even though it may induce significant thermal damages, thus determining a significant worsening of dried products quality. On the contrary, the utilization of mild or very mild operating conditions does certainly improve the organoleptic properties of dried foods, but could not assure a proper decontamination of the final product. It is, therefore, necessary to identify the set of operating conditions that are to

[7] Corresponding author

be chosen so as to achieve high quality and safe dried foods. This was actually achieved by means of a transport model, accounting for the simultaneous transfer of momentum, heat and mass occurring in the drying air and in the food sample, coupled to both a product decontamination model describing the microbial inactivation kinetics of *Lysteria monocytogenes* and to another model aimed at predicting the kinetics of color changes occurring during drying. The proposed model was tested over a very wide range of process and operating conditions so as to identify, on the basis of a dynamic optimization algorithm, a trajectory of operating conditions that has to be tracked by means of proper control systems so as to optimize the performance of drying process.

1.Introduction

Convective drying is a thermal intensive operation consisting in moisture reduction from a solid product. In food industry this process is performed up to a definite moisture level, which can reduce the microbial spoilage and limit the deterioration chemical reactions (Triphaty and Kumar, 2008). The main objective of food drying is, therefore, the product decontamination so as to enhance its safety and improve its shelf-life. Both the heat effect and the induced reduction of food water content avoid the growth of the microbial species since they are incapable to survive below a water activity (a_w) threshold limit, after a mild heat treatment (Valdramidis et al., 2006).

During thermal drying, food quality is strongly deteriorated: the loss of water causes indeed profound modifications to both the mechanical and the structural properties of food, together with a degradation of many essential attributes, such as color. Color is usually considered as the key quality attribute of foodstuffs due to its relation with flavor and aroma (Morris et al., 1953).

On the basis of the above reported discussion, the optimization of drying process consists in the identification of a set of operating conditions capable of guaranteeing the safety and quality of dried foods in the cheapest way. Usually, a dynamic optimization, actually resulting in a trajectory of operating conditions that has to be tracked by means of proper control systems, is to be preferred over other types of common practices (Aversa et al., 2007a).

The control of inherent non linear and unsteady state processes, such as food drying, is a challenging area of research; nonlinear control plays an increasing important role in the area of process control engineering and, within this frame, neural networks may represent an attractive alternative to traditional model-based control techniques (Stephanopoulos,1984; Ogunnaike & Ray, 1994). Neural networks can be used in different kinds of control schemes such as (a) inverse model-based control, (b) predictive control and (c) adaptive control (Scott and Ray, 1994).

In the inverse-model-based control what is specified *a priori* is the "desired" dynamic behavior of the controlled system and not the controller structure; actually, the design procedure is invoked to derive the controller structure that is called to achieve a set of pre-specified objectives (Ogunnaike & Ray, 1994). In particular, in a direct inverse controller, the inverse model of the process performs as the actual controller without any feedback loop. The predictive control scheme with neural networks makes use of a neural network model to predict the future response of the plant. In the adaptive control approach the controller has to be able to adjust its parameters in an optimal way so as to cater for the unsteady-state, non-linear behavior characterizing the chemical processes (Scott and Ray, 1994).With the aim of testing the above-mentioned control schemes so as to improve drying process performance, a mathematical model should be, however, available so as to simulate the process at hand, thus verifying the controlled system responses to either set-point or disturbances changes.

In this work a fundamental model was preliminary proposed to predict food drying behavior over a wide range of operating conditions; then, a processing strategy was developed so as to achieve proper control objectives, characteristic for vegetables drying. In particular, the proposed model, accounting for the simultaneous transfer of momentum, heat and mass both in the drying air and in the food sample, is capable of describing the bacterial starvation and the color degradation occurring during food drying. The bacterial starvation and the color degradation were chosen as model outputs since they represent the actual controlled variables of the process, due to the strong relationships existing between them and both the reduction of water content determining microorganisms starvation and the dried food quality, expressed in terms of its external aspect.

2.Model development

When a moist and cold food sample is put in contact with dry and warm air, two different transport mechanisms simultaneously occur: heat is transferred from air to the material, water, instead, is transferred from food to air. Within the solid material, heat is transported by conduction and convection; the transport of water, as liquid, is due to both gas pressure and capillary pressure gradients, whereas vapor is transferred by pressure and concentration gradients.

To develop the present theoretical model it was assumed that: a) capillary pressure prevailed over gas pressure assuming that the hygroscopic material under study was highly unsaturated, like in most drying applications. The transport of liquid water, therefore, occurred essentially by capillary pressure. b) The term containing the pressure driven flow in vapor transfer equation was neglected and the molecular diffusion was considered as the prevailing mechanism. c) The contribution of convection to heat transport was considered negligible as compared to conduction. d) Evaporation

occurred over the entire food domain and also at food outer surfaces. e) Moisture removal from the surface took place by vapor transport, diffusing into the boundary layer developing in the drying air, and by liquid water transport, evaporating at the outer food surfaces. Both vapor and liquid water were convected away by the drying air, whose velocity field is expected to affect strongly the interfacial rates of heat and mass transfer. f) The continuity of both heat and mass fluxes occurred at the food/air interfaces. g) All the phases, i.e. solid, liquid, and gas, were continuous and were in local thermal equilibrium. h) The vapor pressure was expressed as a function of both temperature and moisture content. i) The turbulent momentum transfer referred to drying air flowing in the drying chamber around the food sample was described by the k-ω model.

On the basis of the above assumptions, a system of transport equations was obtained, respectively for food and air.

In particular, the resulting unsteady-state mass and energy balance equations referred to the transport of liquid water and of vapor in the food sample were reported in the following. It is worthwhile remarking that the physical and the transport properties of food were expressed in terms of the local values of temperature and of moisture content:

$$\partial C_w / \partial t + \underline{\nabla} \cdot \left(- D_w \underline{\nabla} C_w \right) + \dot{I} = 0 \qquad (1)$$

$$\partial C_v / \partial t + \underline{\nabla} \cdot \left(- D_v \underline{\nabla} C_v \right) - \dot{I} = 0 \qquad (2)$$

where C_w was the liquid water concentration, C_v was the vapor concentration, $\dot{I}$ was the volumetric rate of evaporation, D_w and D_v were the capillary diffusivity of water and the effective diffusion coefficient of vapor in food, respectively.

The energy balance in the food material led, according to Fourier's law, to the unsteady-state heat transfer equation:

$$\rho_s C_{p_s} \partial T / \partial t - \underline{\nabla} \cdot \left(k_{eff} \underline{\nabla} T \right) + \lambda \cdot \dot{I} = 0 \qquad (3)$$

where T was the food temperature, ρ_s was the density of food sample, C_{ps} its specific heat, k_{eff} was the effective thermal conductivity and λ the latent heat of vaporization of water.

The unsteady-state momentum balance (i.e. the so-called Reynolds-averaged Navier-Stokes equations) coupled to both the continuity equation and the transport equations for k and ω, the energy balance (accounting for both convective and conductive contributions) and the mass balance (accounting for both convective and diffusive contributions) were used to model the transport phenomena in the drying air:

$$\partial \rho_a / \partial t + \underline{\nabla} \cdot \rho_a \underline{u} = 0 \qquad (4)$$

$$\rho_a \partial \underline{u} / \partial t + \rho_a \underline{u} \cdot \underline{\nabla} \underline{u} + \underline{\nabla} \cdot \left(\overline{\rho_a \underline{u}' \otimes \underline{u}'} \right) = -\underline{\nabla} p + \underline{\nabla} \cdot \left[\eta_a \left(\underline{\nabla} \underline{u} + (\underline{\nabla} \underline{u})^T \right) \right] \quad (5)$$

$$\rho_a \partial k / \partial t + \rho_a \underline{u} \cdot \underline{\nabla} k = \underline{\nabla} \cdot [(\eta_a + \sigma_k \eta_t)(\underline{\nabla} k)] + \frac{\eta_t}{2} \left(\underline{\nabla} \underline{u} + (\underline{\nabla} \underline{u})^T \right)^2 - \beta_k \rho_a k \omega \quad (6)$$

$$\rho_a \partial \omega / \partial t + \rho_a \underline{u} \cdot \underline{\nabla} \omega = \underline{\nabla} \cdot [(\eta_a + \sigma_\omega \eta_t)(\underline{\nabla} \omega)] + (\alpha \omega / 2k) \eta_t \left(\underline{\nabla} \underline{u} + (\underline{\nabla} \underline{u})^T \right)^2 - \beta \rho_a \omega^2 \quad (7)$$

where p was the pressure within the drying chamber, $\underline{u}$ was the averaged velocity field, $\otimes$ was the outer vector product, $\underline{u}'$ was the fluctuating part of velocity field and β_k, σ_k, σ_ω, α, β were constants. Air density, ρ_a, and its viscosity, η_a, were expressed in terms of the local values of both temperature and moisture content, considering drying air as a gas mixture whose vapor concentration may vary point by point within the drying chamber.

Heat balance equation

$$\rho_a C_{pa} \partial T_2 / \partial t - \underline{\nabla} \cdot (k_a \underline{\nabla} T_2) + \rho_a C_{pa} \underline{u} \cdot \underline{\nabla} T_2 = 0 \quad (8)$$

where T_2 was the air temperature, C_{pa} was its specific heat and k_a was the air thermal conductivity, actually comprised by both a laminar and a turbulent contribution to energy transport by conduction.

Vapor balance equation

$$\partial C_2 / \partial t + \underline{\nabla} \cdot (-D_a \underline{\nabla} C_2) + \underline{u} \cdot \underline{\nabla} C_2 = 0 \quad (9)$$

where C_2 was the water concentration, as vapor, in the air and D_a was the diffusion coefficient of vapor in air; also in this case, both a laminar and a turbulent contribution were considered to express mass transfer due to a diffusion mechanism.

A set of initial conditions, typically prevailing in an industrial drying process, was set to perform the numerical simulations. As far as the boundary conditions were concerned, at the food-air interface, where no accumulation occurs, the continuity of heat and water fluxes, both as liquid and vapor, was imposed. Moreover, a thermodynamic equilibrium at the air-food interface was formulated and expressed in terms of water activity, thus accounting also for the effects of physically bound water. At the drier outlet, it was assumed that conduction and diffusion were neglected in favour of convection, which prevailed. Finally, the boundary conditions for momentum balance at the solid surfaces were expressed in terms of a logarithmic wall function.

It is worthwhile observing that the formulated theoretical model can be considered as very general since it does to make use of any transport coefficient aimed at estimating the heat and mass fluxes at food/air interfaces.

The above-described transport model, as represented by Eqs. 1-9 together with the corresponding boundary and initial conditions, was capable to describe the time evolution of drying process but actually did not give any indication about the progress of product decontamination and about the quality of dried product. For this reason, two additional models were developed and included in the more general transport model with the aim of relating the calculated local values of both moisture content and temperature in the food to microbial inactivation and to color degradation, as determined by the operating conditions chosen to perform the drying process.

In particular, product decontamination was described considering the microbial inactivation kinetics of *Lysteria monocytogenes* expressed as a function of temperature and water activity (Valdramidis et al. 2006). Among all the microorganism that may proliferate on vegetables Lysteria is definitely the most studied due to the safety problems that may arise if it is not properly inactivated during processing.

The following "primary" model, i.e. a model describing the microbial population as a function of time, was chosen:

$$\frac{dN}{dt} = -k_{\max} \cdot \left(\frac{1}{1+Cc} \right) \cdot N \tag{10}$$

where N represents the microbial population, k_{max} is the so-called specific inactivation rate and Cc is the physiological state of cells and is a function of time as well.

$$\frac{dCc}{dt} = -k_{\max} \cdot Cc \tag{11}$$

Eqs. 10-11 can be integrated knowing the initial microbial population, *No*, and the initial value of the parameter Cc that for the Lysteria in macerated potatoes was estimated to be constant and equal to 10^{-4} (Valdramidis et al. 2006).

A "secondary" model was then identified to relate k_{max} to the local values of both temperature and water activity in the food sample:

$$k_{\max}(T, a_w) = \frac{\ln 10}{1.8} \exp\left(\frac{\ln 10}{7.11}(T - 60) \right) \cdot \exp\left(\frac{\ln 10}{0.231}(a_w - 1) \right) \tag{12}$$

where T was expressed in °C.

To describe the kinetics of color changes occurring during drying the model proposed by Krokida et al. (1998) was exploited. This model describes the color changes kinetics in terms of the so called

Hunder parameters, i.e. (a) redness, (b) yellowness, (L) lightness. Each of these parameters follows a first order kinetics that is given by the following general equation:

$$\frac{C - C_e}{C_0 - C_e} = \exp(-k_c t) \tag{13}$$

where C is each of the color parameter (a, b, L), *Co* and *Ce* are their corresponding initial and equilibrium values, *kc* is a rate constant and *t* is the drying time. The dependence of color parameters on the operating conditions, i.e. the dry bulb temperature, *Ta*, and the relative humidity, *H*, of drying air, was taken into consideration through the effect that *Ta* and *H* determines on both the equilibrium value and the rate constant as expressed by the following equations:

$$Ce = C_{eo}(T_a / 70)^{a_T} (H / 30)^{a_H} \tag{14}$$

$$k_c = K_{c0}(T_a / 70)^{m_T} (H / 30)^{m_H} \tag{15}$$

The empirical parameters of Eqs. 14-15- are actually available for potatoes.

The system of PDEs and ODEs as represented by Eqs. 1-15 was solved by the Finite Elements Method implemented by the commercial package Comsol Multiphysics 4.2, defining a proper two-dimensional domain representing the potato sample and the drying chamber. The proposed model was simulated over a very wide range of process and operating conditions so as to identify, on the basis of a dynamic optimization algorithm, a trajectory of operating conditions that has to be tracked by means of proper control systems so as to optimize the performance of drying process.

References

Aversa, A., Curcio, S., Calabrò, V., Iorio, G. (2007a) Experimental evaluation of quality parameters durying drying of carrots samples. Food and Bioprocess technology. DOI 10.1007s/11947-009-0280-1.

Aversa, A., Curcio, S., Calabrò, V., Iorio, G. (2007b). An analysis of the transport phenomena occurring during food drying process. Journal of food engineering, 78, 922-932.

Krokyda, M.K., Tsami, E. and Maroulis, Z.B. (1998) Kinetics on colour changes during drying of some fruits and vegetables. Drying technologies, 16, 667-685.

Morris, N.J., Lohmann, I.W., O'Conner, R.T., freeman, A.F. (1953). Determination of colour of peanut butter by spectral reflectance method. Food Technology, 7, 393-373.

Ogunnaike, B. A., Ray, W. H.(1994). Process dynamics, modeling and control. Oxford university press.

Scott, G.M. & Ray, W.H. (1993).Experiences with model based controllers based on neural network process models. Journal of Process control, 3, 179-196.

Stephanopoulos, G. (1984). Chemical process control, an introduction to Theory and Practice. Prentice-Hall.

Triphaty, P.P. and Kumar, S. (2008). Determination of temperature dependent drying parameters for potato cylinders and slices during solar drying. Energy conversion and Management, 49, 2941-2948.

Valdramidis, V.P., Geeraerd, A. H., Gaze, J.E., Kondjoyan, A., Boyd, A.R., Shaw, H. L., Van Impe, J. F. Quantitative description of Listeria monocytogenes inactivation kinetics with temperature and water activity as the influencing factors; model prediction and methodological validation of dynamic data. Journal of Food Engineering, 76, 79-88.

CONCLUSIONS

In the present thesis, the modeling of biotechnological and food-industry processes was discussed. Several case-studies were analyzed and, for each of them, different modeling approaches were tested.

It was showed that the choice of the best modeling strategy was case-study-dependent: actually, a higher complexity of the observed phenomena determines a greater difficulty in the formulation of proper and reliable theoretical models. In particular, for a wide variety of both biotechnological and food-industry processes, the fundamental description of kinetics and mass transfer phenomena can be precluded by the huge number of chemical compounds actually involved in the reaction, by the complex behavior of bio–catalyst, whose activity could be lowered by an improper choice of pH or of temperature or even inhibited by substrate and/or by product and by the complicated phenomena occurring at the fluid/solid interface(s) where momentum, heat and mass are simultaneously transported. In such situations, neural modeling can be useful to perform quantitative calculations about the process and to rationally develop it. Furthermore, when artificial neural networks are properly interconnected to a theoretical model, thus achieving a hybrid structure, it is possible to exploit the knowledge provided by one or more fundamental relationships about process dynamics, assigning only the difficult-to-be-described aspects of the process to an empirical model. It is worthwhile observing that whether partly or totally describing the process, the artificial neural networks differ from theoretical models not only for their capability to describe any kinds of dynamics (as long as the system inputs and its responses are actually known) but also for the lower computational effort that is generally required. Independently on the specific process under study, a versatile methodology aimed at modeling the behavior of complex systems has been actually developed, proving that it provides consistent predictions of the actual system behavior in a wide range of operating conditions.

The future development of the research activity carried out during this PhD course is represented by the optimization and the control of the analyzed processes. This can be performed exploiting the intrinsic characteristics of neural networks that easily allow implementing either neuro- or adaptive or intelligent controllers, i.e. a variety of controllers employing techniques which can sense and reason about their environment and execute commands in a flexible and robust manner.

REFERENCES

Bailey, J. E. and Ollis, D. F. (1986). Biochemical Engineering Fundamentals, McGraw-Hill Book Co., Singapore.

Dunleavy P: Authoring a PhD. How to Plan, Draft, Write and Finish a Doctoral Thesis or Dissertation. New York: Palgrave Macmillan; 2003. p. 8, 9.

Engineering Chemistry 43, 1460-1467.

Feyo de Azevedo, S., Dahm, B., & Oliveira, F.R. (1997). Hybrid modelling of Biochemical Processes: A comparison with the conventional approach. Comput. Chem. Eng., 21, 751

Kahrs, O., & Marquardt, W. (2007). The validity domain of hybrid models and its application in process optimization. Chem. Eng. Process., 46, 1054

Lubbert, A., & Jorgensen, S. B. (2001). Bioreactor performance: a more scientific approach for practice. J. Biotechnol., 85, 187-212.

Luque, R., Campelo J., Clark, J.(2010). Handbook of biofuels production. Woodhead Publishing Ltd.

Psichogios, D. C., Ungar, L.H (1992). A hybrid neural network-first principles approach to process modeling. AIChe J., 38, 1499

Stephanopoulos, G. Chemical process control : an introduction to theory and practice (1984). Prentice Hall.

Zhang, G., Patuwo, B.E., Hu, M. J. (1998). Forecasting with Artificial Neural Network: the state of Art. Int. J. of Forecasting, 14, 35

LIST OF PUBLICATIONS

1 **Saraceno, A.,** Curcio, S., Calabrò, V., Iorio, G. (2010). *A hybrid neural approach to model batch fermentation of "ricotta cheese whey" to ethanol.* Computers & Chemical Engineering, 2010, 34 (10), 1590

2 **Saraceno, A.,** Sansonetti, S., Calabrò, V., Iorio, G., Curcio, S., (2011*). A comparison between different modeling techniques for the production of bioethanol from dairy industry wastes.* Chemical and Biochemical Engineering Quarterly, 25(4).

3 **Saraceno, A.,** Aversa, M., Curcio, S. *Advanced modeling of food convective drying: artificial neural networks and hybrid approaches*. Food and Bioprocess Technology, DOI 10.1007/s11947-010-0477-3.

4 Calabrò, V., Curcio, S., **Saraceno, A.,** Ricca, E., De Paola, M.G., Iorio, G. *Biodiesel production from waste oils by enzymatic trans-esterification: process modeling with hybrid neural model.* The abstract of the paper has been published on Journal of Biotechnology, 2010, 150, 371. The paper is ready to be submitted for publication on ISI ranked scientific journals.

5 **Saraceno, A.,** Curcio, S., Calabrò, V. *How hybrid neural model might help on the optimization of biofuels product.* It was submitted to Biomass & Bioenergy and at present, it is under review.

6 **Saraceno, A.,** Ricca, E., Curcio, S., Calabrò, V., Iorio, G. *A mass transport/kinetic model for the description of inulin hydrolysis by immobilized enzyme.* The paper is ready to be submitted for publication on ISI ranked scientific journals.

7 **Saraceno,** A., Sansonetti, S., Curcio, S., Calabrò, V. *A hybrid neural approach to model batch fermentation of dairy industry wastes.* In Computer Aided Chemical Engineering, 28, pp.(739-744). Doi: 10.1016/S1570-7946(10)28124-5.

BOOK CHAPTER

1 Curcio, S., Aversa, M., **Saraceno, A.** (2010). *Advanced modeling of food convective drying: a comparative study among fundamental, artificial neural networks and hybrid approaches* published in Food Engineering, Eds. Brendan-Siegler, Nova Publisher.

CONFERENCE PROCEEDINGS

1 **Saraceno, A.,** Sansonetti, S., Curcio, S., Calabrò, V., Iorio, G. A hybrid neural approach to model batch fermentation of dairy industry. ESCAPE20 Symposium, 6-9 June 2010, Ischia

2 **Saraceno, A.,** Curcio, S., Calabrò, V., Iorio, G., De Bari, I., Cuna D., Stillo, V. *Modeling of an integrated bioreactor/pervaporation system.* IBIC 2010 conference, 11-14 April 2010, Padova

3 **Saraceno, A.,** Curcio, S., Calabrò, V. *How hybrid neural model might help on the optimization of biofuels product*. 19th Biomass Conference and Exhibition, Berlin, 6-9 June, 2011.

4 Calabrò, V., Curcio, S., Ferraro, F., **Saraceno, A.** *Biogas production with bioconversion of organic solid wastes (manure) and "pastazzo" or husks residual from olive oils mills.* 19th Biomass Conference and Exhibition, Berlin, 6-9 June, 2011.

5 Calabrò, V., Basile, A., Pinacci, P., Drago, F., Liguori, S., Iulianelli, A., **Saraceno, A**. *An application of water gas shift reaction via PSS supported Pd-based membrane reactor for hydrogen production.* 19th Biomass Conference and Exhibition, Berlin, 6-9 June, 2011.

6 Calabrò, V., Di Bari, I., Verardi A., **Saraceno, A.,** Curcio, S., Liuzzi, F. *Integrated bioreactor / pervaporation system, for bioethanol production from lignocellulosic biomasses.* The 6th Conference of the Aseanian Membrane Society In Conjunction with the 7th International Membrane Science and Technology Conference, Sydney, 22-26 November 2010

7 **Saraceno, A.,** Calabrò, V., Curcio, S., Iorio, G., De Bari, I., Liuzzi, F., Cuna, D. *Modeling of an integrated bioreactor / pervaporation system, for bioethanol production, based on a hybrid neural approach.* The 14th International Biotechnology Symposium and Exhibition Biotechnology for the Sustainability of Human Society, Rimin, 14-18 September, 2010

8 **Saraceno, A.,** Aversa, M., Curcio, S. *A theoretical model for the control of color degradation and microbial spoilage occurring in food convective drying.* Submitted for an oral presentation to the 20th International Congress of Chemical and Process Engineering, CHISA 2012, Prague

ACTIVITIES

- Research project “Ottimizzazione e controllo del processo di essiccamento di vegetali” Funded by University of Calabria “Progetto Giovani Ricercatori 2010/2011, Area CUN09”
- Supervisor of six thesis in Chemical Engineering Degree, 2009-2011
- Tutor of the academic course “Laboratorio di ingegneria Chimica”, Chemical Engineering Degree, 2010/2011,
- Tutor of the academic course” Biotecnologie Industriali 2”, Chemical Engineering Degree, 2010/2011
- Gricu PhD national School “Mathematical Methods for Chemical Engineering”, 25-30 September, 2011
- PhD School “Sustainable Hydrogen and Energy Production from Renewable Sources, Catalytic and Bio-catalytic Membrane reactors, Fuel Cells and Biotechnology, Università della Calabria, 26-29 April 2010.
- Participation to the 19th Biomass Conference and Exhibition, Berlin, 6-9 June, 2011. Oral and Visual Presentations.
- Participation to ESCAPE20 Symposium, 6-9 June 2010, Napoli. Oral presentation.
- Representative of the PhD students in ”Ambiente, Salute e processi eco-sostenibili” in the Department of Engineering Modeling Council, 2009-2011
- Achievement of the *First Certificate of Spoken English* (FIRST), 2009
- English Course, B2 level, University of Calabria, July-October 2009
- English course, Advanced level, Kaplan Aspect Institute of New York, 1-30 June, 2009
- Thermodynamics course, Prof. Bruno de Cindio, April 2010.